Impact of extreme events on particulate trace metal transfer from the continent to the deep sea

Chloé Dumas

THÈSE

Pour obtenir le grade de

Docteur

Délivré par

UNIVERSITE DE PERPIGNAN VIA DOMITIA

Préparée au sein de l'école doctorale Energie et Environnement (ED 305)
Et de l'unité de recherche CEFREM UMR 5110

Spécialité : **Océanographie**

Présentée par **Chloé DUMAS**

Impact of extreme events on particulate trace metal transfer from the continent to the deep sea

Soutenue le 02/06/2014 devant le jury composé de

J. SCHAFER, Professeur, EPOC	***Rapporteur***
C. GARNIER, Maitre de conférence, PROTEE	***Rapporteur***
C. GROSBOIS, Professeur, GeHCO	***Examinateur***
A. PALANQUES, Professeur, CSIC	***Examinateur***
W. LUDWIG, Professeur, CEFREM	***Directeur de thèse***
D. AUBERT, Maitre de conférence, CEFREM	***Co-directeur de thèse***

b

TABLE OF CONTENT

ABBREVIATIONS

CCC	Cap de Creus Canyon
CTD	Conductivity-Temperature-Depth
DSWC	Dense Shelf Water Cascading
EF	Enrichment Factor
GoL	Gulf of Lion
LDC	Lacaze-Duthiers Canyon
OOC	Open-Ocean Convection
POC	Particulate Organic Carbon
PTM	Particulate Trace Metals
Q	Liquid discharge
REE	Rare Earth Elements
SOS	South Open Slope
SPM	Suspended Particulate Matter
UCC	Upper Continental Crust

h

LIST OF FIGURES

LIST OF TABLES

Table 4.5 Grain-size, OC and PTM concentrations in HERMES sediment traps. Flux-weighted mean contents and concentrations are indicated for each trap. Each sample is named after the reference date of the 15-days sampling interval.

Table 4.6 a) Pearson correlation matrices, during and pre and post DSWC conditions and b) correlation coefficients between Al-normalized concentrations and POC in CCC sediment trap samples.

Table 4.7 Mean EFs calculated in CCC sediment trap samples and standard deviation. For the local Rhone riverbank reference samples, correlation coefficients (r^2) were calculated between EF and POC content (significance > 99% with 9 degrees of freedom). Those EF values are compared to EFs calculated by Dumas et al. (2014) in CCC sediment trap samples, high-frequency water sampling samples and the first centimeter of the fresh sediment deposit recovered in the CCC after the E-SE storm studied. Mean EF values calculated by Roussiez et al. (2012) in superficial shelf sediments are also shown.

Table 4.8 a) Comparison between HERMES sediment traps' mass and trace metal fluxes. All fluxes are in $mg.m^{-2}.d^{-1}$ except for Al, which is in $g.m^{-2}.d^{-1}$ and for Cd, which is in $\mu g.m^{-2}.d^{-1}$. b) Comparison between CCC PTM daily fluxes and total export calculated in this work and in Dumas et al., 2014.

Table 5.1 Location and length of the deep sediment cores from the North Western Mediterranean sea investigated in this study.

Table 5.2 PTM Concentrations, grain-size distribution, C_{org} and carbonate contents, C:N ratios and calculated datation in deep cores.

Chapter I

Introduction

Although coastal areas represent only 18% of the worldwide ocean, they are the connexion between continent, ocean and atmosphere domains. They are the scene for production, transformation, transfer, export and storage of both natural and anthropogenic inputs. Indeed, rivers hydrology is dependent on seasonal and regional climate (snowmelt, intense rainfalls) which cause elevated discharge of freshwater and particulate matter on coastal margins, called seasonal or oceanic flood according to the size of the drainage basin (*Drake & Cacchione, 1985; Mulder & Syvitski, 1996; Sommerfield & Nittrouer, 1999; Mullenbach & Nittrouer, 2000; Roussiez et al., 2005*). Deposition of sediment in estuaries and river prodeltas is ephemeral as mechanisms such as bottom nepheloid layers, winter storms and/or mesoscale circulation patterns rework the inner shelf, resuspending and redistributing this particulate load along and across-shelf to the mid-shelf and beyond (*Puig & Palanques, 1998; Ogston & Sternberg, 1999; Geyer et al., 2000*).

High-energy oceanographic processes such as storms, waves and dense water formation occur on continental margins and induce currents that rapidly transfer important amounts of water, sediment particles, organic matter but also litter and chemical pollutants, from the continental shelf to the deep-ecosystems, which are very sensitive to external inputs. Coastal zones hence play a key role in marine biogeochemical cycles and primary production by providing nutrients to the open-ocean. A good understanding of the ecosystems functioning and behaviour will help anticipate their evolution, but also to identify the major threats they face, their potential impact and, ultimately, it will provide the tools required to improve the sustainable management of living (deep-sea benthic and pelagic organisms) as well as inert ressources (*Canals et al., 2013*). For example, particulate material is regularly removed from coastal and deep-sea regions to sand up beaches but, only recently, few studies have been carried out in the Manche area, regarding the impact of this sediment load's extraction on the remobilization and transfer of contaminants (*Lozach, 2011; Duclos, 2012*).

Indeed, coastal zones are also subjected to increasing anthropogenic pressures over the years : more than 60% of the world's population lives within 150km of the coast and uses coastal areas as a source of food (*Holligan and de Boois, 1993*) or leisure. Unfortunately marine pollution arises from this constant increase in population density and industrialization. Anthropogenic impacts, either direct through bottom trawling or litter and chemical pollutants release, or indirect, through global warming, do have a central part in deep-sea environment functioning (*Glover et al., 2003*). Indeed, repetitive droughts in summers, as well as more frequent and more violent torrential precipitations in autumns and winters could lead to modifications of hydrological regimes, then biogeochemical cycles and environments to some

extent. For example, it is known that climate change will have profound effects on the frequency, intensity and eventually the location of key oceanographic processes like Dense-Shelf Water Formation (DSWC) and eastern storms or open-ocean convection, the three tenors of the NW Mediterranean Sea (*Canals et al., 2013*). In order to know how those changes will also impact the role those key processes have on sustaining the deep ecosystems but also on carrying chemical pollution, one has to fully understand how those processes function nowadays.

As the development of industrial societies is linked to discovery and use of metals, their consumption has increased by 300% in the last fifty years and anthropogenic release of metallic elements such as Pb, Hg, Zn, Cd, Cu and Cr have tripled since the beginning of the industrial era (*INERIS, 2006*). Trace metals hence seem like a good indicator of anthropogenic pressures because it is possible to distinguish natural from man-made contribution. Most trace metals are naturally present in the continental crust in low concentrations, but additionnal inputs from anthropogenic origin are now frequent.

Some trace metals are essential, like Cu, Zn or Se; some have specific roles, like Ni in urease; but others have no biological functions and are toxic, like Cd, Hg or Pb. And even essential trace metals can be lethal in high levels or under bioavailable forms. This labile, bioavailable stock becomes exchangeable with the surrounding environment and is usually introduced by anthropogenic activities (*Salomons and Forstner, 1984*).

Hence, management of risks related to trace metals imply monitoring and controlling trace metal fluxes in each compartment of the ecosystem (*Berthelin & Bourrelier, 1993*).

As trace metal distribution in the marine environment is largely controlled by the particulate phase (*Turekian, 1977*), especially by fine sediment particles, due to their affinity for silt and clay (*Gibbs, 1973*), therefore, their fate is also linked to suspended particulate matter discharge to the sea, dispersal dynamics and ultimately, sequestration in the sedimentary strata. Those are controlled by rapid physico-chemical and hydro-meteo-climatic forcings (floods, storms, primary production…) as well as slow ones (diagenesis and climate change).

In estuaries, during the passage from the freshwater to the marine environment, throughout the salinity gradient, trace metals undergo remobilization processes. For example, some are removed from the dissolved phase and taken up by particulate matter, which can be deposited then resuspended during larger estuarine mixing episodes (*Duinker et al., 1978*).

Sediment-bound contaminants are dependant on the rivers regime and their episodic discharges events, on the strength and length of mixing and advection processes that will be

able to resuspend and disperse them step by step until they reach the deep environments in episodic pulses. However, very few informative and systematic studies have been conducted on contaminant concentrations and fluxes in deep-sea environments.

In this context, the Mediterranean Sea seems well fitted. With a surface of 2.5 10^6 km^2 the Mediterranean Sea represents only 1% of the global ocean surface (*Amblas et al., 2004*), and due to its enclosed character and restricted exchanges with the open ocean, it is strongly influenced by continental inputs of water, sediment, nutrients and chemical pollutants, but also by coastal-pelagic interactions and hydrodynamic functioning. It is also susceptible to climate change and anthropogenic pressures, as years of intense development and exploitation have resulted in significant changes of its fragile natural resources. Coastal urbanisation, industrialisation and touristic exploitation, intensive agriculture, riverine and atmospheric inputs and fisheries are only some of the anthropogenic forcings which have exerted a progressively growing pressure on the mediterranean environment.

The Gulf of Lion (GoL) in particular (Fig.1.1) exhibits specific characteristics like small tidal currents, variable wind-driven circulation and dense-water formation. It is probably an area in the Mediterranean Sea advantaged for across-shelf export because the GoL is often affected by relatively stronger storms, dense shelf water cascading and wind-induced cyclonic circulation (*Durrieu de Madron et al., 2005; Palanques et al, 2006; Canals et al., 2006; Ogston et al., 2008*). As the NW Mediterranean margins are the most densely canyoned in the entire basin, the GoL is also a privileged area for down-shelf export. Indeed Puig et al. (*2013*) demonstrated how submarine canyons are preferential conduits for matter and energy transfer from the surface to the deep ecosystem. Their distribution, characteristics and functioning have a strong influence on sediment transfer and deep ecosystem functioning and they are likely to significantly contribute of the propagation of anthropogenic signals (e.g. PBDE accumulation at the end of the Cap de Creus and Lacaze-Duthiers submarine canyons, *Salvadó et al., 2012*).

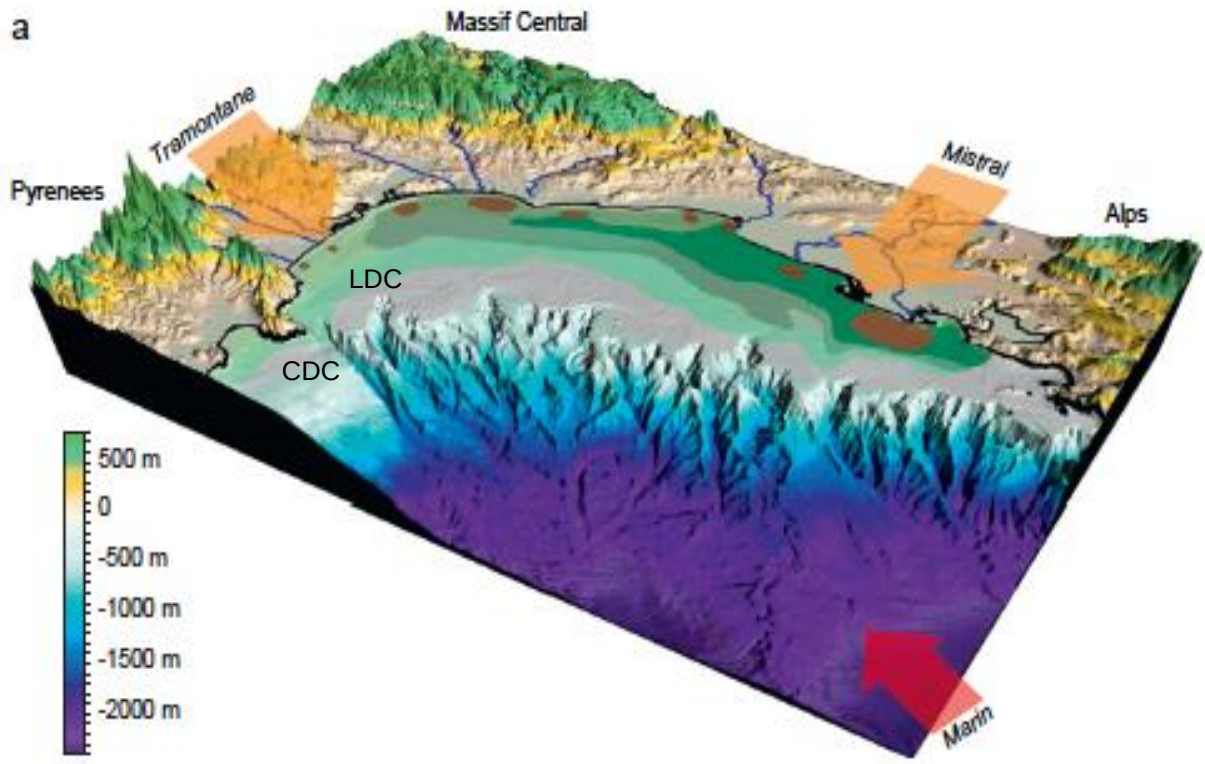

Fig.1.1 Map of the GoL (from Durrieu de Madron et al., 2008) with moutains (Pyrenees, Massif Central and Alps), rivers and bathymetric features (Lacaze-Duthiers and Cap de Creus submarine canyons in particular)

The GoL is hence considered as a test-zone for the long-term evolution of sediment transport and has been the place of numerous European research programs for the past 20 years. EUROpean Margin STRATA FORMation (EUROSTRATAFORM, 2002-2005) was developed to understand sedimentary processes, deposits and stratigraphy in areas of the northeast Atlantic and Mediterranean systems, representative of the European continental margin (*Syvitski et al., 2004*; *Weaver et al., 2006*). It provided the opportunity to study the effects of the DSWC (2004-05 event), extreme floods (December 2003 event on the Rhone river) and storms which are the most effective processes controlling sediment dynamics in the GoL's continental shelf. Results and modelling emphasized the predominant role of E-SE storms in wave-induced resuspension and along-shelf cyclonic transport of fine sediment on the inner shelf but also during periods of dense water formation driven by N-NW winds. These two wind-driven processes induce most of the export of suspended sediment and associated elements from shelf, primarily at the southwestern end of the Gulf. These events displayed a clear seasonality and large interannual variability and are likely to be sensitive to climatic changes.

Following this program, HERMES (Hotspot Ecosystem Research on the Margins of European Seas, 2005-2009), HERMIONE (Hotspot Ecosystem Research on Man's Impact on European Seas, 2009-2012) and now PERSEUS (Policy-oriented marine Environmental Research in the Southern EUropean Seas, 2012-2015), were designed to deepen the current understanding of the Mediterranean marine ecosystems and their response to spatial and temporal modifications of physico-chemical forcing linked to changing environmental conditions and increasing human pressure. Those integrated approaches always considered the continuum between the coastal zone and the open sea. Such scientific data are used in the frame of the Marine Strategy Framework Directive (MSFD), a European initiative which aims at attaining good environmental status in marine waters by 2020, notably in the deep-sea ecosystem.
As some of these programs are still ongoing, the scientific community recognizes the need to quantify and assess the fluxes of trace metals in our case, from the continent, which acts as a source, to the marine environments acting as a receiver. Improving our knowledge on land-to-sea transfer of sediment, organic matter (a PhD is currently conducted on this topic at the CEFREM) and bound contaminants and knowing what happens to it once it is delivered to the coastal waters is one of the priorities for a better understanding of global biogeochemical cycles (*Sanchez-Vidal et al., 2013*).

In the GoL, trace metals have been well studied. They were used as geochemical tools: fine sediment fraction normalizer (*Roussiez et al., 2005*) or geochemical tracers of atmospheric fallout pattern (*Miralles et al., 2006*) or lithogenic sources (*Roussiez et al., 2013*).
On the continental shelf, spatial and temporal studies were conducted to elucidate their fate in the sedimentological cycle (*Roussiez et al., 2006, 2011; Radakovitch et al., 2008*), often resulting in budget calculations. Ollivier et al. (*2011*) and Roussiez et al. (*2012*) estimated the flood contribution to annual Particulate Trace Metal (PTM) input fluxes to be between 15 and 91%, depending on the element. Radakovitch et al. (*2008*) showed that, between 2000 and 2003, particulate input fluxes of trace metals from the Rhone River were 2 to 10 times higher than particulate atmospheric deposition. He compared his results with estimations of dissolved and particulate metals fluxes (from *Guieu et al., 1997*) deposited from various sites of the northwestern Mediterranean Sea for which he used mean flux values. Regarding atmospheric particulate deposition of trace metals, Guieu et al. (*1997)* highlighted the importance of dry deposition (i.e. Saharan dust). Moreover, Guieu et al. (*1997*) and Elbaz-Poulichet et al. (*2001*) showed that, concerning dissolved trace metal fluxes, atmospheric inputs represent more than 50% of the total dissolved trace metal inputs to the NW

Mediterranean Sea. In the canyon environments, Grousset et al. (*1995*) studied the distribution of PTMs in the Lacaze-Duthiers canyon and Roussiez et al. *(2012, 2013*) looked at the output fluxes in the head of the Cap de Creus canyon. In the deep-sea basin, Marin et al. (*2001*) studied the forcing factors controlling the distribution of Mn and Fe in sediment cores from the GoL continental shelf and deep-basin and Angelidis et al. (*2011*) highlighted the accumulation of anthropogenic Cd, Pb and Zn in surficial sediment of deep cores, but suspected atmospheric deposition to be the main source for trace metal inputs in this deep-basin area.

Since PTMs have been well documented in the past (Fig.1.2), the objectives of this study were not to develop a new analytical technique. We rather wanted, with the help of long-term surveys, to fill in some gaps of specific situation consequences on PTM dynamics. For example, until now, great attention was focused on the Rhone river but less was granted to small coastal rivers and their respective contribution to the annual PTM inputs.

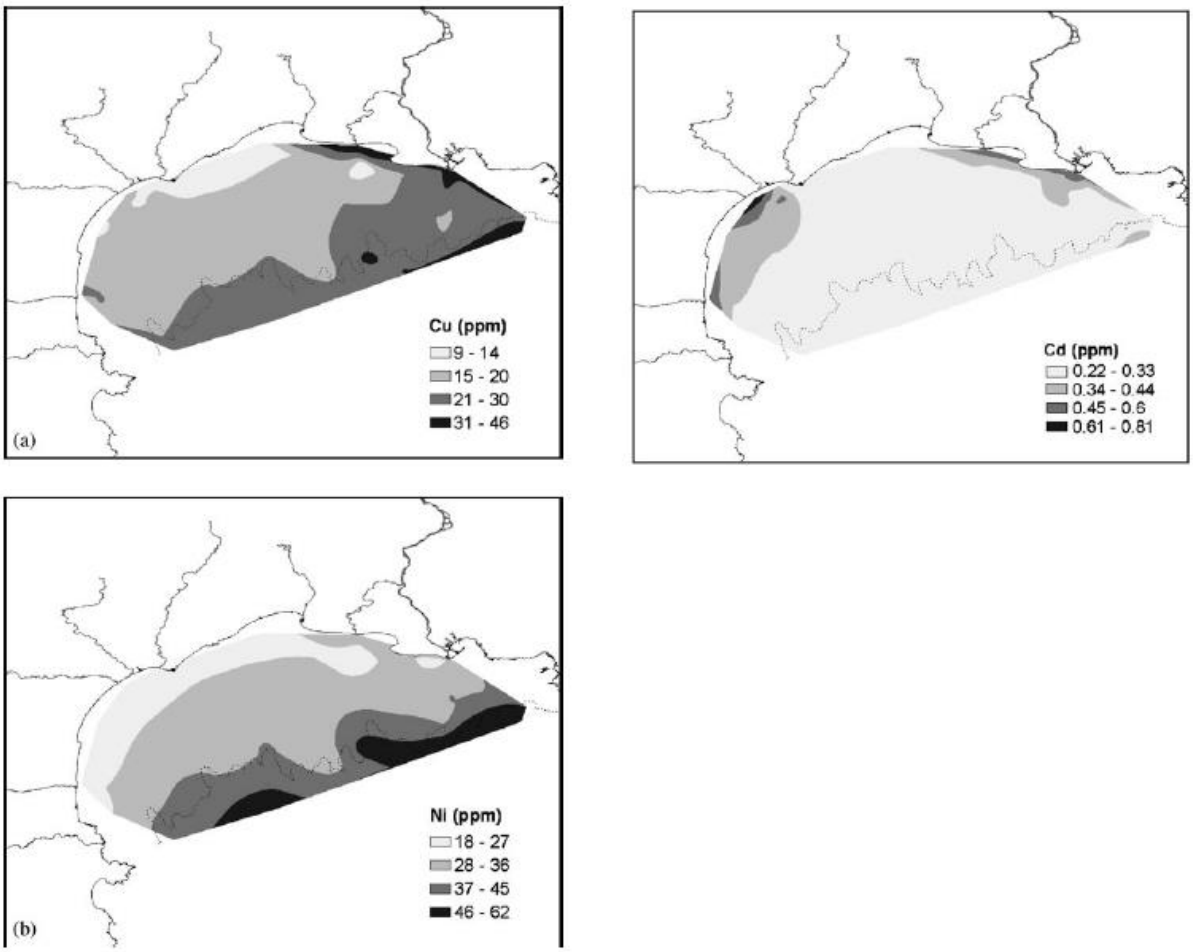

Fig.1.2 From Roussiez et al. (2006). Spatial distribution of Cu, Cd and Ni contents in less than 63 µm sediment fraction on the GoL continental shelf

In this way, we also aimed at proposing a sampling strategy for PTM export budgets calculation, through the example of the Tet and Rhone rivers.

Those methods might ease potential decision in sustainable management decisions for the future of the coastal zones. Also, the sedimentological cycle of PTM was extensively studied on the continental shelf (from prodeltas to mid and outer shelf) but less studies were conducted on PTM transport processes and fate in submarine canyons and beyond. Objectives of this study are first to quantify the fluxes transferred and deposited from the continental shelf to the deep basin. Since this export mostly takes place under extreme hydro-meteo-dynamic processes, we focused on floods, E-SE storm and DSWC case studies. Input fluxes by rivers, which happen mainly during flood events, and output fluxes due to hydrodynamic processes will help us in assessing the role of continental shelf as a source or sink of trace metal and its flushing potential from the shelf toward deep environments.

We also aim at characterizing the origin of those PTM, through the study of specific Rare Earth Elements and of their natural and residual fraction but also to evaluate the anthropogenic part of those fluxes and its potentially bioavailable nature. Through those spatial and temporal resolution studies of heavy metal downward fluxes from the GoL coastal rivers and in the southwesternmost canyons, we will help understand the input, transfer and deposition fluxes of heavy metals from the GoL continental area to deeper environments.

The manuscript is organized in the following manner :

The second chapter will present in more detail the study area, the samples and sampling strategies used in this work as well as the analytical and calculation methods.

In order to follow the general land-to-sea continuum reasoning, we will first present the results of our study on riverine inputs in the third chapter. The results from this chapter were obtained after a 5-year monitoring of the GoL coastal rivers, which makes it the most up-to-date dataset in the GoL coastal system regarding metallic contaminants. Particular attention was paid to flood events and their respective contribution to the annual riverine input.

The fourth chapter will deal with transfer processes through submarine canyons : transfer triggered by E-SE storm in the first part and by DSWC in the second part. We will also quantify their relative output contribution of PTM compared to annual riverine input in order to assess and compare both event-related export and depurating potential.

In the fifth chapter, we will focus on the deep basin through analysis of the trace metal contents of three deep sediment cores which are the result of previously described transport and input.

Finally, the sixth chapter will present the general conclusions and perspectives of this study.

References

Amblas, D., Canals, M., Lastras, G., Berne, S., Loubrieu, B. (2004). Imaging the seascapes of the Mediterranean. *Oceanography*, 17 (4), 144–155.

Angelidis, M.O., Radakovitch, O., Veron, A., Aloupi, M., Heussner, S., Price, B. (2011). Anthropogenic metal contamination and sapropel imprints in deep Mediterranean sediments. *Marine Pollution Bulletin*, 62, 1041-1052.

Berthelin, J., Bourrelier, P.H. (1998). Contamination des sols par les éléments en traces : les risques et leur gestion. *Académie des Sciences, Tec et doc (éd.)*, rapport n°42.

Canals, M., Puig, P., Durrieu de Madron, X., Heussner, S., Estournel, C. (2006). Flushing submarine canyons. *Nature*, 444, 354-357.

Canals, M., Company, J.B., Martín, D., Sànchez-Vidal, A., Ramírez-Llodrà, E. (2013). Integrated study of Mediterranean deep canyons: Novel results and future challenges. *Progress in Oceanography*, 118, 1-27.

Drake, D.E., Cacchione, D.A. (1985). Seasonal variation in sediment transport on the Russian River shelf, California. *Continental Shelf Research*, 4, 495-514.

Duclos, P.A. (2012). Impacts morpho-sédimentaires de l'extraction de granulats marins. Application au bassin oriental de la Manche. Université de Rouen, 286 p.

Durrieu de Madron, X., Zervakis, V., Theocharis, A., Georgopoulos, D. (2005). Comments on "Cascades of dense water around the world ocean", *Progress in Oceanography*, 64(1), 83-90.

Elbaz-Poulichet, F., Guieu, C., Morley, N.H. (2001). A Reassessment of Trace Metal Budgets in the Western Mediterranean Sea. *Marine Pollution Bulletin*, 42(8), 623-627.

Geyer, W.R., Hill, P., Milligan, T., Traykovski, P. (2000). The structure of the Eel River plume during floods. *Continental Shelf Research*, 20, 2067-2093

Gibbs, R.J. (1973). Mechanisms of trace metal transport in rivers. *Science*, 180, 71-72.

Glover, A.G., Smith, C.R. (2003). The deep-sea floor ecosystem: current status and prospects of anthropogenic change by the year 2025. *Environmental Conservation*, 30, 219–241.

Grousset, F.E., Quetel, C.R., Thomas, B., Donard, O.F.X., Lambert, C.E., Guillard, F., Monaco, A. (1995). Anthropogenic vs. lithogenic origins of trace elements (As, Cd, Pb, Rb, Sb, Sc, Sn, Zn) in water column particles: northwestern Mediterranean Sea. *Marine Chemistry*, 48(3–4), 291-310.

Guieu, C., Chester, R., Nimmo, M., Martin, J.M., Guerzoni, S., Nicolas, E., Mateu, J., Keyse, S. (1997). Atmospheric input of dissolved and particulate metals to the northwestern Mediterranean. *Deep Sea Research Part II: Topical Studies in Oceanography*, 44(3–4), 655-674.

Holligan, P.M., de Boois, H.E. (1993). The LOICZ Science Plan. IGBP Report n°25. Stockholm, IGBP : 50 p.

INERIS, (2006). Recommandations pour la modélisation des transferts des éléments traces métalliques dans les sols et les eaux souterraines. *Rapport d'étude N°INERIS-DRC-06-66246/DESP-R01a.*

Lozach, S. (2011). Habitats benthiques marins du bassin oriental de la Manche : enjeux écologiques dans le contexte d'extraction de granulats marins. Université de Lille Nord de France, 308 p.

Marin, B., Giresse, P. (2001). Particulate manganese and iron in recent sediments of the Gulf of Lions continental margin (north-western Mediterranean Sea): deposition and diagenetic process. *Marine Geology*, 172(1–2), 147-165.

Miralles, J., Veron, A., Radakovitch, O., Deschamps, P., Tremblay, P., Hamelin, B. (2006). Atmospheric lead fallout over the last century recorded in Gulf of Lions sediments (Mediterranean Sea). *Marine Pollution Bulletin*, 52 (11), 1364-1371.

Mullenbach, B.L., Nittrouer, C.A. (2000). Rapid deposition of fluvial sediment in the Eel Canyon, northern California. *Continental Shelf Research*, 20(16), 2191-2212.

Ogston, A.S. and Sternberg, R.W., (1999). Sediment transport events on the northern California continental shelf. *Marine Geology*, 154, 69-82.

Ogston, A., Drexler, T., Puig, P. (2008). Sediment delivery, resuspension, and transport in two contrasting canyon environments in the southwest Gulf of Lions. *Continental Shelf Research*, 28(15), 2000-2016.

Ollivier, P., Radakovitch, O., Hamelin, B. (2011). Major and trace element partition and fluxes in the Rhône River. *Chemical Geology*, 285(1–4), 15-31.

Palanques, A., Durrieu de Madron, X., Puig, P., Fabres, J., Guillén, J., Calafat, A., Canals, M., Heussner, S., Bonnin, J. (2006). Suspended sediment fluxes and transport processes in the Gulf of Lions submarine canyons. The role of storms and dense water cascading. *Marine Geology*, 234, 43-61.

Puig, P., Palanques, A. (1998). Nepheloid structure and hydrographic control on the Barcelona continental margin, northwestern Mediterranean. *Marine Geology*, 149(1-4), 39-54.

Puig, P., Palanques, A., Sanchez-Cabeza, J.A., Masqué, P. (1999). Heavy metals in particulate matter and sediments in the southern Barcelona sedimentation system (North-Western Mediterranean). *Marine Chemistry*, 63, 311-329.

Puig, P., Palanques, A., Martin, J. (2014). Contemporary Sediment-Transport Processes in Submarine Canyons. *Annual Review of Marine Science*, 6(5), 53-77.

Radakovitch, O., Roussiez, V., Ollivier, P., Ludwig, W., Grenz, C., Probst, J.L. (2008). Input of particulate heavy metals from rivers and associated sedimentary deposits on the Gulf of Lion continental shelf. *Estuarine, Coastal and Shelf Science*, 77, 285-295.

Roussiez, V., Ludwig, W., Probst, J.L., Monaco, A. (2005). Background levels of heavy metals in surficial sediments of the Gulf of Lions (NW Mediterranean): an approach based on ^{133}Cs normalization and lead isotope measurements. *Environmental Pollution*, 138, 167-177.

Roussiez, V., Ludwig, W., Probst, J.L., Monaco, A., Bouloubassi, I., Buscail, R., Saragoni, G. (2006). Sources and sinks of sediment-bound contaminant in the Gulf of Lions (NW Mediterranean Sea): a multi-tracer approach. *Continental Shelf Research*, 26, 1843-1857.

Roussiez, V., Ludwig, W., Radakovitch, O., Probst, J.-L., Monaco, A., Charrière, B., Buscail, R. (2011). Fate of metals in coastal sediments of a Mediterranean flood-dominated system: An approach based on total and labile fractions. *Estuarine, Coastal and Shelf Science*, 92(3), 486-495.

Roussiez, V., Heussner, S., Ludwig, W., Radakovitch, O., Durrieu de Madron, X., Guieu, C., Probst, J.-L., Monaco, A., Delsaut, N. (2012). Impact of oceanic floods on particulate metal inputs to coastal and deep-sea environments: A case study in the NW Mediterranean Sea. *Continental Shelf Research*, 45, 15-26.

Roussiez, V., Aubert, D., Heussner, S. (2013). Continental sources of particles escaping the Gulf of Lion evidenced by rare earth elements: flood vs. normal conditions. *Marine Chemistry*, 153, 31-38.

Salomons, W., & Förstner, U. (1984). *Metals in the hydrocycle*. Berlin-Heidelberg-New York-Tokyo : Springer-Verlag, 349 p.

Salvadó, J.A., Grimalt, J.O., López, J.F., Durrieu de Madron, X., Heussner, S., Canals, M. (2012). Transformation of PBDE mixtures during sediment transport and resuspension in marine environments (Gulf of Lion, NW Mediterranean Sea). *Environmental Pollution*, 168, 87-95.

Sanchez-Vidal, A., Higueras, M., Martí, E., Liquete, C., Calafat, A., Kerhervé, P., Canals, M. (2013). Riverine transport of terrestrial organic matter to the North Catalan margin, NW Mediterranean Sea. *Progress in Oceanography*, 118, 71-80.

Sommerfield, C.K., Nittrouer, C.A. (1999). Modern accumulation rates and a sediment budget for the Eel shelf: a flood-dominated depositional environment. *Marine Geology*, 154(1–4), 227-241.

Syvitski, J.P., Peckham, S.D., Hilberman, R., Mulder, T. (2003). Predicting the terrestrial flux of sediment to the global ocean: a planetary perspective. *Sedimentary Geology*, 162(1–2), 5-24.

Turekian, K.K. (1977). The fate of metals in the oceans. *Geochimica et Cosmochimica Acta*, 41(8), 1139-1144.

Weaver, P.P.E., Canals, M., Trincardi, F. (2006). EUROSTRATAFORM Special Issue of Marine Geology. *Marine Geology*, 234(1–4), 1-2.

Chapitre I

Introduction

Bien que les zones côtières ne représentent que 18 % de l'océan mondial, elles sont l'interface entre continent, océan et atmosphère. Elles sont le lieu de production, de transformation et de transfert de matière mais aussi des zones d'export et de stockage des apports naturels et anthropiques. En effet, le climat régional et une forte saisonnalité des régimes (fonte des neiges, pluies abondantes) influencent l'hydrologie des rivières et peuvent provoquer des élévations de débits significatives et par conséquent des apports en matières en suspension élevés sur les marges côtières. Ces hausses de débits sont alors appelées inondations saisonnières ou océaniques en fonction de la taille du bassin versant correspondant (*Drake & Cacchione, 1985; Mulder & Syvitski, 1996; Sommerfield & Nittrouer, 1999; Mullenbach & Nittrouer, 2000; Roussiez et al., 2005*). Le dépôt de ces sédiments dans les estuaires et prodeltas des rivières est éphémère car des mécanismes tels que les couches néphéloïdes de fond, les tempêtes hivernales et/ou la circulation générale « retravaillent » le plateau, provoquant la remise en suspension et la redistribution de ces dépôt de particules à travers et le long du plateau continental et au-delà vers la pente (*Puig et Palanques, 1998; Ogston & Sternberg, 1999; Geyer et al., 2000*).

Les processus océanographiques intenses tels que les tempêtes, les vagues et la formation d'eau dense se produisent sur les marges continentales et induisent des courants qui transfèrent rapidement d'importantes quantités d'eau, de sédiments, de matière organique, mais aussi de déchets et de contaminants chimiques, du plateau continental vers les écosystèmes profonds, eux-mêmes très sensibles aux apports externes. Les zones côtières jouent donc un rôle clef dans les cycles biogéochimiques marins et la production primaire en fournissant notamment, par les processus cités ci-dessus, des nutriments essentiels à l'océan ouvert. Une bonne compréhension du fonctionnement des écosystèmes et de leur comportement contribue à anticiper leur évolution, mais aussi à identifier les principales menaces auxquelles ils sont confrontés, leurs impacts potentiels et, en fin de compte, fournit les outils nécessaires à l'amélioration de la gestion durable des ressources vivantes (organismes benthiques et pélagiques de fond) ainsi que des ressources inertes (*Canals et al., 2013*). Par exemple, des stocks sableux sont régulièrement extraits des régions côtières et du large afin de ré-ensabler le littoral. Jusqu'à récemment, peu d'études ont été menés sur l'impact de l'extraction de ce stock sédimentaire, sur la remobilisation de particules fines protégées par le drapage sableux ou sur les conséquences de ce transfert sédimentaire en terme d'apport potentiel en contaminants à la zone littorale (*Lozach, 2011*; *Duclos, 2012*).

Les zones côtières ont été soumises à des pressions anthropiques croissantes au fil des ans : actuellement plus de 60% de la population mondiale vit à moins de 150 km de la côte et utilise les zones littorales en tant que zones de production de ressources alimentaires (*Holligan et de Boois, 1993*) ou de loisirs. Malheureusement la pollution marine provient de l'augmentation constante de cette densité de la population et de l'industrialisation de ces zones. Les impacts anthropiques, soit directs par le chalutage de fond ou par le relargage de déchets et de polluants chimiques, ou indirects, de par le réchauffement climatique par exemple, ont un rôle central dans le fonctionnement des environnements profonds (*Glover et al., 2003*). Par exemple, les sécheresses répétitives en période estivale, ainsi que les précipitations torrentielles plus fréquentes et plus violentes en automne et en hiver pourraient conduire à des modifications des régimes hydrologiques, et par la même des cycles biogéochimiques et des environnements dans leur ensemble. Ainsi, il est connu que le changement climatique peut avoir des effets importants sur la fréquence, l'intensité et éventuellement l'emplacement des processus océanographiques clefs comme la formation d'eaux denses côtières (cascading) et les tempêtes d'Est ou la convection, les trois ténors de la Méditerranée Nord-Occidentale (*Canals et al., 2013*). Il est donc nécessaire de comprendre le fonctionnement actuel de ces processus afin de comprendre l'influence d'éventuels futurs changements sur le maintien des écosystèmes profonds, mais également sur le transport de la pollution chimique.

Le développement des sociétés industrielles étant lié à la découverte et à l'utilisation des métaux, leur consommation a augmenté de 300% au cours des cinquante dernières années et les rejets anthropiques d'éléments métalliques tels que Pb, Hg, Zn, Cd, Cu et Cr ont triplé depuis le début de l'ère industrielle (*INERIS, 2006*). Les métaux traces semblent donc être un bon indicateur des pressions anthropiques, car il est possible de distinguer la contribution naturelle de celle due à l'homme. En effet, la plupart des métaux traces sont naturellement présents dans la croûte continentale en faibles concentrations, mais des apports additionnels d'origine anthropique sont maintenant fréquents.

Certains métaux sont essentiels, comme Cu, Zn ou Se; certains ont des rôles spécifiques, comme Ni avec l'uréase; mais d'autres n'ont pas de fonctions biologiques et sont toxiques, comme Cd, Hg ou Pb. Il en est de même pour les métaux traces essentiels qui peuvent être mortels à fortes doses ou sous des formes biodisponibles. Ce stock de métaux labiles et potentiellement biodisponibles peut être échangé avec le milieu environnant et est généralement introduit par les activités anthropiques (*Salomons et Forstner, 1984*).

Par conséquent, la gestion des risques liés aux métaux traces implique de surveiller et de contrôler leurs flux dans chaque compartiment de l'écosystème (*Berthelin et Bourrelier, 1993*). Comme la distribution des métaux traces dans l'environnement marin est en grande partie contrôlée par la phase particulaire (*Turekian, 1977*), en particulier par les particules fines, en raison de l'affinité des ces métaux avec les silts et les argiles (*Gibbs, 1973*), leur sort est également lié aux particules en suspension rejetées en mer, à leur dynamique de dispersion et, finalement, à leur séquestration dans les couches sédimentaires. Tous ces paramètres sont contrôlés par les forçages physico-chimiques et hydro-météo-climatiques rapides et intenses (crues, tempêtes, production primaire, ...) mais aussi par des forçages plus lents (diagenèse et changement climatique). En effet, les contaminants liés aux sédiments dépendent du régime hydrologiques des rivières et de leurs événements épisodiques de rejet, et de la force et de la durée des processus de mélange et d'advection qui seront en mesure de les remettre en suspension et de les disperser sporadiquement, de proche en proche, jusqu'à ce qu'ils atteignent les environnements profonds. Cependant, très peu d'études systématiques ont été menées à ce jour sur les concentrations et les flux de contaminants dans les environnements profonds.

Dans ce contexte, la Méditerranée un lieu d'étude privilégié. Avec une surface de $2{,}5.10^6$ km^2, elle ne représente que 1% de la surface de l'océan mondial (*Amblas et al., 2004*), et en raison de son caractère fermé et des échanges restreints avec l'océan ouvert, elle est fortement influencée par les apports continentaux en eau, en sédiments, en nutriments et en contaminants chimiques, mais aussi par les interactions côtières-pélagiques et le fonctionnement hydrodynamique global. Elle est également sensible au changement climatique et aux pressions anthropiques, car des années de développement intense et d'exploitation ont entraîné des modifications importantes de ses ressources naturelles fragiles. L'urbanisation du littoral, l'industrialisation et l'exploitation touristique, l'agriculture intensive, la fluctuation des apports fluviaux et atmosphériques et la pêche sont une partie seulement des forçages anthropiques qui ont exercé une pression progressivement croissante sur l'environnement méditerranéen.

Le Golfe du Lion (GdL) en particulier (Fig.1.1) présente des caractéristiques spécifiques comme un faible marnage, une circulation soumise aux vents et est une zone de formation d'eaux denses. C'est probablement une zone privilégiée de la mer Méditerranée pour l'export du plateau continental, car le GdL est souvent affecté par des tempêtes relativement fortes, des cascades d'eaux denses et par une circulation cyclonique induites par les vents (*Durrieu*

de Madron et al., 2005; Palanques et al., 2006; Canals et al., 2006; Ogston et al., 2008). Comme les marges méditerranéennes nord-occidentales sont les plus densément entaillées par des canyons, le GdL est également un lieu privilégié pour les processus d'export hors du plateau. En effet Puig et al. (*2013*) ont démontré que les canyons sous-marins sont des conduits préférentiels pour le transfert de matière et d'énergie de la surface vers l'écosystème profond. Leurs répartitions, leurs caractéristiques et leurs fonctionnement ont une forte influence sur ce transfert de sédiments et sur le fonctionnement des écosystèmes profonds puisqu'ils sont susceptibles de contribuer de manière significative à la propagation des signaux anthropiques (exemple de l'accumulation de PBDE au bas des canyons sous-marins du Cap de Creus et Lacaze-Duthiers, *Salvadó et al., 2012*).

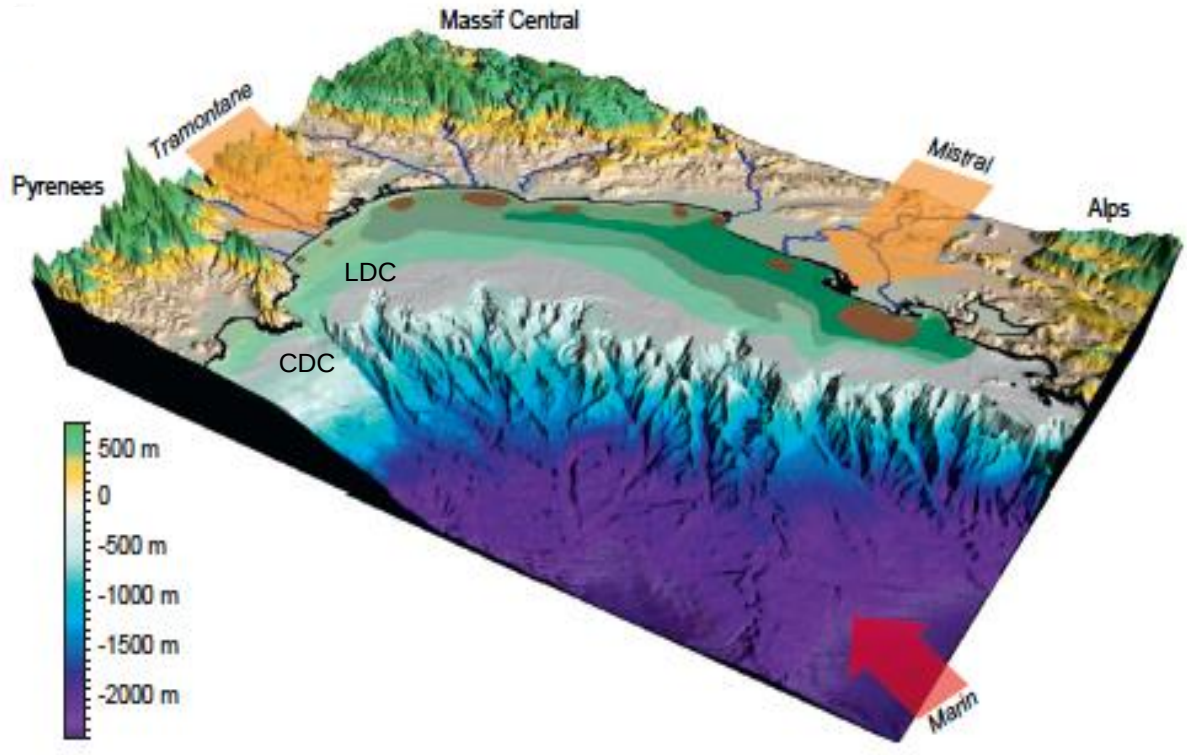

Fig.1.1 Carte du GdL (de Durrieu de Madron et al., 2008). Les massifs montagneux (Pyrénées, Massif Central et Alpes), les principaux fleuves, les caractéristiques bathymétriques (canyons sous-marins Lacaze-Duthiers (LDC) et Cap de Creus (CDC), en particulier) ainsi que les régimes de vents dominants sont représentés

Le GdL est donc considéré comme une zone-test de l'évolution à long terme du transport sédimentaire et a été le lieu de nombreux programmes de recherche européens ces 20 dernières années. EUROpean marge STRATA formation (EUROSTRATAFORM, 2002-2005) a été développé pour comprendre les processus sédimentaires, de déposition et

stratigraphiques dans les systèmes Atlantique-Nord et méditerranéens, représentants de la marge continentale européenne (*Syvitski et al., 2004; Weaver et al., 2006*). Ce programme a permis d'étudier les effets du cascading (événement de l'hiver 2004-05), des crues extrêmes (événement de Décembre 2003 sur le Rhône) et des tempêtes, considérés comme les procédés de contrôle de la dynamique sédimentaire les plus efficaces sur le plateau continental du GdL. Ces résultats et la modélisation ont souligné le rôle prépondérant des tempêtes E-SE dans la remise en suspension induites par leurs vagues et le transport cyclonique des sédiments fins le long du plateau interne mais aussi pendant les périodes de formation d'eaux denses induites par les vents de N-NO. Ces deux processus dus au vent induisent la majeure partie de l'export de particules en suspension et d'éléments associés hors du plateau, principalement à l'extrémité sud-ouest du golfe. Ces événements ont montré une saisonnalité claire et une grande variabilité interannuelle qui sont susceptibles d'être modifiées suite aux changements climatiques.

Après ce programme, HERMES (Hotspot Ecosystem Research on the Margins European Seas, 2005-2009), HERMIONE (Hotspot Ecosystem Research on Man's Impact on European Seas, 2009-2012) et maintenant PERSEUS (Policy-oriented marine Environmental Research in the Southern European Seas, 2012-2015), ont été conçus pour approfondir la compréhension actuelle des écosystèmes marins méditerranéens et leur réponse face aux modifications spatiales et temporelles des forçages physico-chimiques liés à l'évolution des conditions environnementales et à l'augmentation de la pression humaine. Ces approches intégrées ont toujours considéré le continuum entre la zone côtière et l'océan ouvert. De telles données scientifiques sont utilisées dans le cadre de la Directive-Cadre Stratégique sur le Milieu Marin (DCSMM), une initiative européenne qui vise à atteindre un bon état écologique dans les eaux marines d'ici à 2020, notamment des écosystèmes profonds.

Comme certains de ces programmes sont encore en cours, la communauté scientifique reconnaît la nécessité de quantifier et d'évaluer les flux, de métaux traces dans notre cas, du continent, qui agit comme une source, vers le milieu marin agissant comme un puits. Améliorer les connaissances sur le transfert terre-mer de sédiments, de matière organique (une thèse est actuellement menée sur ce sujet au CEFREM) et de contaminants associés et comprendre leur devenir lors de leur arrivée dans les eaux côtières et leur transfert plus au large est l'une des priorités pour une meilleure compréhension des cycles biogéochimiques globaux (*Sanchez- Vidal et al., 2013*).

Dans le GdL, la problématique des éléments trace métalliques a déjà été largement abordée. Ils ont été utilisés comme des outils géochimiques : afin de normaliser la fraction fine des sédiments (*Roussiez et al., 2005*) ou comme traceurs géochimiques des retombées atmosphériques (*Miralles et al., 2006*) et des sources lithogènes (*Roussiez et al., 2013*). Sur le plateau continental, des études spatiales et temporelles ont été menées pour déterminer leur comportement dans le cycle sédimentaire (*Roussiez et al., 2006, 2011; Radakovitch et al., 2008*), donnant lieu à des calculs de bilans. Ollivier et al. (*2011*) et Roussiez et al. (*2012*) ont estimé à 15 à 91 % (en fonction de l'élément) la contribution des crues à l'apport annuel de métaux traces particulaires (MTP). Radakovitch et al. (*2008*) ont montré que, entre 2000 et 2003, les flux d'entrée de MTP du Rhône étaient de 2 à 10 fois plus élevés que le dépôt atmosphérique particulaire. Ils se sont servis des estimations de flux métalliques dissous et particulaires (faites par *Guieu et al., 1997*) déposés en divers endroits de la méditerranée nord-occidentale, et pour lesquelles ils ont pris les valeurs moyennes de flux. En ce qui concerne le dépôt atmosphérique de MTP, Guieu et al. (*1997*) ont souligné l'importance du dépôt sec et en particulier des poussières sahariennes. En outre, Guieu et al. (*1997*) et Elbaz-Poulichet et al. (*2001*) ont montré que, concernant les flux de métaux traces dissous, les apports atmosphériques représentent plus de 50% des apports totaux de MTP dissous en mer Méditerranée Nord-Occidentale. Dans les canyons, Grousset et al. (*1995*) ont étudié la distribution des MTP dans le canyon Lacaze-Duthiers et Roussiez et al. (*2012, 2013*) ont étudié les flux exportés en tête de canyon du Cap de Creus. Marin et al. (*2001*) se sont focalisés sur les forçages qui contrôlent la distribution de Mn et Fe dans les carottes de sédiments du plateau continental du GdL et de son bassin profond. Dans ce dernier Angelidis et al. (*2011*) ont mis en évidence l'accumulation de Cd, Pb et Zn d'origine anthropique dans les sédiments de surface de carottes profondes, en suspectant la déposition atmosphérique d'être la source principale dans le bassin profond.

Puisque les MTP ont été bien documentés par le passé (Fig.1.2), les objectifs de ce travail n'étaient pas de développer de nouvelles techniques analytiques. Il s'agissait plutôt, grâce au suivi à long terme, de combler certaines lacunes sur la conséquence de situations particulières sur la dynamique des MTP. Par exemple, jusqu'à présent, une grande attention a été accordée au Rhône mais moins aux petits fleuves côtiers et à leurs contributions respectives aux apports annuels de MTP sur le plateau continental. Ainsi, nous avons également cherché à proposer une méthode d'échantillonnage pour le calcul de flux de MTP exportés, grâce à l'exemple de la Têt et du Rhône. Ces méthodes permettront peut-être de faciliter de potentielles décisions de gestion durable pour l'avenir des zones côtières.

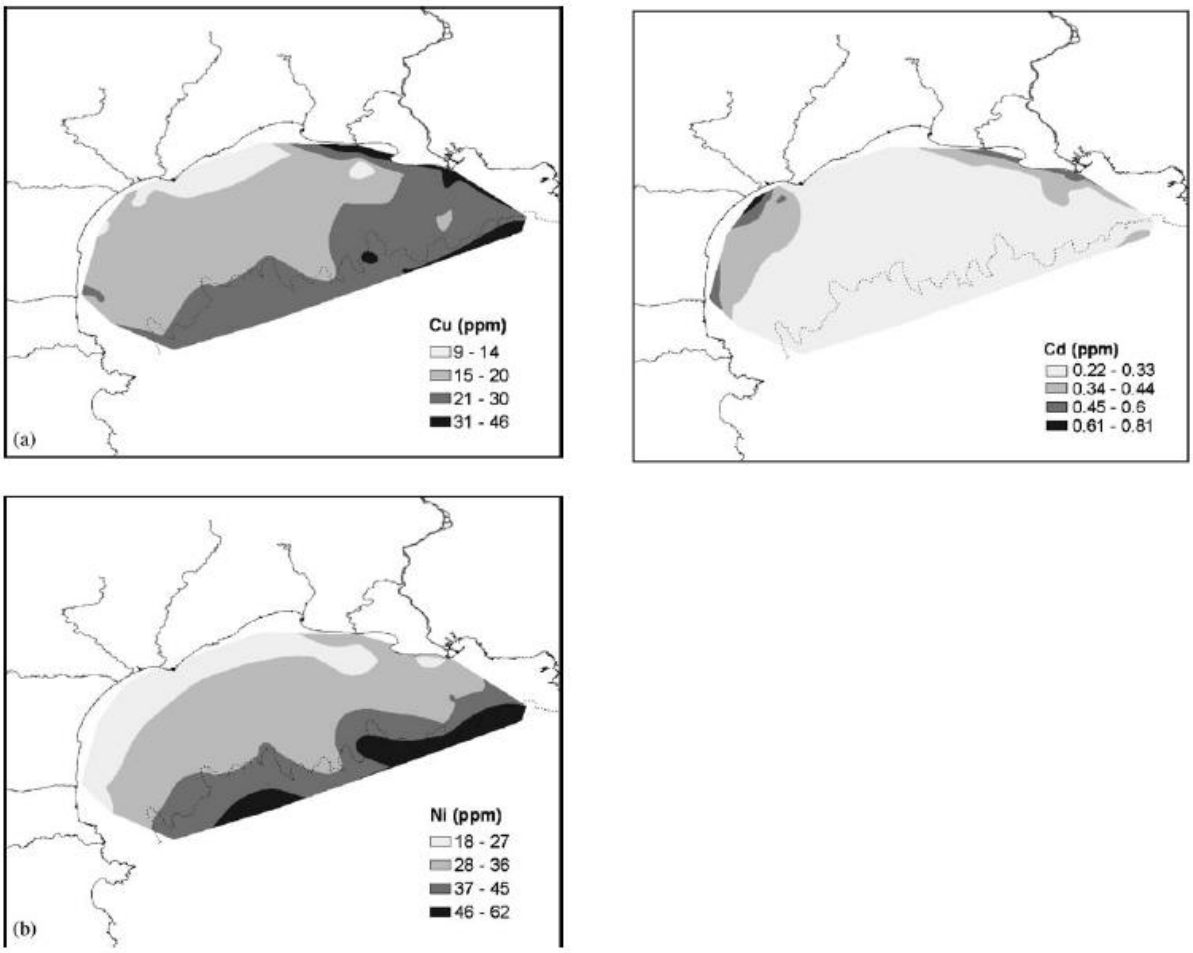

Fig.1.2 Tirée de Roussiez et al. (2006). La distribution spatiale des concentrations en Cu, Cd et Ni contenues dans la fraction < à 63 µm des sédiments du plateau continental du GdL.

En outre, le cycle sédimentaire des MTP a été largement étudié sur le plateau continental (des pro-deltas au plateau intermédiaire et externe), mais moins d'études ont été menées sur les processus de transport des MTP et sur leur devenir, dans les canyons sous-marins et au-delà. Les objectifs de cette étude étaient donc aussi destinés à quantifier les flux transférés, et déposés, du plateau continental vers le bassin profond. Puisque cette exportation se déroule principalement lors de processus hydro-météo-dynamiques extrêmes, nous nous sommes particulièrement intéressés aux crues, aux tempêtes d'E-SE et au cascading. Les flux exportés par les rivières, qui se déroulent majoritairement pendant les événements de crues, et les flux exportés par ces processus hydrodynamiques nous aideront à évaluer le rôle du plateau continental en tant que source ou puit de métaux traces, et le potentiel d'épuration côtière de ces processus.

Nous visons également à caractériser l'origine de ces MTP, par l'étude spécifique des terres rares et des fractions résiduelles et naturelles, mais aussi à évaluer la part anthropique de leurs flux et leurs caractères potentiellement biodisponibles. Grâce à ces investigations à haute résolution spatiale et temporelle des flux de métaux traces exportés, cette synthèse aidera à la compréhension des mécanismes d'apports, de transfert et de dépôts des métaux traces particulaires, de la zone continentale du GdL vers les environnements plus profonds.

Le manuscrit s'organise de la manière suivante :

Le deuxième chapitre présente plus en détail la zone d'étude, les échantillons et les stratégies d'échantillonnage utilisées dans ce travail ainsi que les méthodes d'analyses et de calculs.

Afin de suivre le raisonnement général d'un continuum terre-mer, nous allons d'abord présenter les résultats de notre étude sur les apports fluviaux dans le troisième chapitre. Les résultats de ce chapitre ont été obtenus après un suivi de 5 ans des rivières côtières du GdL, ce qui en fait la base de données la plus à jour dans le GdL sur les contaminants métalliques en milieu côtier. Une attention particulière a été accordée aux événements de crues et à leurs contributions respectives aux apports fluviaux annuels sur le Rhône et la Têt (pris comme un exemple caractéristique des autres fleuves côtiers).

Le quatrième chapitre portera sur les processus de transfert à travers les canyons sous-marins : transfert déclenché par les tempêtes E-SE dans la première partie et par le cascading dans la deuxième partie. Nous quantifierons également leurs contributions relatives à l'export de MTP par rapport aux apports fluviaux annuels afin d'évaluer et de comparer les deux événements en termes d'export et de potentiel d'épuration côtière.

Dans le cinquième chapitre, nous nous concentrerons sur le bassin profond grâce à l'analyse des concentrations en métaux traces de trois carottes profondes, la résultante du transport et des apports décrits précédemment.

Enfin, le sixième chapitre présentera les conclusions générales et les perspectives de cette étude.

Chapter II

Material & Methods

1. Study area

1.1 Geomorphological characteristics of The Gulf of Lion

The Gulf of Lion (GoL) is a crescent-shaped passive margin located in the northwestern Mediterranean sea. It is extending from the Cap de Creus of northern Spain to the Cap Croisette of eastern France. At those promontories, the GoL (GoL) continental shelf almost vanishes: at the west end, near the cap de Creus canyon, it narrows to less than 2km. Its slope is indented by a dozen submarine canyons, coalescing into two major channels and extending down to the deep basin (2000 m). The most important of those canyons, in terms of both export of water and particles, is the Cap de Creus canyon at the southwestern limit of the Gulf (*see Monaco et al., 1990; Raimbault and Durrieu de Madron, 2003; Canals et al., 2006; Durrieu de Madron et al., 2008 and references therein*).

This export is mainly fed by riverine inputs. Indeed, the continental shelf is fed by the Rhone river on one hand : with a drainage basin of 97,800 km^2 it is the largest river in the Mediterranean in terms of water and solid discharge as it releases a mean of 10.10^6 $T.yr^{-1}$ (*Durrieu de Madron et al., 2000*; *Roussiez et al., 2012*). It is thus the main source of freshwater (90%) and suspended sediment to the GoL continental margin (*Bourrin and Durrieu de Madron, 2006*). On the other hand the smaller southwestern rivers Herault, Orb, Aude and Tet, subjected to a Mediterranean regime of intense flash-floods, are also providers of freshwater and particulate matter during those events (*Serrat et al., 2001*). Sediment transport processes on the shelf are controlled by the Rhone River sediment source but also by the morphology of the shelf and its circulation patterns (*Ludwig et al., 2003; Drexler and Nittrouer, 2008*). Indeed fine sediments delivered to the continental shelf are temporarily stored off river mouths, until advected and redistributed by the action of storms *(Guillen et al., 2006)* and anticlockwise current that flows along the continental shelf called Liguro-provencal-Catalan or Northern Current (*Millot, 1990*).

1.2 Hydrological and Hydrodynamical processes

Predominant meteorological regimes induce intense hydrodynamical events such as floods, marine storms, downwelling and dense water formation, which steer the sediment inputs, resuspension and transport on the shelf (*Guillen et al., 2006*; *Palanques et al., 2006*; *Bonnin*

et al., 2008; Bourrin et al., 2008; *Durrieu de Madron et al., 2008*; *Palanques et al., 2008; Ulses et al., 2008a and b*).

As stated previously, terrigeneous material and sediment-bound contaminants inputs in the GoL are largely controlled by the intensity and frequency of the Rhone and smaller coastal rivers' flood events. Indeed, the annual mean water discharge of the Rhone river, measured at the Beaucaire gauging station, is around 1700 $m^3.s^{-1}$ (*Ibanez et al., 1997*; *Arnau et al., 2004*). Discharges of 5000 $m^3.s^{-1}$ are regularly recorded in spring and autumn due to flood events (*Estournel et al., 1997*). These last few years, the highest peak discharge was recorded in December 2003 with 11,000 $m^3.s^{-1}$ (*Antonelli et al, 2007*). Based on historical discharge river data, such extreme floods (discharge > 10,000 $m^3.s^{-1}$) have an expected return period of 100 years. However, four occurred in the past 20 years: in autumns of 1993, 1994, 2002, and 2003 (*Estournel et al., 1997*; *Maillet et al., 2006*).

Although freshwater and sediment inputs to the GoL originate mainly from the Rhone River, the smaller southwestern coastal rivers Herault, Orb, Aude, Agly, Tech and Tet, subjected to a mediterranean regime of intense flash-floods, may occasionally deliver substantial amounts of freshwater and SPM. Those coastal rivers have a strong dynamicity due to their quick answer to climatic variations and have episodic discharges that are difficult to quantify (*Certain et al., 2005*). Consequently, little is known about their role and importance in water and sediment inputs to the GoL.

In this study, the Tet River was chosen as a model for small coastal rivers. In autumn, after long periods of dryness induced by the Mediterranean climate, short but strong marine winds trigger intense rainfalls that lead to flood events of the small coastal rivers like the Tet River. Although the mean liquid discharge measured at the Perpignan gauging station is 6.3 $m^3.s^{-1}$ (2006-2011), during one of those extreme events instantaneous liquid discharge can reach up to 1800 $m^3.s^{-1}$ (*Serrat et al., 2001*). However smaller, those flash flood events are not negligible as *Serrat et al.* (2001) showed that between 1980 and 1999, 78% of the total sediment flux in the Tet River occurred in 0.7% of the total time (50 days).

After its deposition off those river mouths, sediment is exported along and across-shelf by wind-induced currents, that transport sediments towards the southwestern shelf (*Durrieu de Madron et al., 2008*). Indeed, the GoL is subjected to severe winter meteorological conditions were long-lasting cold and dry winds cool and evaporate surface shelf water inducing downslope sinking of surface water masses, which are channelized in submarine canyons. The steep slope of those canyons induces increasing horizontal and vertical near-bottom

current speed that allows erosion and transport of sediment. This phenomenon is known as Dense Shelf-Water Cascading or DSWC (*Ivanov et al., 2004*).

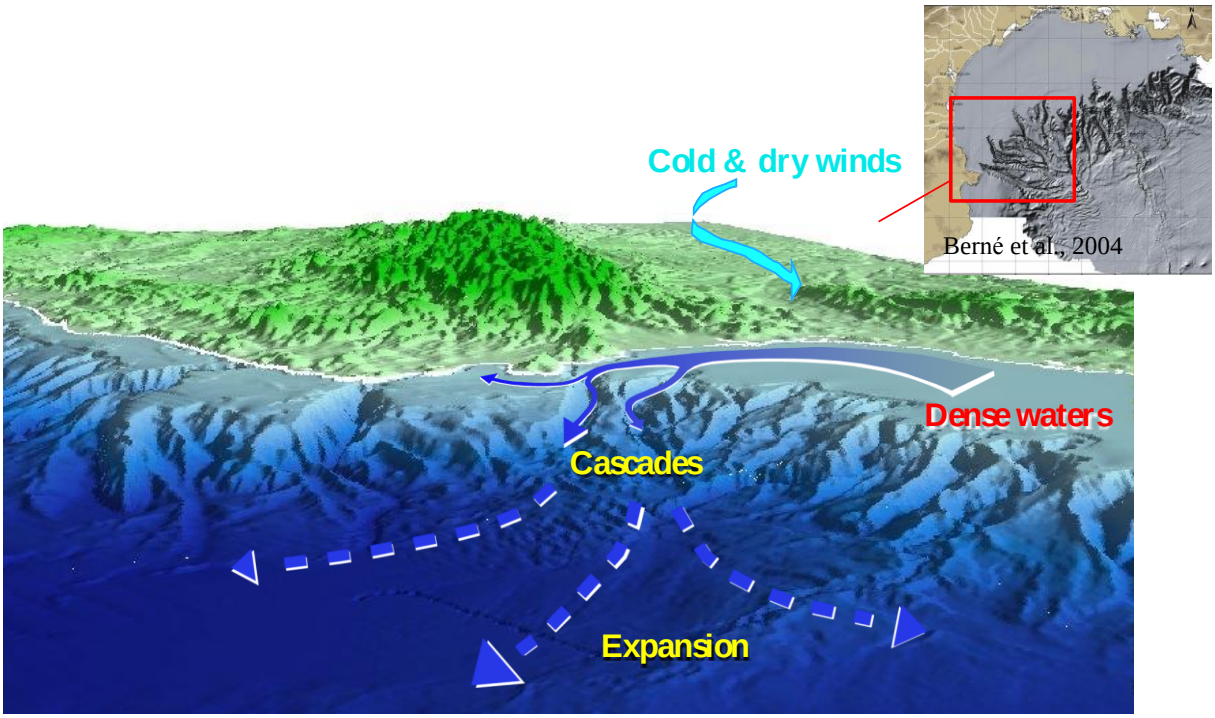

Fig.2.1 Schematic view of the GoL and DSWC process

In the GoL, in the past twenty years, this phenomenon has happened recurently twice a decade. In winter 1999-2000, in winter 2003-2004 and in winter 2005-2006 which was one of its most important occcurence with about 2000 km^3 of water i.e. the equivalent of 40 years of the average Rhone river discharge, was flushed, mainly down the Cap de Creus submarine canyon (*Ulses et al., 2008c*); and in winter 2012-2013.

Independently, E and SE winter winds still produce large swells and storm-induced downwelling, allowing the redistribution of particulate matter from the GoL continental shelf to the open sea. It is the coupling of both phenomenon (DSWC and E-SE storms) that greatly increases the transport of resuspended shelf and slope towards the deep basin (*Canals et al., 2006, Palanques et al., 2006, 2012*).

2. Sample dataset

During this PhD work, different kinds of samples were obtained, in various media, and from several scientific projets and past sampling campaigns. The riverine samples were, and still are, collected under the MOOSE observatory (http://www.moose-network.fr/) which aims at

following the evolution of the Mediterranean environment in the long-term and under climate change conditions in order to detect trends.

Sediment trap and core samples were collected within the framework of the HERMES and HERMIONE (CASCADE oceanographic cruise) projects. While HERMES was focused on the whole GoL shelf and slope, CASCADE focused on the Cap de Creus canyon. Indeed, HERMES results showed that most of the particulate export takes place in the southwesternmost canyon.

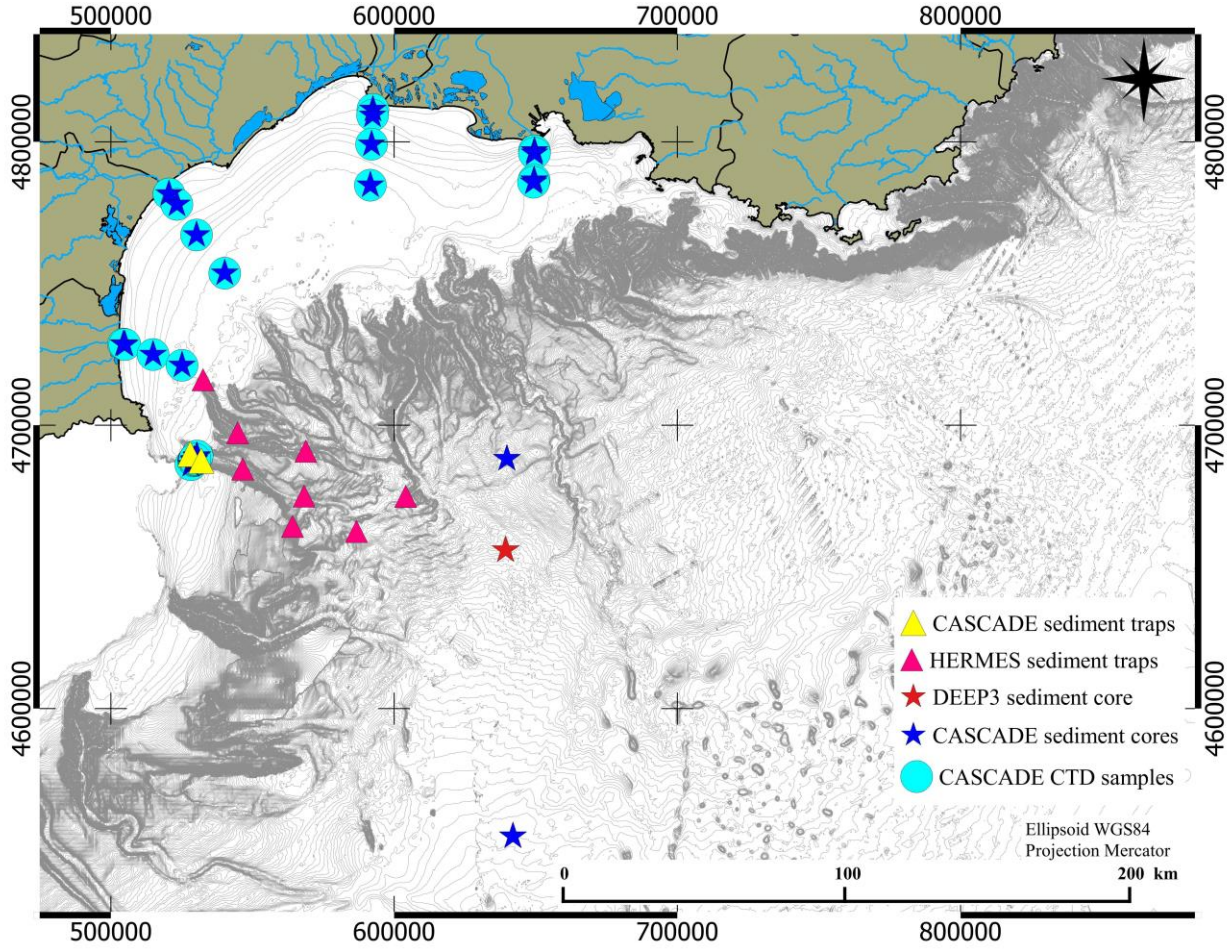

Fig.2.2 Position of the samples collected and analyzed during this work

2.1 River samples

The Rhone, Orb, Herault, Aude, Agly and Tet rivers were sampled once a month from January 2006 to May 2011. During my thesis, a focus was made on the Rhone river, as it is the major conveyor of liquid and solid discharge in the NW Mediterranean; but also on the

Tet river, which was chosen as a model for all the other coastal mediterranean rivers. Samples were always collected close to the river mouth in order to be representative of the whole catchment's input to the marine environment.
On the Rhone River, samples were collected at the SORA observatory station near the CNR gauging station in Arles, 45 km upstream of the river mouth. For the Tet River, samples were taken whether by the POEM automatic sampling station, located 10 km upward from the river mouth, or manually at the same place.
Over the sampling period (2005-2011), the climate was rather dry and only a few floods happened. Some of those flood events (November 2005 and April 2007 for the Tet River, and June and November 2008 for the Rhone River) were sampled more frequently (e.g. on an hourly basis for the Tet River).

2.2 Sediment traps samples

In winter 2005-06, the HERMES program monitored the Lacaze-Duthiers (LDC) and Cap de Creus (CCC) submarine canyons, as well as the southern open slope (SOS) from mid-October to mid-April. Particulate fluxes, currents and temperature were measured along canyons axes at 300, 1000, 1500 and 1900 m depth and at 1000 and 1900 m depth on the open slope.
Particle fluxes were measured by sequential PPS3/3 Technicap sediment traps at 30 m above bottom (mab) and currents and temperature by an Aanderaa current meter (RCM7/8/9) at 5 mab. Sediment traps were programmed to sample the downward particle flux at 15 days intervals. The cups were poisoned with a buffered 5% formaldehyde solution in filtered seawater before deployment.
Failure of sediment trap rotating motor resulted in the absence of samples in the CCC300 station.

Fig.2.3 Sediment trap device, as well as the collecting cups after the CASCADE campaign
Same equipments were used in the HERMES deployment.

Two instrumented mooring lines were deployed along the southern flank of the Cap de Creus canyon (CCC) during the CASCADE cruise in March 2011: one at 290m depth (T1) and one at 365m (T2). Each mooring was equipped with acoustic Doppler current profiler (ADCP) at 160 m above bottom (mab), turbidimeters at 10, 75 and 115 mab, and a Technicap PPS3/3 sequential sampling sediment trap at 40 mab.

Sediment traps are equipped with 12 cups (Fig.2.3) and were set to sample during the period of the CASCADE cruise. Hence the collecting plates were programmed to sample the downward particle flux at 35h intervals. The cups were poisoned with a buffered 2% formaldehyde solution in filtered seawater before deployment.

2.3 Open water samples

Station CX located between the two CASCADE moorings, was continuously sampled with a CTD/Rosette (Fig.2.4) from the 13th to the 15th of March 2011, providing high frequency changes of the hydrology, suspended sediment concentration during the storm. Since the

CTD could not be loaded on board during the monitoring due to the very harsh sea state, profiles were repeated in a Yo-Yo mode (without taking the CTD out of the water) and only one water sample was taken every 6 profiles (2-3 hours) close to the bottom (2-3 mab) using 1010X Clean Niskin bottles mounted on the rosette for the trace metal analysis purpose.

Fig.2.4 CTD/Rosette equipped with clean Niskin bottles.

Eleven near-bottom water sampling were collected from 13th March 2011 at 07:34 to 14th March 2011 at 10:31 (UTC time).

2.4 Sediment cores

A serie of sediment samples was collected during the CASCADE cruise. One serie across the southern flank of the CCC from 120m to 497m water depth, right after the E-SE storm. The first 4 stations from 120 to 347m were sampled with a box-corer as the sediment was very stiff and coarse (Fig.2.5). The last 2 stations at 442 and 497m were also sampled with a multi-tube corer as softer sediment was encountered.

Fig.2.5 Left side : box-corer ; Right side : multi-tube corer

A serie of 5 sediment cores was also sampled in the deep northwestern mediterranean basin but only 3 were studied in this thesis : M01, M08 and SC2400, collected between 1957 and 2657m depth, using a multi-corer collecter.

3. Sample treatment and analyses

All manipulations took place under a laminar flow hood or in a clean room to avoid contaminations.

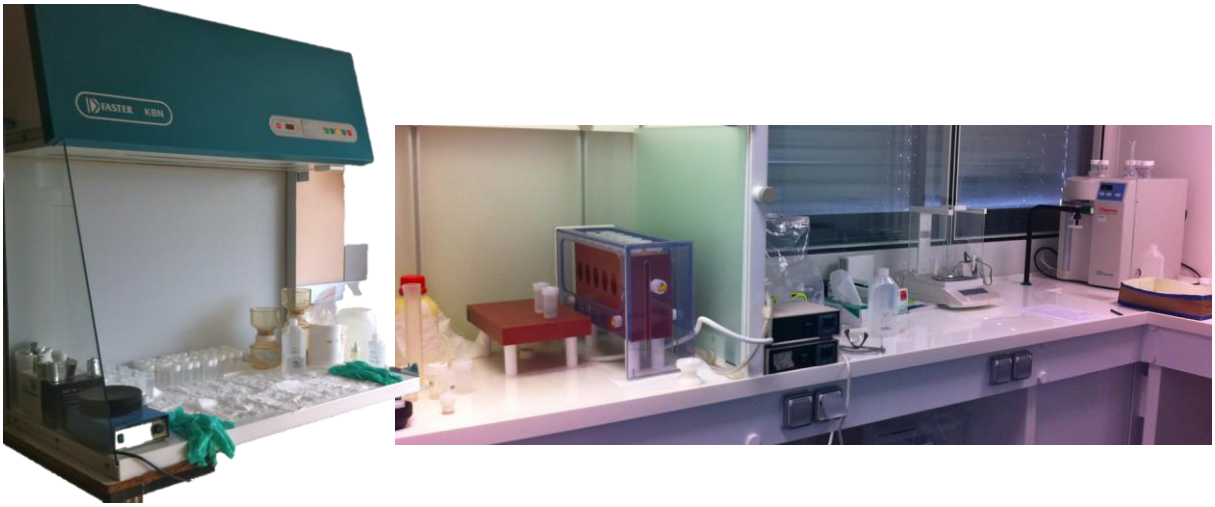

Fig.2.6 Left side : laminar flow hood ; Right side : view of the clean room

3.1 Pre-treatment of riverine samples

After field sampling, water was stored in 1N HCl pre-cleaned polypropylene bottles, in a dark refrigerated room (4°C) and rapidly filtered in the laboratory through pre-weighed cellulose acetate filters (47 mm in diameter and 0,45 µm in pore size) for trace metal analysis. Immediately after filtration, filters were dried at 40°C for at least 24h in a clean oven for dry weight determination. Filters were then sonicated in polypropylene bombs filled with milli-Q water so as to recover the particulate phase. Filters were then weighted to establish recovering rates while polypropylene bombs were placed on a hot-plate until complete evaporation. The same procedure (*Aubert et al., submitted*) was used during floods (recovery between 85 and 116%).

3.2 Preparation of sediment trap samples

After recovery, trap samples were stored in the dark at 2-4°C until processed in the laboratory. In each trap sample, swimmers were removed and subsamples were taken by diluting the original sample in a given volume of seawater and, while still stirring, by pouring small equal volumes of the suspension successively and repetedly until the whole original sample is divided. Each subsample is then constituted of a number of small volume of suspension. Four of those subsamples were then filtered on 0.45 µm Millipore acetate filters, rinsed with distilled water and dried at 40°C for 24h in order to measure sample dry weights, from which total mass fluxes (TMF expressed in $g.m^{-2}.d^{-1}$) were determined. The procedure is fully described by Heussner et al. (*1990, 2006*).

Subsamples dedicated to the determination of particulate flux constituents were recovered in clean conditions, after several rinses to eliminate traces of formaldehyde solution, then filtered on pre-weighted glass-fiber filters for organic carbon analysis and on pre-weighed cellulose acetate filters (47 mm in diameter and 0.45 µm in pore size) for trace metals analysis. They were then rinsed with distilled water in order to remove salt and dried at 40°C for at least 24h for dry weight determination.

3.3 Preparation of sediment core samples

Canyon cores were carefully sliced on board in layers of 1 cm from the surface to 5 cm-depth using acid-cleaned plastic spatulas whereas deep cores were sliced over their whole length,

which approximated 20 cm. Individual samples were then stored in polyethylene plastic bags and kept at 4°C. Samples were freeze-dried and homogenized in agate mortar prior to analysis.

3.4 Analytical Protocols

i) Mineralization

Particulate matter from open-water and sediment trap samples was recovered from the polypropylene bombs and weighted (around 30 mg) for trace metals analysis. Mineralization of the dried material was performed in Teflon beakers. The first step was to remove carbonates by adding 0.5 mL of nitric acid (all acids were of high quality, i.e TraceSELECT®, Fluka or Suprapur, Merck) and sonicating the mixture for 15 minutes. 0.5 mL of hydrofluoridric acid were then added to destroy silicates and sonicated again, then placed on a hot-plate for at least 12 hours at 100°C (Fig.2.7).

Fig.2.7 Hot plate and heating device for teflon beakers in the clean room

After cooling, samples were dried at 80°C until complete evaporation. Organic matter was mineralized in the next step by first addition of 0.5 mL of nitric acid, sonication and warming during 4h at 100°C. After cooling, 0.2 mL of hydrogen peroxide were succesively added to the sample, 3 times, in order for the exothermic reaction to be controlled. Between each addition, samples were sonicated. Clear samples were then dried at low temperature (< 50°C) to avoid projections due to hydrogen peroxide degradation.

The last step was to solubilize our remaining sample in 2 mL of concentrated nitric acid before proceeding to the final dilution.

ii) Micro-wave digestion

Fig.2.8 Teflon bombs and Anton Paar Multiwave 3000

Sediment core samples were digested in Teflon bombs in a micro-wave (Anton Paar Multiwave 3000) (Fig.2.8). Basically, 60 mg of sample was mixed with 1.5 mL of nitric acid, 0.7 mL of hydrofluoridric acid and 4.5 mL of HCl, then placed in the micro-wave for 30 minutes at 600 W. After cooling, the clear liquid solution was placed in polypropylene beakers and the Teflon bombs were rinced with deionized water. The mixture was evaporated to dryness and the residues were solubilized with 2 mL of nitric acid before proceeding to the final dilution.

iii) Acid-leaching procedure

HCl-single extraction (*Langston et al., 1999*; *Audry et al., 2006*) allowed to discriminate the potentially bioavailable and the residual fraction of each sample. The HCl-available fraction was extracted by adding 12.5 mL of HCl 1M to 200 mg of sample, continuously agitated for 24 h in previously acid-cleaned centrifuge tubes (*Dabrin et al., 2013*), in order to desorb elements fixed onto particles that are sensitive to HCl. Samples were then centrifuged during 30 mn at 4000 rpm. Aliquots of supernatant were transferred into acid-cleaned polypropylene beakers and evaporated to dryness at 100°C. Residues were solubilized in 2 mL concentrated nitric acid before the final dilution.

The non-reactive (residual) fraction is simply the difference between the total mineralization and the HCl-sensitive fraction. The residual part would represent the natural mineral signature of the catchment from which the particles originate.

The HCl-single extraction experiment was conducted on particulate matter from the HERMES and CASCADE sediment trap samples and also on SPM from the Rhone and Tet

rivers, two potential sources of the particulate matter recovered in the traps. Indeed, the Rhone is the main conveyor of particles in the NW Mediterranean Sea but the Tet is located nearest to the CCC, hence its signature in the sediment traps could be less diluted by other sediment sources.

iv) ICP-MS analysis

Major, trace element and REE concentrations were measured by Inductively Coupled Plasma Mass Spectrometry (ICP-MS, Agilent 7000x) at the CEFREM laboratory (Perpignan, France, Fig.2.9) or by ICP-MS (Thermo Xseries 2) at the Hydrosciences laboratory (University of Montpellier, France).

Fig.2.9 The Agilent 7000x ICP-MS

All digested samples (in 2 ml concentrated HNO_3) were further diluted with deionized water in order to stay under the 1 $g.L^{-1}$ threshold of initial mineralized material. Too concentrated solutions could generate analytical bias during the analysis and provoke also quick fouling of the device . We aimed for 10 mL of samples concentrated to 0.2 $g.L^{-1}$.

Reference material (GSMS-2 and GSMS-3 from NRCGA-CAGS, China and 1646a from NIST) were mineralized and analyzed under the same conditions as the samples and provided suitable recoveries (errors < 5% for all elements, except for Cr in GSMS-3 and Cd in GSMS-2 for which recoveries ranged from 85% to 95% and 67% to 73% respectively; and errors < 5% for Al, Co, Ni and Pb in 1646a; recoveries of Cr, Cu, Zn and Cd ranged from 90% to 96%, 111% to 122%, 109% to 146% and 86% to 95% respectively).

Analytical blanks did not reveal any sign of contamination (contribution < 0.5% for Al, Cr, Co, Ni, Cs and Pb, < 2% for Cu and Zn) except for Cd (blanks < 10%). Results for this last element have therefore to be considered with more caution but could still be indicative for general considerations.

3.5 Grain-size and organic carbon analysis

CASCADE samples for organic carbon analysis were decarbonated with repeated additions of H_3PO_4 (1M) and HCl (2M) with drying steps in between until no effervescence occurred. Particulate Organic Carbon (POC) content was measured using a VarioMAX CN, Elementar instrument at the CEFREM laboratory (Perpignan, France).
Grain-size analysis of sediment trap samples was performed on a Coulter LS 230 Laser Particle Size Analyzer in the GRC Geociències Marines laboratory (Barcelona, Spain), whereas grain-size analysis of the deep sediment cores was performed in the Observatoire Océanologique de Banyuls/mer (France) on a Mastersizer 2000 (Malvern).

4. Calculation methods

4.1 Enrichment Factors

Anthropogenic inputs in trace metal concentrations were assessed in sediment trap samples on the basis of background-normalized metal ratios, commonly designated as Enrichment Factors (EF). The calculation of EFs allows determining the origin of the sinking material and the trace metals it contains: natural (rock and soil erosion) vs. anthropogenic. EF result from a normalization of the analyzed samples compared to a sample that is considered to reflect natural conditions. In fact, a two-fold normalization is needed. On one hand, PTM concentrations have to be divided by the concentration of a given element (C) in the samples that is of natural origin and that is highly associated with the grain size fraction of clays. This is because PTM are generally associated with this fraction and differences in the grain size distributions can strongly impact the overall PTM concentrations. On the other hand, normalization is needed, with a reference sample that reflects natural PTM concentrations in the local environment (basically pre-dominant soil or rock type) :

$$EF = \frac{\left(\frac{X}{C}\right) sample}{\left(\frac{X}{C}\right) background}$$

where C is a conservative element strongly associated with the finest sediment fraction (clays), used in order to prevent the effect of variation in supply of major sediment components with which the trace metals are associated. In this study, the proxy of crustal carrier chosen as a normalizer is Al. It is a proxy for clay minerals, which are commonly recognized as the most important carrier of trace metals together with their coating formations like organic matter. It has then been widely used in previous studies on marine environments as a normalizer of grain-size variations, as well as in the calculation of EF in heavy metal contamination studies (*Din, 1992*; *Tam and Yao, 1998; Roussiez et al., 2005*).

It is generally admitted that EF > 2 reflects PTM enrichment from anthropogenic sources (*Sutherland, 2000*). If natural background concentrations can be determined regionally, this may be already the case for EF > 1.5 (*Roussiez et al., 2006*). Hence, the choice of the background has to be adjusted to the sample environment. Upper Continental Crust (e.g. *Wedepohl, 1995*) is commonly used by default in many studies but the use of a global reference does not take into account the local lithology that can be highly variable from site to site. That is why, when calculating EFs in sediment trap samples, we compared different local references (chapter 4.1). Indeed, in the GoL the Rhone River is known to be the dominant source of particles. Hence pre-industrial reference values were determined in deep-samples of a Rhone riverbank core, drilled downstream in order to be representative of the whole "natural" Rhone River catchment. This core has already been used as a reference in Ferrand et al. (*2012*). Core levels were dated using radiocarbon dating to ensure the reference was pre-industrial. In chapter 3, we were careful to use different local references as we were calculating EFs on Tet and Rhone riverine particles.

However, at 2500m depth in the middle of the NW Mediterranean basin, inputs might come from various sources impossible to differentiate so EFs in deep cores were calculated over Upper Continental Crust composition.

4.2 Calculation of suspended particle mass fluxes and associated PTM

In this study, hourly water discharge data were obtained by the Perpignan gauging station and the HYDRO database (*www.hydro.eaufrance.fr*) for the Tet River, whereas daily water discharge data of the Rhone River were provided by the Compagnie Nationale du Rhone

(CNR) for the Arles and Beaucaire gauging stations. In both cases, data were interpolated to a 15 minutes resolution in order to calculate reliable SPM fluxes at this resolution. If the gauging station of the Tet River was to be stopped for more than 4 days, SPM fluxes were derived from the relation by Serrat et al. (*2001*).

PTM concentrations obtained by monthly sampling over the 2006-2011 period allowed us to build Q/PTM rating curves. This approach was successful for estimating dissolved element concentrations before (*Vanni et al., 2001*; *Stelzer and Likens, 2006*) but innefective when applied to sediment-associated chemical contaminants (*Horowitz, 2008*). In our case, strong correlations between SPM and sediment-associated PTM were found ($r^2 > 0,9$) for both rivers. Correlations were statistically significant and used to reconstruct each PTM content, using the 15-minute resolution dataset of liquid and solid discharges.

References

Antonelli, C., Eyrolle, F., Rolland, B., Provansal, M., Sabatier, F. (2008). Suspended sediment and ^{137}Cs fluxes during the exceptional December 2003 flood in the Rhone River, southeast France. *Geomorphology*, 95(3-4), 350-360.

Arnau, P., Liquete, C., Canals, M. (2004). River mouth plume events and their dispersal in the Northwestern Mediterranean Sea. *Oceanography*, 17, 22-31.

Aubert D., Probst A., Probst J.L. (submitted). Influence of hydrological conditions on metal behaviour and dissolved/particulate partitioning in the upper Garonne and Ariège rivers (SW, France). *Journal of Hydrology*.

Audry, S., Blanc, G., Schäfer, J. (2006). Solid state partitioning of trace metals in suspended particulate matter from a river system affected by smelting-waste drainage. *Science of the Total Environment*, 363, 216-236.

Bonnin, J., Heussner, S., Calafat, A., Fabres, J., Palanques, A., Durrieu de Madron, X., Canals, M., Puig, P., Avril, J., Delsaut, N. (2008). Comparison of horizontal and downward particle fluxes across canyons of the Gulf of Lions (NW Mediterranean): Meteorological and hydrodynamical forcing. *Continental Shelf Research*, 28(15), 1957-1970.

Bourrin, F., Durrieu de Madron, X. (2006). Contribution to the study of coastal rivers and associated prodeltas to sediment supply in the Gulf of Lions (NW Mediterranean Sea). *Vie et Milieu-Life and Environment*, 56, 307-314.

Bourrin, F., Durrieu de Madron, X., Heussner, S., Estournel, C. (2008). Impact of winter dense water formation on shelf sediment erosion (evidence from the Gulf of Lions, NW Mediterranean). *Continental Shelf Research*, 28(15), 1984-1999.

Canals, M., Puig, P., Durrieu de Madron, X., Heussner, S., Palanques, A., Fabres, J. (2006). Flushing submarine canyons. *Nature*, 444, 354– 357.

Certain, R., Tessier, B., Barusseau, J.-P., Courp, T., Pauc, H. (2005). Sedimentary balance and sand stock availability along a littoral system. The case of the western Gulf of Lions littoral prism (France) investigated by very high resolution seismic. *Marine and Petroleum Geology*, 22(6–7), 889-900.

Dabrin, A., Schäfer, J., Bertrand, O., Masson, M., Blanc, G. (2013). Origin of suspended matter and sediment inferred from the residual metal fraction: application to the Marennes Oleron Bay, France. Continental Shelf Research, 72, 119-130.

Din, Z.B. (1992). Use of aluminium to normalize heavy-metal data from estuarine and coastal sediments of Straits of Melaka. *Marine Pollution Bulletin*, 24(10), 484-491.

Drexler, T.M., Nittrouer, C.A. (2008). Stratigraphic signatures due to flood deposition near the Rhône River: Gulf of Lions, northwest Mediterranean Sea., *Continental Shelf Research*, 28(15), 1877-1894.

Durrieu de Madron, X., Abderrazzak, A., Heussner, S., Monaco, A., Aloisi, J.C., Radakovitch, O., Giresse, P., Buscail, R., Kerherve, P. (2000). Particulate matter and organic carbon budgets for the Gulf of Lions (NW Mediterranean). *Oceanologica Acta*, 23(6), 717-730.

Durrieu de Madron, X., Wiberg., P.L., Puig, P. (2008). Sediment dynamics in the Gulf of Lions : the impact of extreme events. *Continental Shelf Research*, 28, 1867-1876.

Estournel, C., Kondrachoff, V., Marsaleix, P., Vehil, R. (1997). The plume of the Rhone: numerical simulation and remote sensing. *Continental Shelf Research*, 17(8), 899-924.

Ferrand, E., Eyrolle, F., Radakovitch, O., Provansal, M., Dufour, S., Vella, C., Raccasi, G., Gurriaran, R. (2012). Historical levels of heavy metals and artificial radionucleides reconstructed from overbank sediment records in lower Rhône River (South-East France). *Geochimica et Cosmochimica Acta*, 82, 163–182.

Guillén, J., Bourrin, F., Palanques, A., Durrieu de Madron, X., Puig, P., Buscail, R. (2006). Sediment dynamics during « wet » and « dry » storm events on the Têt inner shelf (SW Gulf of Lions). *Marine Geology*, 234, 129-142.

Heussner, S., Ratti, C., Carbonne, J. (1990). The PPS 3 time-series sediment trap and the trap sample processing techniques used during the ECOMARGE experiment. *Continental Shelf Research*, 10, 943-958.

Horowitz, A.J. (2008). Determining annual suspended sediment and sediment-associated trace element and nutrient fluxes. *Science of The Total Environment*, 400(1–3), 315-343.

Ibàñez, C., Canicio, A., Day, J.W., Curcó, A. (1997). Morphologic development, relative sea level rise and sustainable management of water and sediment in the Ebre Delta, Spain. *Jounal of Coastal Conservation*, 3, 191-202.

Ivanov, V.V., Shapiro, G.I., Huthnance, J.M., Aleynik, D.L., Golovin, P.N. (2004). Cascades of dense water around the world ocean. *Progress in Oceanography*, 60(1), 47-98.

Langston, W.J., Burt, G.R., Pope, N.D. (1999). Bioavailability of Metals in Sediments of the Dogger Bank (Central North Sea): A Mesocosm Study. *Estuarine, Coastal and Shelf Science*, 48(5), 519-540.

Ludwig, W., Meybeck, M. and Abousamra, F. (2003). Riverine transport of water, sediments, and pollutants to the Mediterranean Sea. Athens: *UNEP MAP Technical report*, Series 141, UNEP/MAP, 111p.

Maillet, G.M., Vella, C., Berné, S., Friend, P., Amos, C., Fleury, T., Normand, A. (2006). Morphological changes and sedimentary processes induced by the December 2003 flood event at the present mouth of the Grand Rhône River (southern France). *Marine Geology*, 234(1–4), 159-177.

Millot, C. (1990). The Gulf of Lions' hydrodynamics. *Continental Shelf Research*, 10(9–11), 885-894.

Monaco, A., Courp, T., Heussner, S., Carbonne, J., Fowler, S.W., Deniaux, B. (1990). Seasonality and composition of particulate fluxes during ECOMARGE-I western Gulf of Lions. *Continental Shelf Research*, 10, 959-988.

Palanques, A., Durrieu de Madron, X., Puig, P., Fabres, J., Guillén, J., Calafat, A., Canals, M., Heussner, S., Bonnin, J. (2006). Suspended sediment fluxes and transport processes in the Gulf of Lions submarine canyons. The role of storms and dense water cascading. *Marine Geology*, 234, 43-61.

Palanques, A., Puig, P., Durrieu de Madron, X. (2008). Storm-driven shelf-to-canyon suspended sediment transport at the southwestern Gulf of Lions. *Continental Shelf Research*, 28, 1947-1956.

Palanques, A., Puig, P., Durrieu de Madron, X., Sanchez-Vidal, A., Pasqual, C., Martín, J., Calafat, A., Heussner, S., Canals, M. (2012). Sediment transport to the deep canyons and open-slope of the western Gulf of Lions during the 2006 intense cascading and open-sea convection period. *Progress in Oceanography*, 106, 1-15.

Raimbault, P., Durrieu de Madron, X. (2003). Research activities in the Gulf of Lion (NW Mediterranean) within the 1997–2001 PNEC project. *Oceanologica Acta*, 26(4), 291-298.

Roussiez, V., Ludwig, W., Probst, J.L., Monaco, A. (2005). Background levels of heavy metals in surficial sediments of the Gulf of Lions (NW Mediterranean): an approach based on ^{133}Cs normalization and lead isotope measurements. *Environmental Pollution*, 138, 167-177.

Roussiez, V., Ludwig, W., Probst, J.L., Monaco, A., Bouloubassi, I., Buscail, R., Saragoni, G. (2006). Sources and sinks of sediment-bound contaminant in the Gulf of Lions (NW Mediterranean Sea): a multi-tracer approach. *Continental Shelf Research*, 26, 1843-1857.

Roussiez, V., Heussner, S., Ludwig, W., Radakovitch, O., Durrieu de Madron, X., Guieu, C., Probst, J.-L., Monaco, A., Delsaut, N. (2012). Impact of oceanic floods on particulate metal inputs to coastal and deep-sea environments: A case study in the NW Mediterranean Sea. *Continental Shelf Research*, 45, 15-26.

Serrat, P., Ludwig, W., Navarro, B., Blazi, J. L. (2001). Variabilité spatio-temporelle des flux de matières en suspension d'un fleuve côtier méditerranéen: la Têt (France). *Comptes Rendus de l'Académie des Sciences-Series IIA-Earth and Planetary Science*, 333(7), 389-397.

Stelzer, R. S., Likens, G. E. (2006). Effects of sampling frequency on estimates of dissolved silica export by streams: The role of hydrological variability and concentration‐discharge relationships. *Water resources research*, 42(7), W07415, doi:10.1029/2005WR004615.

Tam, N.F.Y., Yao, M.W.Y. (1998). Normalisation and heavy metal contamination in mangrove sediments. *Science of The Total Environment*, 216(1–2), 33-39.

Ulses, C., Estournel, C., Durrieu de Madron, X., Palanques, A. (2008)a. Suspended sediment transport in the Gulf of Lions (NW Mediterranean): impact of extreme storms and floods. *Continental Shelf Research*, 28, 2048-2070.

Ulses, C., Estournel, C., Bonnin, J., Durrieu de Madron, X., Marsaleix, P. (2008)b. Impact of storms and dense water cascading on shelf-slope exchanges in the Gulf of Lion (NW Mediterranean). *Journal of Geophysical Research*, 113, C02010, doi:*10.1029/2006JC003795*.

Ulses, C., Estournel, C., Puig, P., Durrieu de Madron, X., Marsaleix, P. (2008)c. Dense shelf water cascading in the northwestern Mediterranean during the cold winter 2005: quantification of the export through the Gulf of Lion and the Catalan margin. *Geophysical Research Letters*, 35, L07610, doi:10.1029/2008GL033257.

Vanni, M.J., Renwick, W.H., Headworth, J.L., Auch, J., Schaus, M.H. (2001). Dissolved and particulate nutrient flux from three adjacent agricultural watersheds: a five-year study. *Biogeochemistry*, 54, 85–114.

Wedepohl, K.H. (1995). The composition of the continental crust. *Geochimica et Cosmochimica Acta*, 59(7), 1217-1232.

Chapter III

Riverine transfer of anthropogenic and natural trace metals to the Gulf of Lion (NW Mediterranean Sea)

In this chapter, we investigate the fluxes of particulate Cd, Co, Cr, Cu, Ni, Pb, Zn in two contrasting river system of the Gulf of Lion (NW Mediterranean Sea) : the Tet and the Rhone rivers.

Rivers are the main source of particulate trace metals to the coastal zone. Although most of the load brought through this way is bound to settle and be sequestred in the estuary or prodelta, a part of this particulate discharge and its sediment-bound contaminants will be resuspended and exported along the continental shelf towards deeper environments. Riverine-transferred trace metals are a source for the benthic abyssal environments but it also plays a key role in coastal ecosystems.

In the Gulf of Lion, this particulate transfer mainly happens during flood events which is why we focus on those extreme events, and their relative contribution to the annual budget, at the end of this chapter. Indeed, in the Mediterranean area, floods happen over a very short period of time (2-3 days in general) and are often hard to predict and study thoroughly. But some studies have shown that, in some rivers, they represent the major part of the annual contribution.

My contribution to this chapter was to analyze the Tet and Rhone samples from 2010 following the same protocol that was used for the other years of the long-term survey (2006-2011). The complete set of data is available in appendix A. This study is currently submitted to *Applied Geochemistry*.

Riverine transfer of anthropogenic and natural trace metals to the Gulf of Lions (NW Mediterranean Sea)

Dumas C[1,2], Ludwig W[1,2], Aubert D[1,2], Eyrolle, F[3], Raimbault, P[4], Gueneugues A[1,2,5], and Sotin C[1,2]

[1] Univ. Perpignan Via Domitia, CEntre de Formation et de Recherche sur les Environnements Méditerranéens, UMR 5110, F-66860, Perpignan, France

[2] CNRS, CEntre de Formation et de Recherche sur les Environnements Méditerranéens, UMR 5110, F-66860, Perpignan, France

[3] Laboratoire d'Etudes Radioécologiques en milieu Continental et Marin, Institut de Radioprotection et de Sûreté Nucléaire (IRSN), F-13115 Saint Paul Lez Durance, France

[4] Mediterranean Institute of Oceanography - MIO Campus de Luminy, 162 Av. de Luminy, F-13288 Marseille cedex9.

[5] present address: UMR 7621 Océanographie Microbienne, Observatoire Océanologique de Banyuls sur Mer, Avenue du Fontaulé, F – 66650 Banyuls sur Mer.

Abstract

During 2005-2011, two contrasting river systems in the Gulf of Lions (southern France) have been monitored for particulate trace metal (PTM) loads (Cd, Co, Cr, Cu, Ni, Pb, Zn). These are the Rhone River, one of the largest Mediterranean rivers and a significant source of man-made contaminants to this semi-enclosed sea, and the Tet River, a small river which is representative for the numerous coastal rivers in the Mediterranean area. The objectives were to understand the transport mechanisms of PTM and to identify specific anthropogenic pressures in the corresponding drainage basin. Concentrations of all elements are highly associated with the concentrations of suspended particulate matter (SPM), but relative metal enrichment in these particulates can be variable depending on the considered elements, rivers and hydrological conditions. Concentrations of Co, Cr and Ni are generally more constant, whereas concentrations of Cd, Cu, Pb and Zn depict much greater variability, likely the result of anthropogenic contributions. Because of its large basins size and particle mixing during transport, variability in the Rhone River is reduced compared to the Tet River, which underlines the interest of small rivers for the study of transport processes. In both rivers, increasing water discharge and SPM concentrations generally reduce PTM enrichment, but

flushing of enriched PTM during floods can have a strong positive impact on the average PTM budgets. Through the definition of natural background concentrations for both catchments, we further propose discrimination of the total PTM fluxes into their anthropogenic and natural counterparts. When subtracting the natural counterparts, specific anthropogenic pressures consistent with the prevailing land use practices can be identified. Greater specific anthropogenic fluxes of Cu in the Tet River (0.8 kg km^{-2} yr^{-1} compared to 0.6 kg km^{-2} yr^{-1} for the Rhone River) point to inputs from agricultural sources, whereas greater specific anthropogenic fluxes of Cd and Pb in the Rhone River (respectively 0.009 and 0.7 kg km^{-2} yr^{-1} compared to 0.005 and 0.4 kg km^{-2} yr^{-1} for the Tet River) indicate inputs from industrial sources. Also detailed analyses of the PTM fluxes during floods were helpful for source identification of PTM. In the Rhone River, comparison of two major floods showed that Pb is mobilized from the upper and more industrialized basins parts. In the Tet River, strong association of anthropogenic PTM and organic matter during floods indicates significant contributions of waste water point sources.

Keywords: Particulate trace metals, anthropogenic and natural fluxes, suspended particulate matter, Rhone River, coastal rivers, flood events, Gulf of Lions.

1. Introduction

Rivers are the principal source of particulate matter for coastal waters and sedimentary systems. Although most suspended particulate matter (SPM) in rivers originate from natural processes, mainly soil erosion (*Lawson et al., 2001*), riverine SPM is also an important vector for the mobilisation of many contaminants which accumulate in the corresponding drainage basins in relation to anthropogenic activities. Trace metals are a good example for this. Because of the reduced solubility of metals in the common pH and redox conditions of surface waters, by far the dominant part of these elements is transported in rivers in association with particulates (in the following: particulate trace metals, PTM).

The Gulf of Lions is one of the largest shelf regions in the Mediterranean Sea and highly interesting for the study of riverine PTM fluxes from land to sea. It is largely influenced by the inputs of the Rhone River, nowadays the biggest Mediterranean river in terms of water discharge (*Ludwig et al., 2009*), and therefore the dominant source of sediments to this particular environment (*Raimbault and Durrieu de Madron, 2003*). The Gulf of Lions is also surrounded by a series of small coastal rivers which contribute to the terrestrial inputs via

short and irregular pulses in relation to major flooding events. Consequently, dynamics and variability of SPM and associated PTM fluxes both in large river systems and small coastal rivers can simultaneously be studied here with regard to their potential impacts on the marine domain.

Previous studies already gave insights in the distribution and enrichment of PTM in recent surface sediments of the Gulf of Lions (*Nolting and Helder, 1991*; *Roussiez et al., 2005*; *2006; 2011*), on the potential contributions of the Rhone River (*Cossa and Martin, 1991*; *Elbaz-Poulichet al., 1996*; *Radakovitch et al., 2008*; *Ollivier et al., 2011*) and other coastal rivers (*Roussiez et al., 2011*; *Nicolau et al., 2012*) to the marine PTM stocks as well as on their further offshore transport to the deep sea environments via the submarine canyons (*Grousset et al., 1995*; *Roussiez et al., 2012*; *Dumas et al., 2014*). Some of them also proposed tentative budgets which detailed the specific PTM inputs from the different drainage basins (*Radakovitch et al., 2008*; *Nicolau et al., 2012*; *Roussiez et al., 2012*). However, most of the previous studies on riverine PTM fluxes relied on general considerations with often limited data availability and/ or on snapshots of specific hydrodynamic events which do not allow fully understanding of the processes governing the transport dynamics of PTM in rivers.

With this study, we intend to fill this data gap. We monitored daily sediment fluxes during more than 6 years in two contrasting river systems of the Gulf of Lions (e.g., the Tet and the Rhone rivers), together with regular analyses of the associated PTM concentrations during different hydrological regimes. Our approach does not only allow for the establishment of reliable PTM fluxes on the long term, but also for a better understanding of the variability of these fluxes in relation to floods. For the first time, we are able to propose discriminations between PTM from natural and anthropogenic sources, which may help to clarify links to prominent land use practices in the corresponding drainage basins and to further track these contaminants in the marine domain.

2. Material and methods

2.1 Study area and sampling periods

The Gulf of Lions is a crescent-shaped passive margin located in the north-western Mediterranean Sea. It extends from the Pyrenees Mountains of northern Spain to the city of

Toulon in south-eastern France (approximately 42–44°N, 3–6°E). More than 10 rivers with a total watershed area of about 125 000 km^2 deliver significant water discharges into the gulf (Fig.3.1). Ignoring the smaller ones, these are the Tech, Tet, Agly, Aude, Orb, Herault, Vidourle, and Rhone rivers (from S to N). Among them, the Tet River has been targeted in this study as representative for the functioning of the coastal rivers in general. This river is also interesting because it is situated close to the south-western border of the gulf, where the platform margin narrows the coast.

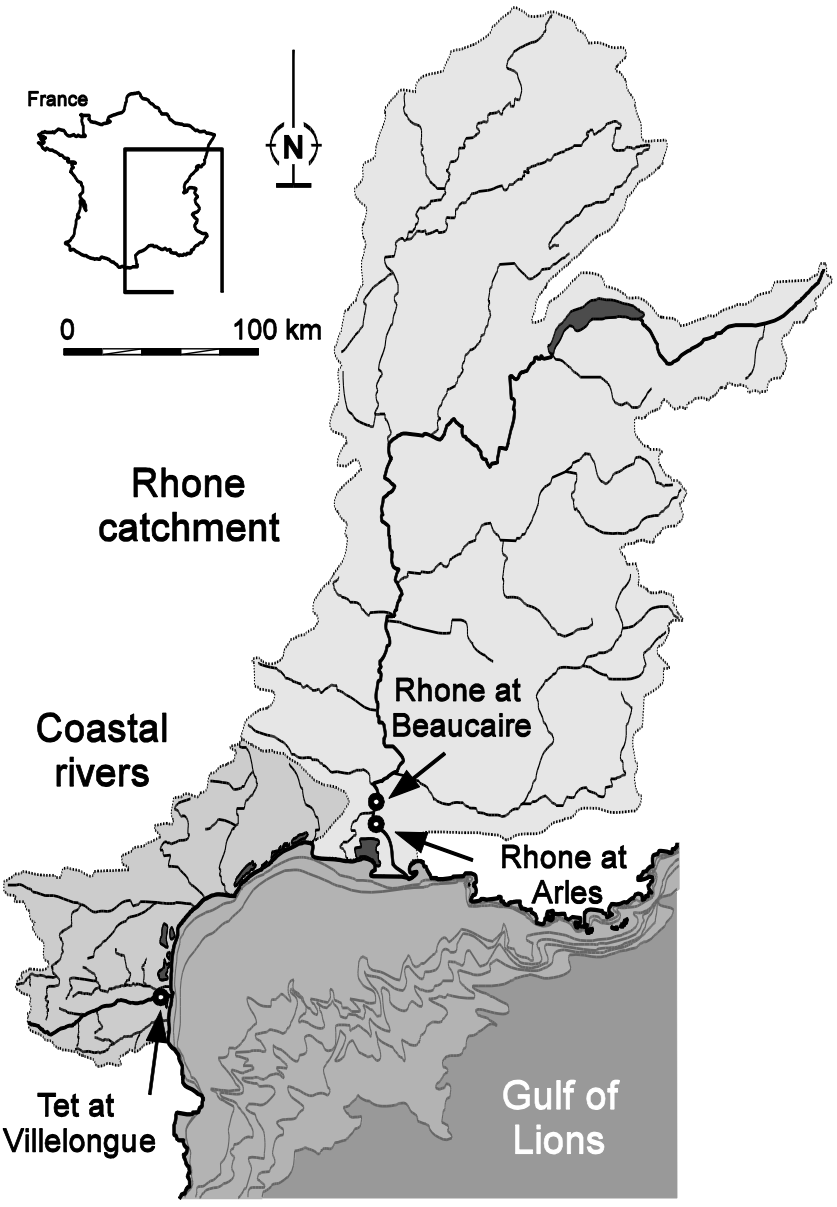

Fig.3.1 Geographic sketch of the studied river basins and the corresponding monitoring stations. Bathimetric lines in the Golf of Lions correspond to the 20, 50, 100, 200, 500, 1000 and 2000m water depths. Modified from Monaco et al. (*2009*)

In combination with the prevalent eastern to western currents, most of the shelf waters and sediments are exported here via the submarine canyons to the deep sea environment (*Canals et al., 2006*). Identification of the geochemical signatures of local rivers is hence useful for the budgeting of PTM export fluxes (*Dumas et al., 2014*).The Tet River drains an area of approximately 1400 km^2 and its average water discharge is about 10 $m^3 s^{-1}$. Considerable water losses due to irrigation occur in the lower drainage basin and its natural water discharge is probably reduced by one third (*Ludwig et al., 2004*). The average river slope is very steep. Its headwaters reach altitudes of >2500m in the eastern flank of the Pyrenees despite a total river length of less than 100 km. The elevated headwaters are responsible for a strong nival component of the river flow, with a maximum value in May during the snowmelt period. However, major peak discharges normally occur in late autumn and winter in relation with short and violent flash-floods. Also in spring, flash-floods can occur. During these flooding events, discharge can rapidly rise to 500-1000 $m^3 s^{-1}$ and even reached 3400 $m^3 s^{-1}$ during the historical flood of 1940 (*Serrat et al., 2001*). There are clear signs that recent climate change already had a negative impact on average water discharge in the Tet and the other coastal rivers in this region (*Lespinas et al., 2009; 2014*).

Discharge trends are absent for the Rhone River (*Ludwig et al., 2003*), the second river which has been monitored in this study. This river alone covers about 80% of the total drainage basin area (Fig.3.1) and contributes almost two thirds of the total riverine freshwater inputs into the north-western Mediterranean Sea (*Ludwig et al., 2009*). Due to its associated nitrate and phosphate loads, it enhances significantly the primary production in the shelf waters of the Gulf of Lions (*Minas and Minas, 1989*). Based on its long term discharge record at Beaucaire, the most downstream station before the river splits into the small and large Rhone River branches, its average water discharge (Q) is estimated to about 1700 $m^3 s^{-1}$ (*Ibanez et al., 1997*). Maximum and minimum water flow normally occur in winter (January) and in summer (August), respectively. Extreme floods with a return period of 100 years can reach peak discharges of >10000 $m^3 s^{-1}$ (*Estournel et al., 1997*; *Maillet et al., 2006*). However, four of these events occurred during the last 20 years (1993, 1994, 2002, 2003), with the maximum discharge recorded in December 2003.

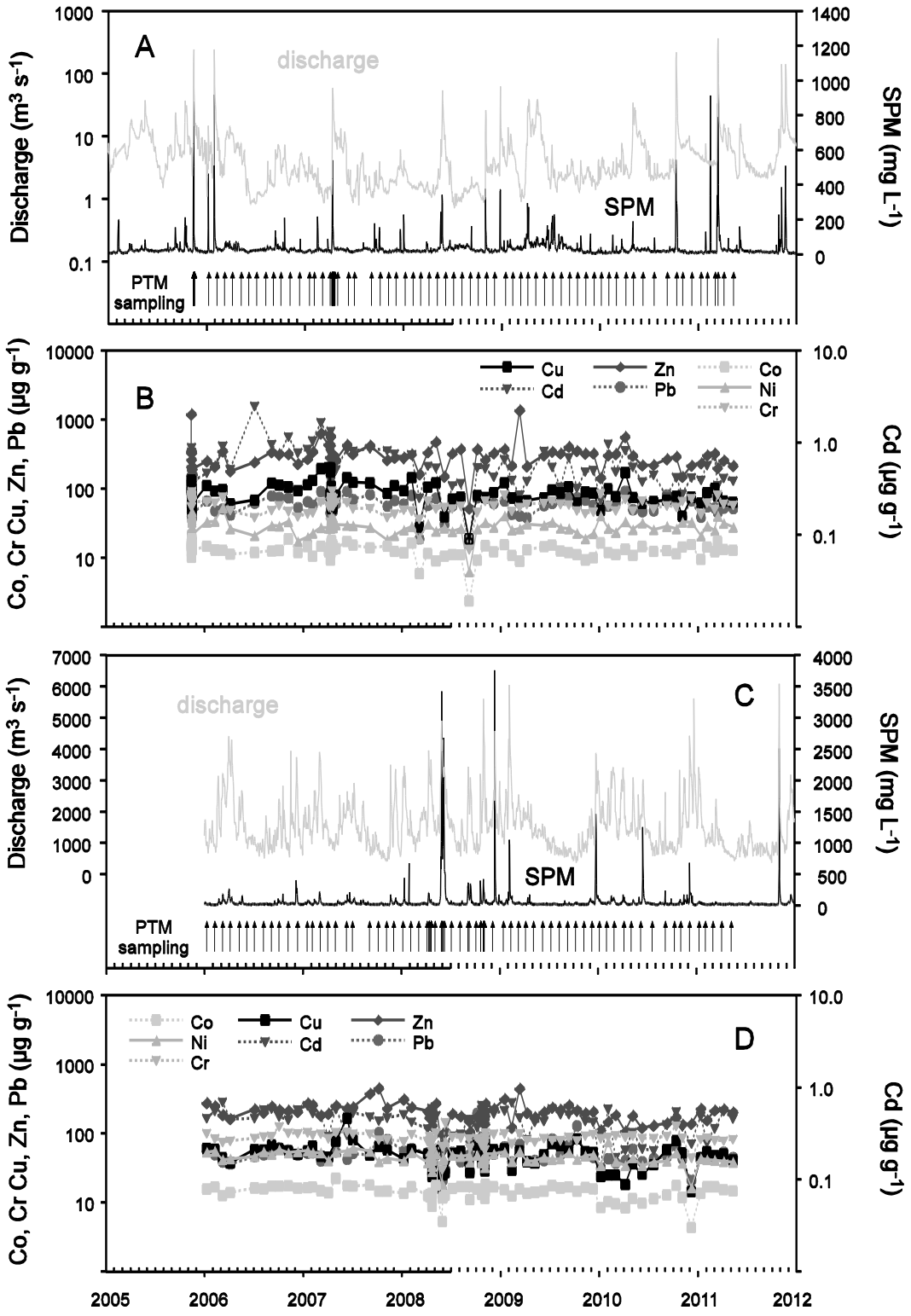

Fig.3.2 Evolution of daily water discharge, daily sediment concentrations, and monitored PTM concentrations in the Tet (A, B) and Rhone (C, D) rivers during the study period. Notice that water discharge for the Tet River is in logarithmic scale for better representation of variability. PTM concentrations and other basic data can be downloaded via (weblink)

Both the Rhone and Tet rivers are equipped with autonomous sampling stations close to their river mouths (Fig.3.1). This allows the determination of realistic SPM fluxes with daily to hourly sampling frequencies. We continuously monitored this parameter from 2005 to 2011 in the Tet River and from 2006 to 2011 in the Rhone River (Fig.3.2a, c). PTM were generally analysed in monthly sampling intervals, but several flooding and high discharge events were analysed with higher frequencies. In the case of the Tet River, this concerns two events in autumn 2005 and spring 2007. In the case of the Rhone River, two floods during 2008 were analysed for PTM. Both occurred in spring and autumn of 2008.

2.2 Calculation of SPM and POC fluxes

During non-flood conditions, automatic sampling of SPM in the Tet River occurred once a day at fixed hours about 10 km upstream the river mouth (station of "Villelongue"), close to the city of Perpignan (Fig.3.1). During floods, detected by a rapid increase of water level, sampling frequency switched to about hourly time steps (higher frequencies at the beginning, lower frequencies towards the end). Each time, 1L of water was sampled and kept refrigerated for a maximum of one week (one or two days during floods) in our sampling station before being filtered on pre-weighed and pre-heated (at 450 °C for 12 h) GFF filters. SPM concentrations between sampling were considered to evolve linearly with time. For flux calculations, we multiplied these concentrations with the corresponding water discharge of the Tet River, calculated as the sum of the "Perpignan" and the "Basse" (last tributary before the river mouth) gauging stations (*BD Hydro, 2013*). As water discharge and SPM concentrations were gauged at irregular time steps, we linearly interpolated all parameters to one value per minute, calculated the corresponding water and SPM fluxes and then condensed the results to daily fluxes.

In some cases, the automatic sampling station of the Tet River was stopped because of technical problems. Whenever the continuous sampling was interrupted for more than 5 days (or when a significant discharge increase occurred without being sampling), we determined the daily SPM concentration on the basis of the SPM – discharge relationship published by Serrat et al. (*2001*). This was, however, only rarely the case. The number of days which were covered by sampling was always greater than 330 days per year, with a minimum coverage in 2011 (332 days) and a complete coverage in 2007 and 2009 (365 days).

In the case of the Rhone River, sampling occurred with an automatic sampling station that exists in the city of Arles (about 45 km upstream the river mouth). Here, average daily SPM concentrations were determined by integrated sampling during 24h (4h during floods). These concentrations can directly be multiplied by the corresponding daily discharge of the Rhone River (or 4h averages in the case of floods). Although there is a water gauging station at Arles, we used for flux calculation the discharge records of the upstream gauging station at "Beaucaire". This station is situated just before the spreading of the Rhone River into its two major branches which flow into the Mediterranean Sea (Fig.3.1). We therefore consider that concentration measurements at Arles are representative for both branches).

Also in the case of the Rhone River, a few days are missing in the continuous sampling record because of technical problems. However, this only concerned 1% of the days in the study period and gaps never lasted longer than a few days. We consequently filled these gaps by linear interpolation of the SPM concentration between closest measurements.

Other water quality parameters were regularly measured in the Tet and the Rhone rivers as well. In this study, we only focus on particulate matter fluxes. Among the monitored parameters, we also present estimates on the associated fluxes of particulate organic carbon (POC), as PTM transport in rivers can be significantly linked to this parameter as well (see section 3.4). POC was not measured with the same sampling frequency as SPM. In the Tet River, high resolution measurements of POC only started in 2011. In the Rhone River, they already started in earlier years. Nevertheless, for both rivers, highly significant log-log relationships between POC ([POC], μmoles L^{-1}) and SPM concentrations ([SPM], mg L^{-1}) could be found, allowing extrapolation of the average POC fluxes during the study period according to (eq. (i) is for the Tet River and eq. (ii) for the Rhone River):

$$\log([POC]) = 0.67 \log([SPM]) + 1.25 \qquad r^2 = 0.77,\ n= 233 \qquad \text{(i)}$$

$$\log([POC]) = 0.73 \log([SPM]) + 0.83 \qquad r^2 = 0.80,\ n= 1887 \qquad \text{(ii)}$$

2.3 Laboratory analysis

Continuous monitoring of SPM was accompanied by regular analysis of PTM in both rivers (see arrows in Fig.3.2a, c). Samples were taken at the sampling stations described above, but immediately recovered after sampling and transported to our laboratory (except during floods

when the samples were kept refrigerated in the station up to one day before recovery). Water was stored in 1N HCl pre-cleaned polypropylene bottles (soaked for at least 48h, rinsed by milli-Q and air-dried) and rapidly filtered in the laboratory through pre-weighed cellulose acetate filters (47 mm in diameter and 0.45 μm in pore size). After filtration, filters were dried at 40°C for at least 24h in a clean oven for dry weight determinations.

Particulate matter was recovered from cellulose acetate filters in de-ionized water by using ultrasonic baths. Mineralization of the dried material was performed in Teflon beakers with successive mixtures of high quality (trace metals grade) nitric and hydrofluoric acids (HNO_3-HF) and nitric acid and oxygen peroxide (HNO_3-H_2O_2). Major and trace element concentrations were measured by Inductively Coupled Plasma Mass Spectrometry (ICP-MS, Thermo Xseries 2) at the Hydrosciences Laboratory (University of Montpellier, France). Reference material of estuarine sediment (1646a from NIST) was mineralized and analysed under the same conditions as the samples and provided suitable recoveries (errors < 5% for Al, Co, Ni and Pb; recoveries of Cr, Cu, Zn and Cd ranged from 90% to 96%, 111% to 122%, 109% to 146% and 86% to 95% respectively). Analytical blanks did not reveal any significant sign of contamination (contribution < 0.5% for Al, Cr, Co, Ni, Zn, Cs and Pb, < 1.5% for Cu and < 3% for Cd).

POC contents in the PTM samples were measured on a Leco CN 2000 elemental analyser (EA) at the CEFREM laboratory, after separate filtration on pre-weighted and pre-heated GFF filters (47 mm in diameter and <0.7 μm in pore size) and removal of inorganic carbon by repeated additions of HCl 25%. POC in the samples of the continuous SPM monitoring was analysed according to the same protocol but in the MIO Laboratory at Marseille (France). Filtration on GFF filters was used for determination of representative SPM concentrations in all samples which were analysed for PTM.

3. Results and Discussion

3.1 Average water, SPM and POC fluxes

Results of the long-term monitoring of water, SPM and POC fluxes in the Tet and the Rhone rivers are summarized in Table 3.1. Notice that the monitoring period was characterized by hydroclimatic conditions which were dryer than on average in both rivers. This is particularly

the case for the Tet River. Here, the average water discharge was below 200 Mm^3 yr^{-1}, corresponding to about 6.3 m^3 s^{-1}. This is less than two thirds of the long-term mean. The years 2007 and 2008 were especially dry. The average water discharge in the Rhone River corresponds to about 1510 m^3 s^{-1} or almost 90% of the long-term mean.

As a consequence, also the average SPM fluxes in both rivers were lower than on average. For the Tet River, one obtains a total of 25900 t yr^{-1}, and for the Rhone River, a total of 4.1 Mt yr^{-1}. Interestingly, this is in both cases about half (or slightly more) of what is considered to be the long-term mean, taking the studies of Serrat et al. (*2001*) and of Pont et al. (*2002*) as references. We also tried to estimate in the Table 1 the flood contribution to these fluxes. Such an approach requires a clear definition of what are flood and non-flood conditions. We therefore performed analyses of peak discharges with the daily 1971 – 2011 (Tet River) and 1960 -2011 (Rhone River) discharge records for different return periods based on the method of Gumbel (*1958*). Fixing the return period to 1.4 years yields a corresponding discharge of 100 m^3 s^{-1} for the Tet River, which is commonly considered for this river to be the threshold for floods (according to *Serrat et al., 2001*, about 10 times the average discharge). For the Rhone River, the same return period yields a corresponding average daily discharge of 4682 m^3 s^{-1}. We retained both values as the limits for defining flood and non-flood conditions. Consequently, it can be calculated that during the study period, 64% and 17% of the total SPM fluxes in the Tet and Rhone rivers were delivered during floods (Table 3.1).

These values have naturally to be considered with caution, as both rivers were monitored during dryer than on average conditions. They are nevertheless interesting as they give insights in the general functioning of both rivers and underline the much more episodic character of coastal rivers like the Tet River. These values may surprise compared to other studies which proposed that also in the Rhone River, a large majority of SPM is delivered during floods (e.g. 80% according to *Antonelli and Provansal, 2003*). However, in many cases, clear definitions about what is considered as flood and non-flood conditions are lacking, making it difficult to use such estimates for inter-comparisons between rivers.

Finally it is also interesting to compare the specific fluxes (fluxes divided by basin area) between both rivers.

Tet River	2005	2006	2007	2008	2009	2010	2011	mean
SPM (Kt yr^{-1})	30.8	29.7	6.4	7.9	11.4	24.4	70.6	25.9
SPM-flood (%)	70	78	0	0	0	69	77	64
Q (Mm^3 yr^{-1})	296	180	106	97	178	218	317	199
Q-flood (%)	11	22	0	0	0	21	30	15
POC (10^3 tC yr^{-1})	1.1	1.0	0.3	0.3	0.6	0.9	2.1	0.9
POC-flood (%)	49	62	0	0	0	56	67	49
Rhone River	2005	2006	2007	2008	2009	2010	2011	mean
SPM (Mt yr^{-1})		2.2	1.8	10.7	3.7	3.4	3.0	4.1
SPM-flood (%)		0	0	14	26	0	53	17
Q (Mm^3 yr^{-1})		48590	46492	57071	43549	54010	36191	47651
Q-flood (%)		0.0	0.0	2.4	2.2	0.9	2.7	1.3
POC (10^3 tC yr^{-1})		56.8	48.9	159.6	68.9	77.6	49.4	76.9
POC-flood (%)		0	0	10	18	0	34	10

Table 3.1 SPM, water and POC fluxes from the Tet and Rhone rivers during the study period.

Table 3.1 shows that the specific SPM flux in the Rhone River basin was on average close to 41 t km^{-2} yr^{-1}, about two times the value in the Tet River basin (19 t km^{-2} yr^{-1}). The Rhone River is known for more elevated mechanical erosion rates which probably were still more enhanced during previous centuries (*Ludwig and Probst, 1998*). In the Tet River basin, resistant metamorphic and magmatic shield rocks are prevalent (*Garcia Esteves et al., 2007*), which can easily explain the lower erosion rates. It should also be mentioned that hydroclimatic conditions in the Rhone River basin are more humid as well. Notice that during the study period, specific water discharge in the Rhone River was three times the value in the Tet River (477 mm and 142 mm, respectively). Specific POC fluxes, however, are comparable (about 0.77 tC km^{-2} yr^{-1} for the Rhone River and 0.64 tC km^{-2} yr^{-1} for the Tet River). SPM in the Tet River is on average more enriched in organic carbon than in the Rhone River.

		Q (m^3 s^{-1})	SPM (mg L^{-1})	POC (%)	Al (mg g^{-1})	Cr (µg g^{-1})	Co (µg g^{-1})	Ni (µg g^{-1})	Cu (µg g^{-1})	Zn (µg g^{-1})	Cd (µg g^{-1})	Pb (µg g^{-1})
Tet	mean	43	117	8.0	68	60	13	28	87	289	0.57	57
	min	0.2	3	1.4	17	13	2	6	19	51	0.07	15
	Q25*	2	9	3.9	54	51	12	25	61	206	0.37	45
	Q50*	5	19	7.9	66	59	13	27	79	259	0.48	55
	Q75*	25	108	12.0	83	68	15	32	105	321	0.73	67
	max	503	1530	18.6	109	92	19	52	198	1344	2.47	97
	n*	96	98	79	89	93	93	93	93	93	93	93
Rhone	mean	1921	133	3.3	62	84	14	44	47	197	0.44	53
	min	270	3	0.7	23	30	4	16	14	57	0.10	12
	Q25*	855	10	2.0	55	77	12	39	37	159	0.37	40
	Q50*	1535	25	3.0	63	84	14	43	46	194	0.47	48
	Q75*	2853	140	4.4	71	92	16	52	57	223	0.54	58
	max	4977	2590	10.5	114	141	22	76	162	443	0.69	192
	n*	77	76	51	77	81	81	81	81	81	81	81

- Q25, Q50 and Q75 correspond to the quantiles 25 %, 50 % and 75 %, respectively; n is the number of concomitant samples (differences between SPM and PTM is because of missing GFF filtrations)

Table 3.2 Variability of PTM concentrations and associated parameters in the Tet and Rhone rivers during the study period.

3.2 Levels and fluxes of PTM

Over the study period, we analysed for each river about 80-90 samples for PTM (Tab. 3.2 and Fig.3.2 b, d). This allows a detailed picture of the variability of the PTM levels and of their relationships with these carrier phases (SPM and Q). Notice that the general concentration levels are not very different in the Tet and Rhone rivers, and that they are close to what has been found in previous studies (*Radakovitch et al., 2008*; *Ollivier et al., 2011*, *Roussiez et al., 2012*). Particulates in the Rhone River seem to be somewhat enriched in Cr and Ni compared to the Tet River, whereas the contrary is the case for Cu, Zn and Cd.

It should also be noticed that the variability of PTM concentrations is clearly lower than the variability of SPM concentrations. Taking the ratio of the Q75 over Q25 percentile as an indicator for this, SPM concentrations are on average 5-10 times more variable than concentrations of PTM. In particular the elements Cr, Co and Ni depict low variability. This rather constant behaviour of PTM in SPM means that fluxes are principally dominated by the variability of SPM. Consequently, highly significant log-log relationships can be found for all elements (Tab. 3.3), linking the PTM concentrations (in µg L^{-1}) to the concentrations of SPM (in mg L^{-1}). We applied these relationships to the long-term SPM records in order to calculate the corresponding PTM budgets (Tab. 3.4). In terms of specific fluxes, the Rhone River depicts systematically higher values than the Tet River, except for Cu. There often exists a factor of 2-3 between the specific fluxes in both rivers, in particular for the elements Ni and Cr. This directly reflects the two times greater SPM fluxes in the Rhone River basin, together with the also more elevated concentration levels for these elements (see above).

	Tet			Rhone		
	a	b	r^2	a	b	r^2
Cr	1.075	-1.353	0.98	1.012	-1.075	0.99
Cu	0.968	-1.046	0.93	0.871	-1.148	0.94
Ni	1.044	-1.631	0.97	0.973	-1.317	0.98
Co	1.044	-1.964	0.98	0.945	-1.774	0.97
Zn	0.884	-0.411	0.91	0.891	-0.554	0.97
Pb	0.961	-1.205	0.96	0.923	-1.187	0.93
Cd	0.890	-3.131	0.89	0.948	-3.312	0.94

Table 3.3 Regression and correlation coefficients between PTM (in µg L^{-1}) and SPM (in mg L^{-1}) according to the general form : log(PTM) = a log(SPM) + b.

Ni, Co and Cr in soils are generally considered to be mostly of natural origins (in the following: "natural PTM"), contrary to Cu, Zn Pb and Cd, which normally have stronger anthropogenic contributions (*Micó et al. 2006*). For these latter elements (in the following: "anthropogenic PTM"), differences in the specific PTM fluxes of the Rhone and Tet rivers are less important. Notice also that in the log-log relationships of the Table 3.3, regression coefficients a (defining the slope of the regressions) are often smaller for anthropogenic elements compared to natural ones, indicating that anthropogenic PTM are more diluted in samples with elevated SPM concentrations. Dilution of anthropogenic PTM during floods was also observed by Oursel et al. (*2014*) in another Mediterranean river system.

Compared to previous literature estimates, the PTM fluxes in Table 4 are systematically lower. Radakovitch et al. (*2008*) proposed values for the Tet and Rhone rivers which are, depending on the element, on average 2 – 3 times greater than ours. Also Roussiez et al. (*2012*) gave estimates for both rivers which are still about 1.5 – 2.5 times greater on average. Part of these differences can be explained by the relative dry conditions during our study period, but probably not all of them. Difference can also be related to our regression method based on the values in Table 3.3. Depending on the SPM levels, this method produces variable PTM concentrations (in $\mu g\ g^{-1}$), while the above cited studies worked with constant PTM concentrations.

It is finally also interesting to compare these river export fluxes with atmospheric deposition rates in this region. Guieu et al. (*2010*) estimated them for the Western Mediterranean Sea, although only for the elements Zn, Cd and Pb. Specific deposition rates for Zn and Cd (in $kg\ km^{-2}\ yr^{-1}$) are clearly more elevated than specific riverine export fluxes: about 3 (Zn) and 5 (Cd) times the values of the Tet River, and 2 (Zn) to 2.5 (Cd) times the values for the Rhone River. Only for Pb, for which atmospheric deposition considerably decreased during recent years (*Guieu et al., 2010*), the atmospheric and riverine values are in about the same range. This suggests that atmospheric deposition can be an important (and even dominant) source of PTM in the studied river basins.

		Cr	Co	Ni	Cu	Zn	Cd	Pb
Tet	total flux (kg yr^{-1})	1775	364	780	1938	5191	10	1288
	specific flux (kg km^{-2} yr^{-1})	1.268	0.260	0.557	1.385	3.708	0.007	0.920
	EF (SPM weighted)	1.40	1.44	1.62	2.39	3.15	3.19	1.83
	anthropogenic (%)	28.5	30.7	38.4	58.1	68.3	68.6	45.2
	anthropogenic (kg km^{-2} yr^{-1})	0.362	0.080	0.214	0.805	2.532	0.005	0.416
	natural (kg km^{-2} yr^{-1})	0.906	0.180	0.343	0.580	1.176	0.002	0.504
Rhone	total flux (kg yr^{-1})	372055	50720	169822	141855	619353	1491	173299
	specific flux (kg km^{-2} yr^{-1})	3.72	0.51	1.70	1.42	6.19	0.015	1.73
	EF (SPM weighted)	1.30	1.59	1.70	1.74	1.63	2.66	1.72
	anthropogenic (%)	23.0	37.0	41.2	42.4	38.8	62.4	41.8
	anthropogenic (kg km^{-2} yr^{-1})	0.854	0.188	0.699	0.601	2.403	0.009	0.725
	natural (kg km^{-2} yr^{-1})	2.866	0.320	0.999	0.817	3.790	0.006	1.008

Table 3.4 Average PTM fluxes in the Tet and Rhone rivers during the study period.

3.3 Natural and anthropogenic origins of PTM

3.3.1 Enrichment factors

Discrimination of natural and anthropogenic origins of PTM in rivers is usually done via the calculation of enrichment factors (EF). They result from a two-fold normalisation of the analysed samples with reference materials. Because PTM are generally associated with the finest particles, PTM concentrations have to be divided first by the concentrations of a given element (C) in the samples that is of natural origin and that is highly associated with the grain size fraction of clays. Then, a second normalisation with a reference background sample is applied. It reflects natural PTM concentrations in the soils derived from local lithologies:

$$EF = [(PTM/C)_{sample}] / [(PTM/C)_{background}] \quad \text{(iii)}$$

It is generally admitted that EF > 2 translate PTM enrichment from anthropogenic sources (*Sutherland, 2000*). If natural background concentrations can be determined regionally, this may be already the case for EF > 1.5 (*Roussiez et al., 2006*). Ideally, if the background concentrations can be determined locally for a given drainage basin, already EF > 1 can translate anthropogenic contributions (P_{anthro}, %) which can be calculated according to:

$$P_{anthro} = (100/EF) * (EF-1) \quad \text{(iv)}$$

Different elements have been proposed to be suitable tracers for clays and hence the best candidate for C in equation (iii). Among the most prominent are Al (e.g., *Din, 1992*; *Tam and Yao, 1998*), Li (*Loring, 1990*), Sc (e.g., *Grousset et al., 1995*), Ti (e.g., *Bi et al., 2014*) and Cs (e.g., *Roussiez et al., 2005*). Not all of these elements are frequently analysed in studies of PTM in natural environments, which complicates the comparison of data from different literature sources. The most widely used tracer element is probably Al and has consequently also been selected in our study. We also tested Sc and Cs instead, but since clay tracer elements are correlated, this had only a minor impact on our results.

Selection of the local background concentrations, however, is more delicate and can have a strong influence on the resulting EF values. A common approach is here to use sediment cores, giving access to samples which accumulated long before anthropogenic activities changed the natural PTM levels. For the Rhone River, a deep sediment core was recovered in the river bank sediments of the lower river course, and the local background values were determined at -30 m (corresponding to 4705 +/-30 BP) by Ferrand et al., (*2012*). After normalisation with Al, we listed them in the Table 3.5, together with statistical analysis (min,

max, percentiles 25, 50 and 75) of the corresponding values in the Rhone and Tet river particulates. We also included the natural backgrounds Roussiez et al. (*2005*) proposed for the surface sediments in the Gulf of Lions. These latter values were originally proposed based on normalisation with Cs, but we recalculated them on the basis of Al as normaliser element.

	Cr/Al	Co/Al	Ni/Al	Cu/Al	Zn/Al	Cd/Al	Pb/Al
Tet – min alluvials (1)	6.4	1.5	3.0	4.6	16.7	0.04	6.1
Rhone – min alluvials (2)	10.0	1.4	5.7	2.2	13.8		3.3
GoL min sediments (3)	13.3	1.9	5.6	3.8	12.8	0.22	4.2
min-Tet	6.4	1.3	2.5	4.6	8.7	0.02	3.5
Q25-Tet	7.8	1.6	3.6	8.0	25.4	0.05	5.7
Q50-Tet	8.9	1.8	4.3	11.9	44.0	0.06	8.9
Q75-Tet	10.0	2.2	4.8	17.9	59.5	0.12	12.7
max-Tet	11.5	4.0	6.4	35.4	250.3	0.61	17.0
min-Rhone	10.4	1.4	4.5	3.4	15.0	0.02	4.1
Q25-Rhone	12.3	2.1	6.4	5.9	26.2	0.05	6.5
Q50-Rhone	13.2	2.2	7.0	7.2	29.6	0.07	7.9
Q75-Rhone	14.4	2.4	7.5	8.4	37.0	0.09	9.6
max-Rhone	26.6	4.3	14.8	19.3	68.1	0.14	27.9

(1) determined in this study ; (2) Ferrand et al., 2012; (3) Roussiez et al. (2005)

Table 3.5 Variability of Al-normalized PTM concentrations in the Tet and Rhone rivers in comparison with potential natural background levels compiled from different sources.

Also for the Tet River, a 1m sediment core close to the village of "Ille sur Tet" was recovered. Activity profiles of $^{210}Pb_{xs}$ and ^{137}Cs reveal that the last 50 years should be included in the first 10-20 cm of the core (*Ferrand, 2010*), indicating that the lowest core parts could reach down to pre-industrial levels. It is here where Al normalised PTM levels are generally lowest (Fig.3.3), and we included these minima in our comparison of Table 3.5 as potential candidates for local background levels. PTM enrichment principally occurs in the uppermost levels for anthropogenic elements (Zn, Pb, Cd), although also some intermediate peaks can exist (Pb, Cu). Natural PTM (Ni, Cr) depict almost no variability over the entire profile.

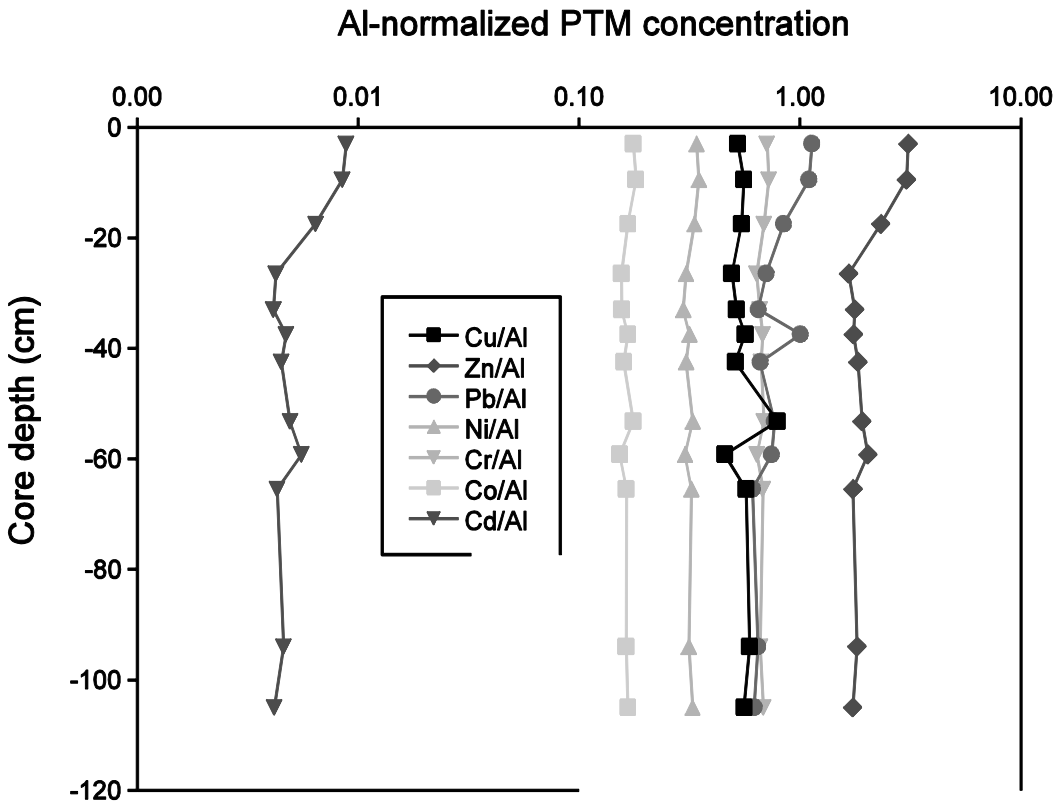

Fig.3.3 Al-normalized PTM concentrations in a sediment core of alluvial deposits in the Tet River near the village of Ille sur Tet (long 2°35'22 E, lat 42°39'43 N)

Some important observations can be made in data of Table 3.5. For natural PTM, minima values in the river SPM are similar to the sediment core backgrounds both for the Rhone and Tet rivers. However, compared to each other, both rivers are different, underlining the general enrichment of Ni and Cr in the Rhone River SPM. This may translate the greater abundance of sedimentary rocks in the drainage basin of the Rhone River compared to the drainage basin of the Tet River, where magmatic and metamorphic rocks are dominant (*Garcia-Esteves et al., 2007*). Also for anthropogenic ETM, there is still a reasonable agreement between the SPM minima in the Rhone River and the sediment core backgrounds of Ferrand et al. (*2012*). But the sediment core backgrounds are generally lower, indicating that the natural levels were probably never entirely reached in the Rhone River during our study period. In the Tet River, on the contrary, river minima are often lower than the sediment core values, in particular for Zn, Pb and Cd. Natural backgrounds were probably not reached in this shallow sediment core for anthropogenic ETM.

Nevertheless, minima values in the river samples are always close to the sediment core backgrounds. We therefore conclude from this comparison that they might be a very general but valuable approximation for the local backgrounds both in the Rhone and Tet rivers. We consequently used them in our study for calculation of the corresponding EF values according to equation (iv).

3.3.2 Variability and controls of PTM enrichment

Once the local backgrounds have been assigned, spatial and temporal variability of PTM enrichment in both rivers can be studied. According to our approach, minimum EF are fixed to 1 by definition. Maximum EF in the Tet River can reach 1.8, 3.1, 2.5, 7.8, 28.6, 35.8, and 4.8 for the elements Cr, Co, Ni, Cu, Zn, Cd, and Pb, respectively. For the Rhone River, the corresponding values are 2.6, 3.1, 3.2, 5.7, 4.6, 6.2, and 6.9. In both rivers, maximum EF are clearly lower for natural than for anthropogenic PTM. With the exception of Pb, the latter reach significantly higher maxima in the Tet River than in the Rhone River. In particular, variability of anthropogenic EF is higher here. Taking again the ratio of the Q75 to Q25 quantiles as an indicator for this, EF variability is on average about 50% greater in the Tet River than in the Rhone River.

Of course, the precise EF values presented above have to be taken with caution. Natural backgrounds and enrichment factors correspond to a theoretical concept which supposes homogeneous functioning of river drainage basins, neglecting spatial variability which can exist. Also variability related to analytical errors is not accounted for. Not all “enrichment” is necessarily of anthropogenic origin. On the other hand, comparison of our data with the deep sediment core backgrounds for the Rhone River indicate that real EF could still be greater (see above), which means that anthropogenic contributions can be underestimated. We are aware about these uncertainties. Our EF values are indicative for anthropogenic contributions in the river particulates rather than representing precise quantifications. They are based on the assumption that “natural” particulates still exist in both basins and that they were at least sampled once during our study period.

In order to use the EF values for discrimination between natural and anthropogenic PTM fluxes on the long term, it is necessary to understand their variability in relation to the variability of the major carrier phases (water, SPM, and POC). The fluxes of these latter phases were reconstructed in detail (see above), defining a solid basis for budget calculations. In both rivers, EF values are generally anti-correlated to (elevated) SPM concentrations

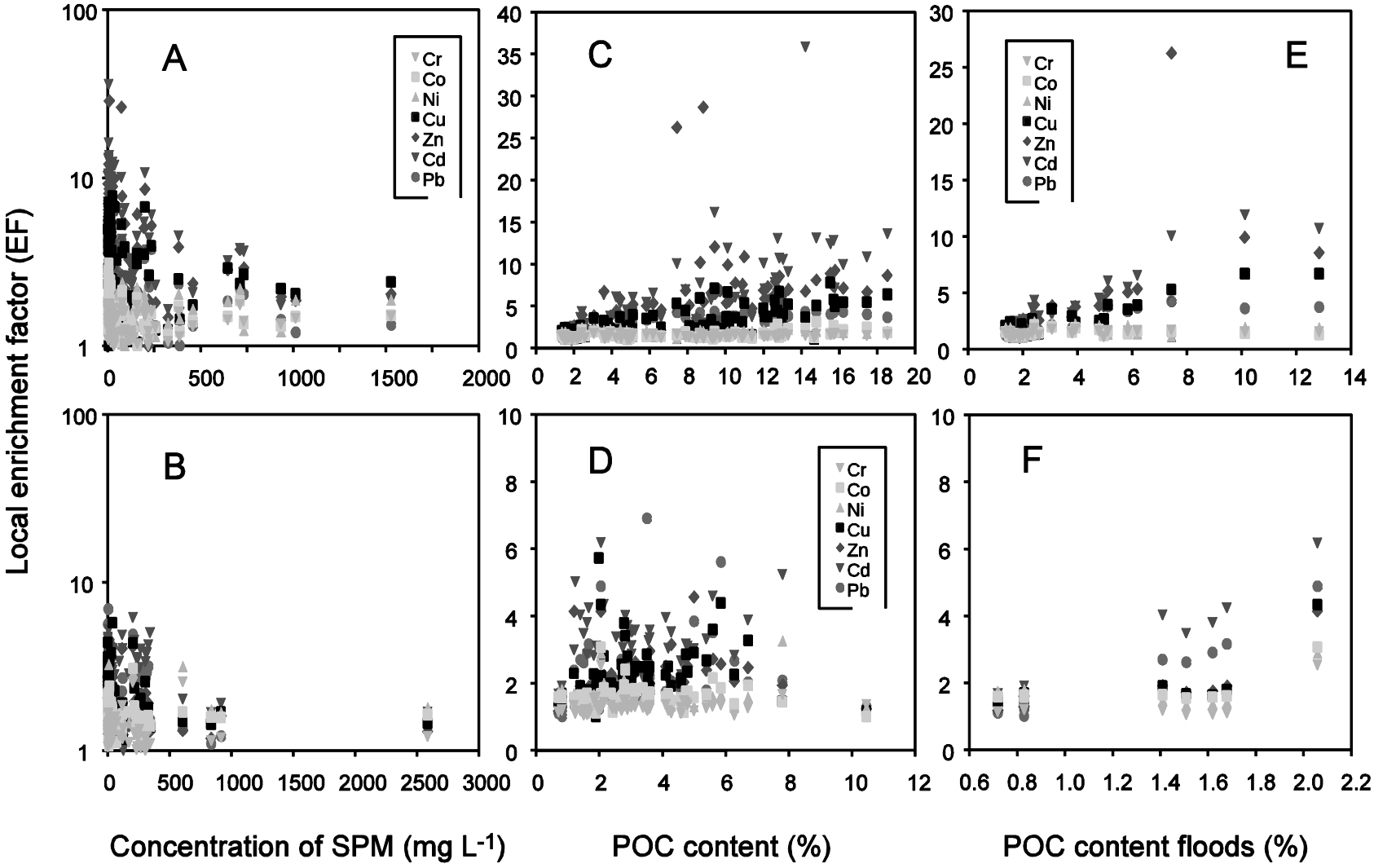

Fig.3.4 Evolution of EF in relation to SPM concentrations and POC contents in the Tet (A, C, E) and Rhone (B, D, F) rivers (data in E and F correspond to the flood samples of Fig.3.5)

(Fig.3.4a, b). This anti-correlation also holds for the PTM-Q relationship, as SPM and Q are highly linked especially when water discharge increases (Fig.3.2a, c). Lowest EF are normally observed both in the Tet and Rhone rivers towards the end of floods, after the first flushing of surface soils and recently accumulated particulates in the river (see also below). This is in agreement with our assumption that here, deeper soil horizons and older river sediments should be mobilized, reflecting closely the natural background concentrations of PTM in the respective river basins.

The degree of anti-correlation between EF and SPM or Q is depending on the PTM of consideration, and on the specific river basin. Anti-correlation is generally significant for anthropogenic PTM, but absent for natural PTM. In the Tet River, correlation coefficients are generally greater for the EF – Q than for the EF – SPM relationships (with r^2 max = 0.53 for the EF_{Zn} - Q correlation). The contrary is the case for the Rhone River (with r^2 max = 0.24 for the EF_{Cu} - SPM correlation). One can also notice some degree of association between anthropogenic PTM and POC in the Tet River (Fig.3.4c), despite the existence of prominent outliers. The correlation between EF and POC is the most evident for anthropogenic PTM during floods (Fig.3.4e). Similar EF-POC relationships do not really exist in the Rhone River (Fig.3.4d), although during floods, also here, some association between both parameters may exist (Fig.3.4f). PTM discharges during floods in both rivers will be further discussed in section 3.4.

3.3.3 Natural and anthropogenic PTM fluxes

The behaviour of PTM and associated EF in relation to the major carrier phases is not identical in the Tet and the Rhone rivers, making it impossible to define one common model for the discrimination of natural and anthropogenic fluxes in both rivers. In particular in the Rhone River, clear relationships are often missing. This is not surprising, given the size of this basin. SPM and associated PTM can originate from very different source regions and slowly mix through “spiralling” (alternation of mobilisation and deposition processes) through the river system. Small coastal rivers like the Tet River are easier to understand in this respect, as the mobilisation of PTM often directly responds to major forcings that affect the entire river basin.

Both rivers have nevertheless in common that EF generally decrease with increasing SPM concentrations (Fig.3.4a, b). Calculation of SPM-weighted average EF for each element should allow a general estimate of the anthropogenic and natural parts in the total PTM

fluxes. These estimates were also included in Table 3.4 and confirm that Cr, Ni and Co fluxes are throughout dominated by natural contributions. For the other elements, anthropogenic contributions are not negligible and can even represent a dominant part. This is the case for the elements Cd, Zn and Cu in the Tet River, and for Cd in the Rhone River. Although specific total PTM fluxes are always greater in the Rhone River (except for Cu, where both rivers have about the same values), specific anthropogenic PTM fluxes of Cu and Zn are greater in the Tet River than in the Rhone River. This suggests the existence of specific sources for these elements in the drainage basin of the Tet River. For Cu, increased pressures are consistent with the land use practices in this part of France, clearly dominated by agricultural land use. Major cultures in the Tet River basin are vineyards and fruit trees (*Garcia Esteves et al., 2007*) which are frequently treated with $CuSO_4$ as fungicide. For Zn, identification of specific sources in the Tet River basin is less evident. This element is characterized by great atmospheric deposition rates (see above), despite a possible decrease during recent years (*Heimbürger et al., 2010*).

With regard to the elements Pb and Cd, one can notice that specific anthropogenic PTM fluxes in the Rhone River are about two times the specific fluxes in the Tet River. This probably reflects the higher degree of industrialisation along the Rhone River and greater inputs of these trace metals from industrial point sources.

3.4. PTM export during floods

Also in the Tet River, point sources could have a considerable influence on the mobilisation of anthropogenic PTM in this river. This particularly concerns the waste water treatment plant (WWTP) of Perpignan. It rejects about 10 km upstream the river mouth and can significantly alter the natural water chemistry (*Garcia Esteves et al., 2007*). By far most of the population in the drainage basin is connected to the Tet River through this station. The hypothesis that this station also impacts the PTM loads in the river is confirmed when looking at the discharge patterns during floods. Two of these events could be monitored with increased sampling frequencies. One event (Tet-F1) occurred in November 2005 and reached Q and SPM peaks of 472 $m^3 s^{-1}$ and 1530 mg L^{-1}, respectively (Fig.3.5a). Both parameters evolved more or less in parallel and during the 5 days of enhanced sampling, and the river discharged SPM about 87% of its average annual SPM flux (Tab. 3.6).

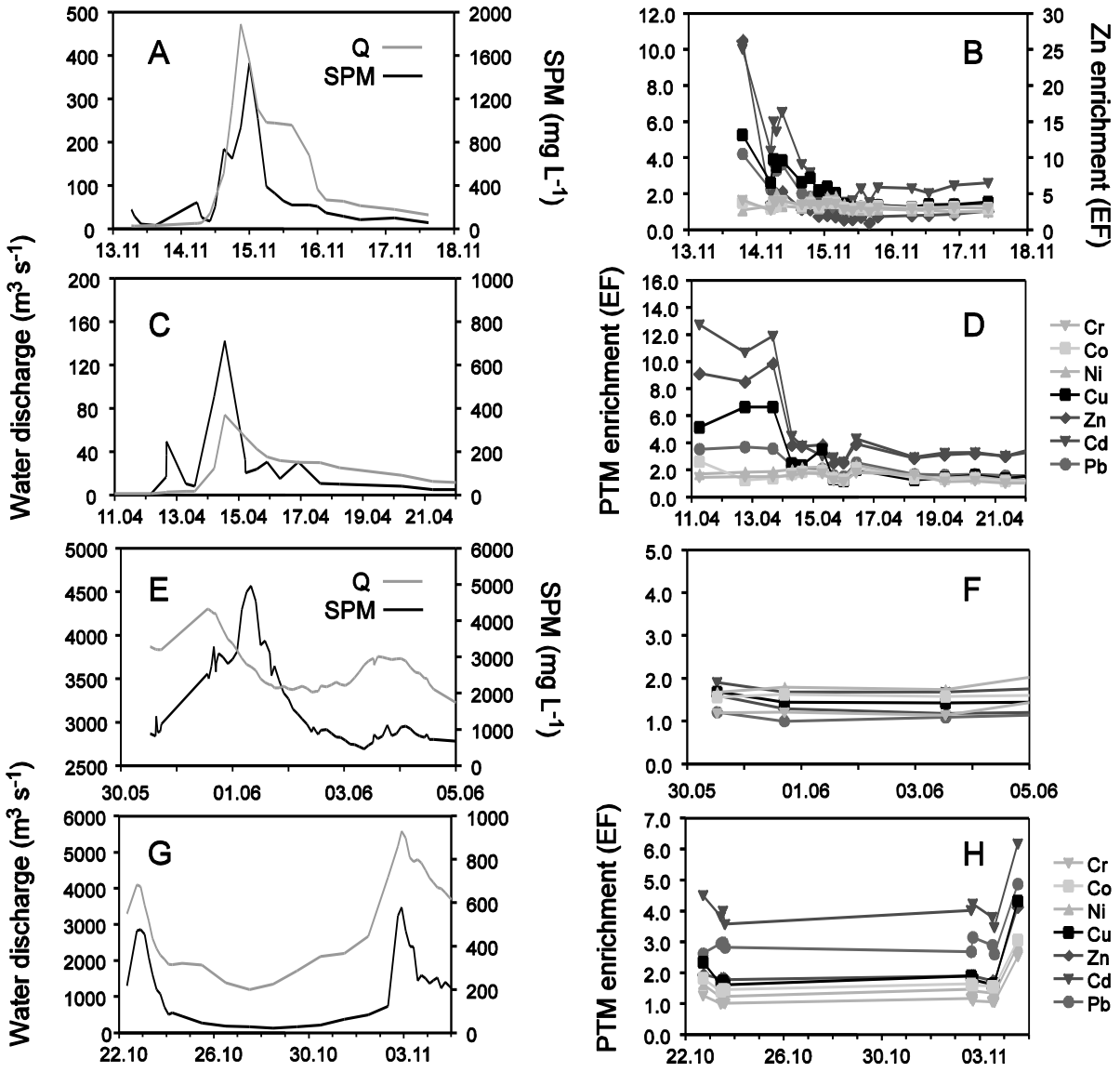

Fig.3.5 Evolution of water discharge, SPM concentrations and EF during flood events in the Tet River in 2005 (A, B) and in 2007(C, D), as well as during two successive flood events in the Rhone River in 2008 (E, F, G, H). Notice that for Zn in B, a separate axis has been drawn

The corresponding value for water discharge is 21%. At the beginning of the flood, all anthropogenic PTM were clearly enriched, reaching maximum EF values of 26 in the case of Zn (Fig.3.5b). Enrichment also continued when Q and SPM started to increase (and hence SPM fluxes), but then rapidly dropped to minimum values. Such a behaviour indicates flushing of enriched particulates which either accumulated in the river during the preceding low water stages and/ or which were injected into the river at the beginning. During floods, WWTP often have to bypass sewage waters. These waters mix with waters from evacuation networks of urban rain and can be particularly enriched in anthropogenic compounds.

Event	days	Flux	Q	SPM	Cr	Co	Ni	Cu	Zn	Cd	Pb
Tet-F1	5	total	21	87	91	91	86	100	98	100	94
		anthropogenic			76	75	62	96	99	99	94
Tet-F2	11	total	11	16	16	17	18	17	19	20	17
		anthropogenic			21	23	23	18	21	22	20
Rhone-F1	6	total	5	90	59	77	84	61	54	44	43
		anthropogenic			43	79	89	46	31	29	6
Rhone-F2	14	total	7	17	13	18	16	19	19	24	27
		anthropogenic			12	21	14	23	25	29	43

* compared to the annual averages listed in the Tables 1 and 4

Table 3.6 PTM fluxes (% mean*) from the Tet and Rhone rivers during the studied floods.

A second flooding event in the Tet River (Tet-F2) could be monitored in spring 2007. Water discharge was moderate and always remained under the flood threshold of 100 m^3 s^{-1} (Fig.3.5c). SPM concentrations, however, could reach values up to 715 mg L^{-1}. This event accounted only for about 16% of the average annual SPM flux during the study period (Tab. 3.6), but the general pattern of PTM discharge is very similar compared to the Tet-F1 event (Fig.3.5d). In both the Tet-F1 and Tet-F2 events, enrichment of anthropogenic PTM was clearly associated with elevated POC contents (Fig.3.4e). When pooling the data of both floods, correlation coefficients between POC (in % of SPM) and EF of the elements are r^2 = 0.90, 0.89, 0.87 and 0.73 for the elements Cd, Zn, Cu and Pb, respectively (n = 27 for Cd, Cu and Pb, and n= 26 for Zn; we omitted here the most prominent outlier of Fig.3.4e). For natural PTM, no significant correlation between POC and EF exist. This indicates that flushing of metallic contaminants is linked to flushing of particulate organic matter in the Tet River.

Also in the Rhone River, two floods could be monitored. One (Rhone-F1) occurred at the end of spring 2008 and had a major impact on the particulate matter transport in this river. Both Q and SPM values were peaking (Fig.3.5e) with a delay of about one day (with maximum Q and SPM values of about 4300 m^3 s^{-1} and 4960 mg L^{-1}, respectively). These exceptionally high SPM concentrations were triggered by the flooding of the Durance tributary (*Eyrolle et al., 2012*), where the outcrop of black marls provoke particularly high mechanical erosion rates (*Descroix and Olivry, 2002*; *Descroix and Mathys, 2003*).

Rhone-F1 alone accounted for about 90% of the annual average sediment discharge of this river (Tab. 3.6). Sampling frequency for PTM was relatively low, but existing data indicate only weak and invariable PTM enrichment throughout the event (Fig.3.5f). At the beginning, slightly increased EF indicate moderate flushing of anthropogenic PTM. At the end, about 10 days after peaking of SPM (data not shown), a significant increase of EF for some natural PTM was detected (Cr, Ni).

The second flood event we followed in the Rhone River (Rhone-F2) occurred in the same year during autumn (Fig.3.5g). Two discharge and SPM peaks appeared here synchronously with a delay of about 11 days. This event was triggered by intense rainfall over the Cevennes and mainly affected the right bank tributaries, such as the Ardeche and Ceze tributaries (but also provoked flooding further upstream up to the north of Lyon). Water discharge reached a much greater maximum than during the spring flood (5580 m^3 s^{-1}), but maximum SPM concentrations remained moderate (about 580 mg L^{-1}). Rhone-F2 contributed on average only to about 17% of the annual average sediment discharge (Tab. 3.6). Enrichment of PTM (Fig. 3.5g) is comparable to the values during Rhone-F1 for most elements, except Pb and Cd, for which enrichment is significantly higher. The general discharge pattern is comparable between both events too. Interestingly, also the second peaking of Q and SPM started with a slight enrichment of most PTM. But the most prominent increase of EF occurred at the end of Rhone-F2. This is consistent with the idea of a general anti-correlation of EF and Q/ SPM in rivers (see above). Also other studies reported increasing PTM concentrations and enrichment ratios at the end of floods (e.g., *Coynel et al., 2007*).

In order to evaluate the impact of flooding on the total PTM fluxes in both rivers, we calculated the respective fluxes for each of the four events described above and compared them with the average annual long-term fluxes during the study period (Tab. 3.6). We assumed linear evolutions of PTM concentrations and EF factors on an hourly basis and then averaged these data to daily means for each day of the floods. The daily mean PTM concentrations were then multiplied with the daily SPM loads and average EF were used for discrimination between the natural and anthropogenic parts. Since PTM are highly linked to SPM in both rivers (Tab. 3.3), PTM fluxes closely match SPM fluxes (Table 3.6). However, some prominent deviations from this general pattern can be noticed. For the Tet-F1 event, fluxes of anthropogenic PTM (especially Cu, Zn and Cd) are relatively more important than fluxes of SPM.

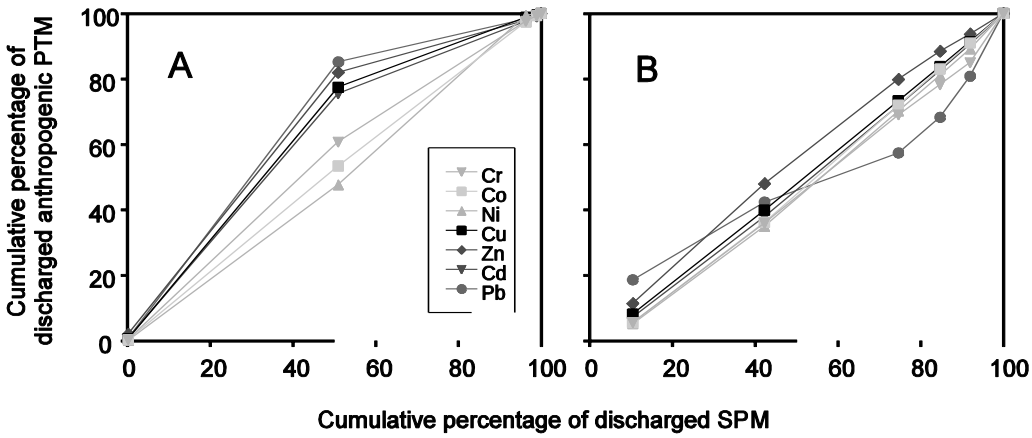

Fig.3.6 Cumulative percentage of discharged anthropogenic PTM versus cumulative percentage of discharged SPM during two major floods in the Tet (A, autumn 2005) and in the Rhone (B, spring 2008) rivers

This behaviour is the case both for total PTM fluxes and for their anthropogenic contributions. Also the temporal evolution of the PTM and SPM fluxes during Tet-F1 clearly supports flushing (Fig.3.6a). In the case of the Rhone-F1 event, discharge patterns are very different and dominated by dilution. Fluxes of anthropogenic PTM are reduced compared to the fluxes of SPM (Tab. 3.6). Anthropogenic parts in these fluxes are even less important, in particular for Pb, where the temporal evolution of the PTM and SPM fluxes indicate a clear dilution pattern (Fig.3.6b).

The Tet-F2 and Rhone-F2 events only had a moderate impact on the particulate matter fluxes in both rivers. PTM fluxes follow more or less the corresponding SPM fluxes, but anthropogenic PTM are slightly more important in the annual budgets compared to SPM. The difference is striking for anthropogenic Pb in the case of Rhone-F2: although this event only discharged 17% of the average annual SPM flux, it contributed to 43% of the anthropogenic Pb flux. This means that enrichment of this element in the Rhone River is not originating from the Durance tributary, but likely from further upstream.

4. Conclusions

We followed over several years two contrasting river systems of the Gulf of Lions and acquired a wide range of PTM concentrations during different hydrological conditions. This allowed the establishment of reliable PTM fluxes for both rivers, probably overestimated in

previous studies because of limited data availability. In comparison with analyses in alluvial sediments, we were also able to postulate natural background concentrations for both study sites and discriminate between natural and anthropogenic origins in the PTM fluxes. For the first time, direct comparison of possible anthropogenic pressures in the two contrasting river systems is therefore possible. Because of more elevated erosion rates, specific total PTM fluxes are throughout greater in the Rhone River compared to the Tet River. Specific anthropogenic PTM fluxes, however, are comparable in both systems. They are greater in the Tet River for Cu, consistent with the dominant agricultural land use practices here. The contrary is the case for Pb and Cd, suggesting a greater influence of industrial sources from point sources in the Rhone River.

Monitoring of PTM in relation to major changes of SPM and water discharge also allowed a better understanding of the transport mechanisms of these elements in the studied river basins. We often observed anti-correlation between EF and SPM concentrations, indicating that anthropogenically enriched PTM from surface soils and point sources were diluted by natural particulates from enhanced erosion and the mobilisation of ancient sediment pools. During floods, however, also flushing of enriched particulates (i.e. the concomitant increase of EF and SPM concentrations) can occur during the initial stages. This was particularly visible in the Tet River for anthropogenic PTM. Flushing can counteract dilution and attribute to floods a dominant role in the long-term fluxes of anthropogenic PTM.

Generalisation of transport mechanisms of PTM in Mediterranean rivers is therefore difficult. In the case of the Rhone River, further studies should focus on the basin internal variability and dynamics of PTM fluxes. In large basins, clear understanding of the encountered signals at the river mouth is not possible without identification of the upstream processes. In the case of coastal rivers like the Tet River, dynamics of PTM in response to major hydroclimatic forcing is likely more uniform and straightforward. Here, local point sources like WWTP can have a strong impact on the mobilisation of anthropogenic PTM and particulate organic carbon is probably their dominant carrier phase.

Acknowledgements

This work was supported by the French National Research Agency (ANR) through the ANR–EXTREMA project (contract no. ANR-06-VULN-005, 2007–2011). Additional funding was

provided by the « Agence de l'eau Rhône–Méditérranée–Corse » (Water Agency Rhone–Mediterranean–Corsica). Liquid discharge data in Arles were available thanks to the CNR (Compagnie Nationale du Rhône). The authors gratefully acknowledge J.M. Fornier for field work We are further grateful to V. Roussiez for recalculation of marine backgrounds with Al-normalisation, to P. Serrat for graphical support with Figure 1, and to L. E. Heimbürger and one anonymous reviewer for their valuable comments during the review process.

References

Antonelli, C., Provansal, M. (2003). Impact des crues méditerranéennes dans le bilan sédimentaire du Rhône aval. Proceeding of Hydrology of Mediterranean and Semi-arid Regions, IAHS publication 278, pp.243–248.

BD Hydro. (2013). Hydrological data bank hosted at the French Ministry of the Environment and of sustainable Development (http://www.hydro.eaufrance.fr/index.php). Consulted in 2013.

Bi, N., Yang, Z., Wang, H., Xu, C., Guo, Z. (2014). Impact of artificial water and sediment discharge regulation in the Huanghe (Yellow River) on the transport of particulate heavy metals to the sea . *Catena*, 121, 232–240 .

Canals, M., Puig, P., Durrieu de Madron, X., Heussner, S., Estournel, C. (2006). Flushing submarine canyons. *Nature*, 444, 354-357.

Cossa, D., Martin, J.M. (1991). Mercury in the Rhône delta and adjacent marine areas. *Marine Chemistry*, 36(1–4), 291-302.

Coynel, A., Schäfer, J., Blanc, G., Bossy, C. (2007). Scenario of particulate trace metal and metalloid transport during a major flood event inferred from transient geochemical signals. *Applied Geochemistry*, 22, 821–836 .

Descroix, L., Olivry, J.C. (2002). Spatial and temporal factors of hydric erosion in black marls badlands of the French southern Alps. *Journal of Hydrological Sciences*, 47 (2), 227–242.

Descroix, L., Mathys, N. (2003). Processes, spatio-temporal factors and measurements of current erosion in the French southern Alps: a review. *Earth Surface Processes and Landforms*, 28 (9), 993–1011.

Din, Z.B. (1992). Use of aluminium to normalize heavy-metal data from estuarine and coastal sediments of Straits of Melaka. *Marine Pollution Bulletin*, 24, 484-491.

Dumas, C., Aubert, D., Durrieu de Madron, X., Ludwig, W., Heussner, S., Delsaut, N., Menniti, C., Sotin, C., Buscail, R. (2014). Storm-induced transfer of particulate trace metals to the deep-sea in the Gulf of Lion (NW Mediterranean Sea). *Environmental Geochemistry and Health*, DOI 10.1007/s10653-014-9614-7.

Elbaz-Poulichet, F., Garnier, J.M., Guan, D.M., Martin, J.M., Thomas, A.J. (1996). The conservative behaviour of trace metals (Cd, Cu, Ni and Pb) and As in the surface plume of stratified estuaries: Example of the Rhône River (France). *Estuarine, Coastal and Shelf Science*, 42(3), 289-310.

Estournel, C., Kondrachoff, V., Marsaleix, P., Vehil, R. (1997). The plume of the Rhone: numerical simulation and remote sensing. *Continental Shelf Research*, 17(8), 899-924.

Eyrolle, F., Radakovitch, O., Raimbault, P., Charmasson, S., Antonelli, C., Ferrand, E., Aubert, D., Raccasi, G., Jacquet, S., Gurriaran, R. (2012). Consequences of hydrological events on the delivery of suspended sediment and associated radionuclides from the Rhone River to the Mediterranean Sea. *Journal of Soils and Sediments*, 12(9), 1479-1495.

Ferrand, E. (2010) Détermination des niveaux historiques en radionucléides et éléments trace métalliques à partir d'enregistrements sédimentaires. Contribution au projet ANR-EXTREMA. Rapport final de Post Doctorat – DEI/SESURE/2010-02 , 54p.

Ferrand, E., Eyrolle, F., Radakovitch, O., Provansal, M., Dufour, S., Vella, C., Raccasi, G., Gurriaran, R. (2012). Historical levels of heavy metals and artificial radionucleides reconstructed from overbank sediment records in lower Rhône River (South-East France). *Geochimica et Cosmochimica Acta*, 82, 163–182.

Garcia-Esteves, J., Ludwig, W., Kerhervé, P., Probst, J. L., Lespinas, F. (2007). Predicting the impact of land use on the major element and nutrient fluxes in coastal Mediterranean rivers: the case of the Têt River (Southern France). *Applied Geochemistry*, 22(1), 230-248.

Grousset, F.E., Quetel, C.R., Thomas, B., Donard, O.F.X., Lambert, C.E., Guillard, F., Monaco, A. (1995). Anthropogenic vs. lithogenic origins of trace elements (As, Cd, Pb, Rb, Sb, Sc, Sn, Zn) in water column particles: northwestern Mediterranean Sea. *Marine Chemistry*, 48(3–4), 291-310.

Guieu, C., Loye-Pilot, M.D., Benhyahya, L., Dufour, A. (2010). Spatial variability of atmospheric fluxes of metals (Al, Fe, Cd, Zn and Pb) and phosphorus over the whole Mediterranean from a one-year monitoring experiment: biogeochemical implications. *Marine Chemistry*, 120, 164–178.

Gumbel, E.J. (1958). Statistics of Extremes. *Columbia University Press*, New York, 375 pp.

Ibàñez, C., Canicio, A., Day, J.W., Curcó, A. (1997). Morphologic development, relative sea level rise and sustainable management of water and sediment in the Ebre Delta, Spain. *Jounal of Coastal Conservation*, 3, 191-202.

Heimbürger, L.E., Migon, C., Dufour, C., Chiffoleau, J.F., Cossa, D. (2010). Trace metal concentrations in the North-western Mediterranean atmospheric aerosol between 1986 and 2008: Seasonal patterns and decadal trends. *Science of The Total Environment*, 408(13), 2629-2638.

Lawson, N., Mason, R., Laporte, J.M. (2001). The fate and transport of mercury, methylmercury, and other trace metals in chesapeake bay tributaries. *Water Research*, 35(2), 501-515.

Lespinas, F., Ludwig, W., Heussner, S. (2009). Impacts of recent climate change on the hydrology of coastal Mediterranean rivers in southern France: case of the Languedoc-Roussillon area (Gulf of Lions). *Climatic Change*, DOI 10.1007/s10584-009-9668-1.

Loring, D. H. (1990). Lithium - A new approach for the granulometric normalization of trace-metal data. *Marine Chemistry*, 29(2-3): 155-168.

Lespinas, F., Ludwig, W., Heussner, S. (2014). Hydrological and climatic uncertainties associated with modeling the impact of climate change on water resources of small Mediterranean coastal rivers. *Journal of Hydrology*, 511, 403-422.

Ludwig, W., Probst, J. L. (1998). River sediment discharge to the oceans; present-day controls and global budgets. *American Journal of Science*, 298(4), 265-295.

Ludwig, W., Meybeck, M., Abousamra, F. (2003). Riverine transport of water, sediments, and pollutants to the Mediterranean Sea. Athens: *UNEP MAP Technical report*, Series 141, 111p.

Ludwig, W., Serrat, P., Cesmat L., Garcia-Esteves, J. (2004). Evaluating the Impact of the recent temperature increase on the Hydrology of the Têt River (Southern France). *Journal of Hydrology*, 289, 204–221.

Ludwig, W., Dumont, E., Meybeck, M., Heussner, S. (2009). River discharges of water and nutrients to the Mediterranean and Black Sea: Major drivers for ecosystem changes during past and future decades? *Progress in Oceanography*, 80(3–4), 199-217.

Maillet, G.M., Vella, C., Berné, S., Friend, P., Amos, C., Fleury, T., Normand, A. (2006). Morphological changes and sedimentary processes induced by the December 2003 flood event at the present mouth of the Grand Rhône River (southern France). *Marine Geology*, 234(1–4), 159-177.

Micó C, Recatalá, L., Peris, M., Sánchez, J. (2006). Assessing heavy metal sources in agricultural soils of an European Mediterranean area by multivariate analysis. *Chemosphere*, 65, 863–872.

Minas, M., Minas, H.J. (1989). Primary production in the Gulf of Lions with considerations to the Rhone River input. *Water Pollution Research Reports*, 13, 112–125.

Monaco, A., Ludwig, W., Serrat, P. (2009). De la terre à la mer : épilogue et perspectives. In : A. Monaco, W. Ludwig, M. Provansal, B. Picon (éds), *Le golfe du Lion. Un observatoire de l'environnement en Méditerranée*. Editions QUAE, 338 pp.

Nicolau, R., Lucas, Y., Merdy, P., Raynaud, M. (2012). Base flow and stormwater net fluxes of carbon and trace metals to the Mediterranean sea by an urbanized small river. *Water Research*, 46(20), 6625-6637.

Nolting, R. F., Helder, W. (1991). Lead and zinc as indicators for atmospheric and riverine particle-transport to sediments in the gulf of lions. *Oceanologica acta*, 14(4), 357-367.

Ollivier, P., Radakovitch, O., Hamelin, B. (2011). Major and trace element partition and fluxes in the Rhône River. *Chemical Geology*, 285(1–4), 15-31.

Oursel, B., Garnier, C., Zebracki, M., Durrieu, G., Pairaud, I., Omanović, D., Cossa, D., Lucas, Y. (2014). Flood inputs in a Mediterranean coastal zone impacted by a large urban area: Dynamic and fate of trace metals. *Marine Chemistry*, 167, 44-56.

Pont, D., Simonnet, J.P., Walter, A.V. (2002). Medium-term Changes in Suspended Sediment Delivery to the Ocean: Consequences of Catchment Heterogeneity and River Management (Rhône River, France). *Estuarine, Coastal and Shelf Science*, 54 (1), 1–18.

Radakovitch, O., Roussiez, V., Ollivier, P., Ludwig, W., Grenz, C., Probst, J.L. (2008). Input of particulate heavy metals from rivers and associated sedimentary deposits on the Gulf of Lion continental shelf. *Estuarine, Coastal and Shelf Science*, 77, 285-295.

Raimbault, P., Durrieu de Madron, X. (2003). Research activities in the Gulf of Lion (NW Mediterranean) within the 1997–2001 PNEC project. *Oceanologica Acta*, 26(4), 291-298.

Roussiez, V., Ludwig, W., Probst, J.L., Monaco, A. (2005). Background levels of heavy metals in surficial sediments of the Gulf of Lions (NW Mediterranean): an approach based on ^{133} Cs normalization and lead isotope measurements. *Environmental Pollution*, 138, 167-177.

Roussiez, V., Ludwig, W., Probst, J.L., Monaco, A., Bouloubassi, I., Buscail, R., Saragoni, G. (2006). Sources and sinks of sediment-bound contaminant in the Gulf of Lions (NW Mediterranean Sea): a multi-tracer approach. *Continental Shelf Research*, 26, 1843-1857.

Roussiez, V., Ludwig, W., Radakovitch, O., Probst, J.L., Monaco, A., Charrière, B., Buscail, R. (2011). Fate of metals in coastal sediments of a Mediterranean flood-dominated system: An approach based on total and labile fractions. *Estuarine, Coastal and Shelf Science*, 92(3), 486-495.

Roussiez, V., Heussner, S., Ludwig, W., Radakovitch, O., Durrieu de Madron, X., Guieu, C., Probst, J.-L., Monaco, A., Delsaut, N. (2012). Impact of oceanic floods on particulate metal inputs to coastal and deep-sea environments: A case study in the NW Mediterranean Sea. *Continental Shelf Research*, 45, 15-26.

Serrat, P., Ludwig, W., Navarro, B., Blazi, J. L. (2001). Variabilité spatio-temporelle des flux de matières en suspension d'un fleuve côtier méditerranéen: la Têt (France). *Comptes Rendus de l'Académie des Sciences-Series IIA-Earth and Planetary Science*, 333(7), 389-397.

Sutherland, R.A. (2000). Bed sediment-associated trace metals in an urban stream, Oahu, Hawaii. *Environmental Geology*, 39, 611–627.

Tam, N.F.Y., Yao, M.W.Y. (1998). Normalization and heavy metal contamination in mangrove sediments. *Science of the Total Environment,* 216, 33-39.

Chapter IV

Transfer of particulate trace metals in the Gulf of Lion submarine canyons

In this chapter we follow the land-to-sea continuum thread of this work by focusing on submarine canyon environments and what is transiting through them.

This chapter is subdivised in two sections, each one centered on a particular extreme event of transfer and its relative contribution to the annual budget of potentially harmful elements brought by the Gulf of Lion rivers. The first section focuses on the impact of a moderate storm event, which was studied during the CASCADE oceanographic cruise; whereas the second section investigates the export caused by cascading events of winter 2005-06.

Storms and the waves they generate are of great importance in sediment dynamic processes. In the Gulf of Lion area, they have been studied but mostly regarding their impact on sediment delivery, reworking and export (e.g. *Guillén et al., 2006*). However very few interest has been given to contaminants and their dynamic, although this is closely related to the physical processes evoked just above. This is why section IV.1 gives a first attempt of a budget of some particulate trace elements exported by the moderate storm of 2011. However this study is located at the upper end of the Gulf of Lion's continental shelf (up to 365m depth). In order to further our understanding of the trace metal cycle in this environment, we studied the impact of cascading events in the Cap de Creus canyon and the adjacent open slope. Indeed, dense shelf water cascading from the shelf has been occurring in, at least, 63 identified sites around the world (*Ivanov et al., 2004; Durrieu de Madron et al., 2005*) and extreme events may be in some regions, a dominant mechanism to remove particulate matter and sediment-bound contaminants from the continental shelf deposits, and to deliver it down the slope and up to the abyssal plain (e.g. *Puig et al., 2013*) in a multistep mechanism (*Palanques et al., 2012*). In the Mediterranean, the Gulf of Lion is one of the 3 important sites where this off-shelf sediment transfer takes place.

Section IV.1 was published in *Environmental Geochemistry and Health* and section IV.2 is currently in preparation for submission.

I actively participated in the CASCADE oceanographic cruise, hence all the data used here were collected, prepared and analyzed by myself. Sediment trap samples used in section IV.2 were collected in the frame of the HERMES program, prior to the start of my Ph.D but they were prepared and analyzed under the same protocol.

Chapter IV-1

Storm-induced transfer of particulate trace metals in the Gulf of Lion

Storm-induced transfer of particulate trace metals to the deep-sea in the Gulf of Lion (NW Mediterranean Sea)

Dumas C. [(1)*], Aubert D. [(1)], Durrieu de Madron X. [(1)], Ludwig W. [(1)], Heussner S. [(1)], Delsaut N. [(1)], Menniti C. [(1)], Sotin C. [(1)], Buscail R. [(1)]

[(1)] *Université Perpignan Via Domitia, CEntre de Formation et de Recherche sur les Environnements Méditerranéens, CNRS, UMR 5110, F-66860 Perpignan, France*

CNRS, CEntre de Formation et de Recherche sur les Environnements Méditerranéens,UMR 5110, F-66860, Perpignan, France

*Corresponding author: chloe.dumas@univ-perp.fr; +33667071729

Abstract

In order to calculate budgets of particulate matter and sediment-bound contaminants leaving the continental shelf of the Gulf of Lion, settling particles were collected in March 2011 during a major storm, using sediment traps. The collecting devices were deployed in the Cap de Creus submarine canyon, which represents the main export route.

Particulate matter samples were analyzed to obtain mass fluxes and contents in organic carbon, Al, Cr, Co, Ni, Cu, Zn, Cd, Pb and La, Nd and Sm. The natural or anthropogenic origin of trace metals was assessed using enrichment factors (EFs). Results are that Zn, Cu and Pb appeared to be of anthropogenic origin, whereas Ni, Co and Cr appeared to be strictly natural. The anthropogenic contribution of all elements (except Cd) was refined by acid-leaching (HCl 1N) techniques, confirming that Zn, Cu and Pb are the elements that are the most enriched. However, although those elements are highly labile (59-77%), they do not reflect severe enrichment (EFs < 4). Most particles originate from the Rhone river. This has been confirmed by two different tracing procedures using Rare Earth Elements ratios and concentrations of acid-leaching residual trace metals. Our results hence indicate that even in this western extremity of the Gulf of Lion, storm events mainly export Rhone derived particles via the Cap Creus submarine canyons to the deep-sea environments. This export of material is significant as it represents about a third of the annual PTM input from the Rhone river.

Keywords: Particulate trace metal, storm event, Gulf of Lion, Cap de Creus canyon, element geochemistry, sediment traps.

1. Introduction

For many continental margins, submarine canyons are preferential transport routes for Suspended Particulate Matter (SPM) transfer, from the coastal zone to the adjacent basin (*Allen & Durrieu de Madron, 2009; Puig et al., 2014*). Many studies have been conducted on these environments throughout the world, especially focusing on processes responsible for sediment transport (e.g., *Genesseaux et al., 1971*; *Palanques et al., 2006*; *Xu et al., 2013*), on fluxes exported by those hydrodynamic events (e.g., *Kao & Milliman, 2008*; *Ulses et al., 2008b; Huh et al., 2009*) and on the geochemical composition of the exported matter (*Puig et al., 1999*; *Pasqual et al., 2010*). Studies on exported particles from the shelf to the canyons are usually derived from sediment trap deployments and their derived downward fluxes calculations (*Biscaye et al., 1988*; *Monaco et al., 1990*; *Heussner et al., 1999 and 2006*).

The Gulf of Lion (GoL) has been the object of numerous studies over the last two decades. This crescent-shaped passive margin is indented by numerous submarine canyons, the most important in terms of export being the Cap de Creus canyon at its southwestern limit (*see Monaco et al., 1990; Raimbault and Durrieu de Madron, 2003; Durrieu de Madron et al., 2008 and references therein*).

The GoL is a continental margin fed by the large Rhone River in its eastern part and smaller coastal rivers in its western part. Sediment transport processes on the shelf are controlled by the Rhone River sediment source (supplying 90% of freshwater and suspended sediment inputs to the GoL), by the morphology of the shelf and its circulation patterns (*Ludwig et al., 2003; Drexler and Nittrouer, 2008*). Predominant meteorological regimes induce intense hydrodynamical events such as floods, marine storms, downwelling and dense water formation, which steer the sediment inputs, resuspension and transport on the shelf (*Guillen et al., 2006*; *Palanques et al., 2006*; *Bonnin et al., 2008; Bourrin et al., 2008*; *Durrieu de Madron et al., 2008*; *Palanques et al., 2008; Ulses et al., 2008a and c*).

Strong marine storms and dense shelf water cascading control off-shelf sediment export, which culminates in wintertime. The regional cyclonic circulation and the narrowing of the shelf in the southwest lead to shelf sediment export via the southwestern-most canyons, namely the Lacaze-Duthiers and Cap de Creus canyons. Sediment effectively bypasses the canyon heads due to the frequent occurrence of intense currents in this part of the GoL. Sedimentation in the canyon heads is asymmetrical with erosion (and coarse sediment) dominating the western flank and main entrance, and drapes of fine-grained sediment on the eastern flank (DeGeest et al., 2008).

The GoL coastal area is heavily inhabited, and thus, subject to significant inputs of contaminants along its coast (EEA, 2006). Indeed, contamination by anthropogenic trace metals has been an issue over the last decade and sources, transport pathways and budgets have been investigated mostly for the coastal zone (Balls et al., 1997; Puig et al., 1999; Radakovitch et al., 2008; Roussiez et al., 2011; Santos-Echeandia et al., 2012).

Trace metals are sediment-bound contaminants associated with fine river particles (Salomons and Förstner, 1984) and they arise from different sources including atmospheric deposition, soil erosion, land runoff and industrial or wastewater discharges. Each of these sources has specific fingerprints, allowing the tracing of its particles once they enter the marine environment.

Particulate Trace Metals (PTM) stored in the GoL shelf sediments are now well documented (Migon et al., 1998; Marin and Giresse, 2001; Radakovitch et al., 2008; Roussiez et al., 2005 and 2006). These studies showed a decreasing enrichment gradient while going seaward and underlined the role of the sediment source and the organic carbon in the distribution of anthropogenic trace metals.

Concentrations of PTM in particles of the shelf were studied in different canyons of the GoL (Grousset et al., 1995; Roussiez et al., 2006). These studies aimed at determining the anthropogenic or lithogenic origins of the PTM, and at assessing the temporal (seasonal) and spatial (along margin and down canyon) variability of the composition.

More recently, Roussiez et al. (2012) investigated the impact of a strong flood and marine storm event, which took place in December 2003, on the budget of the PTM export from the GoL shelf. They demonstrated that export fluxes of PTM in canyon heads could represent more than half the amount of the annually supplied PTM by rivers. The attribution of source specific signatures suggested that the exported particles mainly derive from continuous particle mixing on the shelf. However, the detailed dynamic (i.e. high frequency variability) of the PTM during such an event remains still poorly understood as this study dealt with weekly average sample that blurred the short-lasting signal of the storm.

The CASCADE (Cascading, Storm, Convection, Advection and Downwelling Events) oceanographic cruise, conducted in March 2011, allowed to describe the transport of particulate matter and trace metals exported from the shelf to the basin during a significant marine storm. It also gave opportunity to go further in the tracing of the exported PTM fluxes. Based on a higher sediment trap resolution (daily scale) as well as a high-frequency water sampling (tri-hourly scale), the goals of this study were to characterize the origins, characteristics (concentration, enrichment factors, bioavailability) and fluxes of the PTM

exported in the water column during the storm. Evaluation of the potential of such exporting events to purify the coastal zone from land-derived contaminants is crucial in the understanding of their implication in biogeochemical cycles and the evaluation of their potential impacts on living resources from the canyon and deeper environments.

2. Material and methods

2.1 Characteristics of the March 2011 marine storm

Southeasterly and easterly winds episodes are frequent but short during autumn and winter in the GoL. They generate major storms and floods by bringing humid air masses towards Massif Central and Pyrenean mountains, forcing precipitations (*Ulses et al., 2008c*), as well as large swells and storm-induced downwelling that allow redistribution of the particulate matter from the continental shelf to the open sea. During winter 2011 and the CASCADE oceanographic cruise, an eastern storm occurred between the 12th and 16th of March. Maximum significant wave height of 4.6m measured on the inner shelf and strong along-shore current of more than 60 cm.s^{-1} classify this event as a typical winter storm with a return period of 1 to 2 years. Those rough conditions were observed along the western shelf, and transported large amounts of coastal water and resuspended sediment towards the southwestern end of the shelf and its canyons (see Martín et al., 2013).
Between the 11th and 12th of March, a storm-induced downwelling progressively pushed warmer, fresher and lighter shelf water down the head of the Cap de Creus canyon. By the 13th of March, this coastal water mass reached depths of 350m associated with currents up to 90 cm.s^{-1}. A very large increase of the particulate matter transport was observed during the storm by both turbidity sensors and sediment traps (Martín et al., 2013).

2.2 Sampling strategy

Two instrumented mooring lines were deployed along the southern flank of the Cap de Creus canyon (CCC) during the CASCADE cruise (Fig.4.1): one at 290m depth (T1) and one at 365m (T2). The sampling period was from the 3rd to the 21st of March 2011. Each mooring was equipped with acoustic Doppler current profiler (ADCP) at 160 m above bottom (mab), turbidimeters at 10, 75 and 115 mab, and a Technicap PPS3/3 sequential sampling sediment

trap at 40 mab. All the equipments are fully described by Martín et al. (*2013*).

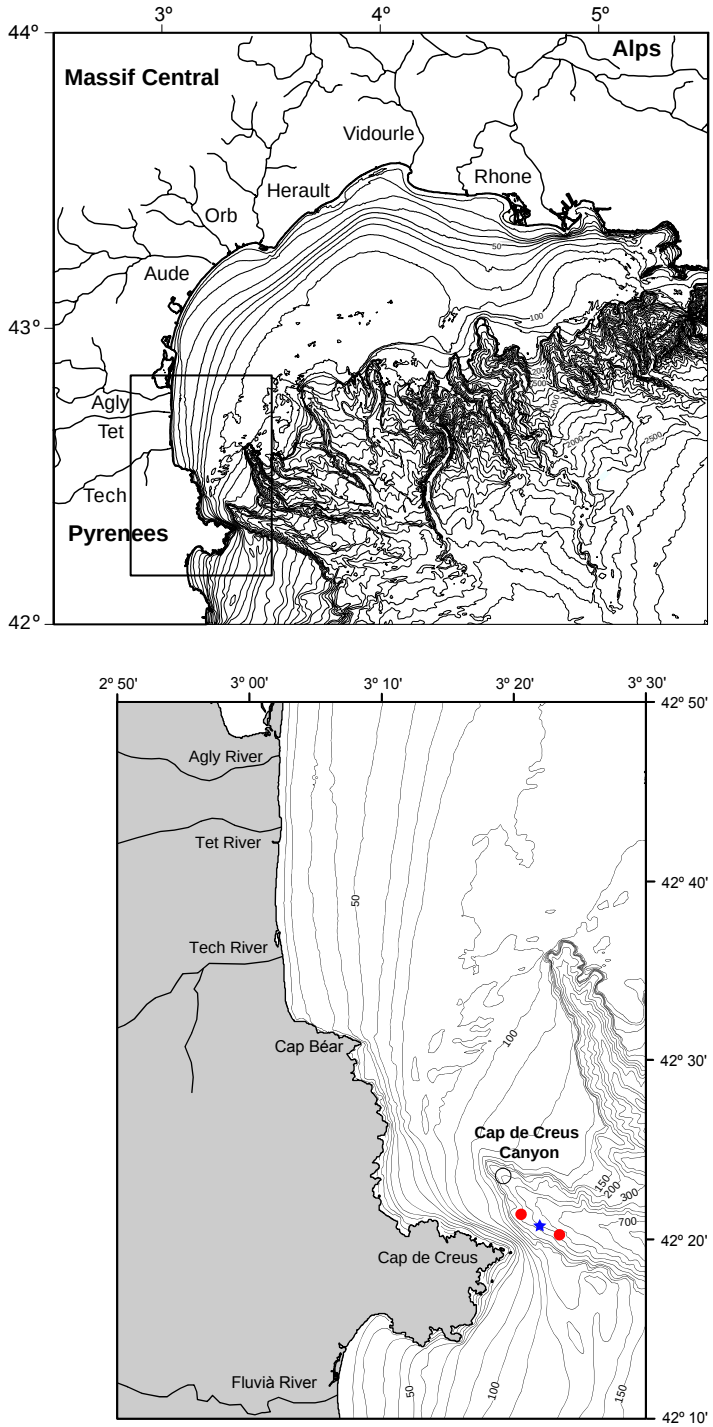

Fig.4.1 Map of the study area, the Gulf of Lion and the Cap de Creus canyon. Red circles indicate the location of both sediment traps deployed on the southern flank of the CCC during the CASCADE campaign (T1 at 290m depth and T2 at 365m depth), and the blue star represents the position of the station CX from which the high-frequency water sampling was performed

Sediment traps are equipped with 12 cups and were set to sample during the period of the CASCADE cruise. Hence the collecting plates were programmed to sample the downward particle flux at 35h intervals. The cups were poisoned with a buffered 2% formaldehyde solution in filtered seawater before deployment.

Station CX (Fig.1), located between the two moorings, was continuously sampled with a CTD/Rosette from the 13th to the 15th of March 2011, providing high frequency changes of the hydrology, suspended sediment concentration and sediment-bound contaminants composition during the storm. Since the CTD could not be loaded on board during the monitoring due to the very harsh sea state, profiles were repeated in a Yo-Yo mode (without taking the CTD out of the water) and only one water sample was taken every 6 profiles (2-3 hours) next to the bottom (2-3 mab) using 1010X Clean Niskin bottles mounted on the rosette for the trace metal analysis. Eleven near-bottom water sampling were collected from 13th March 2011 at 07:34 to 14th March 2011 at 10:31 (UTC time).

After the storm, a series of sediment samples were collected across the southern flank of the CCC from 120m to 497m water depth. The first 4 stations from 120 to 347m were sampled with a box-corer as the sediment was very stiff and coarse. The last 2 stations at 442 and 497m were also sampled with a multi-tube corer as softer sediment was encountered. Cores were carefully sliced on board in layers of 1 cm from the surface to 5 cm-depth using acid-cleaned plastic spatulas, then stored in polyethylene plastic bags and kept at 4°C. Samples were freeze-dried and homogenized prior to analysis. Only the first centimeter of the sediment from each station was analysed in order to compare the material collected in sediment traps and the expectedly deposited material, resulting from the storm resuspension.

2.3 Sample treatment and analytical procedures

After recovery, trap samples were stored in the dark at 2-4°C until processed in the laboratory. The procedure described by Heussner et al. (*1990*) was followed in order to obtain the downward total mass fluxes (TMF expressed in $g.m^{-2}.d^{-1}$).

Samples were recovered in clean conditions, after several rinses to eliminate traces of formaldehyde solution, then filtered on pre-weighted glass-fiber filters for organic carbon analysis and on pre-weighed cellulose acetate filters (47 mm in diameter and 0.22 µm in pore size) for trace metals analysis. They were then rinsed with distilled water in order to remove salt and dried at 40°C for at least 24h for dry weight determination.

Samples for organic carbon analysis were decarbonatated with repeated additions of H_3PO_4 (1M) and HCl (2M) with drying steps in between until no effervescence occurred. Particulate Organic Carbon (POC) content was measured using a VarioMAX CN, Elementar instrument at the CEFREM laboratory (Perpignan, France).

Particulate matter was recovered for trace metals analysis from cellulose acetate filters, in de-ionized water by using ultrasonic baths. Mineralization of the dried material was performed in Teflon beakers with successive mixtures of high quality (TraceSELECT®, Fluka or Suprapur, Merck) nitric and hydrofluoric acids (HNO_3-HF) and nitric acid and oxygen peroxide (HNO_3-H_2O_2). Major, trace element and REE concentrations were measured by Inductively Coupled Plasma Mass Spectrometry (ICP-MS, Agilent 7000x) at the CEFREM laboratory (Perpignan, France).

Marine sediment reference material (GSMS-2 and GSMS-3 from NRCGA-CAGS, China) were mineralized and analyzed under the same conditions as the samples and provided suitable recoveries (errors < 5% for all elements, except for Cr in GSMS-3 and Cd in GSMS-2 for which recoveries ranged from 85% to 95% and 67% to 73% respectively). Analytical blanks did not reveal any sign of contamination (contribution < 0.5% for Al, Cr, Co, Ni and Pb, < 2% for Cu and Zn) except for Cd (blanks < 10%). Results for this last element have therefore to be considered with more caution but should still be indicative for general considerations.

Grain-size analysis was performed on a Coulter LS 230 Laser Particle Size Analyzer in the GRC Geociències Marines laboratory (Barcelona, Spain).

Calculation methods

Anthropogenic inputs in trace metal concentrations were assessed in sediment trap samples on the basis of background-normalized metal ratios, commonly designated as Enrichment Factors (EF). The calculation of EFs allows determining the origin of the sinking material and the trace metals it contains: natural (rock and soil erosion) vs. anthropogenic. An EF superior to 1.5 indicates significant enrichment from anthropogenic origin (*Sutherland et al., 2000*).

In this work, we calculated EFs using the equation below, relative to pre-industrialized reference values:

$$EF = \frac{\left(\frac{X}{C}\right) sample}{\left(\frac{X}{C}\right) background}$$

where C is a conservative element strongly associated with the finest sediment fraction (clays), used in order to prevent the effect of variation in supply of major sediment components with which the trace metals are associated. In this study, the proxy of crustal carrier chosen as a normalizer is Al. It is a proxy for clay minerals, which are commonly recognized as the most important carrier of trace metals together with their coating formations like organic matter. It has then been widely used in previous studies on marine environments as a normalizer of grain-size variations, as well as in the calculation of EF in heavy metal contamination studies (*Din, 1992*; *Tam and Yao, 1998; Roussiez et al., 2005*).

Regarding the choice of the background reference, Upper Continental Crust (e.g. *Wedepohl, 1995*) is commonly used by default in many studies, although the use of a global reference does not take into account the local lithology that can be highly variable from site to site. In the GoL, the Rhone River is known to be the dominant source of particles. Hence pre-industrial reference values were determined in deep-samples from an ancient Rhone riverbank core, drilled downstream in order to be representative of the whole "natural" Rhone River catchment. This core has already been used as a reference in *Ferrand et al.* (*2012*). Core levels were dated using radiocarbon dating to ensure the reference was pre-industrial. This work allowed us to compare different background references as well as normalizers.

Tracing procedures

Discrimination of the particles origin is assessed by two means: (1) the residual signature of particles collected in the traps, after HCl-single extraction (*Langston et al., 1999*; *Audry et al., 2006*), and (2) the use of Rare Earth Elements (REE) as a lithological signature of watersheds from which particles might come from (*Araújo et al., 2002*; *Roussiez et al., 2013*).

The first procedure was realized in order to desorb elements fixed onto particles that are sensitive to HCl. These elements are considered as potentially available when entering the environment. Hence, the residual part would represent the natural mineral signature of the catchment from which the particles originate.

The HCl-single extraction experiment was conducted on particulate matter from the CASCADE sediment traps samples and also on SPM from the Rhone and Tet rivers, two potential sources of the particulate matter recovered in the traps. Indeed, the Rhone is the main conveyor of liquid and solid fluxes in the NW Mediterranean Sea but the Tet is located nearest to the CCC, hence its signature in the sediment traps could be less diluted by other sediment sources.

3. Results & Discussion

3.1 Characterization of the exported material in March 2011

3.1.1 General characteristics of particulate material

The temporal variations of TMF collected by near-bottom traps as well as the dynamic of the POC content are represented in Fig 4.2. Most of the sediment transport observed during the CASCADE cruise occurred within 2 days. As described in Martín et al. (*2013*), two consecutive eastern storms (on the 8th and 13th of March 2011) caused storm-induced downwelling that drove coastal waters down the Cap de Creus submarine canyon, delivering fresh material to the deep-sea environment. Although the first storm on the 8th was visible in terms of TMF in both T1 and T2 (17 and 37 g.m^{-2}.d^{-1} respectively, see Table 4.1), TMF peaked on the 13th in T1 with 119 g.m^{-2}.d^{-1} and on the 14th in T2 with 149 g.m^{-2}.d^{-1} (Fig.4.2a and b). This time frame corresponds to the second storm that was monitored directly from the ship at station CX in-between both moored lines T1 and T2 (Fig.2c). During this sampling period (13-14th March 2011), the water column was characterized by its low salinity (37.65-38.00), low temperature (11.5-12.5°C) and high suspended particulate matter (2.9 to 18.6 mg.L^{-1}) in the bottom layer (Table 1). Currents at 210m depth were strong (up to 90 cm.s^{-1}) and clearly oriented along the canyon flank during the whole period. After the storm, fresh sediment was only encountered at 442m depth, on the first top 2 cm of cores. For the shallower stations, fine sediment samples could hardly be collected as the sediment was very coarse (shells and pebbles) and indurate.

POC content in both sediment traps ranged between 1.2 and 1.9% (Table 4.1). When zooming on the two cups that coincide with the 13-14th March storm event, one can see that POC content variations in the water samples that ranged from 0.7 to 3 % were, on average, larger than in the sediment trap samples. The lowest POC content values were found in the superficial sediment across the southern flank of the canyon. Values ranged from 0.2 % to 1 %. The highest POC content amongst those values corresponded to the deeper station at 442 m depth, where “fresh” deposits of fine sediment were collected. The temporal evolution of TMF was opposite to the temporal evolution of the POC content in the different media (trap samples, water samples). POC in sediment traps was maximum (1.9 %) when TMF was minimum before the storm, and dropped (1.2 %) when TMF peaked during the storm

	reference date	Flux (g.m^{-2}.d^{-1})	POC (%)	Clay (%)	Silt (%)	Sand (%)	D_{50} (mm)	Al (mg.g^{-1})	Cr (µg.g^{-1})	Co (µg.g^{-1})	Ni (µg.g^{-1})	Cu (µg.g^{-1})	Zn (µg.g^{-1})	Cd (µg.g^{-1})	Pb (µg.g^{-1})	La (µg.g^{-1})	Nd (µg.g^{-1})	Sm (µg.g^{-1})
T1	04/03/11	6.0	1.7	13.0	70.6	16.4	16.6	58.6	78.6	10.8	36.6	60.6	190.7	0.12	40.5	27.4	24.0	4.6
(290m)	05/03/11	17.0	1.5	15.7	74.0	10.3	12.9	57.4	75.2	10.5	35.2	41.9	163.3	0.12	39.0	27.0	23.9	4.8
	07/03/11	8.3	1.6	15.5	74.1	10.4	12.7	59.4	79.1	10.9	38.2	54.8	184.2	0.41	39.9	27.5	23.9	4.6
	08/03/11	17.2	1.3	18.3	74.8	6.9	11.8	58.2	75.5	10.6	35.4	37.1	164.3	0.11	38.8	25.4	22.3	4.3
	10/03/11	3.9	1.6	13.9	77.7	8.4	13.4	57.7	81.4	11.0	39.7	64.5	188.1	0.11	40.2	26.6	23.2	4.4
	11/03/11	6.7	1.9	14.7	79.6	5.7	12.7	59.0	82.1	11.4	40.7	55.9	184.3	0.21	40.6	27.5	23.9	4.4
	13/03/11	119.2	1.2	15.7	76.7	7.6	12.9	57.1	73.2	10.1	33.0	38.1	161.6	0.15	39.7	27.2	23.9	4.5
	14/03/11	103.3	1.4	19.7	76.9	3.4	10.0	57.2	76.3	9.7	34.4	40.2	161.4	0.14	41.1	27.0	23.3	4.6
	16/03/11	95.3	1.3	19.0	77.7	3.3	10.6	60.7	82.3	10.7	37.2	40.9	153.5	0.14	44.5	29.7	25.7	4.9
	17/03/11	5.9	1.6	14.4	78.5	7.1	12.9	56.2	80.6	11.1	39.3	58.8	171.4	0.11	39.4	33.5	28.3	5.2
	19/03/11	3.4	1.6	14.9	78.3	6.8	12.6	55.1	81.4	10.9	42.0	68.5	181.6	0.11	39.4	27.2	23.5	4.5
	MEAN	**35.1**	**1.5**	**15.9**	**76.3**	**7.8**	**12.6**	**58.2**	**77.1**	**10.3**	**35.2**	**41.4**	**161.7**	**0.15**	**41.2**	**27.8**	**24.2**	**4.7**
T2	04/03/11	7.0	1.7	14.8	74.5	10.7	14.1	59.9	80.7	11.2	37.8	48.7	140.4	0.70	40.5	28.3	24.3	4.5
(365m)	05/03/11	11.7	1.7	14.4	73.3	12.3	14.4	61.5	82.9	11.7	40.0	44.6	152.4	0.14	40.3	28.8	24.4	4.7
	07/03/11	16.7	1.6	18.4	75.4	6.2	11.2	59.5	78.8	11.2	38.3	32.9	144.5	0.13	39.2	28.1	24.2	4.8
	08/03/11	37.4	1.3	16.6	73.5	9.9	13.3	59.2	78.1	10.9	36.6	40.4	146.1	0.13	40.9	27.6	24.0	4.7
	10/03/11	8.4	1.7	15.8	80.9	3.3	11.7	58.9	79.7	11.1	38.8	45.9	159.5	0.11	39.9	26.2	22.8	4.4
	11/03/11	6.7	1.8	13.3	80.5	6.2	13.2	57.8	79.1	11.1	39.4	49.2	164.8	0.15	38.4	26.5	23.6	4.4
	13/03/11	125.5	1.2	16.0	77.9	6.1	12.2	59.5	76.0	10.6	35.6	37.8	184.6	0.239	41.3	26.4	23.4	4.6
	14/03/11	149.0	1.3	20.5	76.7	2.8	9.6	59.2	78.5	10.2	35.4	41.1	172.4	0.13	41.9	28.1	24.3	4.7
	16/03/11	41.8	1.3	18.1	77.1	4.8	10.6	60.8	80.3	10.7	36.9	41.2	172.9	0.06	41.8	28.5	25.0	4.8
	17/03/11	7.6	1.5	15.4	78.0	6.6	12.2	59.8	82.8	11.4	41.1	47.4	181.1	0.19	39.4	30.1	25.8	4.8
	19/03/11	6.3	1.6	14.9	77.8	7.3	12.8	59.2	82.6	11.3	40.5	54.4	181.5	0.12	39.8	27.5	23.4	4.6
	MEAN	**38.0**	**1.5**	**16.2**	**76.9**	**6.9**	**12.3**	**59.5**	**78.2**	**10.6**	**36.3**	**40.5**	**171.4**	**0.16**	**41.2**	**27.6**	**24.1**	**4.7**
High-frequency temporal sampling		**(mg.L^{-1})**																
	13/03/11 07:34	3.5	3.0					61.4	75.9	10.0	33.7	20.6	165.4	0.18	41.9	27.7	24.2	4.5
	13/03/11 10:23	6.3	1.3					57.2	74.4	9.0	31.9	20.2	121.9	0.25	41.8	24.2	20.7	3.9
	13/03/11 13:07	2.9	2.1					48.9	71.2	8.3	29.9	25.5	104.5	0.37	42.0	19.3	16.9	3.3
	13/03/11 15:25	4.1	2.0					64.1	81.7	10.0	35.4	22.2	133.9	0.18	42.3	27.2	23.3	4.4
	13/03/11 17:18	8.5	1.1					69.9	91.2	10.8	39.0	28.1	136.6	0.23	52.1	28.0	24.4	4.8
	13/03/11 19:30	8.9	1.4					53.4	73.1	8.4	29.7	22.4	203.4	0.21	39.7	22.4	19.1	3.7
	13/03/11 22:13	4.5	1.9					69.1	88.9	10.7	38.9	24.5	153.6	0.22	47.9	28.2	24.5	4.7
	14/03/11 00:22	8.3	1.2					53.9	72.7	8.7	31.2	22.1	131.3	0.31	60.0	22.3	19.4	3.7
	14/03/11 02:40	7.3	1.5					58.9	74.3	9.1	32.7	20.3	131.1	0.17	38.8	24.5	20.9	4.1
	14/03/11 04:44	18.6	0.7					53.0	68.9	8.2	30.1	20.9	133.5	0.20	37.8	21.5	18.8	3.5
	14/03/11 10:31	4.4	2.5					69.0	90.2	10.9	40.8	24.2	130.2	0.20	46.5	27.4	23.6	4.6
	MEAN	**7.0**	**1.7**					**58.6**	**76.6**	**9.2**	**33.1**	**22.5**	**141.8**	**0.22**	**44.1**	**24.1**	**20.9**	**4.0**
Sediment core (CCC)		**Prof. (m)**	**POC (%)**															
	CE08 (Mtd)	442	1.0	10.6	77.7	11.7	24.3	64.1	88.5	10.3	34.1	22.3	/	0.14	43.0	29.4	25.0	4.7
	CE09 (Mtd)	497	0.4	26.0	64.6	9.5	9.7	36.4	27.7	5.8	10.3	5.7	/	0.05	20.7	12.1	10.9	2.2

Table 4.1. TMF and SPM fluxes, POC content, grain-size parameters and particulate trace metal concentrations from the CASCADE sediment trap samples, high-frequency water sampling and sediment cores. Mean trace element concentrations are flux-weighted mean concentrations.

(Fig.4.2a, b). In water samples, the high-frequency SPM and POC dynamics (Fig.4.2c) were more noisy, but generally showed opposite fluctuations.

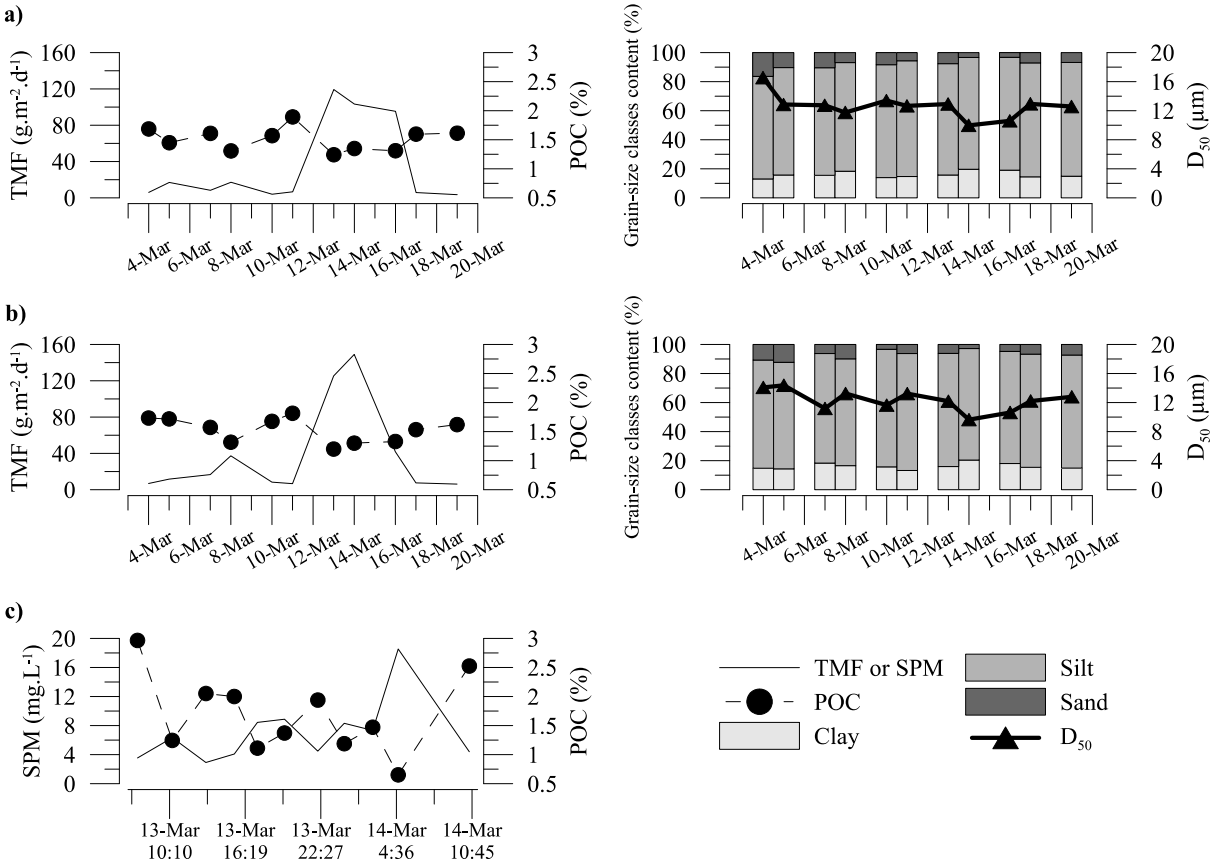

Fig.4.2 TMF fluxes in $g.m^{-2}.d^{-1}$ and SPM flux in $mg.L^{-1}$, POC content (●) in %, mass median diameter (▲) in mm and grain-size classes content (%) in a) CASCADE T1 sediment trap; b) CASCADE T2 sediment trap and c) CASCADE high-frequency water sampling

The composition of exported particles was also characterized by the relative proportion of each grain-size class (clay, silt and sand) and by the modal grain size (D_{50}) (Fig.2d,e). Sinking particulate material in traps contained mostly silt (70-80%), and in a lesser extent clay (13-20%) and sand (3-16%) (Table 4.1). Superficial sediment for the deepest coring stations at 442m and 497m equally comprised mostly silt (65-78%), and in a lesser extent sand (10-12%). However, the clay content was higher in the deeper core (26 vs 11%). D_{50} (Fig.2) varied between 10 and 17 µm in the sediment trap samples with a mean modal grain size of 12.4 µm. The composition of the settling particles collected during the storm was dominated by silts. Concomitantly the sand content was lowest (3.4 and 2.8 % in T1 and T2 respectively) and the clay content was highest (up to 19.7 and 20.5 %) compared to the other sediment

collecting cups. This resulted in a decrease of D_{50} size by a factor 1.5 (from 16.6 to 10.0 µm in T1 and from 14.4 to 9.6 µm in T2). After the peak of the storm, the D_{50} re-increased but never reached its initial size before the end of the deployment.

However the D_{50} of the particles deposited in the canyon after the storm was higher than in the sediment traps: 24 µm at 442 m depth. The mean modal grain size and the particle size classes of the exported material showed that the particles flushed down the canyon during the storm were finer than during the rest of the deployment. Also, SPM fluxes and POC content were more variable in the high-frequency water samples.

This difference in the settling particulate material composition could lead to differences in geochemical signatures of the sinking exported material as particulate trace metals are mostly carried by the clay fraction and its coating formations. It has to be noted that deepening and tilting of the sediment traps increased markedly under current speeds surpassing 40 $cm.s^{-1}$ (an approximate 30% of current records were above that threshold at both lines). According to Martín et al. (2013), for maximum current speeds (90 $cm.s^{-1}$) recorded at both moorings, the sediment trap originally at 40 mab deepened to only a few meters above the seafloor and its inclination was nearly horizontal. Such high velocities were rarely reached. At line T2 currents were higher than 80 $cm.s^{-1}$ only 0.4% of the time, while at T1 the highest speed range (70–80 $cm.s^{-1}$) was reached 0.3% of the recording time (*Martín et al., 2013*). The inclination of the traps due to strong currents probably induces a grain size sorting, resulting in different grain size spectra in the sediment compared to traps. Hence, the sediment-trap-derived fluxes during high current speed periods should be considered as qualitative rather than quantitative data.

3.1.2 Particulate trace metal concentrations and dynamics

Trace element and Rare Earth Element (REE) concentrations in each sediment trap are presented in Table 4.1. Individual trace metal concentrations were weighted by their corresponding mass fluxes, in order to take into account the temporal variability of the flux in the calculated mean concentration value. The flux-weighted average PTM concentration is then more representative of what would have been a single sample over the average duration of the collecting period (*Heussner et al., 2006*). Comparison of total trace metal concentrations for sinking material in both sediment traps reveals higher flux-weighted mean concentrations in the T2 trap than in T1, for some elements: Al, Cr, Co, Ni, Zn, Cd and Pb (59.5 $mg.g^{-1}$, 78.2, 10.6, 36.3 and 171.4, 0.2 and 41.3 $µg.g^{-1}$ respectively). T1 sediment trap

displayed the highest flux-weighted mean concentrations of Cu (41.4 µg.g^{-1}). The cups corresponding to the peak of the storm (13th of March 2011) displayed the lowest values of total Cr, Co, Ni and Cu concentrations in both traps and the highest total Cd concentration in T2. However, the dynamic of Zn was opposite in both traps: total Zn concentration decreased during the storm in T1 (from 184 to 162 µg.g^{-1}) but increased in T2 (from 164 to 184 µg.g^{-1}).

Samples from the high-frequency water sampling at station CX displayed flux-weighted mean concentrations of Al, Cr, and Ni (Table 4.1) within the same range as the corresponding sediment traps collecting cups (13-14th March 2011) compared to the sediment traps (58.6, 76.6 and 33.1 µg.g^{-1} respectively). But those water samples also had higher flux-weighted mean Cd and Pb (0.2 and 44.1 µg.g^{-1} respectively) and lower Co, Cu and Zn concentrations (9.2, 22.5 and 141.8 µg.g^{-1} respectively). Hence sinking particles sampled at the peak of the storm display lower concentrations of Cu and Zn, elements of a supposedly anthropogenic origin, compared to the sediment trap collection. But PTM of an admittedly crustal origin are within the same range of concentration in both kinds of samples. If we compare the particulate trace metal concentrations of the sediment trap samples with the concentrations found in the sediment deposit at 442 and 497m depths, we encountered the highest concentrations of Al and Cr in the 442 m depth core (64.1 mg.g^{-1} and 88.5 µg.g^{-1} respectively). Concentrations of Cu and Pb in the sediment were within the same range as the flux-weighted mean concentrations from the high-frequency water sampling. However the concentration of Cu was higher, and the concentration of Pb lower, in the sediment compared to the flux-weighted mean concentrations of the sediment trap samples.

In the 497 m depth core, PTM concentrations decreased by a factor 2 to 3 compared to the concentration of the 442 m depth sediment. This is clearly the result of fresh sediment deposition at 442 m. This depocenter was located around 440-450 m only, because values from shallower sediment cores were similar to those reported here for 497 m depth (data not shown). As suggested by DeGeest et al. (*2008*), the CCC southern flank is an occasional depocenter of fine-grained sediment, advected by various oceanographic processes like storm-induced downwelling. Such ephemeral deposits are supposed to be remobilized toward deeper environments when submitted to more intense hydrodynamic processes. When looking at linear relationships between POC content and trace element concentrations from sediment trap samples (Fig.3), correlation coefficients only showed significant values in T1 between Co, Cu, Zn and POC (r^2 = 0.61, 0.60 and 0.69 respectively). The same calculations for T2 or the high-frequency water samples were not statistically significant.

Particulate trace metal concentrations in sinking material or in sediment are generally influenced by their particulate matter physical properties and particularly by the grain size.

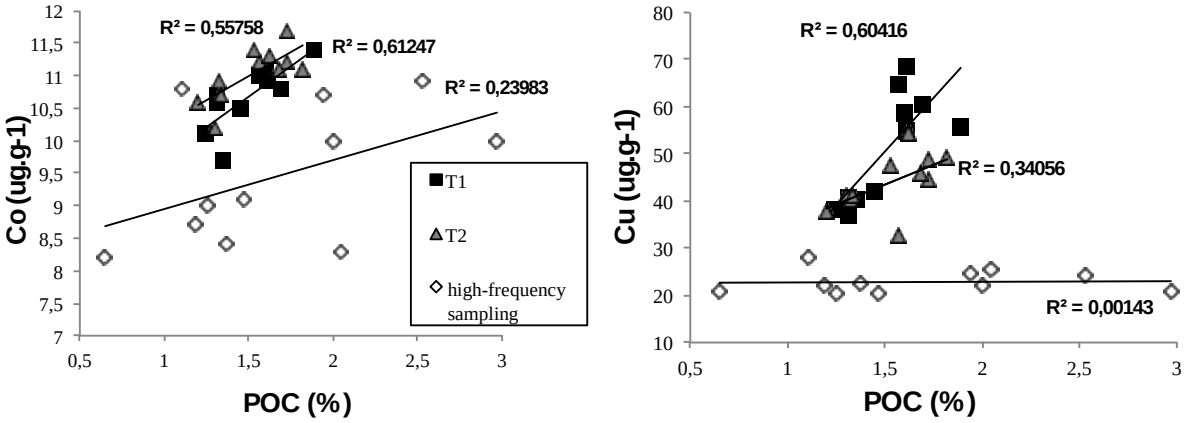

Fig.4.3 Relationships between Co and Cu concentrations and POC content in both sediment traps and during the high-frequency water sampling

In order to compare the chemical characteristics of the different material collected at different times and in different hydrological conditions, normalization is commonly applied. Many studies have documented the normalization with major or minor lithogenic elements like Fe (*Lee et al., 1998*; *Schiff and Weisberg, 1999*), Sc (*Audry et al., 2004*), Cs (*Ackermann, 1980*; *Roussiez et al., 2005*) or Th (*Coynel et al., 2007*; *Dabrin et al., 2013*). But Al is most commonly used, as it is considered a tracer for clay and provides efficient correction of grain-size bias (*Balls et al., 1997*; *Rubio et al., 2000*; *Hieu Ho et al., 2012*). The temporal evolution of trace metal concentrations can then be related to variations of sinking particulate matter.
Results from Al normalization are displayed in Fig.4.4. Spider diagrams of T1 (a) and T2 (b) sediment traps showed homogeneous normalized-PTM ratios throughout March 2011. However, during the high-frequency water sampling (c), an input of Zn is noticeable on the 13th of March 2011 (19:30) whereas Pb peaked later, on the 14th of March (00:22). Otherwise, Al-normalized PTM ratios from the high-frequency water sampling were within the same range as those from the sediment traps.

3.1.3 Enrichment factors and anthropogenic impact

EFs values are presented in Table 4.2 for sediment trap, water and sediment samples. Results with different background values and normalizer are also displayed.

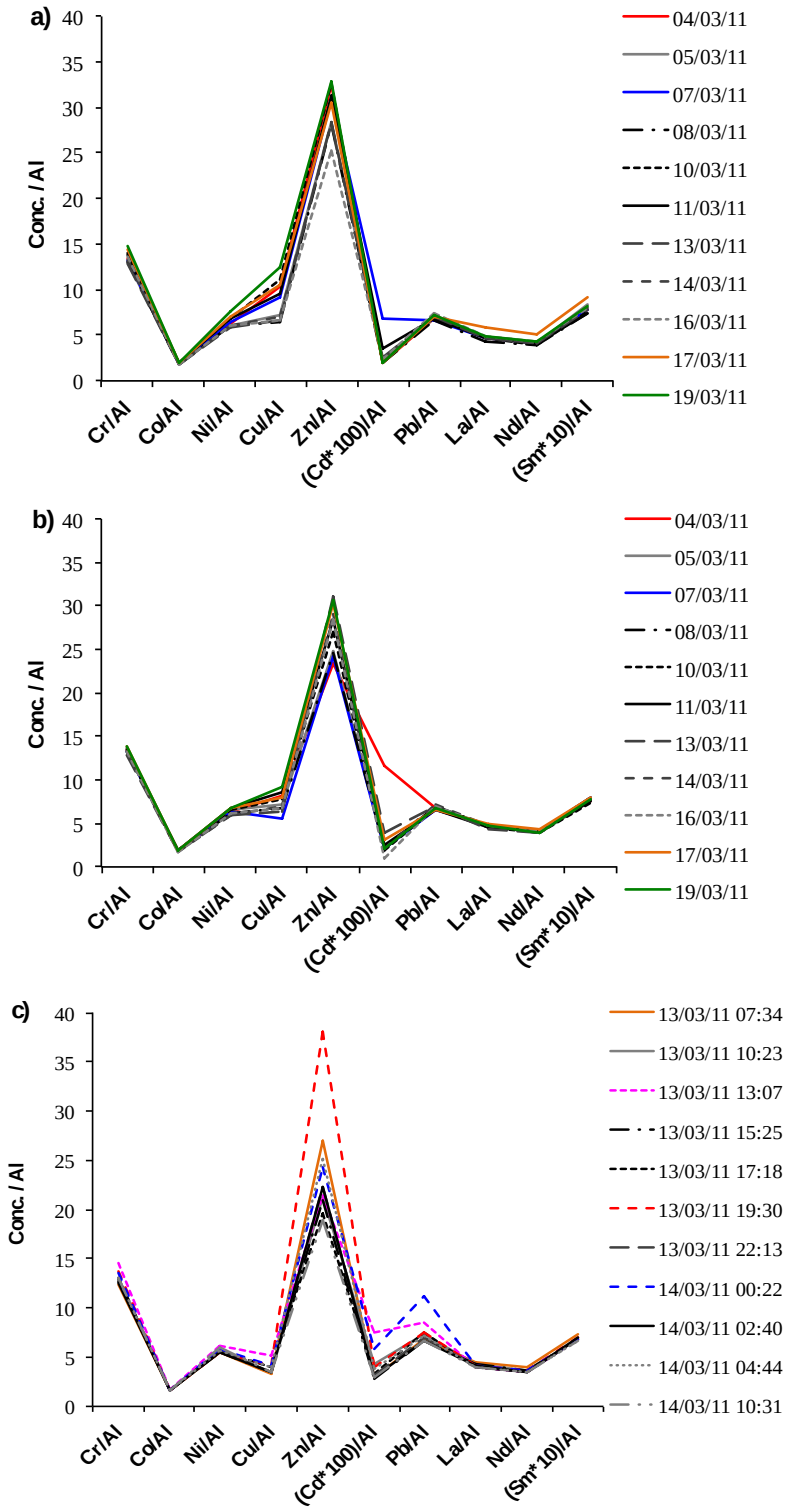

Fig.4.4 Spider diagrams of normalized concentrations in a) CASCADE T1 sediment trap, b) CASCADE T2 sediment trap and c) during the CASCADE high-frequency water sampling. All concentrations are normalized to Al concentration in order to remove grain-size bias

When using the Upper Continental Crust (UCC) reference concentrations (*Wedepohl, 1995*) but different clay tracers (Al, Th or the sum of rare earth elements La, Nd and Sm), we found similar values for a given PTM. Hence, Al was maintained as a suitable normalizer. When using a local Rhone riverbank core as the background reference sample, we noticed that corresponding EF values were lower. This is because the UCC reference does not reflect the local lithology that seems to be naturally enriched in Cu and Zn and to a lesser extent in Cr, Ni and Pb. However our results are in good agreement with the EF calculated by Roussiez et al. (*2012*) who also used a local background reference (Table 4.2). Hence, we selected the local (Rhone) reference.

In both T1 and T2 sediment traps, trace metal enrichment showed the same pattern: Cr, Co and Ni had steady EF under 1.5 and synchronous temporal evolution of EFs; Cd was episodically enriched (one sample above the 1.5 threshold); Pb was slightly enriched (EF $\geq$ 2) but constant throughout the duration of the deployment. Cu and Zn, however, were regularly impacted by anthropogenic contribution as their EFs were mostly above 3 and 2 respectively. For Cu, Zn and Pb, EFs were slightly higher in T1 than in T2 but the storm event did not seem to have any impact on EF variations. This indicates that, regarding potential anthropogenic enrichment, the sinking material was of the same origin in both traps throughout the whole deployment. Mean EFs for each trace element were in the same range as those calculated by Roussiez et al. (*2012*) for either the shelf-sediments or the material exported in the head of canyons in December 2003. One can finally notice that EFs of Cu are higher within sediment trap samples but remain in the range of EFs calculated by Roussiez et al. (*2012*) for the Tet River. The temporal evolution of EF ratios calculated from the high-frequency sampling was also variable: Cr, Co and Ni enrichments were inexistent; Cd was occasionally affected by anthropogenic enrichment as its EF rose from 1.5 to 4.5 in less than 6 hours; Pb EFs were also less constant at this increased sampling rate. EFs of Cu and Zn were intermittently peaking above the 1.5 threshold. Mean EF ratios were equal or lower in high-frequency samples than in T1 and T2, except for Pb mean EF ratios that was slightly higher (2.3 compared to 2.1 in both traps). Relationships between EF and POC have been studied and significant correlation coefficients are reported in Table 2. In both traps, EFs profiles of Cr, Co, Ni and Cu were similar to the POC profiles whereas, EFs profiles of Cd and Pb were completely different from POC. However the best correlation coefficients were found in T2 for Co and Ni (r^2 = 0.82 and 0.75 respectively) whereas, r^2 of Cu and Zn were higher in T1 compared to the deeper trap (0.74 and 0.76 respectively).

	Reference			Cr	Co	Ni	Cu	Zn	Cd	Pb
This work	UCC / Al	*T1*	*March 2011*	3.0	1.2	2.7	4.8	4.5	2.1	3.2
		T2	*March 2011*	3.0	1.2	2.7	4.0	4.1	2.4	3.1
		HFS	*13-14th March 11*	2.9	1.1	2.4	2.1	6.8	3.0	3.4
		sediment deposit	*deposit*	2.5	1.1	2.1	1.8		1.4	3.0
	UCC / REE	*T1*	*March 2011*	2.5	1.0	2.2	4.0	3.7	1.7	2.6
		T2	*March 2011*	2.5	1.1	2.3	3.4	3.5	2.1	2.6
		HFS	*13-14th March 11*	2.8	1.0	2.3	2.0	6.3	2.9	3.3
		sediment deposit	*deposit*	2.3	1.0	1.9	1.6	/	1.3	2.7
	UCC / Th	*T1*	*March 2011*	2.6	1.1	2.3	4.1	3.8	1.8	2.7
		T2	*March 2011*	2.5	1.0	2.3	3.4	3.5	2.0	2.6
		HFS	*13-14th March 11*	2.7	1.0	2.2	2.0	6.2	2.8	3.2
		sediment deposit	*deposit*	/	/	/	/	/	/	/
	local / Al	*T1*	*March 2011*	1.4 ± 0.1	1.3 ± 0.1	1.1 ± 0.1	3.9 ± 0.9	2.2 ± 0.2	1.5 ± 0.8	2.1 ± 0.1
		r^2					*0.74*	*0.76*		
		T2	*March 2011*	1.3 ± 0.03	1.3 ± 0.05	1.1 ± 0.1	3.3 ± 0.5	2.0 ± 0.2	1.8 ± 1.7	2.1 ± 0.1
		r^2			*0.82*	*0.75*				*-0.75*
		HFS	*13-14th March 11*	1.3 ± 0.1	1.1 ± 0.04	1.0 ± 0.03	1.7 ± 0.2	1.7 ± 0.4	2.2 ± 0.9	2.3 ± 0.4
		sediment deposit	*deposit*	1.1	1.1	0.9	1.5	/	1.1	2.0
Roussiez et al. (2012)	local / Cs	*Rhone*	*flood Dec 03*	0.9	1.0	1.2	1.8	2.2	2.2	2.2
		Tet	*flood Dec 03*	0.9	1.3	1.0	3.1	2.4	1.9	2.1
		Lacaze	*flood Dec 03*	0.9	1.0	1.1	1.44	2.0	0.8	2.1
			29 Dec-4 Jan	1.0	1.0	1.2	1.8	2.4	0.7	2.0
		Shelf sed	*flood Dec 03*	1.0	1.0	1.1	1.0	1.7	1.3	2.2

Table 4.2. Mean EFs calculated in both sediment traps samples, high-frequency water sampling samples and the first centimeter of the fresh sediment deposit recovered by multi-corer, with different references. For the local Rhone riverbank reference samples, correlation coefficients (r^2) were calculated between EF and POC content (significance > 99% with 9 degrees of freedom). Those EF values are compared to EFs calculated by Roussiez et al. (2012).

This shift in the relationships could be explained by a different source of material entering T2 and T1. The material from the deeper trap may have a more distinctive lithogenic origin, possibly emanating from advection of shelf sediments and/or erosion of the canyon flank sediments. Canyon flank erosion has been documented by Pasqual et al. (*2010*) during the deployment of sediment traps that monitored an intense dense-shelf water cascading event. The mean EF values calculated for the sediment deposit in our work were very close to the values calculated by Roussiez et al. (*2012*) for the continental shelf sediment.

3.2 Origin of the particulate trace metals

In the following section, we want to determine the origin of the sinking material entering sediment traps in March 2011. It is well established that most sediments deposited on the shelf of the GoL originate from the Rhone River (*Durrieu de Madron et al., 2000; Ludwig et al., 2003; Révillon et al., 2011*). However, material from other coastal rivers (Herault, Orb, Aude and Agly) is regularly delivered to the continental shelf, mainly through short and intense flash-flood events (*Bourrin et al., 2006*). As the Cap de Creus canyon is located at the southern-end of the shelf, facing the mouth of the Tet River, it is not trivial to test the influence of this local on the geochemical signature of material exported in the canyon. Indeed, a previous study in the adjacent Lacaze-Duthiers submarine canyon detected significant exported material at the canyon head, originating from the Tet River (*Grousset et al., 1995*). For this purpose, two different approaches were conducted.

3.2.1 Signature from the Rare Earth Element (REE) concentrations

The first tracing procedure used the REE signatures of particles, following the general idea that shelf-exported particles have integrated REE signatures reflecting their lithogenic source signal. This geochemical tool has been successfully used in previous studies to describe different weathering end-members (e.g. *Aubert et al., 2006*; *Araújo et al., 2002*). More recently, Roussiez et al. *(2013)* showed that it was possible to identify, in the GoL, the individual signature of particulate matter in each coastal river by using La/Sm and La/Nd ratios. This further allowed to determine the origin of particulate matter exported in canyon heads during various hydrological conditions (storm events and normal conditions). We refined here the established relationships of Roussiez et al. (*2013*) by adding Rhone and Tet SPM samples collected by the CEFREM laboratory (France) during an 8-years survey

(Dumas et al., *in prep*), and compare them with the samples presented in this study (Fig.4.5 and Table 4.1). Signatures of the Rhone and Tet SPM under normal and highly turbid conditions have been isolated, as they tend to be different. Their respective ratios decreased in the following order: Rhone SPM > Rhone highly turbid samples > Tet SPM > Tet highly turbid samples. In different stream discharge conditions, both rivers likely mobilize materials of different grain-size and mineralogical contents, resulting in different REE signatures.

It is commonly agreed that particles delivered by rivers enter the continental shelf by being temporarily stored in rivers pro-deltas. Under the action of storms and strong currents they are affected by several resuspension, transport, mixing and deposition cycles until they are definitively exported or deposited. Potentially, all coastal rivers contribute to the signature of the submarine canyons particles exported at the southwestern end of the shelf (Fig.4.5).

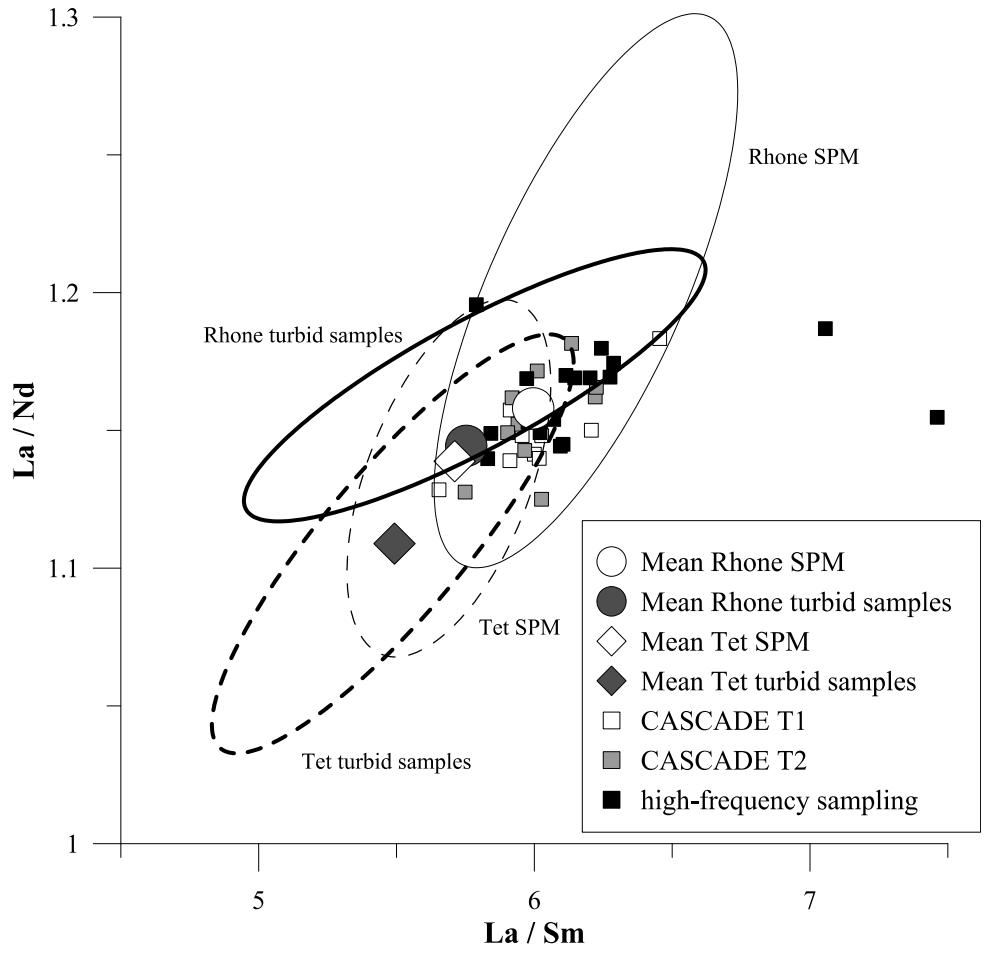

Fig.4.5 REE signatures from river SPM and settling particles of CASCADE sediment traps as well as from SPM of the high-frequency water sampling of the storm, plotted in La/Sm vs. La/Nd diagram

Sediment trap and water samples are plotted in multiple domains. Even if they all end up in the Rhone SPM and turbid samples areas, the storm samples overlap with the Tet SPM domain and half of the Tet turbid samples area. The domain that contains most of our samples is the Rhone SPM area. However, the great variability of the sample plots does not allow a straightforward interpretation and another procedure is hence necessary to corroborate our conclusions.

3.2.2 Signature from the residual metal fraction

The other tracing experiment conducted in this work was an HCl-single extraction, as it is commonly admitted that acid-soluble metals are bound to the reactive phase of the particle and likely to be potentially available once released in the environment. The non-reactive (residual) metal fraction, contained in the mineral phase of the particle, is considered stable during the transport of the particle from its source to its deposition spot. HCl-extracted metal concentrations are displayed in Table 4.3. The residual metal fraction, which is the signature of the sediment source at the watershed scale (*Schäfer and Blanc, 2002*), was calculated from the difference between total and acid-soluble metal concentrations. Riverine particles from the Rhone and Tet rivers used during this procedure were the same than in section 3.2.1 (part of an 8-year survey). In this study, Cr_{res} (Cr concentration in the particulate residue after extraction) and Ni_{res} were significantly lower in suspended particulate matter (SPM) from the Tet River, whereas, Cu_{res}, Zn_{res} and Pb_{res} were higher than in Rhone River SPM (Fig.6a). As explained by Dabrin et al. (*2013*) we grouped the Al-normalized values of Cr_{res} and Ni_{res} on one hand and Cu_{res}, Zn_{res} and Pb_{res} on the other, in order to provide two distinct watershed signatures (Al residual concentrations being very similar for both rivers, Al can be used as a normalizer). As the Rhone and Tet SPM samples were taken during high water and low water conditions, the watershed signatures are valid for all hydrological conditions. Indeed, the plot of $(Cr_{res} + Ni_{res})/Al_{res}$ over $(Cu_{res} + Zn_{res} + Pb_{res}) /Al_{res}$ showed two well-separated domains, representing the signature of the Rhone and Tet rivers SPM. If the same operation is conducted on any particle originating from one or the other watershed, it is expected to plot in its domain. This is what was done with sediment trap particles (Fig.4.6b). Unfortunately, only 5 cups were tested, as there was not enough material left in every cup of both T1 and T2 sediment traps, but each sample plot in the Rhone River domain. As said before, under meteo-climatic forcings, riverine particles may go through several mixing cycles until they are definitively exported at the southwestern end of the shelf.

a)

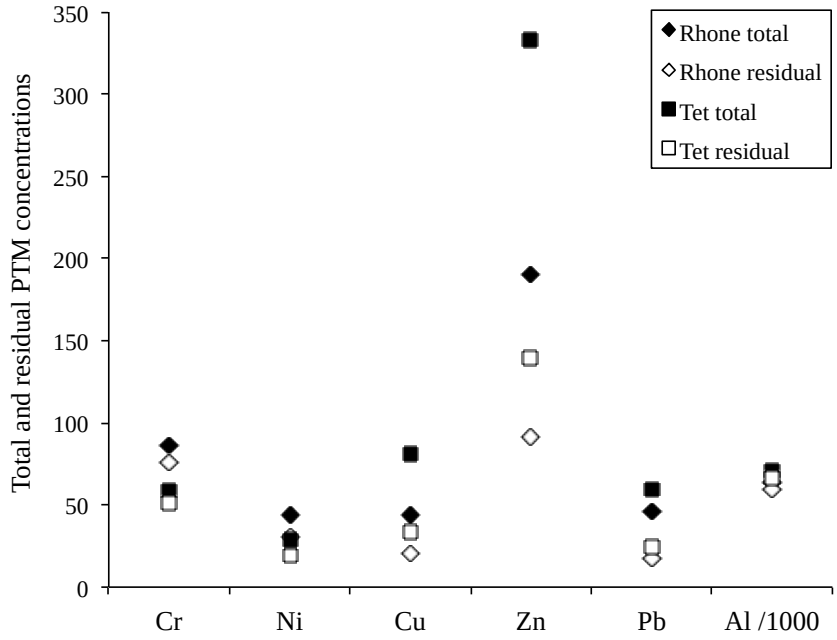

b)

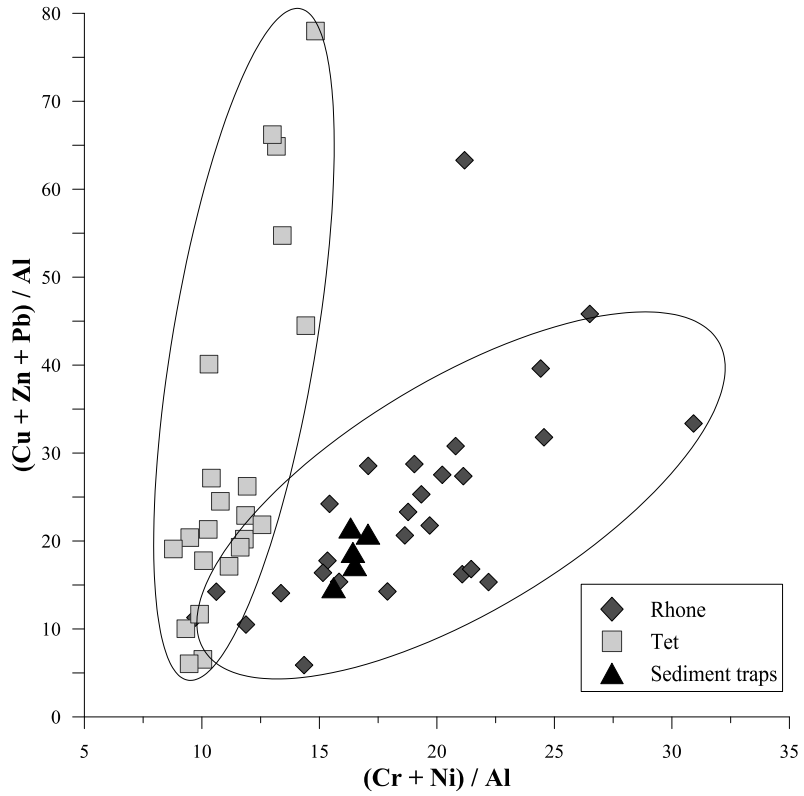

Fig.4.6 Signatures of exported particles using the acid-leaching procedure. a) Average total and residual metal concentrations (µg.g^{-1}) in SPM from the Rhone (◆) and Tet (■) rivers, and b) Plot of $(Cu_{res}+Zn_{res}+Pb_{res})/Al_{res}$ vs $(Cr_{res}+Ni_{res})/Al_{res}$ in SPM from the Rhone and Tet rivers and in samples from the CASCADE sediment traps as well as from SPM of the high-frequency water sampling of the storm

		Date start	Date end	n° days	mass flux	Cr	Co	Ni	Cu	Zn	Cd	Pb
PTM daily fluxes					**($g.m^{-2}.d^{-1}$)**	**($mg.m^{-2}.d^{-1}$)**	**($mg.m^{-2}.d^{-1}$)**	**($mg.m^{-2}.d^{-1}$)**	**($mg.m^{-2}.d^{-1}$)**	**($mg.m^{-2}.d^{-1}$)**	**($\mu g.m^{-2}.d^{-1}$)**	**($mg.m^{-2}.d^{-1}$)**
T1	*(moderate storm)*	12/03/11	15/03/11	3	32.2	3.6	0.5	1.6	1.9	7.6	6.9	1.9
	Potentially bioavailable PTM in T1					(16.9)	(57.2)	(34.8)	(63.6)	(59.0)	/	(77.0)
	Contribution of the storm to the total March 2011 export				*58*	*56*	*56*	*55*	*54*	*58*	*57*	*56*
PTM export					**(Mt)**	**(T)**	**(T)**	**(T)**	**(T)**	**(T)**	**(T)**	**(T)**
This work	*Total*	12/03/11	15/03/11	3	0.4	29	4	13	10	56	0.07	16
	Contribution to the total 2011 export of the Rhone river					*31*	*27*	*26*	*23*	*30*	/	*31*
Roussiez et al., 2012	*Total*	01/12/03	07/12/03	7	/	193	28	97	69	303	0.43	93
	Contribution to the total 2011 export of rivers					*40*	*44*	*42*	*30*	*36*	/	*39*

Table 4.3. CASCADE mass and PTM fluxes. All fluxes are in $mg.m^{-2}.d^{-1}$ except for Cd, which is in $\mu g.m^{-2}.d^{-1}$. Values in brackets represent the percentage of lability (HCl-leaching) from sediment trap T1. Values in italics are the contribution of the storm (PTM fluxes and storm-induced export) to the March 2011 daily fluxes and total export. The total March 2011 export (in tons) was calculated from the estimation of sediment transport by Bourrin et al. (2012). Comparison is made with the results from Roussiez et al. (2012) who studied the flood and storm of December 2003.

However, the diagram in Fig.6b indicates that it does not result in changes of the geochemical signature of the particles and that the Rhone River is clearly the dominant contributor of particulate material compared to the Tet River. The previous approach indicated that small coastal rivers could contribute to the input of particulate matter, mainly during flash floods, but this one confirms that the signal from those particles is widely diluted by the signal from the Rhone SPM.

3.3 Shelf-exported PTM fluxes

For the moderate storm event witnessed in March 2011, calculated elemental fluxes (Table 4.3) for both traps were in the same range: up to 7.6 $mg.m^{-2}.d^{-1}$ of Zn and around 1.9 $mg.m^{-2}.d^{-1}$ of Cu and Pb. However the particulate trace metal fluxes were slightly higher in the second and deeper sediment trap due to a higher suspended particulate matter exportation. This can be explained by the hydrodynamic conditions in the Cap de Creus submarine canyon (*DeGeest et al., 2008*; *Martín et al., 2013*). Storm-induced currents bypass the head of the canyon but due to the coastal topographic constraint of the Cap de Creus peninsula they change course and enter the canyon deeper, through its southern flank. This would have impacted the second and deeper trap more than the upper one. Despite the brevity of the storm (3 days), it contributed to 54 and 58% of the monthly (March 2011) fluxes. Hence, compared to background fluxes, a moderate storm does have a strong impact on the amounts of exported particles.

In Table 4.4, the amounts of potentially bioavailable elements exported by this event are also shown. Those data are the result of the extraction of acid-soluble metals (HCl 1M) described in section 2.3 (Table 4.4). HCl-extracted metal fractions were highly variable depending on the metal considered. Cr_{HCl} and Ni_{HCl} represented less than 11% and 31% of the respective total metal concentrations in both rivers suspended particulate matter (SPM), whereas Cu_{HCl}, Zn_{HCl} and Pb_{HCl} represented between 50% and 65% of the total exported metal concentrations. In the sediment trap samples, Cr_{HCl}, Ni_{HCl} and Cu_{HCl} fractions were lower than in rivers SPM but Pb_{HCl} was higher (81% of the total Pb concentration), indicating enrichment in potentially bioavailable Pb. This difference could result from the significant addition of particulate Pb of atmospheric origin in open sea as previously reported by Guieu et al. (*1997*) for the GoL. Especially as anthropogenic atmospheric Pb has been identified as highly labile in the marine environment (e.g. *Chester et al., 1993*). From the results obtained in $metal_{HCl}$ in T1, calculations of potentially available fluxes exported in March 2011 are shown in Table 3. 63.6 % of the Cu trapped in the first sediment trap was bound to reactive phases of the sinking particles, and up to 77% of the Pb.

		Cr µg.g^{-1}		**Ni** µg.g^{-1}		**Cu** µg.g^{-1}		**Zn** µg.g^{-1}		**Pb** µg.g^{-1}	
		HCl 1M	%	HCl 1M	%	HCl 1M	%	HCl 1M	%	HCl 1M	%
RHONE	05/07/06	7.6	9	9.4	21	26.6	46	83.9	38	23.2	51
river	07/03/07	11.4	12	14.3	27	24.1	53	78.7	44	24.4	62
	02/05/07	14.2	14	16.5	31	47.0	62	126.9	51	32.5	61
	04/07/07	11.4	12	14.2	24	26.9	33	216.4	92	31.9	63
	05/09/07	10.9	11	14.3	26	26.2	55	216.8	58	32.3	68
	06/08/08	4.6	5	7.4	16	16.5	31	45.5	26	15.9	42
	06/09/08	11.0	13	13.7	29	23.1	61	78.5	53	30.9	65
	05/11/08	12.8	13	11.4	23	37.5	53	119.3	45	52.4	59
	06/12/08	17.3	18	20.6	41	49.6	87	150.2	67	46.3	94
	11/02/09	7.8	11	7.9	20	12.8	45	44.2	37	20.5	54
	12/03/09	9.9	10	12.9	24	27.6	50	101.1	23	44.2	65
	08/04/09	20.8	26	23.1	58	26.3	69	142.5	74	34.7	92
	10/06/09	7.7	9	12.1	27	26.4	54	93.6	47	26.1	66
	10/09/09	8.8	10	13.8	27	27.5	51	113.5	45	43.9	66
	10/11/09	13.7	15	16.9	36	28.9	54	100.0	52	31.5	68
	10/12/09	9.1	9	11.2	23	25.9	50	86.0	42	27.8	63
	06/01/10	8.3	10	10.9	32	21.4	92	76.7	70	25.4	83
	03/03/10	8.3	9	10.9	28	20.7	84	76.9	42	24.1	66
	05/05/10	7.0	8	10.3	23	19.8	55	68.6	39	23.3	40
	21/07/10	5.5	7	10.6	28	18.3	53	54.5	43	20.4	48
	08/09/10	6.8	8	12.5	32	36.2	63	73.5	53	44.8	98
	13/10/10	5.7	5	9.0	17	30.2	39	81.7	48	25.4	39
	04/11/10	6.0	7	11.7	32	11.5	22	46.1	35	13.9	33
	12/01/11	10.7	13	12.2	28	30.0	69	138.9	62	32.1	72
	04/03/11	9.1	12	11.4	28	26.6	57	120.5	57	29.0	65
	14/04/08 12:15	13.7	15	18.0	33	25.4	67	97.9	59	27.1	73
	09/09/08 10:00	7.0	12	12.7	33	15.9	59	40.6	39	18.7	69
	03/11/08 12:00	9.6	17	12.7	40	20.4	72	75.7	56	49.4	82
	Mean		**11**		**29**		**57**		**50**		**65**
	sd		**4**		**8**		**16**		**15**		**16**
TET river	05/07/06	7.7	20	7.7	37	53.3	79	198.2	83	48.6	80
	02/05/07	5.2	8	6.9	23	54.8	69	129.7	51	33.6	56
	12/06/07	10.5	17	13.6	47	123.9	86	416.8	98	74.5	83
	06/05/08	5.6	11	6.3	27	59.3	49	257.8	55	38.6	54
	06/08/08	6.5	12	7.9	30	56.2	75	261.0	71	42.6	61
	06/10/08	8.5	19	10.7	42	49.6	63	227.0	62	38.8	53
	05/11/08	8.2	13	10.6	33	47.5	64	164.6	63	41.3	58
	08/04/09	9.0	15	13.1	44	34.7	52	106.8	52	23.5	63
	10/06/09	8.6	14	12.9	44	64.0	88	273.6	91	47.4	85
	10/07/09	6.1	9	10.2	31	66.1	70	245.2	73	36.7	61
	10/08/09	10.8	18	13.8	52	62.7	73	291.9	92	50.2	75
	10/09/09	7.4	13	8.1	31	68.6	65	290.9	73	40.6	55
	10/10/09	5.6	12	7.5	33	38.9	64	263.8	76	57.9	80
	03/02/10	3.0	5	4.4	17	29.0	29	170.4	57	23.5	43
	07/04/10	5.3	8	8.4	26	53.7	32	260.3	47	31.4	35
	05/05/10	3.6	8	6.1	24	30.2	41	103.9	35	24.6	51
	09/06/10	4.1	6	6.0	19	39.2	65	149.7	70	29.1	63
	08/09/10	4.9	9	6.8	24	50.8	76	201.3	76	34.4	43
	13/10/10	5.2	10	9.0	35	17.5	23	56.4	20	23.0	36
	04/02/11	5.9	9	7.0	25	61.2	71	211.3	70	31.6	59
	04/03/11	4.9	10	7.6	31	71.2	72	241.8	75	22.1	43
	Mean		**12**		**32**		**62**		**66**		**59**
	sd		**4**		**9**		**18**		**19**		**15**
CASCADE	05/03/2011 (T1)	10.4	14	11.7	33	11.6	28	91.0	56	31.4	81
sediment traps	08/03/2011 (T1)	9.9	13	11.5	33	11.4	31	82.8	50	31.9	82
	13/03/2011 (T1)	9.1	12	9.4	28	9.3	24	72.4	45	29.2	74
	14/03/2011 (T1)	9.3	12	9.3	27	9.2	23	76.0	47	29.8	72
	13/03/2011 (T2)	12.6	17	13.2	37	13.1	35	114.3	62	40.2	97
	Mean		**14**		**32**		**28**		**52**		**81**
	sd		**2**		**4**		**5**		**7**		**10**

Table 4.4. HCl-extracted metal concentrations and the contribution to the total, in SPM from the Rhone and Tet rivers as well as the sediment trap samples collected during the CASCADE cruise. All concentrations are expressed in µg.g^{-1}.

Bourrin et al. (*2012*) estimated the particulate matter transport using a coastal Slocum glider equipped with various optical sensors that repeatedly crossed the continental shelf between 30m to 100m bottoms during March-April 2011. The cross-shelf glider transects allowed to characterize sediment dynamics during the storm, showing intense sediment resuspension down to 80 m depth. Use of gliders also provided the estimation of a net suspended particulate matter transport during the storm (13-14th March 2011) of 0.4 Mt (*Bourrin et al., 2012*). Using this estimation, we calculated the total PTM export during the storm (Table 4.3) to be 70 kg of Cd to 56 T of Zn (elements with the lowest and highest export fluxes respectively). When comparing the shelf export by this moderate storm to the annual 2011 PTM export of the Rhone river (Table 4.3), it appears that the storm exported the equivalent of about one third of the Rhone annual PTM input. Our results were also compared with the estimation made by Roussiez et al. (2012) for the December 2003 flood and storm event. The March 2011 storm exported 5 to 7.5 (for Zn and Ni respectively) times less PTM than the large 2003 storm. But the contribution of the 2003 storm export also represented about one third of the 2003 annual riverine input, as for our study. Between 30 and 44% (for Cu and Co respectively) of the PTM input by rivers was exported by the storm. Knowing that moderate storms occur frequently (yearly recurrence), even though they do not last long (3 days in our case), they are an efficient export process.

4. Conclusion

This study aimed at improving the description of the characteristics and dynamics of PTM exported from the Gulf of Lion's shelf. Near-bottom observations gathered during the CASCADE cruise in March 2011 allowed describing the effect of a moderate E-SE storm that flushed the coastal waters down the Cap de Creus Canyon head. The various data sets collected using sediment traps samples (35-hour time step), high frequency water samples (3-hour time step), enabled to assess the variability of PTM fluxes and composition exported from the shelf. Surface sediment samples, collected after the storm, permitted to characterize the material that was deposited on the canyon's floor. The main findings are the following:

- This study confirmed that episodic E-SE storms represent efficient export processes. Particles flushed down the canyon were finer during the storm than during the rest of the deployment, and contained variable amounts of POC and PTM. The high-frequency sampling showed large fluctuations in quantity but also in quality of the exported

material. Pulses of particles enriched in anthropogenic PTM (Cu, Zn, Pb) were observed. These elements also exhibited a high lability determined using acid-leaching extraction.

- Two different tracing procedures (REE, HCl-leaching) both indicated that particles exported down the canyon had a mixed riverine origin. Furthermore, residual PTM concentrations suggest a predominant contribution from the Rhone River. We estimated that each E-SE storm exported, depending on the considered element, the equivalent of one third to nearly half of the Rhone annual PTM input.
- A centimetric deposit of fine sediments was only observed after the storm at 442 m depth on the canyon flank. Such deposits accumulate temporarily, and are likely to be remobilized and transported to deeper environments during intense hydrodynamical events, such as dense shelf water cascading, which periodically gush down the canyon.

Acknowledgements

We are grateful to M. Guart, A. Alonso and E. Pelfort (Grup de Recerca Consolidat en Geociències Marines, Barcelona, Spain) for their help in laboratory work. We also thank all the crew and officials of R/V l'Atalante, the technical and scientific staff involved in the CASCADE cruise. The European research projects PERSEUS (FP7-OCEAN-2011-3-287600) and HERMIONE (FP7-ENV-2008-1-226354), as well as the French programme MERMEX under the MISTRALS framework supported this work. We also thank the anonymous reviewers for their helpful comments.

References

Ackermann, F. (1980). A procedure for correcting the grain size effect in heavy metal analyses of estuarine and coastal sediments. *Environmental Technology Letters*, 1, 518-527.

Allen, S.E., Durrieu de Madron, X. (2009). A review of the role of submarine canyons in deep-ocean exchange with the shelf. *Ocean Science*, 5, 607-620.

Araújo, M.F., Jouanneau, J.M., Valerio, P., Barbosa, T., Gouveia, A., Oliveira, A., Rodrigues, A., Dias, J.M.A. (2002). Geochemical tracers of northern Portuguese estuarine sediments on the shelf. *Progress in Oceanography*, 52, 277-297.

Aubert, D., Le Roux, G., Krachler, M., Cheburkin, A., Kober, B., Shotyk, W., Stille, P. (2006). Origin and fluxes of atmospheric REE entering an ombotrophic peat bog in Black Forest (SW Germany): evidence from snow, lichens and mosses. *Geochimica and Cosmochimica Acta*, 70(11), 2815-2826.

Audry, S., Schäfer, J., Blanc, G., Jouanneau, J.-M. (2004). Fifty-year sedimentary record of heavy metal pollution (Cd, Zn, Cu, Pb) in the Lot River reservoirs (France). *Environmental Pollution*, 132(3), 413-426.

Audry, S., Blanc, G., Schäfer, J. (2006). Solid state partitioning of trace metals in suspended particulate matter from a river system affected by smelting-waste drainage. *Science of the Total Environment*, 363, 216-236.

Balls, P.W., Hull, S., Miller, B.S., Pirie, J.M., Proctor, W. (1997). Trace metal in Scottish estuarine and coastal sediments. *Marine Pollution Bulletin*, 34, 42-50.

Biscaye, P.E., Anderson, R.F., Deck, B.L. (1988). Fluxes of particles and constituents to the eastern United States continental slope and rise: SEEP-I. *Continental Shelf Research*, 8, 855–904.

Bonnin, J., Heussner, S., Calafat, A., Fabres, J., Palanques, A., Durrieu de Madron, X., Canals, M., Puig, P., Avril, J., Delsaut, N. (2008). Comparison of horizontal and downward particle fluxes across canyons of the Gulf of Lions (NW Mediterranean): Meteorological and hydrodynamical forcing. *Continental Shelf Research*, 28(15), 1957-1970.

Bourrin, F., Durrieu de Madron, X., Ludwig, W. (2006). Contribution to the study of coastal rivers and associated prodeltas to sediment supply in the Gulf of Lions (NW Mediterranean Sea). *Vie et Milieu-Life and Environment*, 56, 307-314.

Bourrin, F., Durrieu de Madron, X., Heussner, S., Estournel, C. (2008). Impact of winter dense water formation on shelf sediment erosion (evidence from the Gulf of Lions, NW Mediterranean). *Continental Shelf Research*, 28(15), 1984-1999.

Bourrin, F., Durrieu de Madron, X., Mahiouz, K., Guery, L.B., Houpert, L. (2012). Sediment resuspension observed by an optical slocum glider during a typical Mediterranean winter storm. *Ocean Science Meeting 2012*, Salt Lake City, USA.

Chester, R., Murphy, K.J.T., Lin, F.J., Berry, A.S., Bradshaw, G.A., Corcoran, P.A. (1993). Factors controlling the solubilities of trace metals from non-remote aerosols deposited to the sea surface by the ‘dry’ deposition mode. *Marine Chemistry*, 42(2), 107-126.

Coynel, A., Schäfer, J., Blanc, G., Bossy, C. (2007). Scenario of particulate trace metal and metalloid transport during a major flood event inferred from transient geochemical signals. *Applied Geochemistry*, 22, 821-836.

Dabrin, A., Schäfer, J., Bertrand, O., Masson, M., Blanc, G. (2013). Origin of suspended matter and sediment inferred from the residual metal fraction: application to the Marennes Oleron Bay, France. Continental Shelf Research, *in press, Accepted Manuscript.*

DeGeest, A.L., Mullenbach, B.L., Puig, P., Nittrouer, C.A., Drexler, T.M., Durrieu de Madron, X., Orange, D.L. (2008). Sediment accumulation in the western Gulf of Lions, France: the role of Cap de Creus Canyon in linking shelf and slope sediment dispersal systems. *Continental Shelf Research*, 28, 2031-2047.

Din, Z.B. (1992). Use of aluminium to normalize heavy-metal data from estuarine and coastal sediments of Straits of Melaka. *Marine Pollution Bulletin*, 24(10), 484-491.

Drexler, T.M., Nittrouer, C.A. (2008). Stratigraphic signatures due to flood deposition near the Rhône River: Gulf of Lions, northwest Mediterranean Sea., *Continental Shelf Research*, 28(15), 1877-1894.

Durrieu de Madron, X., Abderrazzak, A., Heussner, S., Monaco, A., Aloisi, J.C., Radakovitch, O., Giresse, P., Buscail, R., Kerherve, P. (2000). Particulate matter and organic carbon budgets for the Gulf of Lions (NW Mediterranean). *Oceanologica Acta*, 23(6), 717-730.

Durrieu de Madron, X., Wiberg., P.L., Puig, P. (2008). Sediment dynamics in the Gulf of Lions : the impact of extreme events. *Continental Shelf Research*, 28, 1867-1876.

EEA (2006). Priority issues in the Mediterranean environment. *European Environment Agency*, report 4/2006, 1-88.

Ferrand, E., Eyrolle, F., Radakovitch, O., Provansal, M., Dufour, S., Vella, C., Raccasi, G., Gurriaran, R. (2012). Historical levels of heavy metals and artificial radionucleides reconstructed from overbank sediment records in lower Rhône River (South-East France). *Geochimica et Cosmochimica Acta*, 82, 163–182.

Genesseaux, M., Guibout, P., Lacombe, H. (1971). Enregistrement de courants de turbidité dans la vallée sous-marine du Var (Alpes-Maritimes). *Comptes-Rendus de l'Académie des sciences de Paris*, 273, 2456-2459.

Grousset, F.E., Quetel, C.R., Thomas, B., Donard, O.F.X., Lambert, C.E., Guillard, F., Monaco, A. (1995). Anthropogenic vs lithogenic origins of trace elements (As, Cd, Pb, Rb, Sb, Sc, Sn, Zn) in water column particles: northwestern Mediterranean Sea. *Marine Chemistry*, 48, 291-310.

Guieu, C., Chester, R., Nimmo, M., Martin, J.M., Guerzoni, S., Nicolas, E., Mateu, J., Keyse, S. (1997). Atmospheric input of dissolved and particulate metals to the northwestern

Mediterranean. *Deep Sea Research Part II: Topical Studies in Oceanography*, 44(3–4), 655-674.

Guillén, J., Bourrin, F., Palanques, A., Durrieu de Madron, X., Puig, P., Buscail, R. (2006). Sediment dynamics during « wet » and « dry » storm events on the Têt inner shelf (SW Gulf of Lions). *Marine Geology*, 234, 129-142.

Heussner, S., Ratti, C., Carbonne, J. (1990). The PPS 3 time-series sediment trap and the trap sample processing techniques used during the ECOMARGE experiment. *Continental Shelf Research*, 10, 943-958.

Heussner, S., Durrieu de Madron, X., Radakovitch, O., Beaufort, L., Biscaye, P.E., Carbonne, J., Delsaut, N., Etcheber, H., Monaco, A. (1999). Spatial and temporal patterns of downward particle fluxes on the continental slope of the Bay of Biscay (northeastern Atlantic). *Deep Sea Research Part II: Topical Studies in Oceanography*, 46(10), 2101-2146.

Heussner, S., Durrieu de Madron, X., Calafat, A., Canals, M., Carbonne, J., Delsaut, N., Saragoni, G. (2006). Spatial and temporal variability of downward particle fluxes on a continental slope: Lessons from an 8-yr experiment in the Gulf of Lions (NW Mediterranean). *Marine Geology*, 234(1–4), 63-92.

Ho, H.H., Swennen, R., Cappuyns, V., Vassilieva, E., Tran, T.V. (2012). Necessity of normalization to aluminum to assess the contamination by heavy metals and arsenic in sediments near Haiphong Harbor, Vietnam. *Journal of Asian Earth Sciences*, 56, 229-239.

Huh, C.A., Lin, H.L., Lin, S., Huang, Y.W. (2009). Modern accumulation rates and budget of sediment off the Gaoping (Kaoping) River, SW Taiwan: a tidal and flood dominated depositional environment around a submarine canyon. *Journal of Marine Systems*, 76, 405-416.

Kao, S.J., & Milliman, J.D. (2008). Water and sediment discharge from small mountainous rivers, Taiwan: the role of lithology, episodic events, and human activities. *Journal of Geology*, 116, 431-448.

Langston, W.J., Burt, G.R., Pope, N.D. (1999). Bioavailability of Metals in Sediments of the Dogger Bank (Central North Sea): A Mesocosm Study. *Estuarine, Coastal and Shelf Science*, 48(5), 519-540.

Lee, C.-L., Fang, M.-D., Hsieh, M.-T. (1998). Characterization and distribution of metals in surficial sediments in Southwestern Taiwan. *Marine Pollution Bulletin*, 36(6), 464-471.

Ludwig, W., Meybeck, M. and Abousamra, F. (2003). Riverine transport of water, sediments, and pollutants to the Mediterranean Sea. Athens: *UNEP MAP Technical report,* Series 141.

Marin, B., Giresse, P. (2001). Particulate manganese and iron in recent sediments of the Gulf of Lions continental margin (north-western Mediterranean Sea): deposition and diagenetic process. *Marine Geology*, 172(1–2), 147-165.

Martín, J., Durrieu de Madron, X., Puig, P., Bourrin, F., Palanques, A., Houpert, L., Higueras, M., Sánchez-Vidal, A., Calafat, A., Canals, M., Heussner, S., Delsaut, N., Sotin, C. (2013). Sediment transport along the Cap de Creus Canyon flank during a mild, wet winter. *Biogeosciences*, 10, 3221-3239.

Migon, C., Nicolas, E. (1998). The trace metal recycling component in the North-western Mediterranean. *Marine Pollution Bulletin*, 36(4), 273-277.

Monaco, A., Courp, T., Heussner, S., Carbonne, J., Fowler, S.W., Deniaux, B. (1990). Seasonality and composition of particulate fluxes during ECOMARGE-I western Gulf of Lions. *Continental Shelf Research*, 10, 959-988.

Palanques, A., Durrieu de Madron, X., Puig, P., Fabres, J., Guillén, J., Calafat, A., Canals, M., Heussner, S., Bonnin, J. (2006). Suspended sediment fluxes and transport processes in the Gulf of Lions submarine canyons. The role of storms and dense water cascading. *Marine Geology*, 234, 43-61.

Palanques, A., Puig, P., Durrieu de Madron, X. (2008). Storm-driven shelf-to-canyon suspended sediment transport at the southwestern Gulf of Lions. *Continental Shelf Research*, 28, 1947-1956.

Pasqual, C., Sánchez-Vidal, A., Zúñiga, D., Calafat, A., Canals, M., Durrieu de Madron, X., Puig, P., Heussner, S., Palanques, A., Delsaut, N. (2010). Flux and composition of settling particles across the continental margin of the Gulf of Lion: the role of dense shelf water cascading. *Biogeosciences*, 7, 217-231.

Puig, P., Palanques, A., Sanchez-Cabeza, J.A., Masqué, P. (1999). Heavy metals in particulate matter and sediments in the southern Barcelona sedimentation system (North-Western Mediterranean). *Marine Chemistry*, 63, 311-329.

Puig, P., Palanques, A., Martin, J. (2014). Contemporary Sediment-Transport Processes in Submarine Canyons. *Annual Review of Marine Science*, 6(5), 53-77.

Radakovitch, O., Roussiez, V., Ollivier, P., Ludwig, W., Grenz, C., Probst, J.L. (2008). Input of particulate heavy metals from rivers and associated sedimentary deposits on the Gulf of Lion continental shelf. *Estuarine, Coastal and Shelf Science*, 77, 285-295.

Raimbault, P., Durrieu de Madron, X. (2003). Research activities in the Gulf of Lion (NW Mediterranean) within the 1997–2001 PNEC project. *Oceanologica Acta*, 26(4), 291-298.

Révillon, S., Jouet, G., Bayon, G., Rabineau, M., Dennielou, B., Hemond, C., Berné, S. (2011). The provenance of sediments in the Gulf of Lions, western Mediterranean Sea. *Geochemistry, Geophysics, Geosystems*, 12.

Roussiez, V., Ludwig, W., Probst, J.L., Monaco, A. (2005). Background levels of heavy metals in surficial sediments of the Gulf of Lions (NW Mediterranean): an approach based on ^{133}Cs normalization and lead isotope measurements. *Environmental Pollution*, 138, 167-177.

Roussiez, V., Ludwig, W., Probst, J.L., Monaco, A., Bouloubassi, I., Buscail, R., Saragoni, G. (2006). Sources and sinks of sediment-bound contaminant in the Gulf of Lions (NW Mediterranean Sea): a multi-tracer approach. *Continental Shelf Research*, 26, 1843-1857.

Roussiez, V., Ludwig, W., Radakovitch, O., Probst, J.-L., Monaco, A., Charrière, B., Buscail, R. (2011). Fate of metals in coastal sediments of a Mediterranean flood-dominated system:

An approach based on total and labile fractions. *Estuarine, Coastal and Shelf Science*, 92(3), 486-495.

Roussiez, V., Heussner, S., Ludwig, W., Radakovitch, O., Durrieu de Madron, X., Guieu, C., Probst, J.-L., Monaco, A., Delsaut, N. (2012). Impact of oceanic floods on particulate metal inputs to coastal and deep-sea environments: A case study in the NW Mediterranean Sea. *Continental Shelf Research*, 45, 15-26.

Roussiez, V., Aubert, D., Heussner, S. (2013). Continental sources of particles escaping the Gulf of Lion evidenced by rare earth element: flood vs. normal conditions. *Marine Chemistry*, 153, 31-38.

Rubio, B., Nombela, M.A., Vilas, F. (2000). Geochemistry of major and trace elements in sediments of the Ria de Vigo (NW Spain): an assessment of metal pollution. *Marine Pollution Bulletin*, 40(11), 968-980.

Salomons, W., & Förstner, U. (1984). *Metals in the hydrocycle*. Berlin: Springer-Verlag.

Santos-Echeandía, J., Prego, R., Cobelo-García, A., Caetano, M. (2012). Metal composition and fluxes of sinking particles and post-depositional transformation in a ria coastal system (NW Iberian Peninsula). *Marine Chemistry*, 134–135, 36-46.

Schäfer, J., Blanc, G. (2002). Relationship between ore deposits in river catchments and geochemistry of suspended particulate matter from six rivers in southwest France. *Science of the Total Environment*, 298, 103-118.

Schiff, K.C., Weisberg, S.B. (1999). Iron as a reference element in determining trace metal enrichment in Southern California coastal shelf sediments. *Marine Environmental Research*, 48, 161-176.

Sutherland, R.A. (2000). Bed sediment-associated trace metals in coastal sediments and soils in an urban stream, Oahu, Hawaii. *Environmental Geology*, 39, 611-627.

Tam, N.F.Y., Yao, M.W.Y. (1998). Normalisation and heavy metal contamination in mangrove sediments. *Science of The Total Environment*, 216(1–2), 33-39.

Ulses, C., Estournel, C., Durrieu de Madron, X., Palanques, A. (2008)a. Suspended sediment transport in the Gulf of Lions (NW Mediterranean): impact of extreme storms and floods. *Continental Shelf Research*, 28, 2048-2070.

Ulses, C., Estournel, C., Puig, P., Durrieu de Madron, X., Marsaleix, P. (2008)b. Dense shelf water cascading in the northwestern Mediterranean during the cold winter 2005: quantification of the export through the Gulf of Lion and the Catalan margin. *Geophysical Research Letters*, 35.

Ulses, C., Estournel, C., Bonnin, J., Durrieu de Madron, X., Marsaleix, P. (2008)c. Impact of storms and dense water cascading on shelf-slope exchanges in the Gulf of Lion (NW Mediterranean). *Journal of Geophysical Research*, 113.

Wedepohl, K.H. (1995). The composition of the continental crust. *Geochimica et Cosmochimica Acta*, 59(7), 1217-1232.

Xu, J.P., Barry, J.P., Paull, C.K. (2013). Small-scale turbidity currents in a big submarine canyon. *Geology*, 41, 143-14.

Chapter IV-2

Impact of dense shelf water cascading on particulate trace metals transfer to the deep-sea

1. Introduction

Continental margin are a reservoir for sediment, carbon and also contaminants. Nevertheless such material is not necessarily immobile and can be transported out off the shelf and reach the deep sea. Submarine canyons are fast-track corridors for material transported from land to the deep-sea and they play a crucial role in the redistribution of carbon and anthropogenic materials derived from terrestrial runoff (*Thomsen et al., 2003*; *DeGeest et al., 2008*). They also act as temporary deposits for their storage (*Rogers et al., 2003*) and are hotspots of high faunal biomass which uses canyons ability for transportation and burial of organic carbon to sustain. Some communities however, might find overwhelming the sudden mobilisation by rapid, episodic flushing events, of large amounts of sediments. Investigating the fate of particulate material and sediment-bound contaminants is essential to understand the factors impacting benthic habitats and ecosystems, the dispersal and sequestration of carbon and chemical elements and to provide a better sustainable management of the coastal area.

Trace metals are mainly sediment-bound contaminants associated with fine river particles (*Salomons and Förstner, 1984*), and they arise from different sources including atmospheric deposition, soil erosion and runoff and industrial or wastewater discharges. Hence, fate of both natural and anthropogenic inputs of trace metals is associated with transport and deposition of particulate matter (*Gibbs, 1973*) as they reach the coastal zone. Studies on Particulate Trace Metal (PTM) dynamics and export budgets are linked to studies on hydrodynamical events. This is especially true in the Gulf of Lion (GoL) as studies have highlighted the predominant role of E-SE storms (*Roussiez et al., 2012*; *Dumas et al., 2014*) and Dense Shelf Water Cascading (DSWC) in wave and current-induced resuspension, erosion (*Guillen et al., 2006*; *Bourrin et al., 2008a,b*) and down-canyon transport of suspended sediment (*Bonnin et al., 2008; Ogston et al., 2008; Palanques et al., 2008; Puig et al., 2008*) and associated elements. Models have also been used to estimate the particulate matter export caused by those hydrodynamic events since they play a predominant role in the biogeochemical cycles and elements burial (*Ulses et al., 2008*). Models are now able to couple this “transport” module with geochemical data to budget export of contaminants. But such an approach is rarely documented since no extensive set of geochemical data is available.

This work was performed within the framework of the HERMES (Hotspot Ecosystem Research on the Margin of European Seas) project, which aims at better understanding the distribution, resilience and the processes (physical, biogeochemical) that control hotspot ecosystems like canyons. It also aimed at better assessing the quantity and quality of suspended sediment and contaminants fluxes, parameters that are essential in the understanding of the whole ecosystem functioning. This experiment enabled to observe a major event of DSWC along the southwestern end of the GoL margin.

In this way, the main objectives of this work are to evaluate the behavior and characteristics of PTM in settling particulate matter and to assess the impact of a DSWC event (winter 2005-2006) on PTM fluxes delivered to the deep sea. We will also analyze the spatial (in and out of the exporting zone) and temporal variability of the PTM distribution and export during this DSWC event and compare all those results with a moderate storm-induced down-welling.

2. Material and Methods

2.1. Study area

The GoL is a crescent-shaped passive margin located in the northwestern Mediterranean sea (Fig.4.7). It is extending from the Pyrenean mountains of northern Spain to the Alps of eastern France. At those promontories, the GoL continental shelf almost vanishes: at the west end, near the Cap de Creus canyon, it narrows to less than 2 km. Its slope is indented by a dozen submarine canyons, coalescing into two major channels and extending down to the deep basin (2000 m).

The continental shelf is fed by different rivers: on one hand, the Rhone, with a drainage basin of 97,800 km^2, is the largest river in the NW Mediterranean in terms of water (*Ludwig et al., 2009*) and solid discharge as it releases between 5.4 to 10.10^6 $T.yr^{-1}$ (*Durrieu de Madron et al., 2000; Roussiez et al., 2012*). As a consequence, the Rhone River is the main source (90%) of freshwater and suspended sediment to the GoL continental margin (*Bourrin and Durrieu de Madron, 2006*). On the other hand the contribution of the smaller southwestern rivers Herault, Orb, Aude and Tet, to the global suspended particles budget is somewhat difficult to estimate because largely controlled by the intensity and recurrence of intense flash-floods events.

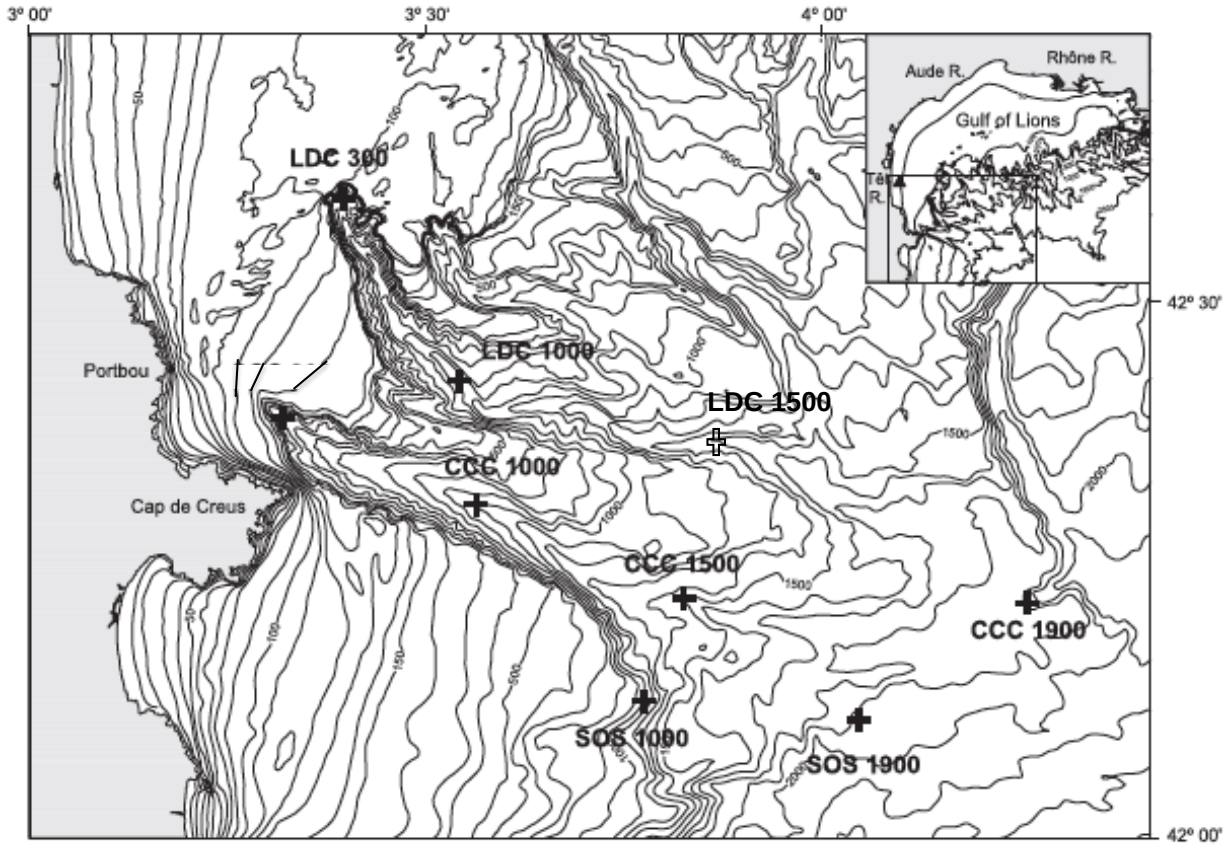

Fig.4.7 Map of the study area, in the SW part of the Gulf of Lion (*modified from Palanques et al., 2012*). Crosses indicate locations of sediment traps in the Lacaze-Duthiers canyon (LDC), Cap de Creus canyon (CCC), and the southern open slope (SOS). Moorings were deployed at 300, 1000, 1500 and 1900m depth and sediment traps are labelled accordingly.

Fine sediments delivered to the continental shelf are temporarily stored off river mouths, until advected and redistributed by the action of wind-induced currents that transport sediments towards the southwestern shelf (*Durrieu de Madron et al., 2008*). Indeed, in winter, the GoL is subjected to severe meteorological conditions where long-lasting cold and dry winds cool and evaporate surface shelf water inducing downslope sinking of surface water masses, which are channelized in submarine canyons. The steep slope of those canyons induces increasing horizontal and vertical near-bottom current speed that allows erosion and transport of sediment. In the GoL, in the past twenty years, major Dense Shelf Water Cascading (DSWC) has happened recurrently twice a decade: in winter 1999-2000, in winter 2005-2006 and in winter 2012-2013 (*Durrieu de Madron et al., 2013*). During these winters, shelf water was dense enough to sink down to the deep slope and basin. Years during which mild DSWC was identified, episodic E and SE winter winds, which generate large swells and storm-induced downwelling, also allowed the export of particulate matter from the GoL continental

shelf to the open sea. It is the coupling of both phenomenon (DSWC and storms) that greatly increases the transport of resuspended shelf and slope sediments towards the deep basin (*Canals et al., 2006; Palanques et al., 2006; Palanques et al., 2012*).

2.2 Experimental design

In order to follow the path of the dense water plume along and across the continental slope of the GoL, the Lacaze-Duthiers (LDC) and Cap de Creus (CCC) submarine canyons, as well as the southern open slope (SOS) were monitored from mid-October 2005 to mid-October 2006. In this work we will focus on the results from the first deployment (October 2005-April 2006) that includes the DSWC event. Currents, temperature and particle fluxes were measured along canyons axis at 300, 1000, 1500 and 1900 m depth and at 1000 and 1900 m depth on the open slope. The hydrology, hydrodynamic and suspended particulate fluxes were described by Palanques et al. (*2012*), and the effect of DSWC on fluxes of major constituents were described by Sanchez-Vidal et al. (*2008*) and Pasqual et al. (*2010*).
Particle fluxes were measured by sequential PPS3 Technicap sediment traps at 30 m above bottom (mab) and currents and temperature by an Aanderaa current meter (RCM7/8/9) at 5 mab. Current and temperature were measured hourly. Sediment traps were programmed to sample the downward particle flux at 15 days intervals. The cups were poisoned with a buffered 5% formaldehyde solution in filtered seawater before deployment. Failure of sediment trap rotating motor resulted in the absence of samples in the CCC300 station.

2.3 Sample treatment and analytical procedures

After recovery, sediment trap samples were stored in the dark at 2-4°C until processed in the laboratory. The procedure described by Heussner et al. (1990) was followed in order to obtain the downward fluxes ($g.m^{-2}.d^{-1}$).
Samples were recovered in clean conditions, after several rinses to eliminate traces of formaldehyde solution, then filtered on pre-weighted glass-fiber filters for organic carbon analysis and on pre-weighed cellulose acetate filters (47 mm in diameter and 0.45 µm in pore size) for trace metals analysis. They were then rinsed with distilled water in order to remove salt and dried at 40°C for at least 24h for dry weight determination.
Particulate matter was recovered for trace metals analysis from cellulose acetate filters, in de-ionized water by using ultrasonic baths. Mineralization of the dried material was performed

in Teflon beakers with successive mixtures of high quality (TraceSELECT®, Fluka or Suprapur, Merck) nitric and hydrofluoric acids (HNO_3-HF) and nitric acid and oxygen peroxide (HNO_3-H_2O_2). Major, trace and rare earth elements concentrations were measured by Inductively Coupled Plasma Mass Spectrometry (ICP-MS, Agilent 7000x) at the CEFREM laboratory (Perpignan, France).

A certified standard (1646a from NIST) was mineralized and analyzed under the same conditions as the samples and provided suitable recoveries (errors < 5% for all element, except for Cu and Cd for which respective recoveries were 83 and 86%). Analytical blanks did not reveal any sign of contamination (< 1 % for Cr, Co, Ni, Cu, Zn, Cd and Pb and < 3% for Al).

Samples for organic carbon (OC) analysis were treated with 25% HCl and analyzed on a Thermo NA 2100 elemental analyzer. Grain-size analyses were performed on a Coulter LS 230 Laser Particle Size Analyzer, after organic matter oxidation with 10% H_2O_2. Both OC and grain-size measurements were realized in the GRC Geociències Marines laboratory (Barcelona, Spain).

Calculation methods

Anthropogenic inputs in trace metal concentrations were assessed in sediment trap samples on the basis of background-normalized metal ratios, commonly designated as Enrichment Factors (EF). The calculation of EFs allows determining the origin of trace metals attached to particles: natural (rock and soil erosion) vs. anthropogenic. An EF superior to 1.5 indicates significant enrichment from anthropogenic origin (*Roussiez et al., 2006*).

In this work, we calculated EFs using the equation below, relative to pre-industrialized reference values:

$$EF = \frac{\left(\frac{X}{C}\right) sample}{\left(\frac{X}{C}\right) background}$$

where C is a conservative element strongly associated with the finest sediment fraction (clays), used as a normalizer to correct variations of major sediment components.

Clays are commonly recognized as the most important carrier of trace metals together with their coating formations like organic matter, and in this study we chose Al as a proxy of this crustal carrier. It has then been widely used in previous studies on marine environments as a normalizer of grain-size variations, as well as in the calculation of EF in heavy metal contamination studies (*Din, 1992*; *Tam and Yao, 1998; Roussiez et al., 2005*).

As for the background reference, Upper Continental Crust (e.g. *Wedepohl, 1995*) is commonly used by default in many studies, although the use of a global reference does not take into account the local lithology that can be highly variable from site to site. In the GoL, the Rhone River is known to be the dominant source of particles. Hence pre-industrial reference values were determined in deep-samples from an ancient Rhone riverbank core, drilled downstream in order to be representative of the whole "natural" Rhone River catchment. This core has already been used as a reference in *Ferrand et al.* (*2012*) and in the previous chapter. Core levels were dated using radiocarbon dating to ensure the reference was pre-industrial.

Tracing procedures

Discrimination of the particles origin is here assessed by the use of Rare Earth Elements (REE) as a lithological signature of watersheds from which particles might come from. REE (from La to Lu) are characterized by their strong affinity with the particulate phase and depict coherent behavior during riverine transport. This tracing method has been widely used in coastal areas (*Sholkovitz, 1988; Jouanneau et al., 1998; Araujo et al., 2002; Prego et al., 2009; Xu et al., 2011*; *Roussiez et al., 2013*). In the research reported here, we will use the same river domains defined in Dumas et al. (*2014*) to determine the lithogenic source of the particles leaving the GoL during winter 2005-2006.

3. Results

3.1 Floods, waves, storm and DSWC chronology in winter 2005-2006

Freshwater discharges (Q) of the Tet and Rhone rivers over the study period are displayed in Fig.4.8. The Rhone river discharge was close to the annual average at the beginning of our study period (Q < 2000 $m^3.s^{-1}$) but increased from early February 2006 until the end of the fisrt deployment (mid-April 2006). On april 12, 2006 the discharge peaked at 4050 $m^3.s^{-1}$.
Even though the water discharge of the other rivers of the Gulf of Lion (Vidourle, Orb, Herault, Aude, Agly, Tet, Tech) was much less important (more than one order of magnitude for the Tet river), all underwent flash-flood events triggered by heavy rainfalls separately from the Rhone River. Indeed, the Tet river was considered flooding in two occasions during the study period: in mid-November 2005 and late January 2006 (Q > 200 $m^3.s^{-1}$ for the Tet

river and up to 1000 $m^3.s^{-1}$ for the the Herault, Orb and Aude). Significant wave height (Hs) measured at the Sète station (Fig.2) showed that moderate storms occurred in early December 2005, mid-January and mid-February 2006, the most important being January 2006 with Hs up to 5.3m.

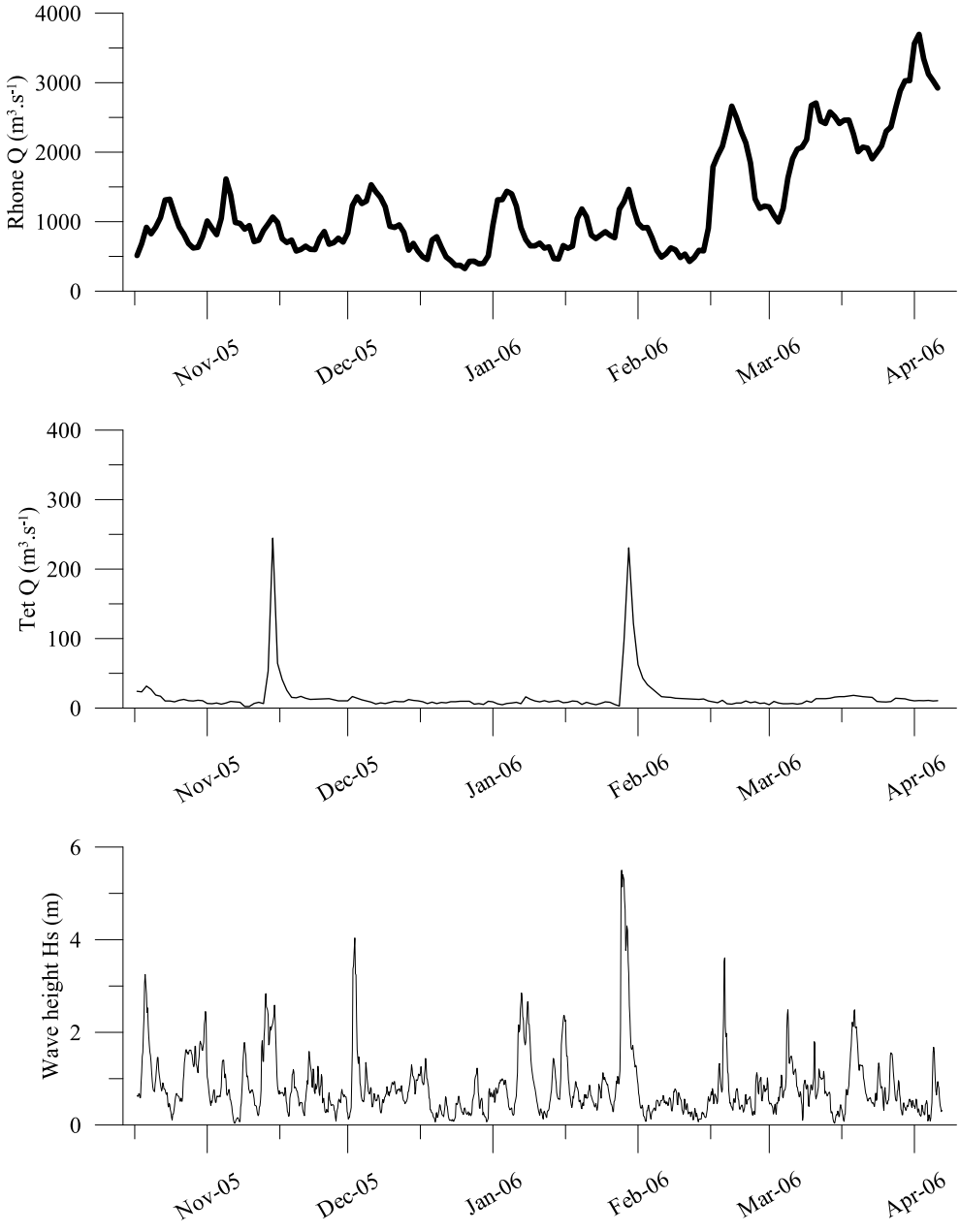

Fig.4.8 Time series of water discharge (Rhone and Tet), as well as significant wave height (Hs) recorded at Sète (France) over the deployment period, from October 2005 to April 2006.

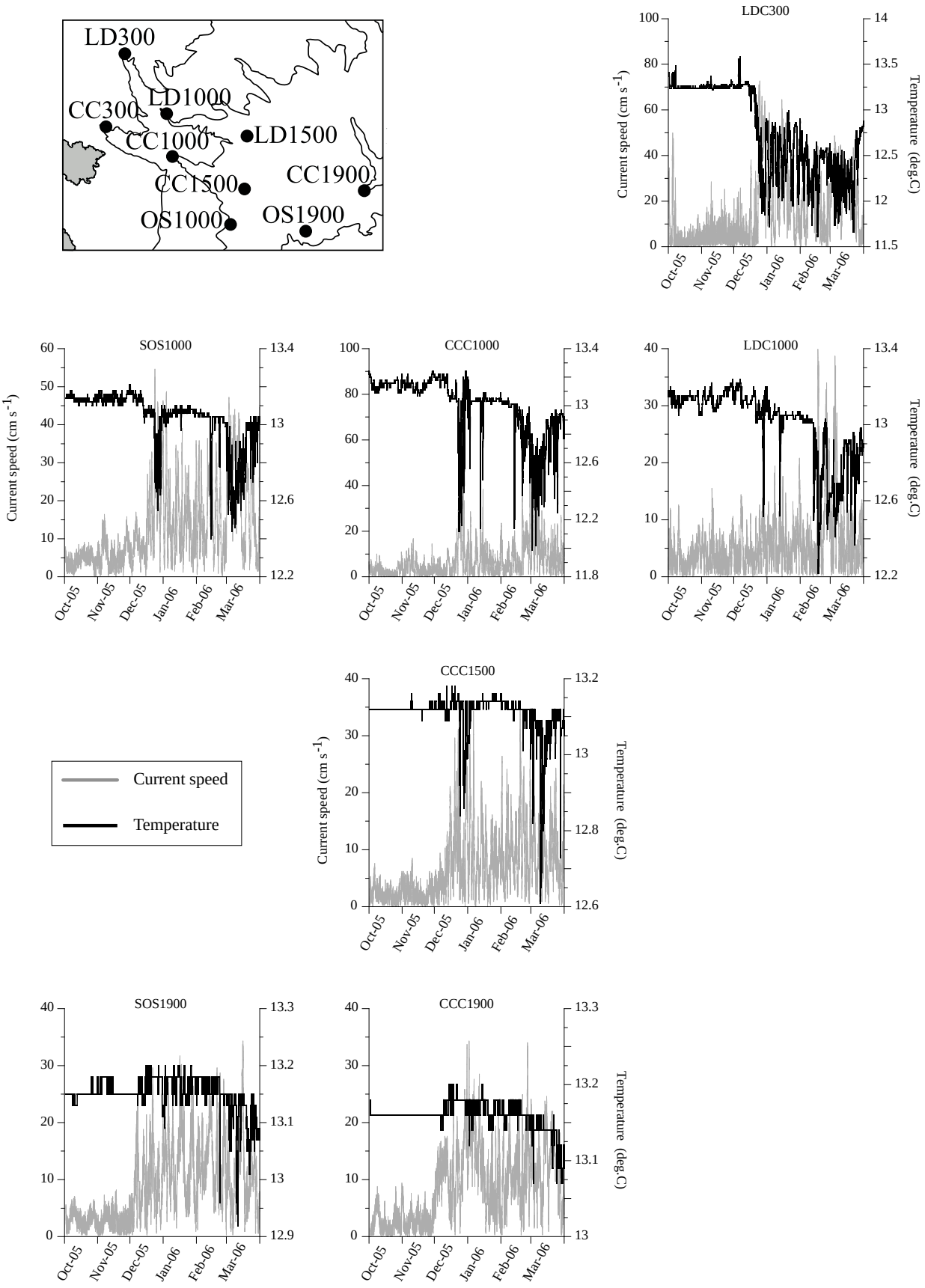

Fig.4.9 Time series of near-bottom current velocity and temperature in the Cap de Creus sediment trap at 1000m depth.

Time series of near-bottom temperature and current speed measured at the different mooring sites are shown in Fig.4.9. Both parameters are quite constant until the end of December 2005, but from early January to April 2006 they show large fluctuations. The strong increase of near-bottom current speed and the drop of near-bottom temperature indicated that occurrence of two major DSWC episodes (January and March-April 2006) affecting the entire slope. The slight warming occurring at the 1900 m deep site in January 2006 prior to the DSWC-induced temperature drop in March was the signature of the bottom-reaching open-convection event that took place in the basin. Hence, storm, DSWC and flood events occurred concomitantly in January 2006, and DSWC and open-ocean convection occurred concomitantly in March 2006.

3.2 Dynamic and composition of the sediment trap material

The temporal variation of total mass fluxes (TMF) collected by the near-bottom sediment traps is represented in Fig.4.10.

As previously described by Pasqual et al. (*2010*), TMF showed a decreasing trend off-shelf: values were higher in the canyons then on the open slope. They were also decreasing concomitantly with depth. For example: TMF_{mean} at CCC1000, CCC1500 and CCC1900 were respectively 20.4, 2.8 and 1.2 $g.m^{-2}.d^{-1}$. This depth-dependent trend is common for the GoL submarine canyons (*Heussner et al., 2006*).

The January 2006 DSWC event induced high TMF in particular in the CCC and its south interfluve. TMF are maximum (up to 1 order of magnitude) at 1000m depth in both canyons and open-slope (39.9, 90.1 and 34.1 $g.m^{-2}.d^{-1}$ at LDC, CCC and SOS1000 respectively) compared to canyon heads and end of the slope (1500 and 1900m depth).

With the DSWC event of March 2006, TMF significantly increase at 1500 (11.9 and 5.1 $g.m^{-2}.d^{-1}$ in LDC and CCC1500 respectively) and 1900m depth (3.2 and 2.4 $g.m^{-2}.d^{-1}$ in CCC and SOS1900 respectively). Open-ocean convection (OOC) is concomitant to the DSWC event (visible on Fig.4.9) and resuspend and redistribute deep-sea floor sediment (*Stabholz et al., 2013*).

Both DSWC events have different impacts: the earlier exports great quantities of continental shelf sediment. This material, deposited at mid-slope is latter transferred to the deep basin during the second event of DSWC and OOC.

Most of the sediment transport identified during this HERMES deployment occurred within 40 days, hence 25% of the total deployment time.

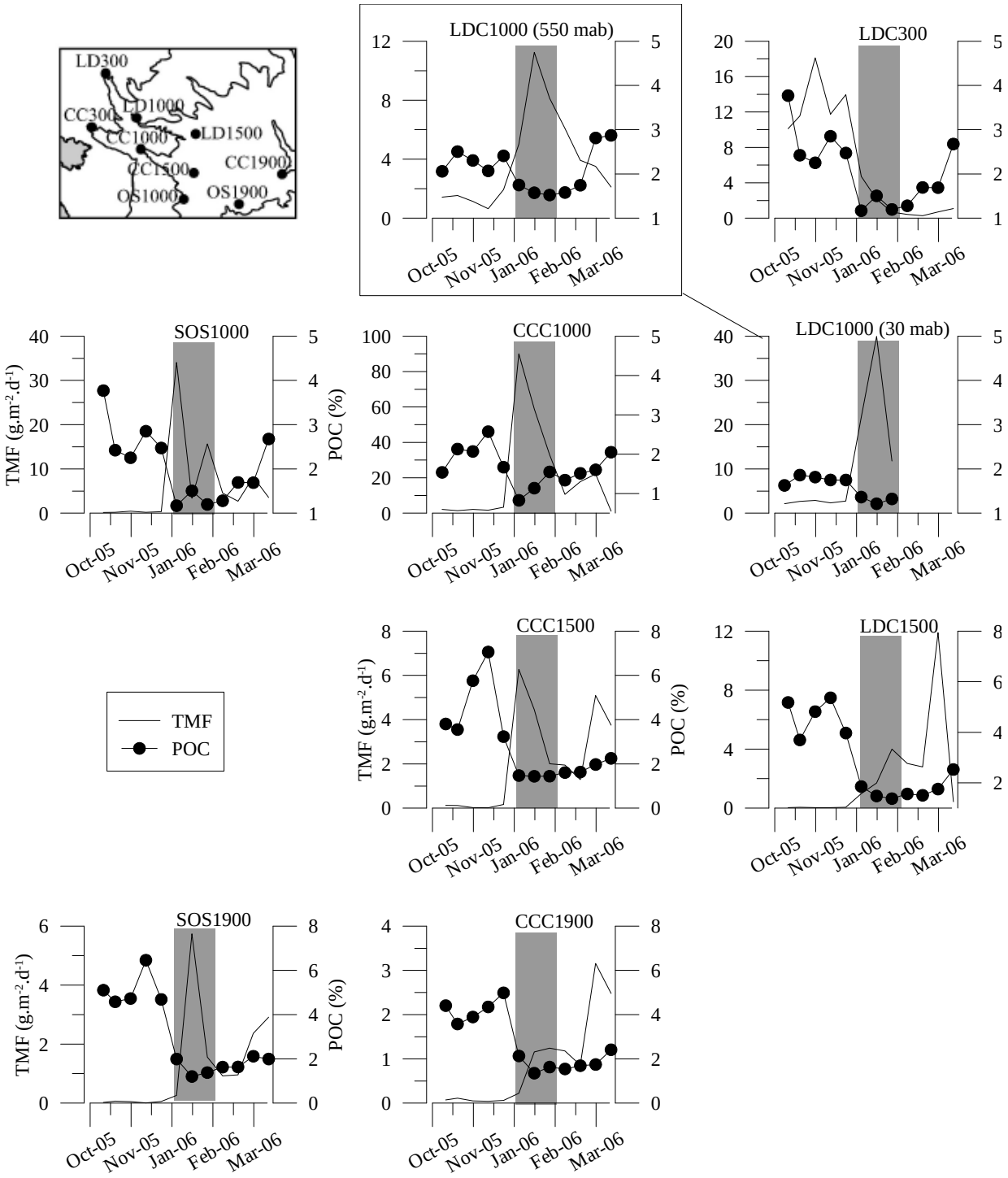

Fig.4.10 Total Mass Fluxes (TMF) and Particulate Organic Carbon (POC) contents of HERMES sediment traps**.**

Particulate organic carbon (POC) content of the material recovered from the sediment traps varied between 0.8 and 5.0%, which is within the same range as what was observed during the CASCADE storm (i.e. between 0.7 and 3%, *Dumas et al., 2014*).

	Reference date	sampling days	TMF $g.m^{-2}.d^{-1}$	C_{org} %	Clay %	Silt %	Sand %	D_{50} µm	Al (µg.g^{-1})	Cr (µg.g^{-1})	Co (µg.g^{-1})	Ni (µg.g^{-1})	Cu (µg.g^{-1})	Zn (µg.g^{-1})	Cd (µg.g^{-1})	Cs (µg.g^{-1})	Pb (µg.g^{-1})	La (µg.g^{-1})	Nd (µg.g^{-1})	Sm (µg.g^{-1})
LDC300	27/10/05	8	10.1	1.7	23	68	4	6.7	72629	94.9	13.2	53.8	48.0	170.4	0.26	10.6	47.1	24.1	21.0	4.0
	07/11/05	15	11.5	1.8	23	73	3	9.9	55751	75.6	10.1	41.9	59.4	157.6		8.0	39.0	19.5	16.8	3.2
	23/11/05	15	18.1	1.8	41	52	4	10.2	62048	88.1	11.8	41.9	44.5	239.4	0.13	8.9	41.3	23.6	20.1	3.8
	07/12/05	15	11.7	1.5	42	49	4	5.1	77954	103.6	14.3	49.9	51.2	246.9	0.17	11.1	47.7	27.0	23.2	4.3
	23/12/05	15	14.0	1.9	39	47	7	5.2	64752	97.9	12.5	45.3	62.8	210.2	0.21	9.1	43.7	25.2	21.4	4.1
	06/01/06	15	4.7	1.5	36	44	6	6.0	61921	84.3	12.6	43.6	39.4	152.9	0.15	10.1	44.0	25.9	22.3	4.1
	22/01/06	15	2.1	1.5	32	56	5	6.6	49071	72.5	11.3	37.8	26.0	119.4	0.12	7.6	40.0	23.3	20.2	3.8
	05/02/06	15	0.7	1.7	28	53	6	6.8	58391	83.6	12.3	43.9	37.6	147.2	0.18	9.5	42.8	25.8	22.2	4.2
	21/02/06	15	0.4	2.1	23	64	5	8.1	66429	110.2	13.5	52.3	58.5	180.8	0.31	9.4	46.4	24.0	20.8	3.7
	08/03/06	15	0.3	2.1					94248	141.0	19.0	68.8	63.5	243.9	0.25	13.1	63.0	33.6	29.0	5.4
	23/03/06	15	0.7	2.6	25	70	4	10.3	57471	87.1	11.8	43.3	41.5	170.1	0.52	7.9	38.9	20.5	19.0	3.4
	06/04/06	15	1.1	2.3	19	71	6	9.2	60930	84.6	11.8	41.8	32.7	182.3	0.21	8.5	38.3	21.2	18.1	3.5
Flux weighted mean			**6.3**	**1.7**	**34**	**56**	**5**		**65154**	**90.9**	**12.3**	**45.6**	**50.7**	**202.0**	**6.83**	**9.4**	**43.3**	**24.0**	**20.6**	**3.9**
LDC1000 (30mab)	27/10/05	15	2.1	1.6	41	48	5	5.3	59032	91.1	17.0	51.5	45.4	152.0	0.18	9.3	44.2	26.0	22.1	4.3
	07/11/05	15	2.7	1.9	47	51	1	4.3	52468	80.8	14.8	44.3	59.1	1443.0	0.73	8.6	43.2	22.5	18.9	3.6
	23/11/05	15	2.9	1.8	44	56	0	4.6	53099	86.6	15.7	46.2	61.1	1035.2	0.58	8.0	46.6	22.6	20.4	3.6
	07/12/05	15	2.3	1.8	44	53	2	4.7	56052	88.3	17.1	46.8	55.0	175.4	0.19	8.7	44.5	23.5	19.6	3.7
	23/12/05	15	2.7	1.8	40	56	2	5.3	61115	91.1	17.0	49.3	61.6	156.1	0.19	9.4	47.0	26.0	21.6	4.2
	22/01/06	15	39.9	1.2	35	57	4	6.1	54545	83.3	12.1	42.4	51.9	172.3	0.16	8.4	40.7	23.9	19.9	4.0
	05/02/06	15	11.8	1.3	37	50	8	6.3	60896	111.4	12.7	58.8	42.1	153.2	0.29	9.3	43.9	25.0	21.1	4.0
Flux weighted mean			**9.2**	**1.3**	**37**	**55**	**4**		**56040**	**89.3**	**13.0**	**46.4**	**51.1**	**258.3**	**0.23**	**8.6**	**42.2**	**24.2**	**20.2**	**4.0**
LDC1000 (550mab)	27/10/05	15	1.4	2.1	46	50	3	4.4	61367	93.3	16.7	50.0	47.9	165.1	0.14	9.8	47.3	26.7	22.1	4.2
	07/11/05	15	1.5	2.5	51	49	0	3.9	56950	120.5	15.1	65.5	59.2	216.7	0.37	8.7	45.7	24.4	20.2	3.8
	23/11/05	15	1.1	2.3	50	50	0	4.0	60780	96.1	18.4	49.7	64.3	217.0	0.27	9.8	50.4	25.7	21.4	4.1
	07/12/05	15	0.6	2.1	47	47	3	4.4	50848	80.1	17.5	42.5	47.4	159.6	0.13	8.0	42.5	21.4	18.3	3.5
	23/12/05	15	1.9	2.4	46	50	3	4.5	54559	87.2	18.9	44.9	70.0	192.0	1.26	8.4	45.5	23.8	19.7	3.8
	22/01/06	15	11.2	1.6	40	51	4	5.5	57093	88.5	13.0	44.1	53.8	203.4	0.17	8.7	43.7	24.0	19.9	3.8
	05/02/06	15	8.1	1.5	42	54	4	5.3	52266	89.3	13.7	47.0	44.3	145.9	0.14	7.6	41.2	23.9	20.1	3.8
	21/02/06	15	6.1	1.6	43	57	1	4.9	45337	94.7	12.8	47.5	31.0	125.4	0.23	6.7	36.3	21.3	17.9	3.4
	08/03/06	15	3.9	1.7	43	53	3	5.1	58525	93.8	15.7	49.6	50.4	170.4	0.18	9.1	44.1	26.0	21.6	4.1
	23/03/06	15	3.5	2.8	43	54	3	5.1	60376	101.2	15.3	52.9	84.5	215.5	0.79	9.4	47.6	26.2	21.8	4.3
	06/04/06	15	2.1	2.9	33	60	5	7.1	61913	107.4	17.7	56.5	62.1	279.7	0.24	9.5	49.9	26.5	23.3	4.3
Flux weighted mean			**3.8**	**1.9**	**42**	**53**	**3**		**55116**	**93.5**	**14.5**	**48.2**	**52.2**	**180.9**	**0.29**	**8.4**	**43.3**	**24.2**	**20.2**	**3.9**
LDC1500	23/12/05	15	0.1	4.0					64581	134.0	34.8	71.0	109.9	335.1	1.79	9.2	69.8	27.6	23.1	4.3
	21/02/06	15	3.0	1.6	24	72	2	9.6	63101	124.8	18.7	64.8	83.9	179.0	1.82	8.6	56.2	27.3	23.2	4.5
	08/03/06	15	2.8	1.5	27	68	3	8.1	60248	114.0	16.5	56.8	51.4	162.5	0.23	8.5	50.9	27.6	23.2	4.5
	23/03/06	15	11.9	1.8	22	70	4	10.5	60703	105.8	14.2	53.4	51.8	185.9	0.25	8.9	47.4	23.4	20.7	4.2
	06/04/06	15	0.4	2.5	21	73	3	10.1	65359	123.4	15.8	61.1	68.1	259.9	0.30	9.5	53.9	30.0	24.9	4.8
Flux weighted mean			**3.6**	**1.7**	**23**	**70**	**3**		**61157**	**110.7**	**15.4**	**56.1**	**57.7**	**183.5**	**0.52**	**8.8**	**49.6**	**24.9**	**21.6**	**4.3**
CCC1000	27/10/05	15	2.1	1.5	32	68	0	6.4	56439	84.1	11.8	44.0	42.4	153.6	0.13	8.4	41.1	21.1	18.5	3.5
	07/11/05	15	1.4	2.1	32	68	0	6.3	66301	97.7	14.5	54.4	58.3	247.8	0.24	9.9	52.6	21.2	18.3	3.5
	23/11/05	15	2.1	2.1	32	66	1	6.3	63682	99.2	13.7	52.2	59.7	229.8	0.47	9.3	49.9	21.3	18.0	3.5
	07/12/05	15	1.7	2.6	46	54	0	4.4	47750	86.8	11.9	46.6	54.6	173.2	0.16	6.8	40.3	17.6	15.3	3.0
	23/12/05	15	3.3	1.7	44	53	2	4.8	64455	100.5	14.7	52.5	74.0	190.5	0.14	8.9	48.5	23.2	20.1	3.9
	06/01/06	15	90.1	0.8	25	49	16	15.8	56198	73.8	11.4	36.3	37.3	139.9	0.22	7.8	39.0	23.0	20.6	4.1
	22/01/06	15	58.8	1.1	30	53	10	9.9	57473	73.9	11.3	37.2	36.7	146.2	0.16	8.4	40.2	24.3	21.5	4.1
	05/02/06	15	33.0	1.6	29	66	3	7.3	61467	87.2	12.8	47.2	44.5	134.4	0.22	9.6	43.1	25.2	21.1	4.0
	21/02/06	15	10.6	1.3	31	63	3	6.9	74814	118.5	17.3	65.9	52.4	213.5	0.49	10.4	56.3	24.6	21.2	3.9
	08/03/06	15	17.8	1.5	29	65	4	7.4	60602	92.3	12.7	48.1	46.1	179.8	0.19	8.2	41.3	20.9	17.6	3.2

	23/03/06	15	22.2	1.6	27	63	6	8.9	67644	93.1	12.4	44.2	37.4	154.3	0.15	8.7	42.7	26.1	23.0	4.4
	06/04/06	15	1.1	2.1	24	65	4	9.1	61936	105.9	13.5	63.4	63.3	246.3	0.33	9.4	46.1	24.7	21.7	4.1
Flux weighted mean			**20.4**	**1.2**	**28**	**56**	**10**		**59590**	**81.7**	**12.1**	**41.6**	**40.5**	**151.0**	**0.21**	**8.4**	**41.5**	**23.8**	**20.8**	**4.0**
CCC1500	07/11/05	15	0.1	3.6					51464	97.0	18.6	54.0	104.1	238.8	0.28	6.8	56.3	21.6	18.5	3.5
	23/12/05	15	0.2	3.2					79402	149.1	27.8	82.8	125.6	409.4	0.55	10.7	85.9	33.2	28.3	5.4
	06/01/06	15	6.3	1.5	40	57	2	6.0	58253	94.3	14.1	48.8	57.8	166.1	0.14	8.9	46.7	28.0	23.7	4.4
	22/01/06	15	4.5	1.4	30	66	3	5.5	60579	113.1	17.7	59.9	67.8	184.2	0.18	8.8	56.0	29.6	24.4	4.6
	05/02/06	15	2.0	1.4	23	74	2	7.3	59919	128.2	18.5	63.4	63.2	131.8	0.25	8.4	58.3	32.2	26.1	4.8
	21/02/06	15	1.9	1.6	23	71	3	9.7	57917	115.5	16.1	60.1	69.1	185.5	0.26	7.9	52.9	24.7	21.4	4.0
	08/03/06	15	1.3	1.6	26	69	3	9.9	54300	128.3	17.8	64.8	65.1	168.8	0.32	7.4	58.1	25.3	21.6	4.0
	23/03/06	15	5.1	2.0	24	71	3	8.6	64107	123.0	15.4	59.7	60.2	187.8	5.92	9.0	54.1	27.1	22.6	4.3
	06/04/06	15	3.8	2.3	20	63	9	9.5	53723	132.3	16.9	63.5	67.9	218.8	0.31	7.4	59.5	25.8	21.3	3.9
Flux weighted mean			**2.8**	**1.7**	**28**	**65**	**4**		**59184**	**115.6**	**16.2**	**58.3**	**63.9**	**182.4**	**1.38**	**8.5**	**54.0**	**27.7**	**23.1**	**4.3**
CCC1900	07/11/05	15	0.1	3.6					52616	95.1	19.5	49.4	131.1	251.5	0.20	5.7	52.2	21.5	17.9	3.5
	23/12/05	15	0.1	5.0					52693	107.3	18.6	60.3	128.8	392.6	0.24	5.8	54.2	22.3	18.4	3.6
	06/01/06	15	0.2	2.1					54666	112.3	17.5	54.7	92.4	262.4	0.24	7.2	54.4	29.1	23.9	4.6
	22/01/06	15	1.2	1.4	39	53	4	5.7	52630	103.1	15.1	56.2	80.1	167.8	0.19	7.1	46.9			
	05/02/06	15	1.2	1.6	40	53	4	5.5	47849	100.0	17.7	55.3	61.9	121.5	0.17	6.5	51.4	27.9	22.8	4.4
	21/02/06	15	1.2	1.5	38	57	3	5.7	56349	110.5	16.2	53.8	60.9	169.4	0.20	6.6	47.8	26.0	21.4	4.1
	08/03/06	15	0.9	1.7	31	56	5	7.4	50584	97.1	14.0	46.4	56.7	141.2	0.36	5.8	40.8	24.9	20.5	3.9
	23/03/06	15	3.2	1.8	38	54	6	6.0	55274	114.7	16.4	56.2	76.5	152.2	0.27	7.2	56.0	28.3	23.8	4.5
	06/04/06	15	2.5	2.4	40	56	3	5.4	52332	114.8	15.7	55.3	76.9	186.3	0.36	7.0	54.4	25.8	21.5	4.1
Flux weighted mean			**1.2**	**1.9**	**37**	**52**	**4**		**53084**	**109.5**	**16.1**	**54.7**	**73.1**	**164.2**	**0.27**	**6.8**	**51.8**	**20.1**	**16.6**	**3.2**
SOS1000	27/10/05	8	0.2	3.8					68699	135.1	24.4	73.4	135.4	306.0	0.37	9.9	73.1	32.1	26.5	4.9
	07/11/05	15	0.2	2.4					69777	119.1	21.8	64.5	99.6	275.3	0.22	9.9	61.4	28.0	23.3	4.5
	23/11/05	15	0.5	2.3					68825	114.6	21.1	61.9	78.7	237.8	2.07	10.2	59.2	26.2	22.1	4.2
	07/12/05	15	0.2	2.9					62676	129.8	22.4	66.6	77.6	201.4	0.52	7.8	62.7	31.9	26.1	5.2
	23/12/05	15	0.3	2.5					56751	97.0	20.7	53.3	75.0	212.3	0.36	8.4	52.1	25.0	21.0	4.0
	06/01/06	15	34.1	1.2	33	57	5	8.0	46701	64.3	9.3	30.5	23.9	98.5	0.14	6.1	28.5	27.3	23.5	4.7
	22/01/06	15	3.4	1.5	37	54	4	6.3	62135	112.9	18.0	61.7	66.7	167.3	0.24	9.6	55.2	31.1	25.3	5.0
	05/02/06	15	15.7	1.2	22	69	5	11.4	65441	95.4	13.3	47.9	37.0	134.7	0.16	10.5	45.2	30.1	25.2	4.7
	21/02/06	15	4.5	1.3	16	80	4	15.5	50952	83.4	12.2	43.6	34.8	127.8	0.18	7.3	38.7	22.1	18.6	3.7
	08/03/06	15	2.7	1.7	24	70	4	9.5	58365	105.0	15.2	53.4	57.4	172.4	0.52	8.1	47.7	26.2	22.0	4.4
	23/03/06	15	8.2	1.7	34	63	3	7.5	55187	86.5	11.9	42.0	40.9	152.6	0.28	7.5	39.5	24.4	20.8	4.0
	06/04/06	15	3.5	2.7	27	68	4	9.0	94542	191.0	23.2	89.3	125.4	356.2	0.53	13.3	79.6	39.4	33.8	6.5
Flux weighted mean			**6.1**	**1.4**	**29**	**62**	**5**		**55699**	**85.4**	**12.2**	**42.0**	**38.5**	**135.0**	**0.21**	**7.9**	**38.9**	**28.0**	**23.8**	**4.7**
SOS1900	23/11/05	15	0.0	4.7					276748	472.7	96.8	256.3	325.5	997.0	0.89	39.5	259.1	125.8	102.3	19.7
	21/02/06	15	0.9	1.6	42	58	0	4.9	47163	110.1	18.3	54.9	75.3	174.6	0.24	5.5	50.8			
	08/03/06	15	1.0	1.6	44	56	0	4.8	11324	221.0	7.8	13.8	33.3	77.7	0.17	1.3	12.9	4.7	3.9	0.8
	23/03/06	15	2.4	2.1	41	59	0	5.2	57176	114.4	18.4	57.4	68.7	159.5	1.01	7.4	54.0	27.7	23.1	4.5
	06/04/06	15	2.9	2.0	39	58	3	5.5	51711	108.4	17.2	55.8	65.7	167.6	0.19	6.9	52.2	27.0	22.5	4.3
Flux weighted mean			**1.4**	**2.0**	**41**	**57**	**1**		**49104**	**128.1**	**17.0**	**52.0**	**65.4**	**159.6**	**0.47**	**6.4**	**48.8**	**14.0**	**11.7**	**2.2**

Table 4.5. Grain-size, OC and PTM concentrations in HERMES sediment traps. Flux-weighted mean contents and concentrations are indicated for each trap. Each sample is named after the reference date of the 15-days sampling interval.

In the LDC, POC content peaked in late November at 1500 m depth (5.2 %). In the CCC, POC peaked in early December at 1000 and 1500 m depth (2.6 and 7.1% respectively), and later in December at 1900 m depth (5.0 %). The lowest POC contents were detected concomitantly with TMF maxima, during the DSWC event. This is explained by the composition of the suspended sediment that is exported: during the cascading event, most of the particulate matter transported is composed of resuspended sediment that had settled on the continental shelf and from which fresh and labile organic carbon has been already removed. The trend was the same on the open slope: POC decreased when TMF increased, but the POC content was higher in the upper open slope than at 1900 m depth.

In Table 4.5, the grain-size of the exported particles is represented by the relative proportion of each size class (clay, silt and sand) and by the modal grain size (D_{50}). Sinking particulate material from the HERMES campaign comprised mostly silt (49-69%) but samples contained a significant part of clay minerals (24-46%). D_{50} (Table 4.5) varied between 4.0 and 15.8 μm over the whole HERMES sediment traps dataset, the coarser being related to the period between the 1^{rst} and the 15th of January (representative date: 7th of January) 2006 in CCC1000, when the cascading event was at its highest. The composition of the settling particles at that time was dominated by silts but the sand proportion increased by a factor 8 (up to 16 %) compared to the other samples, resulting in an increased D_{50} (from 4.8 to 15.8 μm). At 1000m depth, all sediment traps show increased sand proportion during the DSWC event of January, although it is less flagrant in LDC1000, and it happens later in SOS1000 (February 2006). At other depths the trend is opposite: collecting cups corresponding to the January DSWC event have a lower D_{50} size and sand content (e.g. in CCC1500, mean D_{50} is 5.8 μm in January as opposed to 9 μm the rest of the deployment).

It is to be noted that under high current speed (> 70 cm.s^{-1} at the onset of the DSWC in both canyon heads), sediment traps tilt might biase the real TMF. Hence our results are more qualitative than quantitative.

3.3 Spatio-temporal variation of particulate trace metal concentrations in material from the sediment traps

Trace element and Rare Earth Element (REE) concentrations in every sediment trap are presented in Table 4.5. In addition, trace metal mean concentrations were weighted by their corresponding mass flux to calculate flux-weighted mean particulate trace metals (PTM)

concentrations for each trap. This way, mean PTM concentrations reflect the temporal variability of the mass flux.

In most sediment traps, reputed lithogenic metals like Al, Cr or Ni showed almost constant levels throughout the sampling period with slightly lower concentrations during the DSWC event. PTM with supposed higher affinity for organic matter like Cu, Zn, Cd and Pb showed no trend in particular. Looking at the spatial distribution of PTM concentrations, at 1000 m depth, flux-weighted mean concentrations always had the same trend: higher in the LDC compared to the sediment traps of the CCC which were higher than in the SOS1000 trap. This trend was not true for Al which contents did not vary much in any sediment trap. At 1500 m depth, flux-weighted mean concentrations of Cr, Co, Ni, Cu, Cd and Pb seemed higher in the CCC than in the LDC (115.6, 16.2, 58.3, 63.9, 1.4 and 54.0 compared to 110.7, 15.4, 56.1, 57.7, 0.5 and 49.6 $\mu g.g^{-1}$ respectively). The contrary was observed for Al and Zn (CCC < LDC with 59184 and 182.4 compared to 61157 and 183.5 $\mu g.g^{-1}$ respectively). Finally, CCC1900 had slightly higher flux-weighted mean concentrations of Al, Ni, Cu, Zn and Pb than SOS1900 (53084, 54.7, 73.1, 164.2 and 51.8 compared to 49104, 52.0, 65.4, 159.6 and 48.8 $\mu g.g^{-1}$ respectively) but Cr, Co and Cd were found rather higher in the last one (128.1, 17.0 and 0.5 $\mu g.g^{-1}$ respectively in SOS1900 compared to 109.5, 16.1 and 0.3 $\mu g.g^{-1}$ respectively in CCC1900). Although it seems that the particulate export was more concentrated in PTM in the LDC canyon head compared to the CCC, then flowed in the CCC rather than on the open-slope, it is not significant given the inner variability of measures. Instead, it looks like the same material was exported through the LDC and CCC canyons and on the open-slope.

If we now want to inquire on the temporal distribution of PTM and a potential DSWC impact, we have to take into account the variability of the particulate flux composition. As stated in the previous paper (*Dumas et al., 2014*), normalization of PTM concentrations by a clay-tracer is commonly applied to compare chemical characteristics of different materials, and to avoid grain-size bias and dilution effects. Previous studies have compared different clay tracers but in order to test the reliability of Al as an efficient normalizer, we calculated Pearson correlations and results are presented in Table 4.6 under the matrix form.

Hence, during pre and post-DSWC conditions (i.e. excluding samples from January 2006), the distribution of Cr, Co, Ni, Cu and Pb was strongly related to the distribution of Al ($0.80 > r^2 > 0.95$). Only Cd and Zn were not significantly associated with this clay-tracer, which reflects a different carrier phase for both elements (e.g. carbonates). During the DSWC event

however, the situation changed as no elements were linked to Al ($r^2 < 0.50$). Cu and Pb were then correlated with other PTM like Cr, Co and Ni.

a)

DURING DSWC, FOR ALL SAMPLES

	C_{org}	Al	Cr	Co	Ni	Cu	Zn	Cd	Pb
C_{org}	1.00	/	/	/	/	/	/	/	/
Al	0.01	1.00	/	/	/	/	/	/	/
Cr	0.54	0.43	1.00	/	/	/	/	/	/
Co	**0.62**	0.22	**0.88**	1.00	/	/	/	/	/
Ni	0.59	0.40	**0.97**	**0.89**	1.00	/	/	/	/
Cu	0.56	0.07	**0.72**	**0.82**	**0.77**	1.00	/	/	/
Zn	0.29	0.34	0.31	0.26	0.31	0.55	1.00	/	/
Cd	0.03	0.50	0.58	0.32	0.57	0.19	0.05	1.00	/
Pb	0.53	0.45	**0.90**	**0.96**	**0.91**	**0.79**	0.36	0.42	1.00

PRE & POST DSWC. FOR ALL SAMPLES

	C_{org}	Al	Cr	Co	Ni	Cu	Zn	Cd	Pb
C_{org}	1.00	/	/	/	/	/	/	/	/
Al	0.43	1.00	/	/	/	/	/	/	/
Cr	0.47	**0.83**	1.00	/	/	/	/	/	/
Co	0.60	**0.91**	**0.88**	1.00	/	/	/	/	/
Ni	0.54	**0.95**	**0.89**	**0.96**	1.00	/	/	/	/
Cu	**0.77**	**0.80**	**0.81**	**0.91**	**0.89**	1.00	/	/	/
Zn	0.33	0.43	0.37	0.47	0.44	0.47	1.00	/	/
Cd	-0.04	-0.01	-0.07	-0.06	-0.04	-0.01	-0.04	1.00	/
Pb	0.56	**0.95**	**0.88**	**0.98**	**0.99**	**0.91**	0.46	-0.04	1.00

b)

	Cr/Al	**Co/Al**	**Ni/Al**	**Cu/Al**	**Zn/Al**	**Cd/Al**	**Pb/Al**
POC CCC1000	0.79	/	0.74	0.73	0.77	/	0.72
POC CCC1500	/	0.69	/	0.90	0.91	0.68	/
POC CCC1900	/	/	/	**0.89**	**0.93**	/	/

Table 4.6. a) Pearson correlation matrices, during and pre and post DSWC conditions and b) correlation coefficients between Al-normalized concentrations and POC in CCC sediment trap samples.

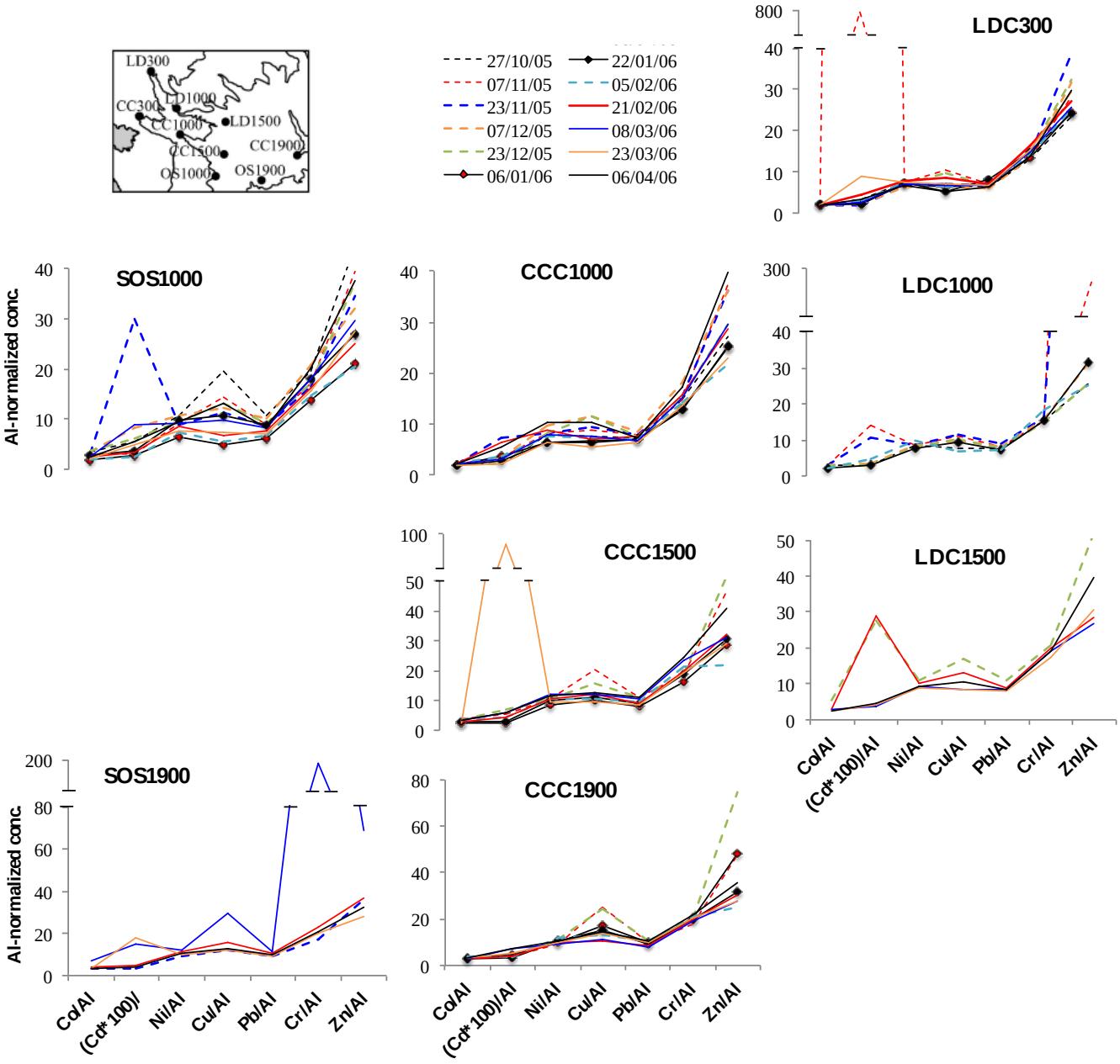

Fig.4.11 Al-normalized Particulate Trace Metal concentrations in HERMES sediment trap samples. Ratios of Cd concentrations were magnified.

We tested this hypothesis by calculating correlation coefficients between Al-normalized PTM concentrations and POC content in the CCC (see Table 4.6b). They had significant correlation coefficients that varied between 0.68 and 0.93. The highest r^2 (ie 0.93) was found for Zn in the CCC1900.

Hence, lower PTM/Al ratios and correlation coefficient with POC in upper sediment traps as opposed to deeper ones reflects the current-induced size sorting (i.e. coarser particles at

canyon heads and finer ones in deeper environments), responsible for a geochemical gradient of settling organic particles but also of sediment-bound trace elements, one of the conclusion by Sanchez-Vidal et al. (*2008*).

4. Discussion

4.1 Origin of the exported material

In the following section, we want to determine the origin of the sinking material entering sediment traps in winter 2005-2006. As we have shown that most of the export due to the DSWC passed through the CCC, we will focus here on this particular site. It is commonly agreed that most sediments deposited on the shelf of the GoL originate from the Rhone river (*Durrieu de Madron et al., 2000; Révillon et al., 2011*). However, previous studies have detected signatures from the Tet river exported material at canyon heads (*Grousset et al., 1995; Roussiez et al., 2013*). As the CCC is facing the mouth of the Tet river, it is not trivial to test the influence of this local river deposit and its impact on the geochemical signature of material exported in the canyon. The tracing experiment conducted here using Rare Earth Element (REE) ratios has been successfully used in previous studies to describe different weathering end-members (e.g. *Araújo et al., 2002; Aubert et al., 2006*), particularly in the GoL (*Roussiez et al., 2013; Dumas et al., 2014*). Established La/Sm and La/Nd relationships (*Roussiez et al., 2013*) were refined by Dumas et al. (*2014*) by adding Rhone and Tet SPM samples collected during a 6-years survey (see chap.III). Signatures of the Rhone and Tet SPM under normal and turbid conditions were isolated, as they tend to differ depending on the hydrological situation. Indeed, in different stream discharge conditions, both rivers likely mobilize materials of different granulometric and mineralogical contents that can result in different REE signatures. The same riverine signatures were used in this study to decipher the origin of the material transferred off-shelf.

Results from this tracing experiment are displayed in Fig.4.12. Samples corresponding to pre-DSWC (blue), DSWC (red) and post-DSWC (black) periods were differentiated in order to detect a potential DSWC impact. The signature from CCC1000 DSWC samples tends closer to the Tet domains, but also fall in the Rhone domains. The rest of the samples from CCC1000 are distributed in the same domains, although some samples have a clear rhodanian signature.

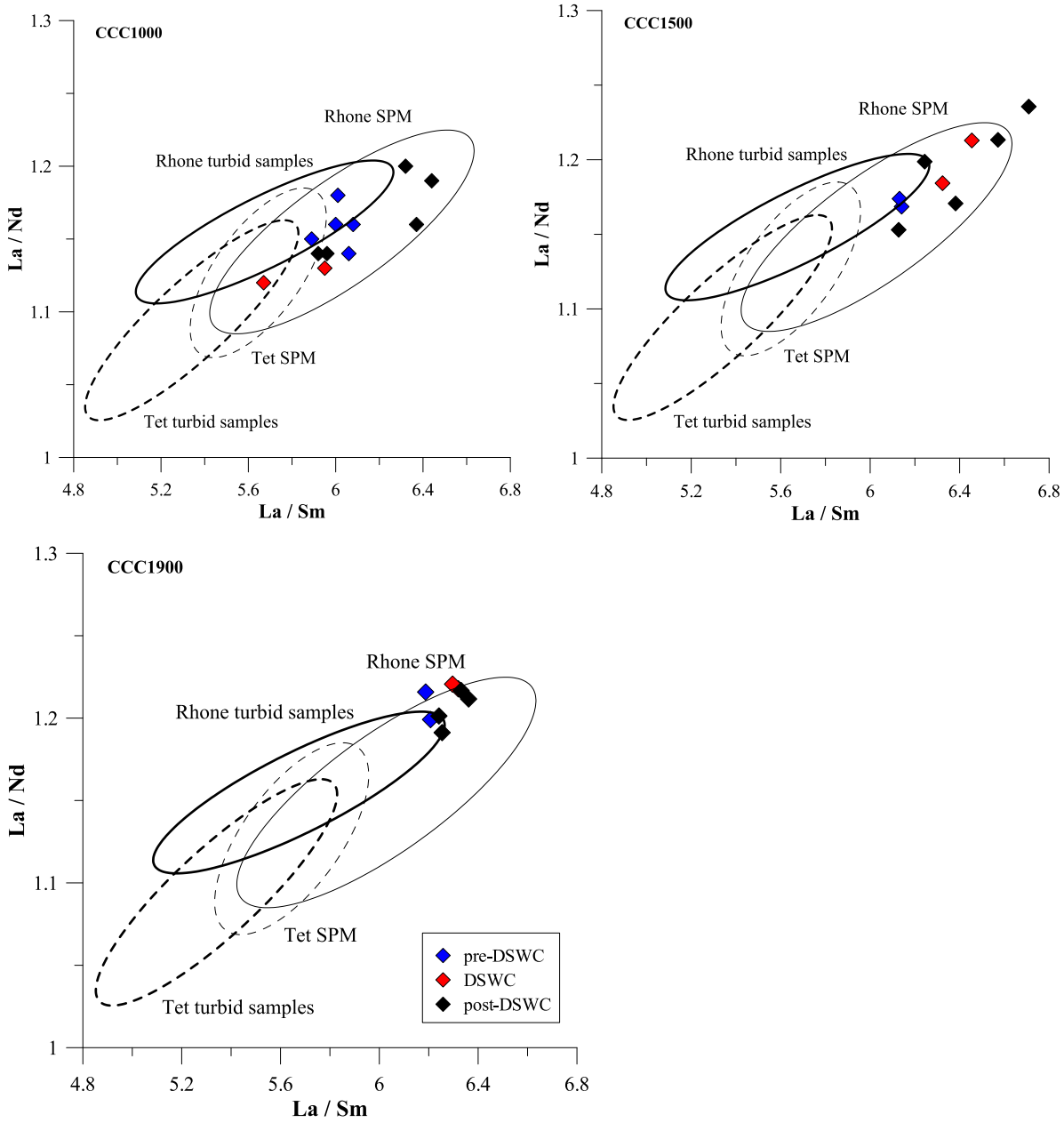

Fig.4.12 Rare Earth Element signatures from Mediterranean coastal rivers (under normal and turbid conditions) and settling particles of CCC sediment traps, plotted in La/Sm vs. La/Nd diagram. In each trap, particles corresponding to pre-DSWC (blue diamonds), DSWC (red diamonds) and post-DSWC (black diamonds) collecting cups were distinguished.

In CCC1500, results are a little different: pre-DSWC samples plot in the coastal rivers domain but DSWC and post-DSWC samples are further away from the Tet areas and in the coastal rivers and Rhone SPM domain.

At CCC1900, samples are even further from the GoL river areas, but are all grouped, probably indicating a different source throughout the whole deployment at this depth. This

could be the result of the abrasion of the canyon walls, the resuspension of temporary canyon deposits and/or the interaction with open-sea convection (*Palanques et al., 2012*).
The result from this method is consistent with the conclusions from other studies. Shelf-exported signals sampled in the Cap de Creus submarine canyon mainly exhibit Rhone SPM imprint but not constantly throughout each event. Indeed, in the CCC, pre-DSWC and DSWC samples plotting in coastal river domains indicate that freshly resuspended flood deposits, probably from the November 2005 flood of coastal Mediterranean rivers, have reached 1000 to 1500m depth. This is also corroborated by the POC content increase in the same sediment traps, although the signal is more and more diluted with depth. This hypothesis was also confirmed by Sanchez-Vidal et al. (*2009*), who showed, with ratios of $\delta^{13}C$ and $\delta^{15}N$, that the proportion of terrestrially derived OC was higher during DSWC.

4.2 Particulate trace metal enrichment factors and anthropogenic influence

Using PTM concentrations of the material collected in sediment traps, and PTM concentrations of a reference sample, we calculated enrichment factors (EF). We tried different reference materials (Upper Continental Crust, a local core from the Rhone river bank) and different clay tracers (Al, Th, REE) and temporal evolution of EF was similar in every sediment trap (data not shown). EF values varied from one reference to another but not much and we chose to represent, in Fig.4.13, EFs calculated as ratios of Al-normalized PTM concentrations, in our samples and in the local reference from the Rhone river, as it is the major conveyor of particles in the GoL.
In all sediment traps, EFs for a given element were in the same range except for SOS1900, which had one sample that brought values higher (i.e. EF_{Cr} of early-March). EF for Co, Cr and Ni ranged between 1.5 and 2.5 (except EF_{Cr} in SOS1900 that reached 19.4); EF values of Pb were quite steady as well (between 1.9 and 3.5); and EF values of Cu, Zn and Cd were the highest and most variable : they ranged from 2.4 to 13.1, 1.5 to 20 and 1.2 to 52 respectively.
Highest EF_{Cu} was found in SOS1900 but also in CCC1900; highest EF_{Zn} was found in LDC1000 whereas highest EF_{Cd} was found in CCC1500. In average, $EF_{Cu} > EF_{Cd} > EF_{Zn} > EF_{Pb} > EF_{Cr} > EF_{Co} > EF_{Ni}$. Looking at their spatial evolution, EFs tended to increase from CCC1000 to CCC1500 and to CCC1900 as opposed to concentrations that decreased with depth.

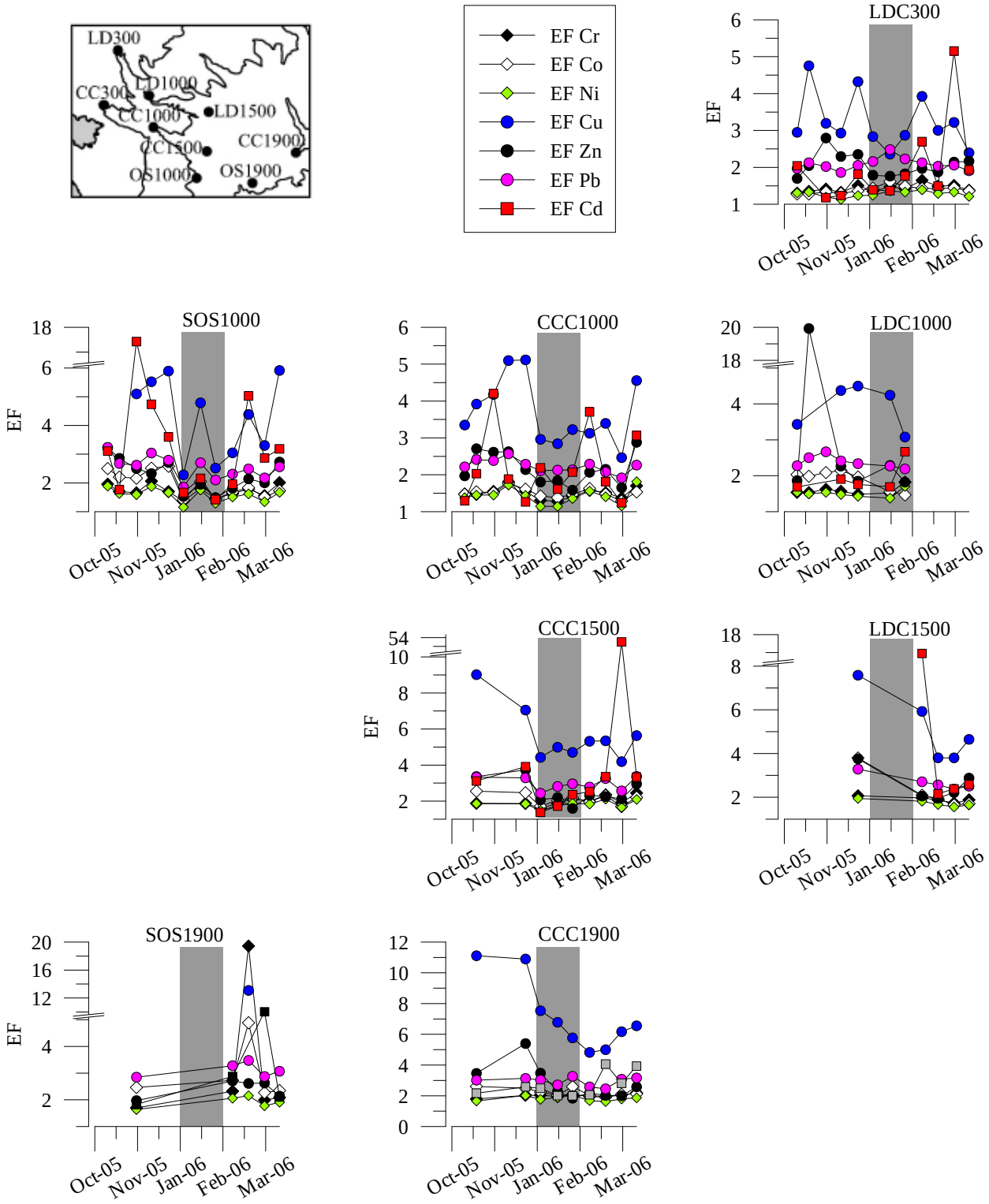

Fig.4.13 Time series of Enrichment Factors in HERMES sediment trap samples.

For example, mean EF_{Cu} were 3.7, 5.6 and 7.2 respectively in those traps. And the same was true in the other canyons (EF_{Cu} = 3.2, 4.2 and 5.2 in LDC300, 1000 and 1500 respectively and 4.8 and 7.3 in SOS1000 and 1900 respectively). The fact that EFs were lower in the upper canyons is probably due to the dilution of the signal by the flow of particulate matter. Indeed, at the head of the canyons, all the grain-size fractions of the flow are transported. But only the finest and lightest particles are transported as deep as 1900m depths and beyond. Indeed, the percentage of clay in deeper sediment traps is higher than in upper ones (*Sanchez-Vidal et al., 2008*). Hence, in upper sediment traps, the signal of anthropogenically enriched PTM is diluted by the larger sand fraction that carries less PTM.

While examining their temporal evolution, it seems that EF_{Ni}, EF_{Co} and EF_{Cr} did not vary much and not highly above the 1.5 threshold of significant anthropogenic enrichment. They had the same behavior in all the sediment traps, except for the exceptional peaks like the one in SOS1900. EF_{Pb} followed the same dynamic as EF_{Cu} but with less amplitude. However, in CCC1000 in particular, EF_{Ni} dropped to 1 during the DSWC event (grey area) indicating a shift in sources of sinking material. It reflects an impoverishment of Ni in the sinking material exported during the cascading process. It suggests that DSWC shelf-exported particles were from one of the coastal rivers (Herault, Orb, Aude or Agly) which local geochemical signature would be impoverished in Ni, or from ancient sediment (from which all the elements' anthropogenic contribution have been released) like the particles that constitute submarine canyon flanks, and that are eroded by intense currents during cascading processes (*Pasqual et al., 2010*).

We compared mean EF values calculated in this work to those calculated during the E-SE storm and we added values from superficial continental shelf sediments (*Roussiez et al., 2012*) as a reference. Results are displayed in Table 4.7. Mean EF values are within the same range in winter 2005-2006 and March 2011 samples. They also are in the range of shelf sediment EFs calculated by Roussiez et al., except for Cu. Significant correlation coefficient are also visible between Cu (or Zn) and POC all along the CCC. This indicates that in winter 2005-2006, most of the material exported off-shelf in the CCC was resuspended continental shelf sediments mixed with material enriched in Cu and Zn. Mean EF_{Cu} and EF_{Zn} increased with depth and with POC content. Hence DSWC has an impact on the spatial distribution of the anthropogenically-enriched PTM, as it induces a grain-size distribution gradient (*Sanchez-Vidal et al., 2008*), which PTM are linked too.

	Reference			Cr	Co	Ni	Cu	Zn	Cd	Pb
This work	local / Al	CCC1000	*winter 2005-06*	1.5 ± 0.2	1.5 ± 0.1	1.4 ± 0.2	3.7 ± 0.9	2.2 ± 0.4	2.2 ± 1.0	2.2 ± 0.2
		r^2 (EF/POC)		*0,79*		*0,74*	*0,73*	*0,77*		*0,72*
		CCC1500	*winter 2005-06*	2.0 ± 0.3	2.1 ± 0.3	1.8 ± 0.2	5.6 ± 1.5	2.5 ± 0.7	8.2 ± 16.6	3.0 ± 0.3
		r^2 (EF/POC)					*0,90*	*0,91*		
		CCC1900	*winter 2005-06*	2.0 ± 0.1	2.2 ± 0.3	1.8 ± 0.2	7.2 ± 2.3	2.8 ± 1.1	2.7 ± 0.8	2.9 ± 0.3
		r^2 (EF/POC)					*0,89*	*0,93*		
Dumas et al. (2014)	local / Al	*T1*	*March 2011*	1.4 ± 0.1	1.3 ± 0.1	1.1 ± 0.1	3.9 ± 0.9	2.2 ± 0.2	1.5 ± 0.8	2.1 ± 0.1
		r^2 (EF/POC)					*0.74*	*0.76*		
		T2	*March 2011*	1.3 ± 0.03	1.3 ± 0.05	1.1 ± 0.1	3.3 ± 0.5	2.0 ± 0.2	1.8 ± 1.7	2.1 ± 0.1
		r^2 (EF/POC)			*0.82*	*0.75*				*-0.75*
		HFS	*13-14th March 11*	1.3 ± 0.1	1.1 ± 0.04	1.0 ± 0.03	1.7 ± 0.2	1.7 ± 0.4	2.2 ± 0.9	2.3 ± 0.4
		Canyon sed. deposit	*deposit*	1.1	1.1	0.9	1.5	/	1.1	2.0
Roussiez et al. (2012)	local / Cs	*Shelf sed*	*flood Dec 03*	1.0	1.0	1.1	1.0	1.7	1.3	2.2

Table 4.7. Mean EFs calculated in CCC sediment traps samples and standard deviation. For the local Rhone riverbank reference samples, correlation coefficients (r^2) were calculated between EF and POC content (significance > 99% with 9 degrees of freedom). Those EF values are compared to EFs calculated by Dumas et al. (2014) in CCC sediment trap samples, high-frequency water sampling samples and the first centimeter of the fresh sediment deposit recovered in the CCC after the E-SE storm studied. Mean EF values calculated by Roussiez et al. (2012) in superficial shelf sediments are also shown.

4.3 Suspended particulate matter and trace metal fluxes

We calculated mean daily elemental fluxes for this major DSWC event and results of those calculations are displayed in Table 4.8a.

For every studied PTM, mean daily elemental fluxes were by far higher in CCC1000, except for Cd, which fluxes were highest in LD300. Mean daily TMF, Al, Cr, Co, Ni, Cu, Zn and Pb fluxes in CCC1000 were 4.5 to 7.5 and 9 to 20 times higher than in CCC1500 and 1900 respectively. Mean daily fluxes in LDC1000 were also higher than in LDC300 and 1500. Fluxes in SOS1000 and 1900 were in the same range as those in LDC1000 and CCC1900 respectively.

The geomorphology of submarine canyons and their interactions with local currents in the Gulf of Lions could explain why the LDC300 fluxes were lower than other upper sediment traps, especially compared to the CCC1000 and LDC1000. The particulate flow tends to be lower at the canyon head because of very strong currents favoring deposition at higher depth (*Bonnin et al., 2008*). Also, it is possible that particulate flux bypassed the head of the

Lacaze-Duthiers canyon to head straight to the Cap de Creus canyon (*DeGeest et al., 2008*). Indeed, fluxes at 300 m depth within the LDC were of the same order of magnitude as at 1000 m depth. This indicates that the DSWC was mostly funneled in the CCC but also that the particulate flow found its isopycnal density somewhere between 1000 and 1500 m depth. This is conclusive with the multi-step sediment transport mentioned by Palanques et al. (*2012*).

If we now compare those mean daily fluxes within the CCC in winter 2005-06 and in March 2011 (Table 4.8b), they are within the same range for T1 (located at 365m depth) and CCC1000.

Numbers in italics (Table 4.8b), indicating the relative contribution of either exporting event (DSWC in 2006 and E-SE storm in 2011) to the total export over the study period, indicate that in CCC1000, between 54 and 61% of the PTM fluxes of winter 2005-06 was due to the DSWC event. In CCC1500 and 1900 it accounted for 5 to 41 and 9 to 12% respectively. Again the contribution of each hydrodynamic event is comparable in both studies as the storm of March 2011 accounted for 54 to 58% of the monthly export.

We used the models' 8 Mt estimate of particulate matter export from the GoL shelf (*Estournel et al., 2010*) for winter 2005-06 (storm and cascading) and calculated total PTM export with mean PTM concentrations from the CCC during the peak of the cascading (January 2006). This calculation gave us an export of 1144 T of Zn to 2 T of Cd over the 2005-06 winter (Table 4.8b). In order to put into perspective particulate fluxes transported by a major DSWC event, which recurrence over the last few decades has been of 5 to 6 years, with a common exporting event like the north-eastern storms that recurrently happen in the GoL 2 to 3 times each winter, we reported the values of particulate fluxes exported in March 2011 during one of those storms (*Dumas et al., 2014*). It seems that the cascading-induced export is 20 to 30 (for Zn and Cu respectively) times more important than the storm-induced export. But again, the storm of March 2011 lasted around 2 days whereas the cascading period was of 30 days. The comparison between the DSWC-induced export and the Rhone input for the same year shows that the 2006 DSWC event had a strong epurating impact.

Moderate storms as well as DSWC are both efficient export processes and even though moderate storms do not last long (3 days against 30 for the January 2006 DSWC) they occur frequently, hence their cumulative export is significant compared to DSWC processes which recurrence is twice a decade.

a)

		Date start	Date end	n° days	TMF ($g.m^{-2}.d^{-1}$)	Al ($mg.m^{-2}.d^{-1}$)	Cr ($mg.m^{-2}.d^{-1}$)	Co ($mg.m^{-2}.d^{-1}$)	Ni ($mg.m^{-2}.d^{-1}$)	Cu ($mg.m^{-2}.d^{-1}$)	Zn ($mg.m^{-2}.d^{-1}$)	Cd ($\mu g.m^{-2}.d^{-1}$)	Cs ($mg.m^{-2}.d^{-1}$)	Pb ($mg.m^{-2}.d^{-1}$)
HERMES	*LDC300*	24/10/05	14/04/06	173	6.3	397	0.56	0.08	0.28	0.31	1.25	44.60	0.06	0.26
	LDC1000 (30mab)	17/10/05	13/02/06	165	9.2	516	0.82	0.12	0.43	0.47	2.38	2.11	0.08	0.39
	LDC1000 (550mab)	17/10/05	14/04/06	105	3.8	209	0.35	0.05	0.18	0.20	0.69	1.09	0.03	0.16
	LDC1500	16/12/05	14/04/06	75	3.6	223	0.40	0.06	0.20	0.21	0.67	1.88	0.03	0.18
	CCC1000	17/10/05	14/04/06	180	20.4	1213	1.66	0.25	0.85	0.82	3.07	4.25	0.17	0.84
	CCC1500	01/11/05	14/04/06	135	2.8	165	0.32	0.05	0.16	0.18	0.51	3.83	0.02	0.15
	CCC1900	01/11/05	14/04/06	135	1.2	62	0.13	0.02	0.06	0.09	0.19	0.31	0.01	0.06
	SOS1000	24/10/05	14/04/06	173	6.1	354	0.54	0.08	0.27	0.24	0.86	1.35	0.05	0.25
	SOS1900	16/11/05	14/04/06	75	1.4	70.9	0.18	0.02	0.08	0.09	0.23	0.67	0.01	0.07

b)

		Date start	Date end	TMF	Cr	Co	Ni	Cu	Zn	Cd	Pb
PTM daily fluxes				**($g.m^{-2}.d^{-1}$)**	**($mg.m^{-2}.d^{-1}$)**	**($mg.m^{-2}.d^{-1}$)**	**($mg.m^{-2}.d^{-1}$)**	**($mg.m^{-2}.d^{-1}$)**	**($mg.m^{-2}.d^{-1}$)**	**($\mu g.m^{-2}.d^{-1}$)**	**($mg.m^{-2}.d^{-1}$)**
This work	***CC1000***	17/10/05	14/04/06	**20.4**	**1.66**	**0.25**	**0.85**	**0.82**	**3.07**	**4.25**	**0.84**
	Contribution of the DSWC to the total winter 2005-06 export (%)			*61*	*55*	*57*	*54*	*56*	*57*	*57*	*58*
	CC1500	01/11/05	14/04/06	**2.8**	**0.32**	**0.05**	**0.16**	**0.18**	**0.51**	**3.83**	**0.15**
	Contribution of the DSWC to the total winter 2005-06 export (%)			*38*	*38*	*41*	*39*	*41*	*41*	*5*	*40*
	CCC1900	01/11/05	14/04/06	**1.2**	**0.13**	**0.02**	**0.06**	**0.09**	**0.19**	**0.31**	**0.06**
	Contribution of the DSWC to the total winter 2005-06 export (%)			*13*	*13*	*13*	*13*	*15*	*15*	*9*	*12*
Dumas et al., 2014	***T1***	04/03/11	21/03/11	**21.5**	**2.56**	**0.34**	**1.17**	**1.37**	**5.37**	**4.85**	**1.37**
	Contribution of the storm to the total March 2011 export (%)			*58*	*56*	*56*	*55*	*54*	*58*	*57*	*56*

PTM export				**(Mt)**	**(T)**	**(T)**	**(T)**	**(T)**	**(T)**	**(T)**	**(T)**
This work	*Total*			8	591	91	294	296	1144	2	317
	Contribution to the total 2006 export of the Rhone river (%)				*374*	*351*	*352*	*375*	*340*	*/*	*350*
Dumas et al., 2014	*Total*	12/03/11	15/03/11	0.4	29	4	13	10	56	0.07	16
	Contribution to the total 2011 export of rivers (%)				*31*	*27*	*26*	*23*	*30*	*/*	*31*

Table 4.8. a) Comparison between HERMES sediment traps' mass and trace metal fluxes. All fluxes are in $mg.m^{-2}.d^{-1}$ except for Al, which is in $g.m^{-2}.d^{-1}$ and for Cd, which is in $\mu g.m^{-2}.d^{-1}$. b) Comparison between CCC PTM daily fluxes and total export calculated in this work and in Dumas et al., 2014.

Ulses et al. (*2008*) calculated the export of shelf water by both intense E-SE storms and DSWC events and concluded that marine storms are powerful mechanisms inducing substantial export of shelf water over short periods, equivalent to cascading episodes lasting several weeks.

Puig et al. (*2013*) showed in their studies of the 1999-2011 period and Durrieu de Madron et al. (*2013*) in winter 2012, that the deep dense water formed by DSWC events spreads across the deep Mediterranean basin after interactions with open-sea convection processes and can last for years (in 2011, Puig et al. detected the deep dense water mass formed in winter 2006). The thick (tenth of meters) bottom nepheloid layer formed in 2006 was mainly composed of clay, the best carrier for PTM. Those resuspended particles coming from continental margins are considered responsible for the fertilization of the deep-sea environments that feed on the arrival of those nutritive particles but also consume sediment-bound contaminants. The spreading of this material could significantly affect biogeochemical cycles of the Western Mediterranean deep basin. Hence, calculating budgets of PTM export is important in order to predict possible impacts.

5. Conclusion

The main objectives of this work were to assess the impact of a DSWC event (winter 2005-2006) on PTM fluxes delivered to the deep sea. Observations gathered during the HERMES deployment allowed analyzing the spatial (in and out of the exporting zone) and temporal variability of the PTM distribution and export during this DSWC event, and comparing all those results with a moderate storm-induced down-welling export. The main conclusions are listed below.

- The rare-earth element tracing methods has shown that, in the Cap de Creus canyon, the material exported up to 1500m depth originate mainly from Rhone particulate input, but mixed with coastal river contribution. This coastal river signal was detected at 1000m and 1500m depths and was probably induced by resuspension of flood deposits from November 2005. At 1900m depth however, the particles originates from a same source but different than upper sediment traps. We suggested that it was either due to resuspension of temporary canyon deposits and erosion of canyon flanks by DSWC-induced strong currents; or to interaction with open-sea convection, as suggested by Palanques et al. (*2012*).

- This study has shown that the material exported in winter 2005-2006 displayed EF values similar to the storm-exported material of March 2011 and to superficial shelf sediment. This indicates that, during both exporting events, exported material was mostly constituted of resuspended shelf sediment, in agreement with the previous conclusion. Enrichment in Cu and Zn, as well as impoverishment in Ni, emphasizes the role of DSWC-induced currents in mixing resuspended shelf sediment with coastal river particles. The spatial distribution of EF, with higher values at 1900m depth highlights the strong affinity of PTM with clay fraction and POC. Hence the geochemical gradient induced by DSWC is also responsible for the spatial distribution of anthropogenically-enriched PTM.
- In terms of quantities, DSWC-induced off-shelf export is 20 to 30 times higher than the storm-induced off-shelf export of March 2011. As both events exported the same material (i.e. resuspended shelf sediment), mean daily PTM fluxes were comparable. But the interaction between DSWC and a moderate storm in January 2006 induced greater particulate and sediment-bound elemental export than a single storm.
- Even though DSWC event are not as recurrent as E-SE storms in the GoL, they have a great flushing potential. It is verified by the imprint they set in water masses and nepheloid layers that spread and set during years on the deep Mediterranean basin.

References

Araújo, M.F., Jouanneau, J.M., Valerio, P., Barbosa, T., Gouveia, A., Oliveira, A., Rodrigues, A., Dias, J.M.A. (2002). Geochemical tracers of northern Portuguese estuarine sediments on the shelf. *Progress in Oceanography*, 52, 277-297.

Aubert, D., Le Roux, G., Krachler, M., Cheburkin, A., Kober, B., Shotyk, W., Stille, P. (2006). Origin and fluxes of atmospheric REE entering an ombotrophic peat bog in Black Forest (SW Germany): evidence from snow, lichens and mosses. *Geochimica and Cosmochimica Acta*, 70(11), 2815-2826.

Bonnin, J., Heussner, S., Calafat, A., Fabres, J., Palanques, A., Durrieu de Madron, X., Canals, M., Puig, P., Avril, J., Delsaut, N. (2008). Comparison of horizontal and downward particle fluxes across canyons of the Gulf of Lions (NW Mediterranean): Meteorological and hydrodynamical forcing. *Continental Shelf Research*, 28(15), 1957-1970.

Bourrin, F., Durrieu de Madron, X., Ludwig, W. (2006). Contribution to the study of coastal rivers and associated prodeltas to sediment supply in the Gulf of Lions (NW Mediterranean Sea). *Vie et Milieu-Life and Environment*, 56, 307-314.

Bourrin, F., Friend, P.L., Amos, C.L., Manca, E., Ulses, C., Palanques, A., Durrieu de Madron, X., Thompson, C.E.L. (2008)a. Sediment dispersal from a typical Mediterranean flood: The Têt River, Gulf of Lions. Continental Shelf Research, 28(15), 1895-1910.

Bourrin, F., Durrieu de Madron, X., Heussner, S., Estournel, C. (2008)b. Impact of winter dense water formation on shelf sediment erosion (evidence from the Gulf of Lions, NW Mediterranean). *Continental Shelf Research*, 28(15), 1984-1999.

Canals, M., Puig, P., Durrieu de Madron, X., Heussner, S., Estournel, C. (2006). Flushing submarine canyons. *Nature*, 444, 354-357.

DeGeest, A.L., Mullenbach, B.L., Puig, P., Nittrouer, C.A., Drexler, T.M., Durrieu de Madron, X., Orange, D.L. (2008). Sediment accumulation in the western Gulf of Lions,

France: the role of Cap de Creus Canyon in linking shelf and slope sediment dispersal systems. *Continental Shelf Research*, 28, 2031-2047.

Din, Z.B. (1992). Use of aluminium to normalize heavy-metal data from estuarine and coastal sediments of Straits of Melaka. *Marine Pollution Bulletin*, 24(10), 484-491.

Dumas, C., Aubert, D., Durrieu de Madron, X., Ludwig, W., Heussner, S., Delsaut, N., Menniti, C., Sotin, C., Buscail, R. (2014). Storm-induced transfer of particulate trace metals to the deep-sea in the Gulf of Lion (NW Mediterranean Sea). *Environmental Geochemistry and Health*, 36(5), 995-1014.

Durrieu de Madron, X., Panouse, M. (1996). Advective transport of suspended particulate matter on the Gulf of Lions continental shelf. Summer and winter situations. *Comptes-Rendus de l'Académie des Sciences de Paris*, 322(12), 1061-1070.

Durrieu de Madron, X., Abderrazzak, A., Heussner, S., Monaco, A., Aloisi, J.C., Radakovitch, O., Giresse, P., Buscail, R., Kerherve, P. (2000). Particulate matter and organic carbon budgets for the Gulf of Lions (NW Mediterranean). *Oceanologica Acta*, 23(6), 717-730.

Durrieu de Madron, X., Wiberg, P.L., Puig, P. (2008). Sediment dynamics in the Gulf of Lions: The impact of extreme events. *Continental Shelf Research*, 28(15), 1867-1876.

Durrieu de Madron, X., Houpert, L., Puig, P., Sanchez-Vidal, A., Testor, P., Bosse, A., Estournel, C., Somot, S., Bourrin, F., Bouin, M.N., Beauverger, M., Beguery, L., Calafat, A., Canals, M., Cassou, C., Coppola, L., Dausse, D., D'Ortenzio, F., Font, J., Heussner, S., Kunesch, S., Lefevre, D., Le Goff, H., Martin, J., Mortier, L., Palanques, A., Raimbault, P. (2013). Interaction of dense shelf water cascading and open-sea convection in the northwestern Mediterranean during winter 2012. *Geophysical Research Letters*, 40, 1-7.

Estournel, C., Ulses, C., Durrieu de Madron, X., Puig, P., Marsaleix, P. (2010). A five-year budget of fine sediment in the Gulf of Lion : Importance of intense events (floods, storms and dense water cascading). *39th CIESM Congress*, 10-14 May 2010, Venice, Italy.

Ferrand, E., Eyrolle, F., Radakovitch, O., Provansal, M., Dufour, S., Vella, C., Raccasi, G., Gurriaran, R. (2012). Historical levels of heavy metals and artificial radionucleides reconstructed from overbank sediment records in lower Rhône River (South-East France). *Geochimica et Cosmochimica Acta*, 82, 163–182.

Gibbs, R.J. (1973). Mechanisms of trace metal transport in rivers. *Science*, 180, 71-72.

Grousset, F.E., Quetel, C.R., Thomas, B., Donard, O.F.X., Lambert, C.E., Guillard, F., Monaco, A. (1995). Anthropogenic vs lithogenic origins of trace elements (As, Cd, Pb, Rb, Sb, Sc, Sn, Zn) in water column particles: northwestern Mediterranean Sea. *Marine Chemistry*, 48, 291-310.

Guillén, J., Bourrin, F., Palanques, A., Durrieu de Madron, X., Puig, P., Buscail, R. (2006). Sediment dynamics during « wet » and « dry » storm events on the Têt inner shelf (SW Gulf of Lions). *Marine Geology*, 234, 129-142.

Heussner, S., Ratti, C., Carbonne, J. (1990). The PPS 3 time-series sediment trap and the trap sample processing techniques used during the ECOMARGE experiment. *Continental Shelf Research*, 10, 943-958.

Heussner, S., Durrieu de Madron, X., Calafat, A., Canals, M., Carbonne, J., Delsaut, N., Saragoni, G. (2006). Spatial and temporal variability of downward particle fluxes on a continental slope: Lessons from an 8-yr experiment in the Gulf of Lions (NW Mediterranean). *Marine Geology*, 234(1–4), 63-92.

Jouanneau, J.M., Weber, O., Grousset, F.E., Thomas, B. (1998). Pb, Zn, Cs, Sc and rare earth elements as tracers of the Loire and Gironde particles on the Biscay shelf (SW France). *Oceanologica Acta*, 21(2), 233–241.

Ludwig, W., Dumont, E., Meybeck, M., Heussner, S. (2009). River discharges of water and nutrients to the Mediterranean and Black Sea: Major drivers for ecosystem changes during past and future decades? *Progress in Oceanography*, 80(3–4), 199-217.

Ogston, A., Drexler, T., Puig, P. (2008). Sediment delivery, resuspension, and transport in two contrasting canyon environments in the southwest Gulf of Lions. Continental Shelf Research, 28(15), 2000-2016.

Palanques, A., Durrieu de Madron, X., Puig, P., Fabres, J., Guillén, J., Calafat, A., Canals, M., Heussner, S., Bonnin, J. (2006). Suspended sediment fluxes and transport processes in the Gulf of Lions submarine canyons. The role of storms and dense water cascading. *Marine Geology*, 234, 43-61.

Palanques, A., Puig, P., Durrieu de Madron, X. (2008). Storm-driven shelf-to-canyon suspended sediment transport at the southwestern Gulf of Lions. *Continental Shelf Research*, 28, 1947-1956.

Palanques, A., Puig, P., Durrieu de Madron, X., Sanchez-Vidal, A., Pasqual, C., Martín, J., Calafat, A., Heussner, S., Canals, M. (2012). Sediment transport to the deep canyons and open-slope of the western Gulf of Lions during the 2006 intense cascading and open-sea convection period. *Progress in Oceanography*, 106, 1-15.

Pasqual, C., Sánchez-Vidal, A., Zúñiga, D., Calafat, A., Canals, M., Durrieu de Madron, X., Puig, P., Heussner, S., Palanques, A., Delsaut, N. (2010). Flux and composition of settling particles across the continental margin of the Gulf of Lion: the role of dense shelf water cascading. *Biogeosciences*, 7, 217-231.

Prego, R., Marmolejo, J., Caetano, M., Vale, C. (2009). Rare earth elements in sediments of the Vigo Ria (NW Iberian Peninsula). *Continental Shelf Research*, 29, 896–902.

Puig, P., Palanques, A., Orange, D.L., Lastras, G., Canals, M. (2008). Dense shelf water cascades and sedimentary furrow formation in the Cap de Creus Canyon, northwestern Mediterranean Sea. Continental Shelf Research, 28(15), 2017-2030.

Puig, P., Durrieu de Madron, X., Salat, J., Schroeder, K., Martín, J., Karageorgis, A.P., Palanques, A., Roullier, F., Luis Lopez-Jurado, J., Emelianov, M., Moutin, T., Houpert, L. (2013). Thick bottom nepheloid layers in the western Mediterranean generated by deep dense shelf water cascading. *Progress in Oceanography*, 111, 1-23.

Révillon, S., Jouet, G., Bayon, G., Rabineau, M., Dennielou, B., Hemond, C., Berné, S. (2011). The provenance of sediments in the Gulf of Lions, western Mediterranean Sea. *Geochemistry, Geophysics, Geosystems*, 12.

Rogers, A., Billett, D., Berger, W., Flach, E., Freiwald, A., Gage, J., Hebbeln, D., Heip, C., Pfannkuche, O., Ramirez-Llodra, E., Medlin, L., Sibuet, M., Soetaert, K., Tendal, O., Vanreusel, A., Wlodarska- Kowalczuk, M. (2003). Life at the edge: Achieving prediction from environmental variability and biological variety. *Ocean Margin Systems*, 387-404, Berlin: Springer-Verlag.

Roussiez, V., Ludwig, W., Probst, J.L., Monaco, A. (2005). Background levels of heavy metals in surficial sediments of the Gulf of Lions (NW Mediterranean): an approach based on ^{133}Cs normalization and lead isotope measurements. *Environmental Pollution*, 138, 167-177.

Roussiez, V., Ludwig, W., Probst, J.L., Monaco, A., Bouloubassi, I., Buscail, R., Saragoni, G. (2006). Sources and sinks of sediment-bound contaminant in the Gulf of Lions (NW Mediterranean Sea): a multi-tracer approach. *Continental Shelf Research*, 26, 1843-1857.

Roussiez, V., Heussner, S., Ludwig, W., Radakovitch, O., Durrieu de Madron, X., Guieu, C., Probst, J.L., Monaco, A., Delsaut, N. (2012). Impact of oceanic floods on particulate metal inputs to coastal and deep-sea environments: A case study in the NW Mediterranean Sea. *Continental Shelf Research*, 45, 15-26.

Roussiez, V., Aubert, D., Heussner, S. (2013). Continental sources of particles escaping the Gulf of Lion evidenced by rare earth element: flood vs. normal conditions. *Marine Chemistry*, 153, 31-38.

Salomons, W., & Förstner, U. (1984). *Metals in the hydrocycle*. Berlin: Springer-Verlag.

Sanchez-Vidal, A., Pasqual, C., Kerhervé, P., Calafat, A., Heussner, S., Palanques, A., Durrieu de Madron, X., Canals, M., Puig, P. (2008). Impact of dense shelf water cascading on the transfer of organic matter to the deep western Mediterranean basin. *Geophysical Research Letters*, 35(5).

Sanchez-Vidal, A., Pasqual, C., Kerhervé, P., Heussner, S., Calafat, A., Palanques, A., Durrieu de Madron, X., Canals, M., Puig, P. (2009). Across margin export of organic matter by cascading events traced by stable isotopes, northwestern Mediterranean Sea. *Limnology and Oceanography*, 54(5), 1488-1500.

Sholkovitz, E. (1988). Rare earth elements in the sediments of the North Atlantic Ocean, Amazon delta, and East China Sea: reinterpretations of terrigenous input patterns to the oceans. *American Journal of Science, 288*, 236–281.

Stabholz, M., Durrieu de Madron, X., Canals, M., Khripounoff, A., Taupier-Letage, I., Testor, P., Heussner, S., Kerhervé, P., Delsaut, N., Houpert, L., Lastras, G., Dennielou, B. (2013). Impact of open-ocean convection on particle fluxes and sediment dynamics in the deep margin of the Gulf of Lions. *Biogeosciences*, 10, 1097-1116.

Tam, N.F.Y., Yao, M.W.Y. (1998). Normalisation and heavy metal contamination in mangrove sediments. *Science of The Total Environment*, 216(1–2), 33-39.

Thomsen, L., Van Weering, T., Blondel, P., Lampitt, R.S., Lamy, F., McCave, I.N., McPhail, S., Meinert, J., Neves, R., d'Ozouville, L., Ristow, D., Waldmann, C., Wollast, R. (2003). Margin building-regulating processes. *Ocean Margin Systems*, 195-203, Berlin: Springer-Verlag.

Ulses, C., Estournel, C., Bonnin, J., Durrieu de Madron, X., Marsaleix, P. (2008). Impact of storms and dense water cascading on shelf-slope exchanges in the Gulf of Lion (NW Mediterranean). *Journal of Geophysical Research*, 113.

Wedepohl, K.H. (1995). The composition of the continental crust. *Geochimica et Cosmochimica Acta*, 59(7), 1217-1232.

Xu, J.P., Barry, J.P., Paull, C.K. (2013). Small-scale turbidity currents in a big submarine canyon. *Geology*, 41, 143-14.

Chapter V

Geochemical characteristics in recent deep sediments from the Gulf of Lion

In this chapter we focus the research on three sediment cores from the abyssal plain of the NW Mediterranean Sea, sampled in continuity to the Cap de Creus and Lacaze-Duthiers submarine canyons. The idea is to look for a signature of those extreme off-shelf export events in the nature of the sediment and/or their particulate trace metals concentrations. Indeed, Puig et al., 2013 identified bottom nepheloid layers formed by different events of dense shelf water cascading off the continental shelf. Those dense water masses are loaded with suspended particles and aggregates and their maintenance on the abyssal plain over time could have an impact on deep-sea biogeochemical cycles. The presence of suspended material ensures presence of sediment-bound contaminants in those pristine environments as well.

As well as describing the contamination level of the north-western mediterranean deep sediments, we attempted to identify its source. However, we saw in the previous section (IV.2) that particulate transport along submarine canyons is a multistep mechanism that includes deposition and resuspension at different depth and at multiple times. Hence, the signature of the original material is most certaintly reworked but very few studies have described the nature and composition of the abyssal sediment of this area of the Mediterranean Sea and this is a first attempt.

I collected two of the sediment cores (M01 and M08) during the CASCADE oceanographic cruise (2011) and the third one (SC2400), which I prepared (digestion and determination of trace metal concentrations) was sampled during the DEEP3 oceanographic cruise (2009).

1. Introduction

Continental margins receive atmospheric as well as riverine inputs of particulate matter but they act either as a sink or a source of material (*Guieu et al., 1993; Migon et al., 1993; Bethoux et al., 1999*). Indeed, they act as a temporary repository until hydrodynamic processes transfer material off-shelf, to the open ocean and deep basin, mainly through submarine canyons (*Guieu et al., 1991; Puig et al., 1999; Roussiez et al., 2006; Palanques et al., 2008*). Sediment-bound contaminants are also supplied through atmospheric and riverine inputs, and marine sediments are a good proxy and record of anthropogenic inputs of pollutants, and particulate trace metals (PTM) in particular.

Most studies in the western Mediterranean Sea have been performed in slope and margin environments of the Gulf of Lion, on the geochemical properties of the sediment (*Buscail et al., 1997; Marin et al., 2001; Miralles et al., 2005*) and on the continental shelf sediments' anthropogenic imprint (*Marin, 1998; Ferrand et al., 1999; Miralles et al., 2006*). On the contrary few have been done in the abyssal plain (*Zuo et al., 1997; Angelidis et al., 2011*) where sedimentation rates have been modeled and where enrichment of contaminants was evidenced even though particles are largely diluted and dispersed compared to near-shore environments (*Fernex et al., 1992, 2001; Martin et al., 2009*). Geochemical characterization of the deep deposits is of importance in the global study of benthic processes (e.g. re-suspension of deep sediments, bioturbation and sediment to pore-water exchanges) and their modifications through anthropogenic inputs. However, discrimination between natural and anthropogenic origins is rather complicated in deep sections of sediment cores due to diagenetic transformations that can cause misinterpretation in trace metals accumulations.

The aim of this work is to describe the geochemical characteristics of the sedimentation, from the surface to the bottom, in deep environments of the Gulf of Lion. The sources of particles and pathways leading to this accumulation are also discussed. We also aim to give insights to the sedimentation rates of those remote environments where inputs are sparse and data are rare. We also wish to enlighten how the transfer observed in submarine canyons is recorded, and to what extent the anthropogenic trace metal contamination reaches the deeper basin environment of NW Mediterranean Sea.

2. Material and methods

As we know that in the GoL, particulate matter and sediment-bound contaminants exit the continental shelf mostly through submarine canyons, one of the sedimentary systems that connect an important source of contamination to the abyssal plain is the Cap de Creus canyon (CCC). Hence we analyzed sediment cores retrieved from the seafloor, at the confluence of GoL canyons, in a north to south transect.

During the CASCADE cruise (1-31 March 2011) a series of 5 sediment cores were sampled in the deep northwestern Mediterranean basin but only 2 were studied in this work: M08 and M01, collected respectively at 1980 and 2657m depth (Fig.5.1 and Table 5.1). A third core, SC2400, collected at 2326m depth during the DEEP3 campaign was also analyzed during this study. The DEEP3 cruise was performed within the framework of the HERMES (Hotspot Ecosystem Research on the Margin of European Seas) project, and XRF-photography was carried out on this particular core at the GRC Geociències Marines laboratory (Barcelona, Spain). All 3 cores were sampled using a multi-corer collecter.

Core	Sampling	Location		Water depth	Core length
	date	Longitude	Latitude	(m)	(cm)
M08	10/03/11	42°N 20.002	04°E 41.799	1957	27
SC2400	29/04/09	42°N 01.518	03°E 51.708	2326	47
M01	08/03/11	41°N 08.008	04°E 41.476	2657	21

Table 5.1 Location and length of the deep sediment cores from the North Western Mediterranean sea investigated in this study

Cores were extruded and carefully sliced on board using acid-cleaned plastic spatulas, in layers of 0.5 cm from the surface to 5 cm depth, and of 1 cm, from 5cm depth to the end of the core. Sub-samples were freeze-dried and homogenized in agate mortar prior to analysis.

Vertical profiles of oxidation-reduction potential (e.g. Eh in mV) in the sediment were performed using a pH/redox meter (Knick apparatus™ and platinum electrode-Pt/Ag/AgCl) immediately after multi-corer sampling. First, the electrode was inserted vertically in the both first five millimeters of the cores. Then, pre-drilled holes in the tubes were used and the electrodes inserted horizontally every 5 mm until 5 cm and every 1 cm down to 30 cm depth.

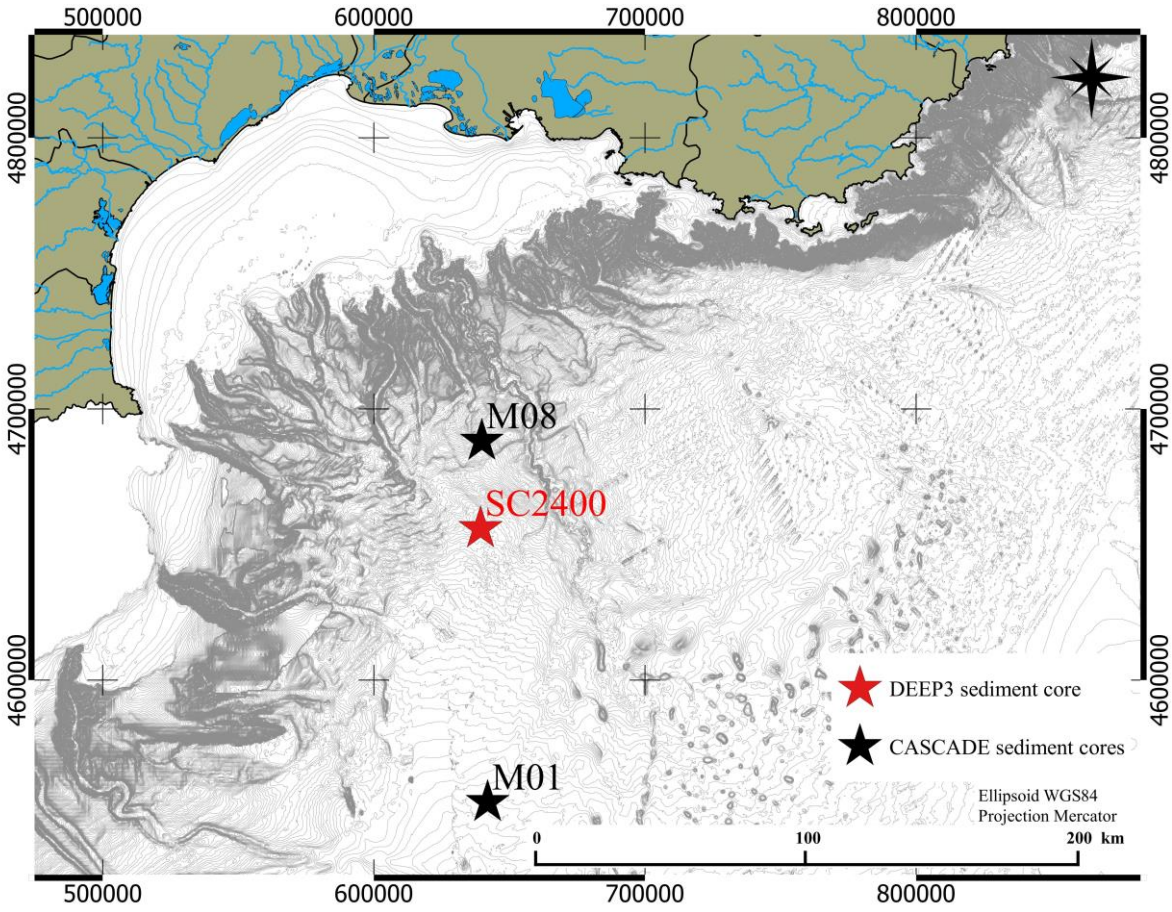

Fig.5.1 Map of the study area and positioning of the deep sediment cores.

Grain-size analyses of the deep sediment cores were performed in the Observatoire Océanologique de Banyuls/mer (France) on a Mastersizer 2000™ (Malvern).

Total carbon (C_t), organic carbon (C_{org}) and total nitrogen (N_t) concentrations were measured using freeze-dried sediment subsamples by combustion in an automatic C-N analyzer (Elementar VarioMax™). Organic carbon values were obtained after removing inorganic carbon by progressive and controlled acidifications with successively 1M H_3PO_4 and 2M HCl (overnights, at 40°C) (*Cauwet et al, 1990*). Precision measurements were about 2% dry weight (DW) for C_{org} and N_t and 0.3% DW for C_t, respectively.

Calcium carbonate contents were calculated from inorganic carbon (C_t - C_{org}) using the molecular mass ratio ($CaCO_3$: C_{inorg}= 100 :12).

Homogenized samples were digested in Teflon bombs in a micro-wave oven with a mixture of HNO_3, HCl and HF acids (TraceSELECT®, Fluka or Suprapur, Merck). Mineralisation solutions were then evaporated to dryness. Residues were solubilized with nitric acid and diluted in deionized water. Solutions were then analyzed for major, trace element and REE

concentrations by Inductively Coupled Plasma Mass Spectrometry (ICP-MS, Agilent 7000x) at the CEFREM laboratory (Perpignan, France).

Marine sediment reference material (GSMS-3 from NRCGA-CAGS, China) was mineralized and analyzed under the same conditions as the samples and provided suitable recoveries (errors < 5% for all elements, except for Cd for which recoveries ranged from 58% to 75%). Analytical blanks did not reveal any sign of contamination (contribution < 0.5% for Al, Co, Ni and Cs, < 2.5% for Cr and Pb and < 3.5% for Cu) except for Cd (blanks < 20%). Results for this last element have therefore to be considered with more caution but should still be indicative for general considerations.

Enrichment factors of the dated samples were estimated using background values from samples within each core. Indeed, at those depths, particulate inputs might come from various sources impossible to differ so, in order to determine a reference sample in each core, we used trace metal concentrations from a certain level as background values.

^{210}Pb activity allowed us to estimate a chronology in the sedimentation by determination of sedimentation rates. They were calculated using flux-constant sedimentation (CFCS), based on ^{210}Pb in excess ($^{210}Pb_{ex}$) distributions (*Appleby & Oldfield, 1978*):

$$[^{210}Pb_{xs}]_z = [^{210}Pb_{xs}]_0 \, e^{-\lambda(z/\tau)}$$

where $[^{210}Pb_{xs}]_{0,\,z}$ are the activities of excess ^{210}Pb at surface, or the base of the mixed layer, and depth z, λ the decay constant of ^{210}Pb (0.03114 yr^{-1}), and τ the sedimentation rate. ^{210}Pb activities of cores M08 and SC2400 were measured through counting of its grand-daughter ^{210}Po via photomultiplicators (*Radakovitch and Heussner, 1999*). ^{210}Pb activities in core M01 were determined using a low-background gamma spectrometer placed at the LAFARA underground laboratory (*van Beek et al., 2013*).

3. Results and Discussion

3.1 Lithological units

It is important to note that all sediment cores do not have the same length. The middle core (SC2400) will give more details of the deeply buried sediment and its top section can be compared with both M01 and M08.

Based on color description, we identified 3 main sedimentological units present in all cores but at different levels (Fig.5.2). Brown mud is observed at the top of each core within the first 3 to 5 cm, sometimes with presence of organisms, possibly orbulines. Then a 15 to 20cm-thick layer of ochre brown mud was also identified in each core, followed by a grey-ochre mud unit.

This last section is intersected with what was identified as black levels in M08 and rust levels in M01. In SC2400, this grey section looks uniform but the bottom of the core ends in a layer of brown mud, like the top section. Although those different sections are present in various thicknesses, they are visible in all three cores but in different estimated periods of time. At 21cm depths in M01 however, benthic coastal foraminifers were identified, probably indicating terrestrial input from the continental shelf.

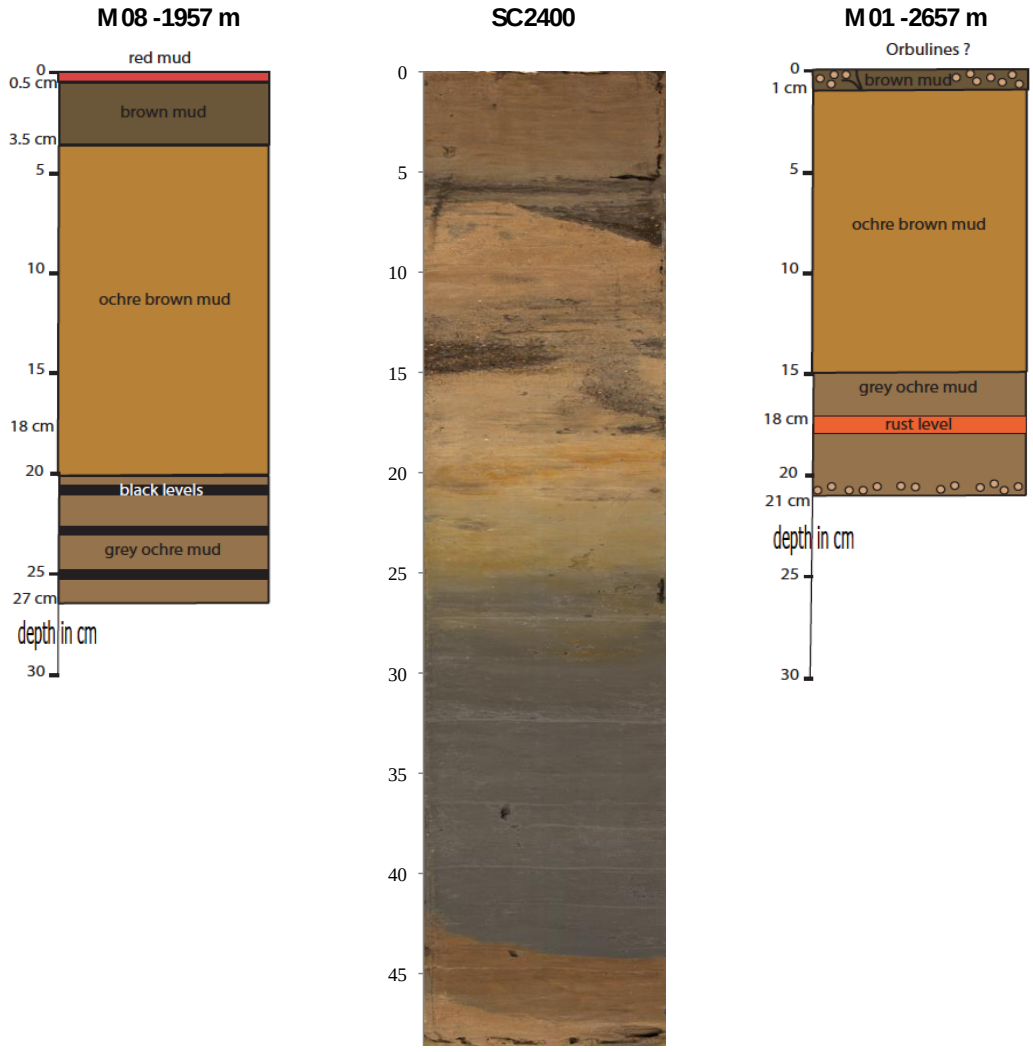

Fig.5.2 Visual description (for M08 and M01) and XRF-photography (for SC2400) of the deep cores.

	Estimated datation	Depth (cm)	C_{org} (%)	C/N molar ratio	$CaCO_3$ %dw	Clays (%)	Silts (%)	Sand (%)	D_{50} (µm)	Al ($\mu g.g^{-1}$)	Ti ($\mu g.g^{-1}$)	Cr ($\mu g.g^{-1}$)	Mn ($\mu g.g^{-1}$)	Fe ($\mu g.g^{-1}$)	Co ($\mu g.g^{-1}$)	Ni ($\mu g.g^{-1}$)	Cu ($\mu g.g^{-1}$)	Zn ($\mu g.g^{-1}$)	Cd ($\mu g.g^{-1}$)	Cs ($\mu g.g^{-1}$)	Pb ($\mu g.g^{-1}$)
M 08	2011	0.5	0.54	8.4	43.5	16	49	35	18.5	36910	2209	66.0	716	19247	9.9	36.4	31.1	81.1	0.10	4.7	30.6
	2004	1.3	0.44	8.7	46.0	21	54	24	11.6	45658	2447	70.7	880	22454	12.1	43.8	35.2	91.0	0.10	5.9	30.6
	2000	2.1	0.41	8.6	46.7	22	55	23	11.3	46893	2507	70.9	924	23089	12.4	46.2	35.8	90.8	0.10	6.2	27.6
	1995	2.8	0.44	9.0	47.3	32	45	22	8.1	47947	2564	70.5	920	23428	12.6	45.3	35.5	88.2	0.10	6.3	25.0
	1991	3.6	0.45	9.2	45.1	34	49	18	7.3	47509	2480	68.9	908	23104	12.4	44.5	34.8	85.7	0.08	6.2	23.3
	1986	4.4	0.45	9.3	43.9	29	44	28	9.8	45873	2344	67.6	891	22525	12.1	42.8	34.1	82.4	0.09	6.1	22.6
	1981	5.1	0.37	7.6	45.0	28	46	26	9.9	45375	2345	67.0	885	22678	12.0	43.7	34.5	82.7	0.04	6.2	22.0
	1977	5.9	0.36	7.7	45.2	29	42	29	10.6	43892	2230	64.7	849	21883	11.6	42.3	33.1	82.0	0.05	5.9	21.1
	1972	6.7	0.39	8.8	44.6	30	44	26	9.3	43807	2303	67.3	840	21804	11.6	42.2	32.6	93.3	0.05	5.9	20.0
	1968	7.4	0.40	10.2	46.5	35	44	20	7.4	42642	2212	64.0	812	21216	11.1	41.4	32.0	87.8	0.06	5.6	18.5
	1961	8.5	0.37	10.0	46.5	32	50	17	7.8	42162	2254	62.4	770	21038	10.7	41.1	30.9	76.9	0.04	5.5	18.2
	1952	9.7	0.33	9.7	48.0	30	40	30	10.9	41669	2149	60.9	739	20761	10.4	40.0	30.4	73.9	0.05	5.6	16.8
	1943	11.0	0.23	6.6	46.7	31	46	23	9.6	42883	2273	65.9	767	21478	10.7	43.0	32.2	79.7	0.02	5.8	34.1
	1934	12.3	0.24	7.2	45.1	36	45	19	7.5	43372	2140	62.6	768	21522	10.6	42.2	31.0	78.9	0.08	5.9	15.1
	1925	13.5	0.24	7.5	45.3	33	46	20	8.3	44817	2329	66.8	799	22225	11.1	43.5	32.4	81.6	0.09	5.9	15.0
	1916	14.8	0.25	7.7	46.3	31	40	29	10.2	42605	2186	62.2	776	21073	10.6	41.3	30.8	76.2	0.07	5.6	15.0
	1906	16.1	0.18	5.0	46.4	32	46	22	9.1	43094	2229	64.8	803	21352	11.0	44.8	31.0	67.4	0.08	5.8	14.4
	1897	17.3	0.22	7.3	46.9	34	46	20	8.2	45321	2341	67.6	866	22289	11.4	46.0	31.5	70.4	0.06	6.1	15.1
	1888	18.6	0.24	7.9	46.9	36	48	15	7.0	44225	2248	65.7	920	21809	11.0	45.6	30.6	69.9	0.07	6.2	14.5
	1879	19.9	0.22	7.0	46.2	36	50	14	7.1	45506	2331	69.5	1025	22535	12.0	47.8	30.3	70.8	0.06	6.4	14.9
	1870	21.2	0.24	7.1	44.3	36	48	16	7.3	43448	2265	67.3	1082	21964	11.8	46.9	29.2	69.4	0.08	6.1	14.8
	1861	22.4	0.26	7.8	43.5	36	48	15	7.2	37759	2354	70.6	1521	22871	11.9	49.9	30.6	71.4	0.07	6.5	14.8
	1852	23.7	0.21	6.6	43.3	36	48	15	7.2	46751	2326	70.8	2789	23034	13.9	60.1	35.4	84.3	0.07	6.5	15.4
	1843	25.0	0.26	7.4	41.7	38	51	11	6.5	47273	2397	72.5	3447	23596	16.6	57.7	32.1	73.8	0.09	6.7	15.6
	1834	26.2	0.21	6.1	42.2	35	50	15	7.3	46353	2334	71.2	4182	22452	24.8	59.5	31.8	71.6	0.05	6.5	15.0
	Δt=0.11																				
SC2400	2009	0.25	0.87	15.1	25.4	34	52	14	6.8	33742	2974	81.4	1092	25378	14.7	50.4	43.0	94.9	0.13	7.3	35.1
	2004	0.75	0.68	12.7	24.4	35	55	11	6.4	28046	2699	74.0	1006	22982	13.7	45.2	38.0	85.6	0.11	6.7	28.1
	2001	1.25	0.50	10.9	25.8	34	57	9	6.8	36693	2813	76.7	1152	24155	14.6	49.9	37.0	85.6	0.09	7.2	42.0
	1998	1.75	0.39	8.6	23.2	35	56	9	6.6	42694	2799	76.0	1252	24017	15.1	51.5	37.3	82.7	0.10	7.2	22.9
	1994	2.25	0.35	6.8	24.9	35	57	8	6.6	48645	2873	78.0	1089	24544	14.8	49.8	35.5	82.9	0.07	7.6	24.3
	1991	2.75	0.34	8.3	23.1	36	58	6	6.2	25106	2885	79.0	1066	24718	15.3	51.2	35.7	89.8	0.09	7.5	23.1
	1988	3.25	0.29	7.2	21.8	35	55	10	6.9	55091	2874	77.5	964	24351	14.6	47.6	33.3	89.5	0.07	7.3	22.7
	1985	3.75	0.32	8.3	22.6	34	59	7	6.8	40582	2920	80.5	882	24222	12.3	47.6	30.1	82.0	0.10	7.3	20.7
	1981	4.25	0.33	9.2	20.0	33	60	8	7.3	36731	2827	62.1	604	20374	8.4	33.7	19.7	69.1	0.08	5.9	16.1
	1978	4.75	0.24	9.8	14.0	26	59	15	13.0	36946	2904	61.1	773	20723	9.0	33.3	15.4	67.8	0.07	5.0	16.7
	1975	5.25	0.25	9.5	18.7	26	61	12	12.2	38035	2681	64.5	681	20316	8.7	36.6	19.1	69.0	0.06	5.8	13.7
	1970	6.00	0.25	11.5	17.1	29	49	22	10.4	46841	2413	61.0	626	19116	7.9	34.0	25.3	61.5	0.08	4.9	14.0
	1964	7.00	0.25	9.2	21.2	28	45	26	11.5	44700	2375	64.2	493	20117	8.3	37.0	30.5	67.4	0.04	5.7	14.6
	1952	8.75	0.25	8.2	20.2	29	53	18	10.0	29920	2203	62.9	688	18394	11.0	39.3	30.7	61.9	0.04	5.1	14.1

	1938	11.00	0.19	6.9	16.1	25	50	25	16.4	43410	2026	53.4	560	17903	10.2	29.4	20.3	91.6	0.02	4.7	14.4
	1925	13.00	0.16	7.4	13.0	18	34	47	52.0	33301	1613	43.9	563	15176	5.6	18.3	12.6	74.4	0.02	3.1	12.0
	1907	15.75	0.23	7.2	22.2	35	51	14	7.4	53454	2794	78.6	1300	23151	14.8	48.5	33.3	127.3	0.02	6.6	17.1
	1887	18.75	0.26	8.2	23.4	38	51	11	5.9	65262	3274	89.1	1779	35039	23.6	70.1	37.7	119.9	0.09	8.6	22.0
	1873	21.00	0.25	8.4	23.3	37	53	10	6.4	58434	2978	90.3	698	30258	14.3	53.4	20.3	126.3	0.07	7.9	20.5
	1858	23.25	0.29	9.6	24.6	36	51	12	6.5	58888	3009	94.9	509	34134	13.3	54.2	22.0	130.5	0.10	8.1	22.2
	1840	26.00	0.37	8.8	25.2	37	50	13	6.1	60519	2963	92.9	546	27829	12.9	53.3	50.4	122.4	0.01	8.3	18.1
	1826	28.25	0.45	10.2	25.1	39	52	9	5.5	60378	2950	100.5	473	28326	12.3	52.0	38.9	130.3	0.06	8.4	22.0
	1814	30.00	0.47	10.0	26.3	37	50	13	6.1	57368	2857	84.8	459	22887	11.3	48.8	35.5	110.0	0.08	7.8	19.0
	1772	36.50	0.51	12.1	23.0	39	51	11	5.6	50799	2531	73.3	428	20817	10.2	39.6	30.5	100.9	0.11	6.9	18.6
	1740	41.50	0.46	12.3	23.0	36	55	9	6.6	51212	2564	71.3	460	20521	9.6	34.5	24.4	107.5	0.17	6.5	17.9
	1728	43.25	0.41	10.2	24.8	34	55	11	7.1	56665	3000	77.4	1225	24671	14.0	45.4	37.2	116.9	0.15	7.0	27.7
	1717	45.00	0.45	10.7	23.8	33	58	9	6.9	58917	3077	79.8	1130	25424	14.5	44.3	33.9	110.1	0.10	7.2	24.6
	1707	46.50	0.37	10.3	20.0	37	51	12	6.4	49557	2667	68.5	1118	22026	12.8	42.4	33.3	93.0	0.07	6.0	18.8
	Δt=0.15																				
M 01	*2011*	0.25	0.68	12.0	47.2	20	54	26	13.3	24608	1895	50.1	801	17968	10.8	31.0	31.7	69.6	0.07	4.7	30.3
	1981	0.75	0.68	9.9	41.4	21	55	23	11.9	42807	2249	60.8	996	21578	13.2	38.3	38.3	81.7	0.12	5.7	35.4
	1931	1.25	0.51	8.7	42.5	23	58	19	10.5	46473	2410	61.0	1061	22671	13.9	39.9	38.9	88.6	0.07	6.1	32.7
	1861	1.75	0.65	10.5	40.6	34	50	16	7.2	40120	2166	35.8	3089	24976	53.9	106.0	230.1	161.0	0.01	4.6	23.1
	1771	2.25	0.63	12.5	40.0	35	44	20	7.3	48704	2631	70.2	1083	24624	14.3	43.1	39.0	84.1	0.08	6.8	24.8
	1661	2.75	0.50	10.5	41.1	38	49	13	6.2	41122	2403	63.1	988	22335	13.2	38.9	35.2	74.4	0.09	6.0	23.6
	1381	3.75	0.39	9.0	43.5	39	47	14	6.0	46844	2494	65.9	1006	23158	13.7	40.5	37.7	73.1	0.08	6.2	21.9
	1201	4.50	0.37	8.7	43.8	40	46	14	5.9	47150	2489	65.8	959	23136	13.5	40.7	38.3	73.3	0.08	6.2	21.1
	981	5.50	0.36	8.3	43.8	38	46	16	6.3	25103	2546	67.2	932	23288	13.2	42.5	38.5	74.9	0.07	6.1	22.1
	721	6.50	0.33	8.6	44.7	40	41	19	6.2	42350	2458	65.1	890	22607	12.5	40.9	37.3	71.3	0.08	6.2	20.0
	421	7.50	0.35	9.5	45.7	38	45	18	6.6	46948	2172	59.7	807	19208	11.4	37.5	33.6	65.6	0.07	5.7	16.3
	81	8.50	0.29	8.5	46.6	38	46	16	6.5	44043	2226	61.3	818	19639	11.7	38.6	34.4	68.7	0.07	5.6	15.5
	-299	9.50	0.32	9.3	45.9	38	43	18	6.5	38228	2275	60.4	792	20930	11.3	38.1	33.7	67.3	0.07	5.6	14.4
	-719	10.5	0.28	8.9	45.2	32	41	27	9.4	37650	2261	58.5	784	20528	11.1	37.5	32.4	65.4	0.09	5.4	14.1
	-1179	11.5	0.22	7.4	32.8	37	51	12	6.6	39381	2400	62.8	818	21957	11.2	39.6	31.5	70.2	0.08	6.0	14.6
	-1679	12.5	0.19	6.7	39.0	35	54	11	6.9	47570	2457	67.4	769	22182	10.0	37.9	25.5	72.7	0.12	6.8	15.4
	-2219	13.5	0.24	7.1	37.3	40	58	2	5.4	46539	2590	69.8	773	23327	10.5	38.7	22.4	78.5	0.10	7.3	15.9
	-2799	14.5	0.19	5.5	37.5	20	67	13	14.0	43835	2449	58.3	717	22746	9.4	33.1	19.2	69.8	0.09	5.8	14.2
	-3419	15.5	0.19	5.7	37.7	8	31	61	104.4	29466	1674	35.9	472	17148	8.9	21.9	11.8	53.4	0.07	3.6	12.7
	-4079	16.5	0.25	11.9	36.0	8	25	67	113.2	29506	1552	33.2	467	15399	8.7	21.7	10.1	55.4	0.09	3.1	12.6
	-4779	17.5	0.24	25.2	34.9	6	19	75	132.2	29107	1382	29.4	430	13346	8.0	20.4	8.5	45.0	0.07	2.8	12.3
	-5519	18.5	0.25	20.8	38.4	6	23	71	110.0	28523	1445	29.0	459	12752	7.4	19.8	7.5	43.2	0.08	2.8	11.3
	-6299	19.5	0.29	28.0	36.4	6	56	38	38.5	25466	1906	31.8	492	13551	6.7	21.4	6.9	43.9	0.09	2.6	10.6
	-7119	20.5	0.31	25.8	34.3	5	34	62	70.6	29008	1908	35.4	476	14833	7.3	21.1	7.0	45.5	0.09	2.8	11.3
	Δt=0.025																				

Table 5.2. PTM Concentrations, grain-size distribution, C_{org} and carbonate contents, C:N ratios and calculated datation in deep cores.

3.2 Physico-chemical parameters in sediments

Physico-chemical conditions such as redox potential, water content, porosity and grain-size distribution were considered in order to evaluate changes in relation with environmental and hydrodynamic factors.

3.2.1 Redox potential and water content

The first indication for diagenetic processes is given by the thickness of the oxidised mud layer. Based on Eh values recorded on the 3 cores (data not shown), as we found positive redox values down to the bottom of each core, in these deep-sea deposits the redox discontinuity was located below 25 cm depth. Oxidized layers were hence important and corresponded to low sedimentation rates, i.e. a long residence time at the sediment-water interface (SWI). A direct relationship ($r^2 = 0.78$) was shown by Buscail et al. (*1997*) between water depth and thickness of the oxidized mud at the sedimentary interface in the Gulf of Lions from the shelf break to around 2500 m depth.

When calculating the water content along the deep cores, we observed that the surface of the deposits are covered by a thin, very fluid and brown layer of unconsolidated mud (around 1.5cm), for which the water content in the first 1.5 centimeter was estimated between 100% DW for M01 and 160% DW for M08. It is an important layer for exchanges (e.g. dissolution and aggregation) with the overlying water due to its superior composition in liquid comparatively to solid phases.

3.2.2 Grain-size

Grain-size distribution allows defining the sedimentological facies and is hence an important parameter in the interpretation of geochemical data. Grain-size and D_{50} profiles along each core are displayed in Fig.5.3 and values in Table 5.2. In the 3 cores, mean clay content varied from 27 to 33% (values in M01 and SC2400 respectively), mean silt content varied from 45 to 53% (values in M01 and SC2400 respectively), and sand content varied from 14 to 28% (values in SC2400 and M01 respectively). It is very noticeable that sand contents are very variable, reaching up to 75% at the bottom of M01 core. Another sand lamina was visible in SC2400 at 13cm depth (47% of sand). The D_{50} profile reflects very well those shifts in grain-size composition (values in Table 5.2).

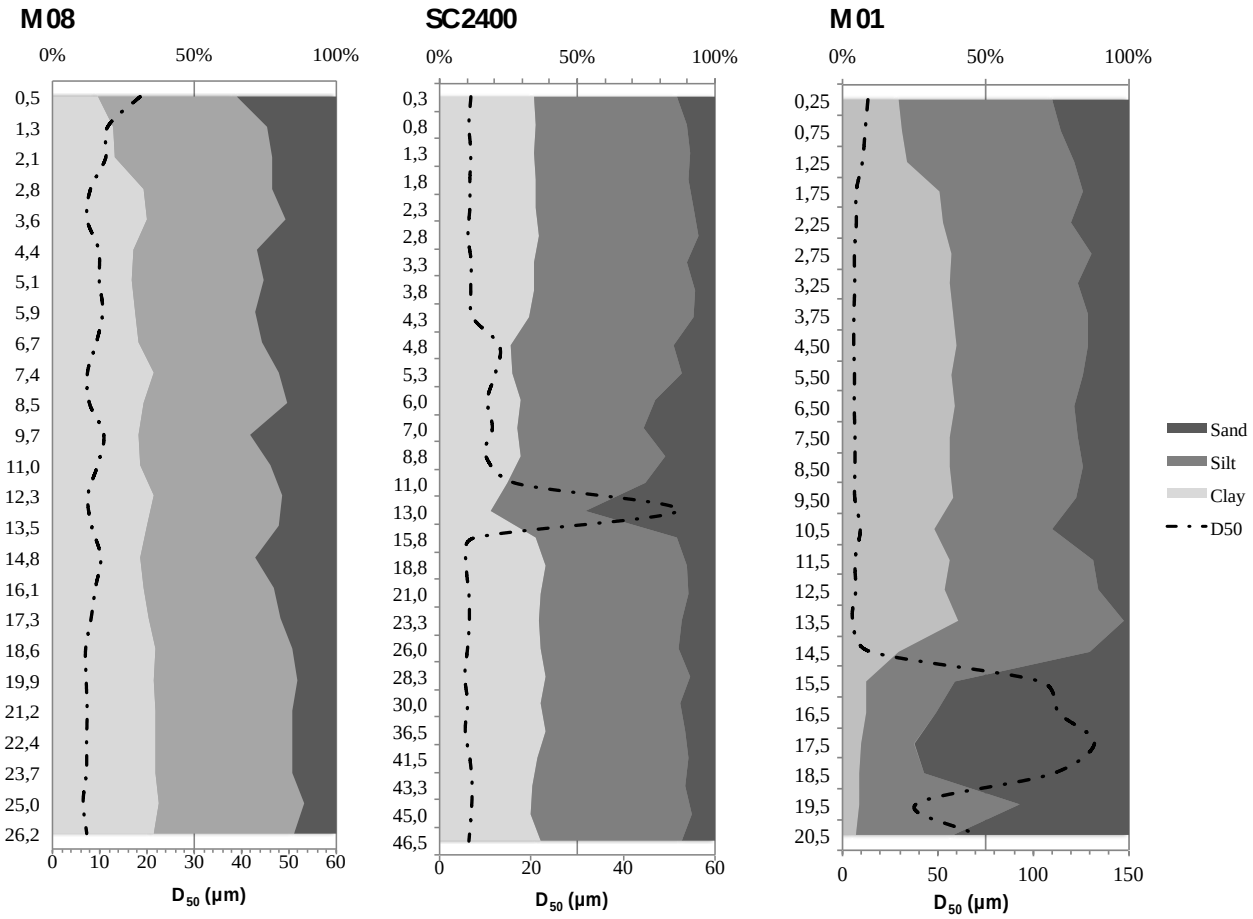

Fig.5.3 Grain-size classes and their relative contribution within each deep core. The D50 is also indicated.

In M01, D_{50} was higher in the top 3 samples than decreased until the sand section where it increased abruptly. In SC2400 the D_{50} was stable from the top to 4.75cm depth, and peaked at 13cm before it re-stabilized around 6 µm. The mean D_{50} in SC2400 top core is comparable to the one found in M01. In M08 however, D_{50} was more variable than in the southern cores. As M08 is located near the canyon mouths, its particulate matter input, particularly recorded at the top of the core here, can be sporadically impacted by pulses of coarser material exported from the shelf. Thus the particulate input could also be more variable than in the deeper environments.

3.2.3 ^{210}Pb chronology and sedimentation rate

^{210}Pb activity allowed us to estimate the date at which the sediment was deposited and hence to calculate the sedimentation rate. The M08 core is located near the extremity of the Marti canyon, where the shelf is the largest; hence we assume that it occasionally receives inputs of particulate matter from riverine origin. Indeed, Roussiez et al. (*2013*) demonstrated that suspended particulate matter with Aude river's characteristics was sampled in the Herault

canyon. Its sedimentation rate is 0.11 $cm.yr^{-1}$. The middle core (SC2400) was selected because, although more remote than M08, it is located at the confluence of the Cap de Creus and Lacaze-Duthiers canyons, both preferential conduits of particulate matter export due to high-energy physical processes, influencing the SC2400 sedimentation rate. Indeed, SC2400 showed the highest sedimentation rate (0.15 $cm.yr^{-1}$), even though it is located deeper than M08. It is also confirmed by the fact that the more distal M01 core, although located not much deeper than SC2400 (2657 and 2326m depth respectively), was retrieved from an environment where the sedimentation rate is much lower (0.025 $cm.yr^{-1}$). All the sedimentation rates estimated in this work are in accordance with values calculated by Miralles et al. (*2005*), that is to say, extrapolated until plausible.

3.3 Description of the organic material in sediments

The role of organic matter and carbonates is especially important with respect to the enrichment and complexation of metallic elements in sediment.

Organic carbon (C_{org}), total nitrogen (N_t) and C:N ratios, were measured in order to determine the organic matter origin, abundance and distribution with burial depth. Vertical profiles of C_{org} contents are displayed in Fig.5.4. C_{org} ranged from 0.18 to 0.54% DW in M08, from 0.16 to 0.87% DW in SC2400 and from 0.19 to 0.68% DW in M01 (Table 5.2). Those values are within the same range as found by different authors at similar depth in the Gulf of Lions, at its northeastern end and in the Balearic basin (*Buscail et al., 1997*; *Martin et al., 2009*; *Zuniga et al., 2007*). Maximum concentrations were always found in the top sample of each core and C_{org} profiles showed a rapid decreasing trend vertically.

M08 and M01 displayed typical decreasing profiles, due to diagenesis. The C_{org} decreasing profile was more accentuated in SC2400 due to a high C_{org} value at the surface of the sediment core. C_{org} values decreased abruptly in the next samples. In addition to C_{org} and N_t, the molecular C:N ratio can be used as a qualitative descriptor of the source and/or degradation state of the organic matter.

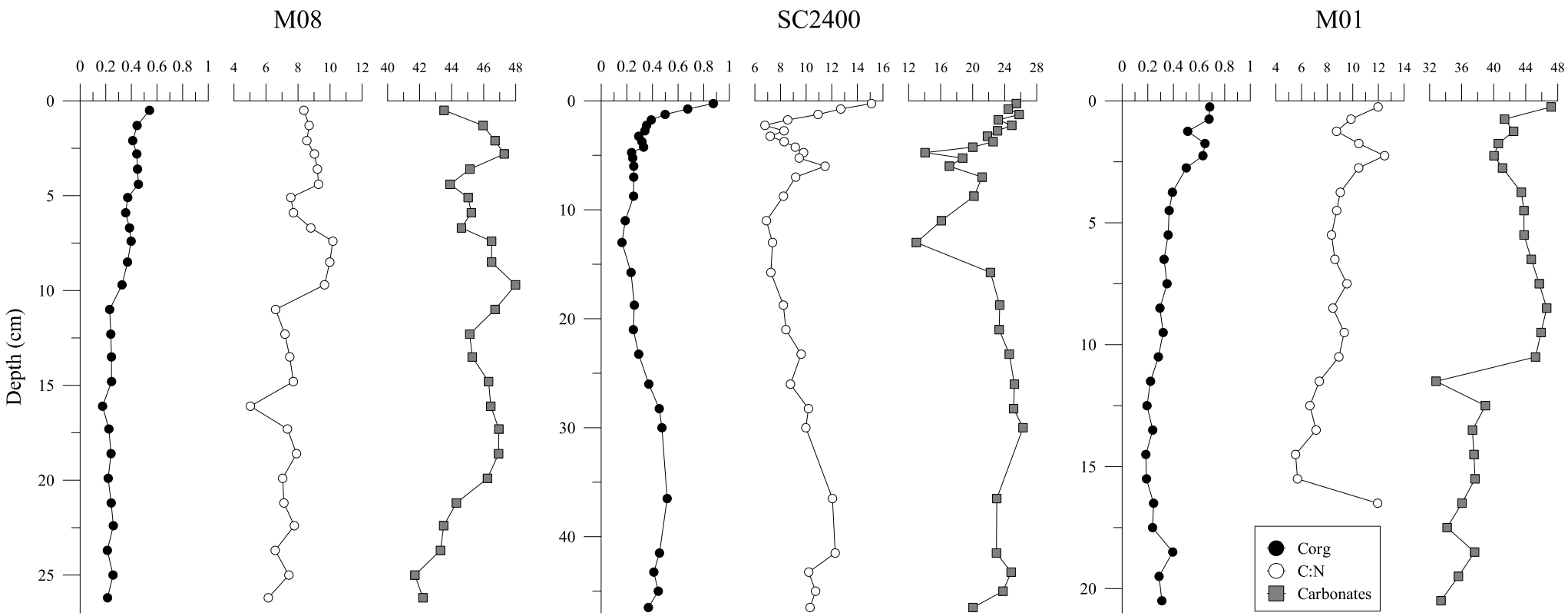

Fig.5.4 Organic Carbon (C_{org}) contents (relative to dry weight, i.e. DW), C:N ratios and carbonate contents in each deep core

Indeed, C:N ratios for organic matter of marine origin generally range from 4 to 6 because of the high protein content of lower organisms such as phytoplankton and zooplankton. On the other hand, plant-derived organic matter from terrestrial origin gives higher C:N ratios than the one derived from marine organisms as it contains a high percentage of non-protein materials (e.g. C:N >20 ; *Meyers and Ishiwatari, 1993*). C:N ratios of deep-sea sediment are normally higher than phytoplankton, zooplankton, zoobenthic and bacterial C:N ratios and lower than terrestrial ratios (low contribution). C:N ratio around 12 in recent marine sediment can imply a terrestrial contribution of organic matter and/or degraded organic detritus, suggesting a breakdown of nitrogenous compounds as a selective mode of organic matter destruction.

Here, C:N ratios in all cores were comprised between 6 and 14. In the shallower core (M08), C:N was rather homogeneous and the mean C:N was 7.9 suggesting higher marine organic matter contribution and low degradation rates of nitrogen (Fig.5.4). At the surface of SC2400, C:N ratio was high (15) but, as Corg, decreased abruptly in the next samples, up to a value of 6.8. This range of C:N ratios indicates a shift in the organic matter source. Organic matter with higher terrestrial contribution (i.e. C:N ≈ 12) was deposited on top of a layer of marine origin. In M01, C_{org} and N_t values were low, close to the detection limits of the C-N analyzer, hence, interpretation of peaks and profiles are to take with caution.

A high proportion of carbonates characterized these deep cores (33% DW to 47 % DW).

High proportions of carbonates result from significant pelagic inputs of calcareous organisms (coccoliths, foraminifera and pteropods). Carbonate-rich sediments have been described in the deepest zones, between 1500 and 2300 m depth, in the Gulf of Lions as biogenic sedimentation (*Buscail and Germain, 1997*). In deep deposits, the biogenic fraction dominates due to abundant planktonic foraminifera (*Vénec-Peyré, 1990*).

3.4 Al, Fe, Mn and Ti

Due to the variable composition of each core with depth, metal concentrations must be normalized to a reference element in order to correct grain-size or mineralogical bias and also to characterize the anthropogenic imprint and/or any biogeochemical processes that could have affected the vertical metal distribution. Al is normally used as a reference element as it is a good clay-tracer. However, no significant correlation was found within all our samples between any reputed terrigenous element (e.g. Ni or Cr) and Al. Instead we used Cs as it is

mostly carried by clay minerals and also considered as a good crustal reference (*Ackermann, 1980; Roussiez et al., 2005*).

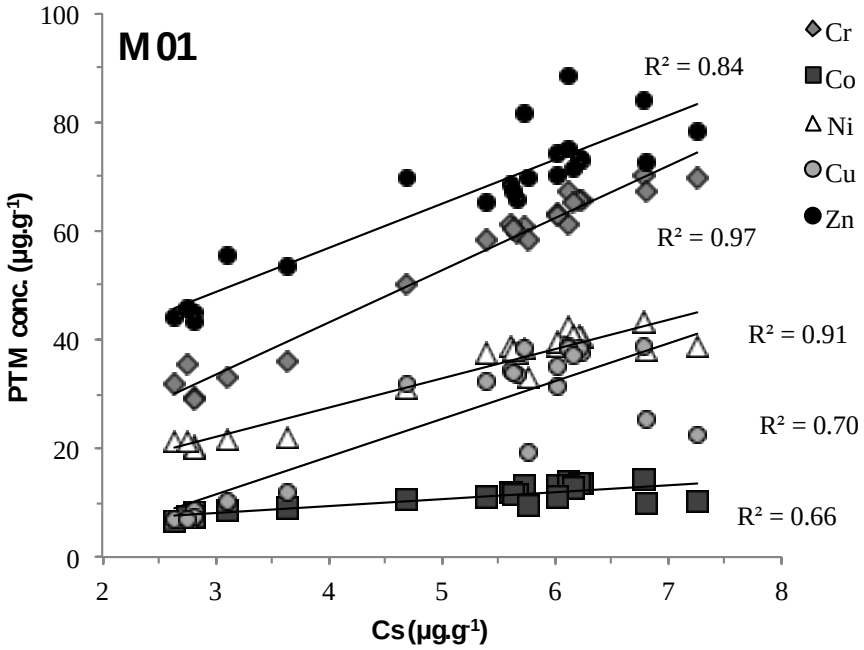

Fig.5.5 Relationships between PTM and Cs in M01 sediment core samples

Correlation coefficients are displayed in Fig.5.5 with the example of the M01 sediment core samples. Good correlations were calculated between Cr and Ni and Cs (r^2 = 0.97 and 0.91 respectively), and to a lesser extent with Co, Cu and Zn (r^2 = 0.66, 0.70 and 0.84 respectively).

Cs-normalized major and redox-sensitive element (Al, Ti, Mn and Fe) concentration profiles are displayed in Fig.5.6. The situation differed between M08 on one side and SC2400 and M01 on the other. Profiles in M08 were rather constant. This core displayed a layer with black levels described (third lithological unit) at the bottom of the core, and corresponds to the increased Mn/Cs ratio. The increase in Mn also indicates an oxidised layer, that is to say low sedimentation rate and long residence time at the sediment-water interface conditions. Hence a stop in the sedimentation process entailed the presence of a redox front. In M08, Al/Cs profile was constant, possibly indicating constant inputs from the same source, except for a peak at 22cm depth, concomitant with the increase in Mn/Cs. This decrease in Al/Cs at the bottom of the M08 core was probably induced by diagenetic processes caused by the redox front burial when the sedimentation started again.

In M01, element profiles were more variable: an increase of Cs-normalized Mn, Fe and Al concentrations together with a decrease of C_{org} at 1.75cm depth could indicate the formation of an oxide layer.

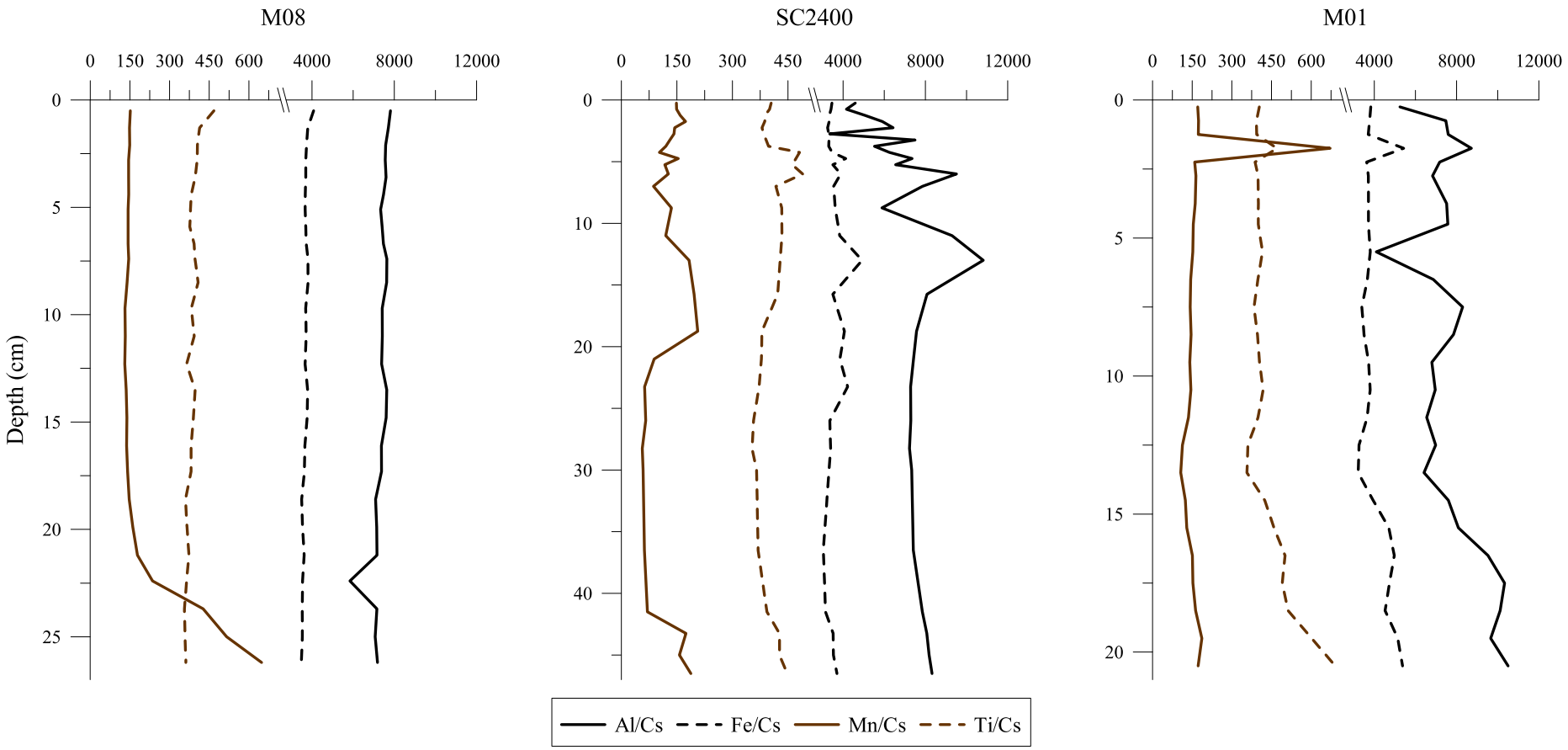

Fig.5.6 Cs-normalized concentration profiles of major trace elements Al, Fe, Ti and Mn in deep cores

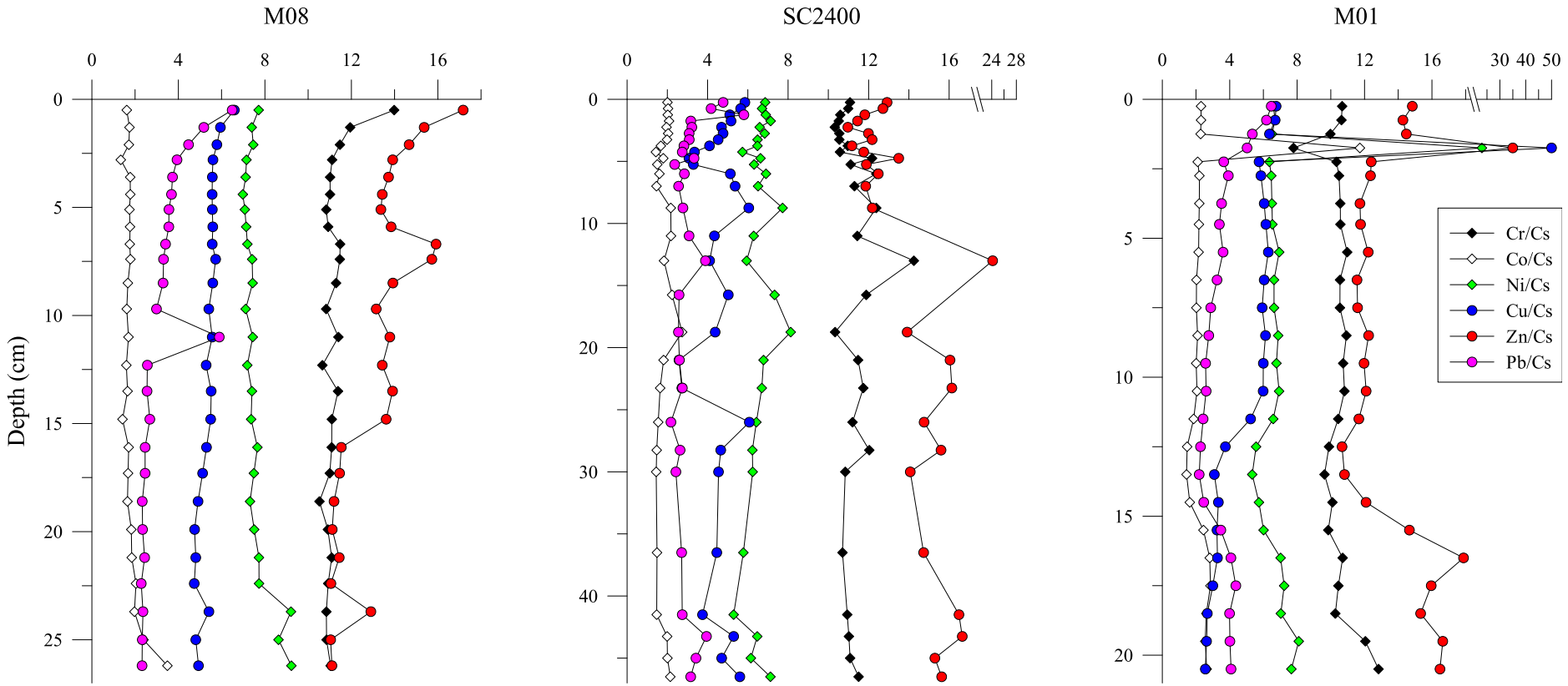

Fig.5.7 Cs-normalized concentration profiles of trace elements (Cr, Ni, Cu, Zn and Pb) in each deep core

In SC2400, the large variability of Al/Cs in the top 13cm, concomitant with variability in C:N and Cs-normalized trace metal concentrations could indicate sparse and regular inputs in this environment, located nearby the confluence of GoL's southwestern submarine canyons. Also, at 13cm depth, slight increases in Al/Cs and slighter peaks of Fe/Cs and Ti/Cs were concomitant with the increase in the sand fraction.

3.5 Trace metals in sediments

Trace metal concentrations are displayed in Table 5.2. In each core, mean PTM concentrations were of the same order of magnitude, although lower in M01 (except for Cu) and were in the range of Earth Upper Crust concentrations, except for Cu and Pb. But as we saw that the sedimentation rate and composition is not the same in those three environments, we also plotted Cs-normalized PTM concentration profiles (Fig.5.7).

Regarding trace element normalized concentrations, profiles from M08 and M01 were similar and different from the SC2400 profile. The south core (M01) is a typical example where values (C_{org}, Cs-normalized PTM concentrations) were high at the top of the core and then decreased with depth (especially Pb/Cs and Zn/Cs).

Nevertheless this core exhibited the highest concentrations of Cu, Zn and Ni (with 230, 160 and 106 $\mu g.g^{-1}$ respectively) and PTM/Cs ratios in a single peak at 1.75 cm depth, concomitant with higher C_{org} values, less carbonates and C:N between 10 and 12. All those parameters could indicate the presence of a terrigenous input enriched in organic matter from terrestrial origin or the burial of a redox front (peak in Mn) that lead to preservation of the organic matter and accumulation of oxydes (*Marin et al., 2001*).

The north core (M08) also displayed classic decreasing PTM/Cs ratios with depths although it showed peaks of Zn at 7cm depth where C_{org} and C:N ratio were higher than upper and lower samples, which could suggest a greater contribution of terrigenous material. Concentrations peaks were also visible at 11cm depth for Pb, and at 23.7cm depth for Cu, Ni and Zn, where Mn profiles started to increase. At those depths however, low C:N ratios (around 6) indicate inputs of autochthonous organic matter of marine origin with high nitrogen degradation due to bacterial activity. As said previously, PTM concentration, and Mn increases in particular indicate burial of a redox front, which could imply "turbidite" deposition. In both cores however, profiles of Cs-normalized Ni and Co concentrations were linear which shows great correlation with clay minerals. It is also true for Cr in M01 but in M08, Cr is less correlated with Cs at the top of the core.

The central core (SC2400) showed less homogeneous profiles, with high variability in the top 10cm and occasional peaks, for example in Cr, Cu and Zn at 11cm depth, which were concomitant with peaks in Fe, Al and Ti together with a slight decrease of C_{org}.

3.6 Origin of the particles

As in the other chapter of this manuscript, we will try to determine the origin of the particles that constitute the deeper basin of the NW Mediterranean Sea. We have seen in the previous chapters that the Rhone River is indeed the major contributor of sediment in the GoL, but also that, after temporary deposition in river pro-deltas, this particulate load is often resuspended by storms and downwelling-induced currents. It is then redistributed in submarine canyons where temporary deposits form (observed around 500m in the Cap de Creus canyon), until intense resuspension events like Dense-Shelf Water Cascading redistribute it, sometimes all over the deep basin of the Mediterranean Sea (*Durrieu de Madron et al., 2013*; *Puig et al., 2013*).

Rare Earth Element (REE) concentration ratios were used in this chapter as well to identify the source of deep sediments in the GoL (Fig.5.8). La/Sm vs La/Nd ratios in the three cores are homogeneously distributed in the Rhone river domain, especially samples from M08. As it is the northern core and located under the Marti canyon, this tracing procedure confirms that the Rhone river particles can reach the deep basin this way. However, REE signatures of the middle core samples are most scattered. They mainly plot in the Rhone river domain but other sources seem to spread the signature. Indeed, some samples plot in the upper corner further away from the other samples, which was also observed in the previous chapter in deeper sediment traps. We then evoked the possibility that this could be the REE signature of canyon wall's eroded particles. This hypothesis is plausible here as the SC2400 core is located at the confluence of the Cap de Creus, Lacaze-Duthiers and Sète submarine canyons.

As stated above in this section, during intense DSWC events, like those witnessed in winters 2005 and 2006, the nepheloid layer formed and carried by high-velocity currents spread all over the deep basin. This nepheloid layer is mainly formed of eroded particles that could have partly sedimented at 2400m depths, as suggested by the heterogeneous Cs-normalized PTM profiles of this core, in favor of varied but sudden inputs of particulate matter from different sources. Also, a group of mixed M01 and SC2400 samples seem to deviate towards higher La/Sm ratios.

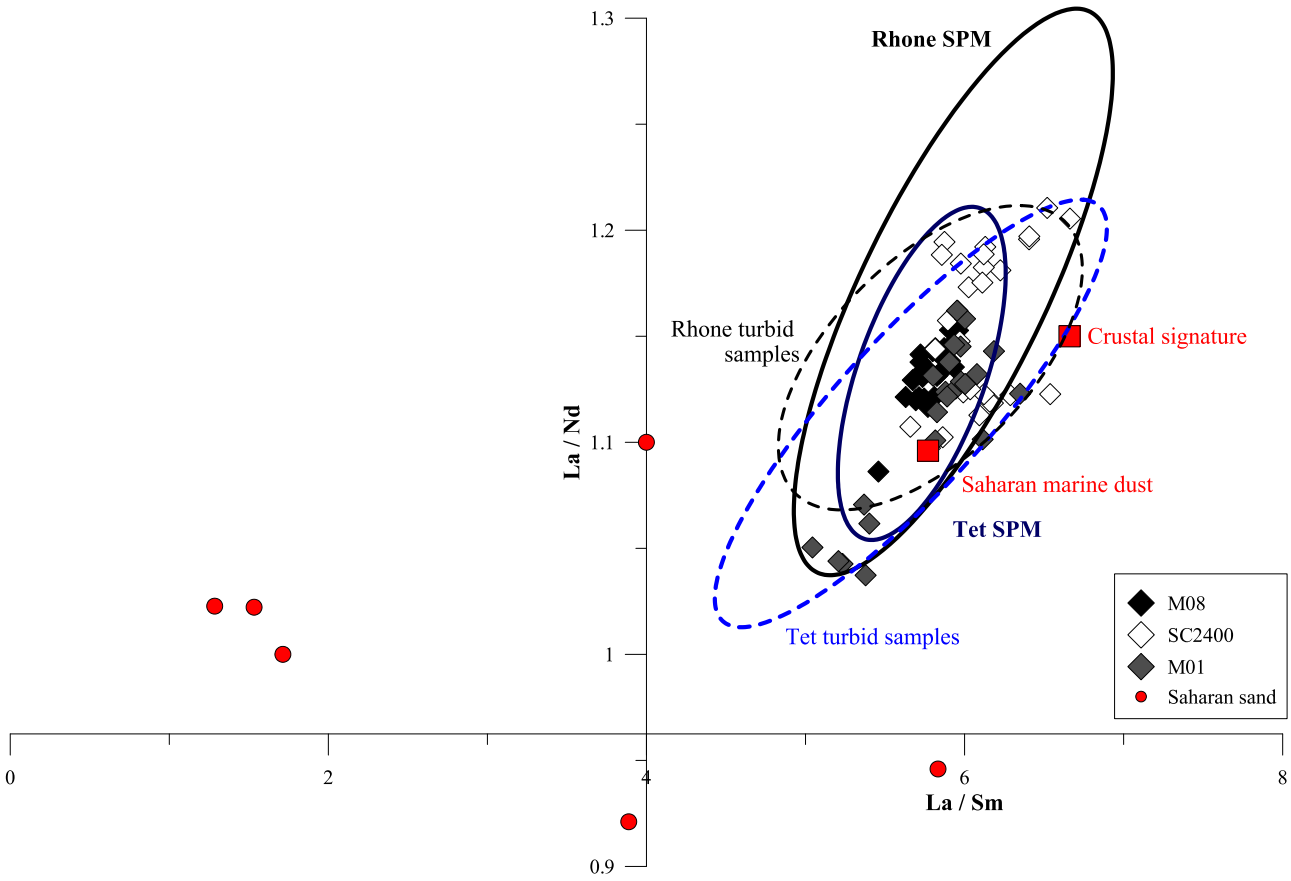

Fig.5.8 La/N vs La/Sm diagram of each core level and of coastal Mediterranean rivers. River SPM and turbid samples are represented as mean value of 58 samples from a 6-year survey. Crustal signature was determined with Upper Continental Crust REE concentrations (*Wedepohl, 1995*); saharan marine dust signature was obtained from Greaves et al. (*1994*) and Saharan sand signatures were calculated with Castillo et al. (*2008*) data.

As those cores are located in remote open-ocean environments, atmospheric inputs can represent more than 50% of the particulate input (*Guieu et al., 1997; Migon et al., 2002*).
In the NW Mediterranean Sea, most crustal particles come from the Saharan area, under the form of dust pulses events (*Guerzoni et al., 1999; Heimburger et al., 2010*).
Hence we tested this hypothesis using values from an atmospheric marine dust of Saharan origin (*Greaves et al., 1994*) and the Upper Continental Crust REE concentrations for a more general origin of crustal aerosols (*Wedepohl, 1995*). The samples showing high La/Sm ratios appear to be a mixing between both atmospheric end-members. This trend also proves that the Saharan component is not the unique atmospheric imprint recorded in deep marine sediments. However, dust sources are multiple and Saharan dust production areas are also numerous and show different relative REE geochemical signatures, as reported by Castillo et

al. (*2008*). But data on REE concentrations in atmospheric particles are still rare in the Western Mediterranean and this needs further investigation. Especially as, on the way from their source to their sink, those natural particles undergo chemical transformations that possibly modify their geochemical signatures.

Another group of samples with different REE signatures (lower ratios, in the low corner of the diagram) is noticeable. All those samples correspond to the bottom of the southern core (M01). They plot at the bottom of the Tet turbid samples area but it could also be due to ancient inputs of another coastal river (French or Catalan). Indeed, Nolting and Helder (*1991*) studied sediment core closer to the Spanish coast and noticed geochemical differences (sub-surface maximum of Pb and Zn concentrations around 7cm depth) with sediment cores from the Gulf of Lion: they stated that the Spanish coast was the source of its sandy sediments.

3.7 Anthropogenic contamination of the deep NW Mediterranean basin

As the main goal of this study was to assess the anthropogenic imprint in deep environments of the Mediterranean Sea, we assessed enrichment factors in each core (Fig.5.9). To do so we used background values of layers above which shifts in geochemical facies were observed in each core (20, 23.5 and 14.5 cm depth respectively in M08, SC2400 and M01) and which also correspond to major color changes at the base of the ochre layer. We plotted EF values regarding the dates estimated with ^{210}Pb activities. EF profiles for both M08 and M01 cores are quite typical, with higher values in the top cm and decreasing downward, but SC2400 EF values are more heterogeneous, reflecting the variability of the particulate inputs and of their origin in this environment.

In the northern core (M08), EF profiles showed a classic decrease from top to bottom, especially significant for Pb. An outlier of EF Pb is noticeable around the estimated date of 1940. At this depth, EF profiles should be cautiously interpreted. In the southern core (M01), EF profiles also showed a decreasing trend, especially when occulting outlier peaks of EF Cu, EF Ni and EF Zn at 2cm depth. At this depth, those concomitant increases could be interpreted as a significant anthropogenic contribution or can also be due to co-precipitation and trapping of different elements. Indeed, Fernex et al. (*1992*) suggested that Mn or Fe-oxide formation in sediment could be responsible for the trapping of Cu, Zn, and Pb in its oxidizing level. In the middle core (SC2400), EF profiles were less smooth.

A peak of EF Pb dated around 1999 could be the record of major anthropogenic input by the dense shelf water cascading event that happened that year.

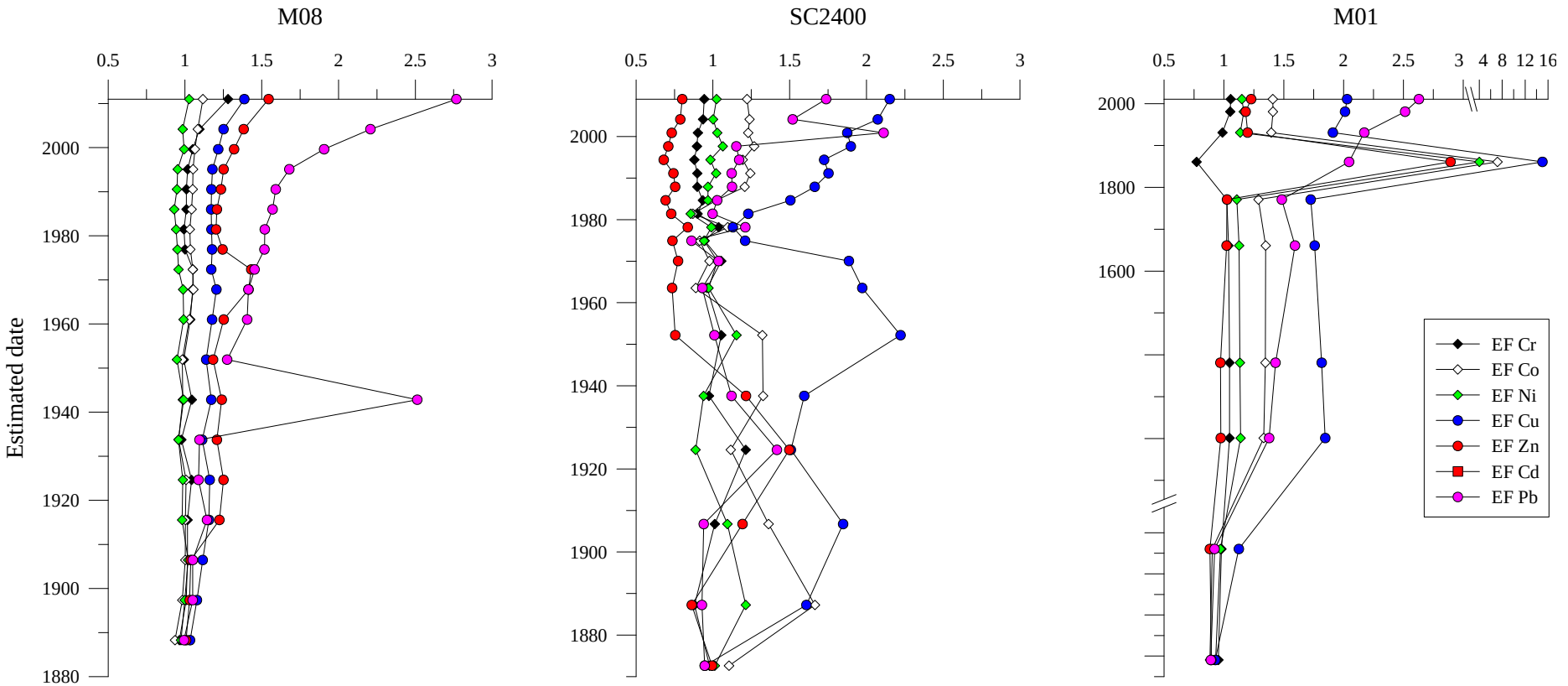

Fig.5.9 EF profiles of PTM in each deep core. Values were calculated using Upper Continental Crust reference (Wedepohl, 1995).

It is to be noted that most EFs are under the 1.5 threshold of anthropogenic contribution (*Roussiez et al., 2006*), except for Pb in the top of the three cores, Zn in the top M08 core and Cu in the top SC2400 and M01 cores. This is in agreement with our previous results stating that Cu issued mostly from the Tet River. Indeed, Tet River's input would preferentially exit the GoL from the Cap de Creus and Lacaze-Duthiers canyons. However, Cu also exhibits high EF values in other Mediterranean coastal rivers like the Herault River (master thesis of J. Sola, 2013) so high EF Cu values in SC2400 and M01 probably are a mix of multiple sources. However, as in all other studies done in this region (*Nolting and Helder, 1991; Martin et al., 2009; Angelidis et al., 2011*), we find that anthropogenic contribution recorded in deep NW Mediterranean sediments is considered as moderate (EFs < 3).

4. Conclusion

All those results allow us to implement the cartography of this abyssal environment in terms of sedimentological and geochemical characteristics:

- Deep cores do record different input events or at least changes in sediment sources. Those can be identified by the composition, quality and degradation state of the organic matter contained in the sediment, as well as by identification of coastal organisms or determination of anthropogenic imprints. The sedimentological properties of the sediment influence the geochemical behavior of the trace metals.

- The REE tracing method allowed us to identify the Rhone as one of the main source of the sediment in the deep environment but more especially in the northern core, located near the continental shelf break. However, other particulate sources are to take into account. In those remote environments, particulate matter sources are as diverse as canyon erosion, gravity flows and also atmospheric deposition of Saharan dust.

- EF values calculated in deep sediment cores show moderate anthropogenic contribution and EFs are higher at the surface of the cores, which correspond to the 20^{th} century.

References

Ackermann, F. (1980). A procedure for correcting the grain size effect in heavy metal analyses of estuarine and coastal sediments. *Environmental Technology Letters*, 1, 518-527.

Angelidis, M.O., Radakovitch, O., Veron, A., Aloupi, M., Heussner, S., Price, B. (2011). Anthropogenic metal contamination and sapropel imprints in deep Mediterranean sediments. *Marine Pollution Bulletin*, 62, 1041-1052.

Appleby P.G., Oldfield F. (1978). The calculation of Lead-210 dates assuming a constant rate of supply of unsupported lead-210 to sediment. *Catena*, 5, 1-8.

Bethoux, J.P., Gentili, B., Morin, P., Nicolas, E., Pierre, C., Ruiz-Pino, D. (1999). The Mediterranean Sea: a miniature ocean for climatic and environmental studies and a key for the climatic functioning of the North Atlantic. *Progress in Oceanography*, 44, 131-146.

Buscail, R., Ambatsian, P., Monaco, A., Bernat, M. (1997). ^{210}Pb, manganese and carbon: indicators of focusing processes on the northwestern Mediterranean continental margin. *Marine Geology*, 137, 271-286.

Buscail, R., Germain, C. (1997). Present-day organic matter sedimentation on the NW Mediterranean margin: importance of off-shelf export. *Limnology and Oceanography*, 42 (2), 217-229.

Castillo, S., Moreno, T., Querol, X., Alastuey, A., Cuevas, E., Herrmann, L., Mounkaila, M., Gibbons, W. (2008). Trace element variation in size-fractionated African desert dusts. *Journal of Arid Environments*, 72(6), 1034-1045.

Cauwet G., Gadel F., De Souza Sierra, M.M., Donard, O., Ewald, M. (1990). Contribution of the Rhône river to organic inputs to the northwestern Mediterranean sea. *Continental Shelf Research*, 10 (9-11), 1025-1037.

Durrieu de Madron, X., Houpert, L., Puig, P., Sanchez-Vidal, A., Testor, P., Bosse, A., Estournel, C., Somot, S., Bourrin, F., Bouin, M.N., Beauverger, M., Beguery, L., Calafat, A.,

Canals, M., Cassou, C., Coppola, L., Dausse, D., D'Ortenzio, F., Font, J., Heussner, S., Kunesch, S., Lefevre, D., Le Goff, H., Martin, J., Mortier, L., Palanques, A., Raimbault, P. (2013). Interaction of dense shelf water cascading and open-sea convection in the northwestern Mediterranean during winter 2012. *Geophysical Research Letters*, 40, 1-7.

Durrieu de Madron, X., Panouse, M. (1996). Advective transport of suspended particulate matter on the Gulf of Lions continental shelf. Summer and winter situations. *Comptes rendus de l'Académie des Science*, 322(12), 1061-1070.

Fernex, F., Février, G., Bénaïm, J., Arnoux, A. (1992). Copper, lead and zinc trapping in Mediterranean deep-sea sediments: probable coprecipitation with Mn and Fe. *Chemical Geology*, 98, 293-306.

Fernex, F.E., Migon, C., Chisholm, J.R.M. (2001). Entrapment of pollutants in Mediterranean sediments and biogeochemical indicators of their impact. *Hydrobiologia*, 450, 31-46.

Ferrand, J.L., Hamelin, B., Monaco, A. (1999). Isotopic tracing of sedimentary fluxes in the Gulf of Lions. *Continental Shelf Research*, 19, 23-47.

Greaves, M.J., Statham, P.J., Elderfield, H. (1994). Rare earth element mobilization from marine atmospheric dust into seawater. *Marine Chemistry*, 46(3), 255-260.

Guerzoni, S., Molinaroli, E., Rossini, P., Rampazzo, G., Quarantotto, G., de Falco, G., Cristini, S. (1999). Role of desert aerosol in metal fluxes in the Mediterranean area. *Chemosphere*, 39(2), 229-246.

Guieu, C., Martin, J.M., Thomas, A.J., Elbaz-Poulichet, F. (1991). Atmospheric versus river input of metals to the Gulf of Lions: total concentrations, partitioning and fluxes. *Marine Pollution Bulletin*, 22 (4), 176–183.

Guieu, C., Zhang, J., Thomas, A.J., Martin, J.M., Brun-Cottan, J.C. (1993). Significance of atmospheric fallout on the upper layer water chemistry of the northwestern Mediterranean. *Journal of Atmosheric Chemistry*, 17, 45-60.

Guieu, C., Chester, R., Nimmo, M., Martin, J.M., Guerzoni, S., Nicolas, E., Mateu, J., Keyse, S. (1997). Atmospheric input of dissolved and particulate metals to the northwestern Mediterranean. *Deep Sea Research Part II: Topical Studies in Oceanography*, 44(3–4), 655-674.

Heimbürger, L.E., Migon, C., Dufour, A., Chiffoleau, J.F., Cossa, D. (2010). Trace metal concentrations in the North-western Mediterranean atmospheric aerosol between 1986 and 2008: Seasonal patterns and decadal trends. *Science of The Total Environment*, 408(13), 2629-2638.

Marin, B. (1998). Répartition et fractionnement géochimique des éléments traces dans les sediments marins, application à la marge continentale du Golfe du Lion. Ph.D.. Université de Perpignan, France. p. 395.

Marin, B., Giresse, P. (2001). Particulate manganese and iron in recent sediments of the Gulf of Lions continental margin (north-western Mediterranean Sea): deposition and diagenetic process. *Marine Geology*, 172, 147-165.

Martín, J., Sanchez-Cabeza, J.A., Eriksson, M., Levy, I., Miquel, J.C. (2009). Recent accumulation of trace metals in sediments at the DYFAMED site (Northwestern Mediterranean Sea). *Marine Pollution Bulletin*, 59, 146-153.

Meyers, P.A., Ishiwatari, R. (1993). Lacustrine organic geochemistry : an overwiew of indicators of organic matter sources and diagenesis in lake sediments. *Organic Geochemistry*, 20, 867-900.

Migon, C. (1993). Riverine and atmospheric inputs of heavy metals to the Ligurian Sea. *Science of the Total Environment*, 138, 289-299.

Migon, C., Sandroni, V., Marty, J.C., Gasser, B., Miquel, J.C. (2002). Transfer of atmospheric matter through the euphotic layer in the northwestern Mediterranean: seasonal pattern and driving forces. *Deep Sea Research Part II: Topical Studies in Oceanography*, 49(11), 2125-2141.

Miralles, J., Radakovitch, O., Aloisi, J.C. (2005). ^{210}Pb sedimentation rates from the Northwestern Mediterranean margin. *Marine Geology*, 216, 155-167.

Miralles, J., Veron, A., Radakovitch, O., Deschamps, P., Tremblay, P., Hamelin, B. (2006). Atmospheric lead fallout over the last century recorded in Gulf of Lions sediments (Mediterranean Sea). *Marine Pollution Bulletin*, 52 (11), 1364-1371.

Monoley, C.L., Field, J.G. (1991). Modelling carbon and nitrogen flow in a microbial plankton community. In : *Protozoa and their role in marine processes*. P.C. Reid et al (eds), Springer, 443-473.

Palanques, A., Masque, P., Puig, P., Sanchez-Cabeza, J.A., Frignani, M., Alvisi, F. (2008). Anthropogenic trace metals in the sedimentary record of the Llobregat continental shelf and adjacent Foix submarine canyon (Nortwestern Mediterranean). *Marine Geology*, 248 (3-4), 213-227.

Puig, P., Palanques, A., Sanchez Cabeza, J.A., Masque, P. (1999). Heavy metals in particulate matter and sediments in the southern Barcelona sedimentation system (northwestern Mediterranean). *Marine Chemistry,* 63, 311-329.

Puig, P., Durrieu de Madron, X., Salat, J., Schroeder, K., Martín, J., Karageorgis, A.P., Palanques, A., Roullier, F., Luis Lopez-Jurado, J., Emelianov, M., Moutin, T., Houpert, L. (2013). Thick bottom nepheloid layers in the western Mediterranean generated by deep dense shelf water cascading. *Progress in Oceanography,* 111, 1-23.

Radakovitch O., Heussner S. (1999). Fluxes and balance of ^{210}Pb on the Bay of Biscay continental margin (northeastern atlantic). *Deep-Sea Res. II,* 46(10-11), 2175-2203.

Roussiez, V., Ludwig, W., Probst, J.L., Monaco, A. (2005). Background levels of heavy metals in surficial sediments of the Gulf of Lions (NW Mediterranean): an approach based on ^{133}Cs normalization and lead isotope measurements. *Environmental Pollution*, 138, 167-177.

Roussiez, V., Ludwig, W., Monaco, A., Probst, J.L., Bouloubassi, I., Buscail, R., Saragoni, G. (2006). Sources and sinks of sediment-bound contaminants in the Gulf of Lions (NW

Mediterranean Sea): A multi-tracer approach. *Continental Shelf Research*, 26(16), 1843-1857.

Sola, J. (2013). Suivi des apports fluviaux en elements traces métalliques au Golfe du Lion. Bilans pour le Rhône, l'Hérault, l'Orb, l'Aude, l'Agly et la Têt de 2006 à 2012. *University of Perpignan Via Domitia, Master thesis,* 45p.

Van Beek, P., Souhaut, M., Lansard, B., Bourquin, M., Reyss, J.L., Jean, P., von Ballmoos, P. (2013). LAFARA: A new underground laboratory in the French Pyrénées for low-background gamma spectrometry. *Journal of Environmental Radioactivity,* 116, 152-158.

Vénec-Peyré, M.T. (1990). Contribution of foraminifera to the study of recent sedimentation in the Gulf of Lions (western Mediterranean Sea). *Continental Shelf Research*, 10, 869-883.

Wedepohl, K.H. (1995). The composition of the continental crust. *Geochimica et Cosmochimica Acta*, 59(7), 1217-1232.

Zuniga, D., Garcia-Orellana, J., Calafat, A., Price, N.B., Adatte, T., Sanchez-Vidal, A., Canals, M., Sanchez-Cabessa, J.A., Masqué, P., Fabres, J. (2007). Late Holocene fine-grained sediments of the Balearic Abyssal Plain, Western Mediterranean Sea. *Marine Geology*, 237, 25-36.

Zuo, Z., Eisma, D., Gieles, R., Beks, J. (1997). Accumulation rates and sediment deposition in the northwestern Mediterranean. *Deep-Sea Research II*, 44, 597-609.

Chapter VI

Conclusion

Through spatial and temporal resolution studies of particulate heavy metal export fluxes and sedimentation in the Gulf of Lion, the main objectives of this work were the following :

- First we aimed at quantifying trace metal (Cr, Co, Ni, Cu, Zn, Cd, Pb in particular) input fluxes transferred by rivers to the GoL. The Rhone River was investigated as well as coastal rivers through the Tet river model. Specific attention was paid to the importance of flood events on the estimation of geochemical fluxes.
- Since the trace metal signature of sediment deposited on the continental shelf has been extensively documented, we focused on the export fluxes from the shelf to the deep basin and the trace metal deposition in this fluvio-marine continuum for whose very few data were available. This export, in NW Mediterranean, mostly takes place under extreme hydro-meteo-dynamic processes such as E-SE storm and DSWC, which we particularly studied in this work.
- We also aimed at characterizing the origin of those Particulate Trace Metals (PTM) in the different investigated areas and kinds of material, that is to say the geographical source of particles initially delivered by rivers. But another goal was also to evaluate the anthropogenic contribution to the exported PTM fluxes. In this aim we used different geochemical tools such as, EF, REE ratios or natural residual fraction method.

This work relies on extensive sample datasets: 6-year survey (2006-2011) of two Mediterranean rivers which I partially analyzed; sediment cores, sediment trap and CTD samples from the CASCADE campaign to which I actively participated; and a 6-month survey (2005-2006, part of the european HERMES program) of 9 sediment traps for which I analyzed trace metal concentrations.

Particulate trace metal transfer from the coastal rivers of the Gulf of Lion

The 6-years survey of coastal mediterranean rivers on a monthly basis provided, to date, the largest dataset on PTM concentrations and particulate fluxes from the Rhone and Tet rivers. This long-term monitoring allowed the extensive determination of PTM concentrations but also of essential parameters (liquid discharge, suspended particulate matter, particulate organic carbon) that help understand their transport and behavior processes. It enabled us to determine the influence of liquid and solid discharges on the composition of the fluxes. This important set of data allowed the calculation of good rating curves and hence the determination of accurate fluxes (suspended particulate matter and PTM). This model could

help making rigorous PTM input estimations in the Gulf of Lion over which policy-making decisions are based.

Previous studies in the GoL had already shown that small coastal rivers have a sparser delivery but are proner to intense flash-flood events whereas large rivers like the Rhone River has a more diffuse and constant outflow. Hence, in order to keep implementing the existent model, the sampling strategy has to be adjusted to the system in question. On those coastal rivers, particles composition highly varies during flood events. It is thus essential to adapt the sampling stategy to better define export fluxes of trace metals. In this context the use of automatic sampling systems was also usefull in terms of tracking intense but impredictable hydro-meteorological events. The analysis of the 2006-2011 dataset and its comparison with preexisting data on previous years or events outlined the high temporal variability of SPM and sediment-bound contaminants transport.

Over this study period, two flood events were studied on each river but showed similar dynamic, whether in spring or autumn. They contributed to around 80% of the annual PTM exportation. However, differences in PTM concentrations (lithogenic PTM more concentrated on the Rhone river, whereas the Tet river exhibits higher Cu and Zn concentrations) were observed as both systems' drainage basins have different lithologies and tributaries. The Rhone River still accounts for 70 to 90% of SPM input to the GoL, and associated particulate trace metals inputs to the continental shelf of the GoL.

Particulate trace metal transfer to the deep-sea in Gulf of Lion submarine canyons

Once delivered to the continental shelf, SPM and sediment-bound trace metals are subjected to along and across-shelf transport then advection towards submarine canyon environments.

- In the second part of this manuscript, we discussed the importance of storm-induced transport at first. The moderate E-SE storm of March 2011 (annual recurrence) proved to be an efficient export process of riverine particles of mixed (Rhone and coastal rivers) origin, as we estimated that between 30 to 50% of the Rhone's annual PTM input was flushed down the CCC. The wide range of samples and time steps gave us the opportunity to study the temporal variability of PTM fluxes and composition in the material exported from the shelf. We concluded that the variability of SPM composition observed by CTD sampling was well transcribed in sediment trap samples, although they function on larger timeframe. Particles flushed down-canyon were finer during the storm than during the rest of the deployment, and contained variable amounts of POC and PTM as well as occasionnal inputs of particles

enriched in anthropogenic PTM (Cu, Zn, Pb). After 3 days of storm, a centimetric deposit of fine sediments was only observed at 442 m depth on the canyon flank. Those temporary deposits are themselves likely to be remobilized and transported to deeper environments during more intense hydrodynamical events, such as dense shelf water cascading, which periodically gush down the canyon.

- Hence, we studied the first deployment samples from the HERMES campaign that witnessed the winter 2005-2006 DSWC event, in order to study the spatial and temporal variability of PTM concentrations and fluxes and to budget those fluxes. Previous studies and observations on the same samples had already given a good approach of the hydrodynamical context. When comparing the exporting capacities of E-SE storm and DSWC-induced off-shelf export of SPM and sediment-bound contaminants, the latter is 20 to 30 times more efficient. As both events exported the same material (i.e. resuspended shelf sediment with the same geochemical characteristics), mean daily PTM fluxes within the CCC were comparable. Compared to E-SE storms, DSWC events have a low recurrence and do not always happen with the same intensity in the GoL. However, this study on the winter 2005-06 event has highlighted their great flushing capacities. Indeed, we estimated that around 300% of the Rhone annual SPM and PTM input was exported that winter.

Geochemical characteristics of recent deep sediments from the Gulf of Lion

Recent studies have detected the presence of water masses formed during this winter 2005-2006 over the whole NW Mediterranean deep-basin. After having flown off the submarine canyons, the dense nepheloid layer has spread and set. Chapter 4.2 conclusions stated that anthropogenically-enriched PTM, together with organic matter, were preferentially distributed in deep sediment traps. Hence, it is not trivial to wonder what is the anthropogenic imprint in those deep sediments and PTM are a good proxy to answer this question.

The deep cores we analyzed did record different input events or at least changes in sediment sources, identified by inclusions of coastal organisms, layers of different grain-size composition, composition and quality of the organic material and/or concomitant increase of different geochemical parameters.

Tracing the origin of exported particles

- Tracing methods (Rare Earth Element ratios and Residual fractions) allowed discriminating the geographical origin of the particles recovered in canyons and deep cores, as

a mix of rhodanian and coastal river inputs. But in deepest environments, in particular in the southernmost core area, we suspect particulate inputs from either resuspension of previously identified temporary deposits, erosion of the canyon walls, resuspension of deep-sea floor sediments due to OOC, gravity flow, or even atmospheric deposition of Saharan dust and sinking of pelagic production.

- Through the calculation of EFs, we determined the natural or anthropogenic origin of the particles and the contribution of the latter to PTM fluxes. EFs showed that during flood events, particles enriched in POC and hence, anthropogenically-enriched and labile PTM were the first exported to the GoL. Anthopogenically-enriched elements in storm-induced fluxes also exhibited a high lability, which was determined using acid-leaching extraction. EFs calculated in surface sediment samples, collected after the storm in the Cap de Creus canyon, permitted to characterize the material that was deposited by the storm-induced currents on the canyon's floor. Those characteristics led us to the conclusion that it was the same material as collected in the sediment traps and originating from resuspension of continental shelf sediments. EFs also showed that hydrodynamic processes act on the suspended particulate matter composition (POC content and clay fraction mainly), which will itself influence the quality and quantity of sediment-bound trace metals fluxes. Indeed, the DSWC-induced geochemical gradient of POC in the CCC was also responsible for the spatial distribution of anthropogenically-enriched PTM in this canyon. DSWC-induced currents were also able to occasionally mix resuspended shelf sediment with coastal river flood deposits.

- Hence, anthropogenic imprint is visible, even tenth of kilometers offshore, but to what extent? Mean EF in all the analyzed samples indicate a low to moderate pollution of the GoL sediments (i.e. $1.5 < EF < 3$, *Roussiez et al., 2006a*). In order to give a better representation of those findings, we drawn a cartography of normalized PTM concentrations and EFs by gathering our extensive dataset on PTM concentrations in surface sediment with others (*Roussiez et al., 2006b; Stabholz et al., 2013a*). Results are presented below and highlight the purveyor role of coastal mediterranean rivers in numerous PTM. To stay consistent with the methods used in this manuscript, we have drawn Al-normalized PTM concentrations in order to avoid grain-size bias, especially as we consider many different environment with different characteristics. We saw in the last chapter that Al was not the best clay-proxy in the first centimeters of the SC2400 sediment core, which is influenced by inputs induced by intense hydrodynamical event in deep environments.

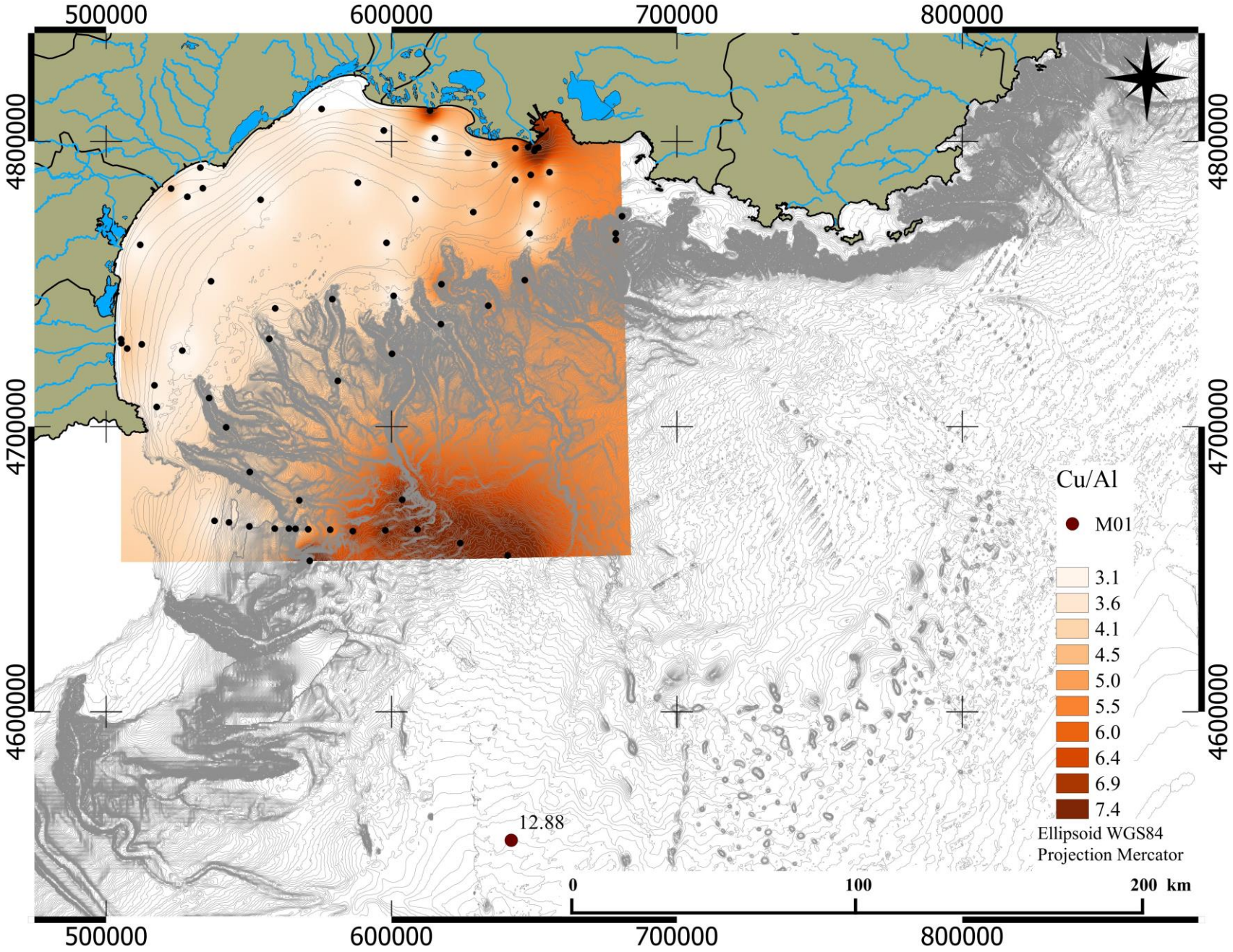
500000
600000
700000
800000
4800000
4700000
4600000
Cu/Al
M01
3.1
3.6
4.1
4.5
5.0
5.5
6.0
6.4
6.9
7.4
12.88
Ellipsoid WGS84
Projection Mercator
0
100
200 km

500000
600000
700000
800000
4800000
4700000
4600000
Cd/Al
M01
0.02
0.03
0.04
0.05
0.06
0.07
0.08
0.09
0.10
0.03
Ellipsoid WGS84
Projection Mercator
0
100
200 km

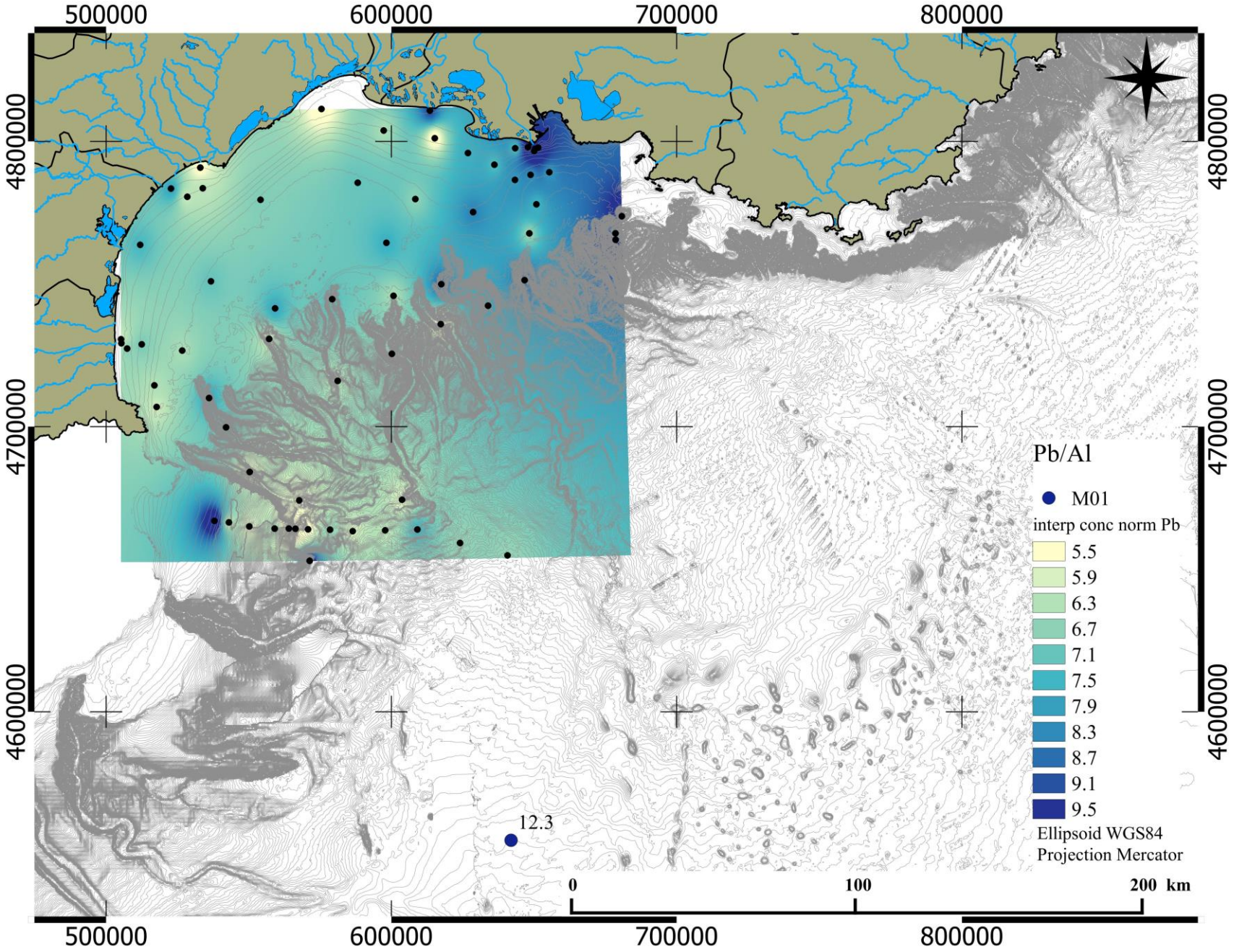
500000
600000
700000
800000
4800000
4700000
4600000
Pb/Al
M01
interp conc norm Pb
5.5
5.9
6.3
6.7
7.1
7.5
7.9
8.3
8.7
9.1
9.5
Ellipsoid WGS84
Projection Mercator
12.3
0
100
200 km

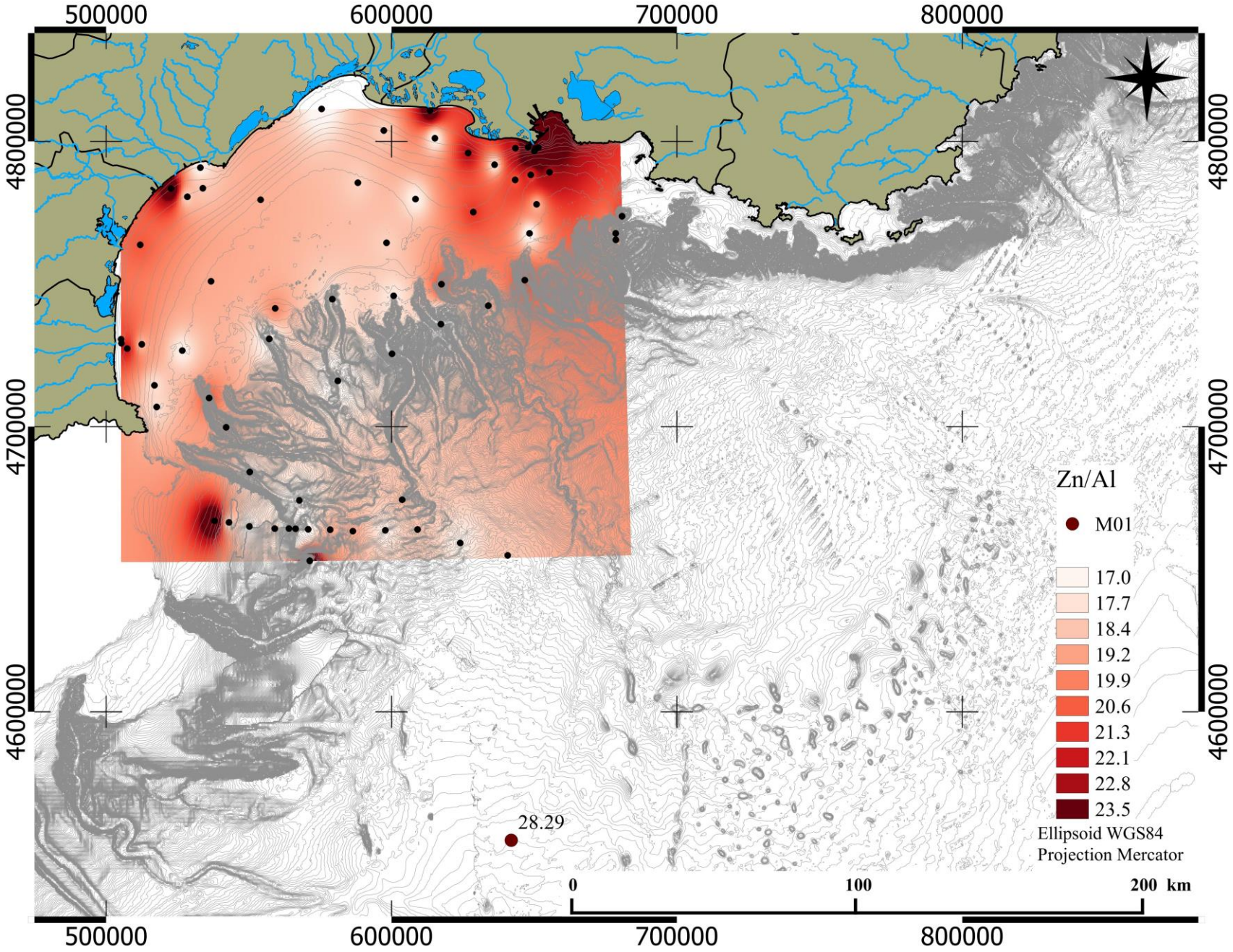
500000
600000
700000
800000
4800000
4700000
4600000
Zn/Al
M01
17.0
17.7
18.4
19.2
19.9
20.6
21.3
22.1
22.8
23.5
28.29
Ellipsoid WGS84
Projection Mercator
0
100
200 km

Those maps evidence the deposition of most PTM in rivers' prodeltas. The continental shelf is poorly concentrated or most probably, regularly remodeled by hydrodynamical processes induced currents. In deeper environments, deposition of Zn and Pb looks emphasized on the open-slope south from the Cap de Creus canyon, where water masses overflow the canyon walls. Al-normalized Zn and Pb concentrations are also quite elevated in the southermost point (M01) because of the low Al concentrations. For Cu however, it seems that this element is concentrated in the whole abyssal plain sediments.

We realised the same QGis plotting of the surficial sediment enrichment factors. For this calculation, we used the deep level of the Rhone riverbank (*Ferrand et al., 2012*) as the reference as it was proven successful in previous chapters of this work. We also did the same calculations using the Upper Continental Crust reference (*Wedepohl, 1995*) and the general profiles were the same, as expected. For all the elements, EF values calculated with the UCC reference were higher than when using a local reference, except for Pb. This is explained by the fact that UCC does not take into account the local lithology which is enriched in some elements and most probably in Cu and Zn for example. Those maps outlined the fact that the PTM depocenters identified with Al-normalized concentrations are also enriched in anthropogenically-enriched PTM.

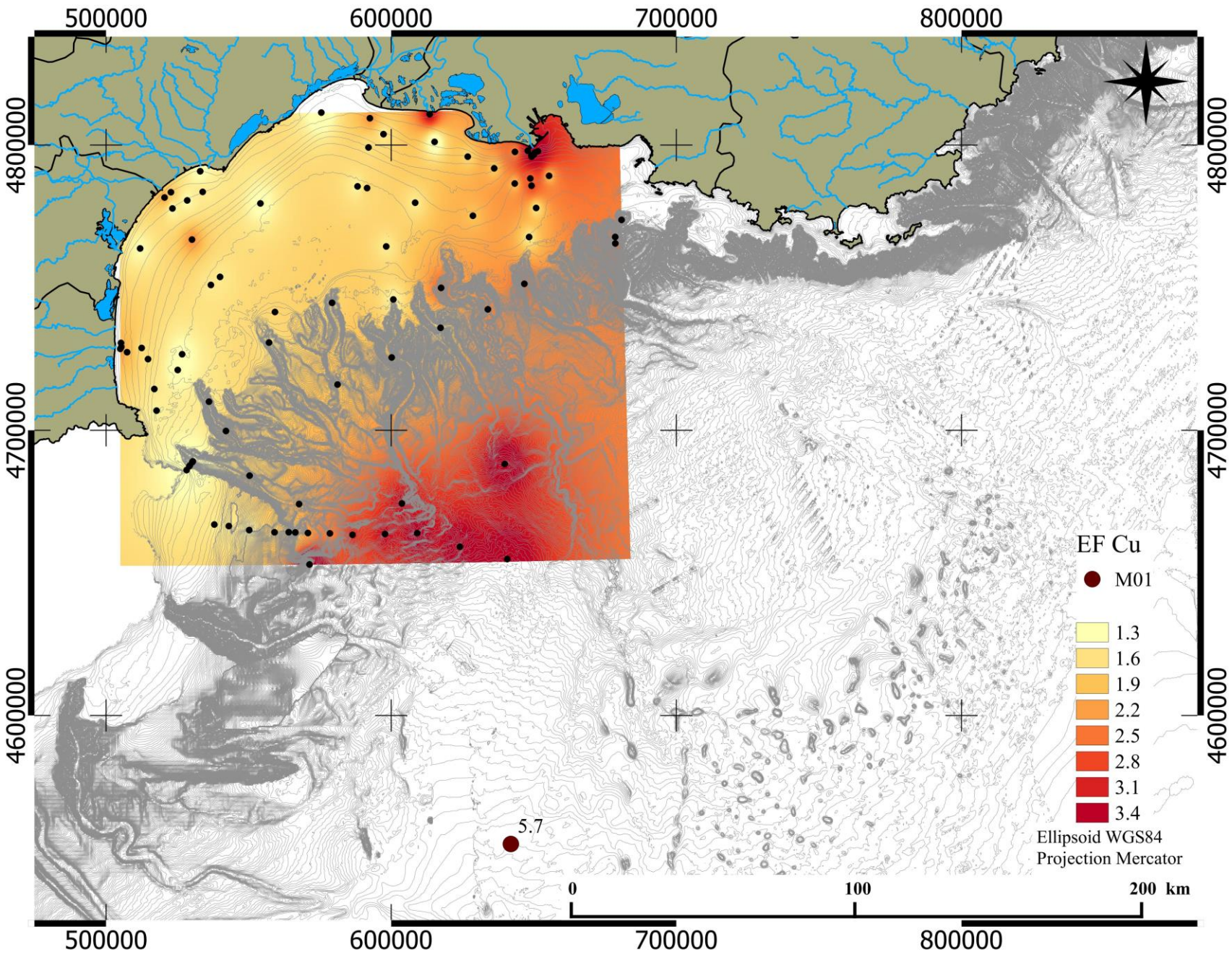
500000
600000
700000
800000
4800000
4700000
4600000
EF Cu
M01
1.3
1.6
1.9
2.2
2.5
2.8
3.1
3.4
5.7
Ellipsoid WGS84
Projection Mercator
0
100
200 km

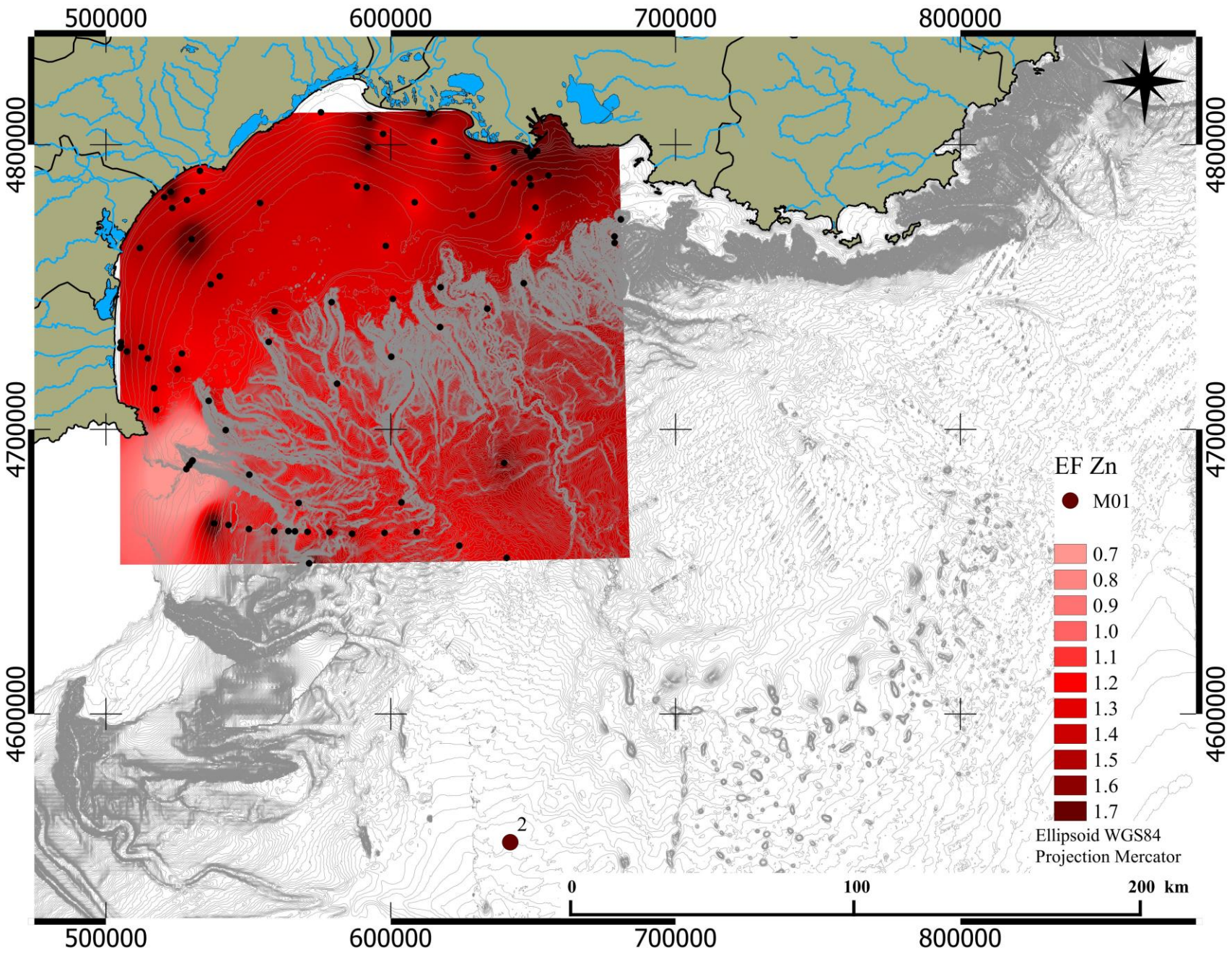
500000
600000
700000
800000
4800000
4700000
4600000
EF Zn
M01
0.7
0.8
0.9
1.0
1.1
1.2
1.3
1.4
1.5
1.6
1.7
Ellipsoid WGS84
Projection Mercator
2
0
100
200 km

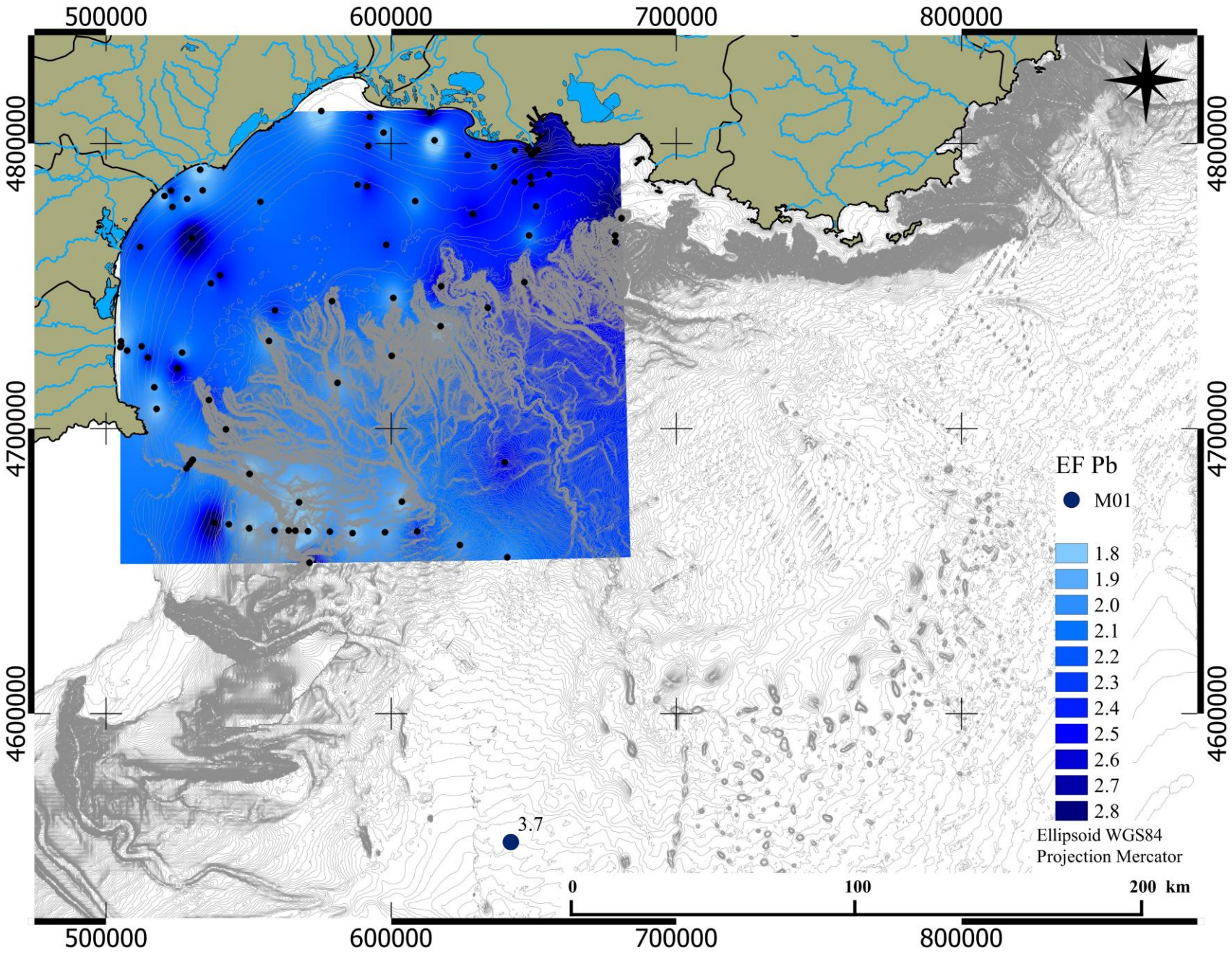
500000
600000
700000
800000
4800000
4700000
4600000
EF Pb
M01
1.8
1.9
2.0
2.1
2.2
2.3
2.4
2.5
2.6
2.7
2.8
3.7
Ellipsoid WGS84
Projection Mercator
0
100
200 km

Perspectives

- After examining case studies of flood, storms and cascading impact on PTM fluxes, one can also wonder the impact of deep Open Ocean Convection (OOC) which was identified as a major resuspension process for deep sediments (*Stabholz et al., 2013b*). We saw in chapter 4.2 that intense OOC does interact with DSWC mass fluxes and we know that this hydrodynamic event is recurrent in the GoL (*Houpert et al., 2012; Durrieu de Madron et al., 2013*). This would be an interesting perspective as OOC remobilized a different stock of particles than all the other processes studied in this work (i.e. continental shelf sediment). Heimburger et al. (*2014*) showed the OOC impact on vertical fluxes of PTM at the DYFAMED site but what is its impact on PTM redistribution in the GoL?
But in order to answer this question, an intensive study of the deep basin sediments of the NW Mediterranean Sea must be carried out. Indeed, to investigate potential mixing with other PTM sources like biological production, we need to characterize the deep sediment signature more extensively.

- This work highlighted the important quantities of PTM exported from the shelf towards canyon and deep-sea environements. The maps described above outline the contribution of anthropogenically-enriched PTM in those fluxes. It is known that PTM of anthropogenic origin are also the most labile and potentially bioavailable for uptake. Hence, it would be interesting to investigate the impact of this PTM distribution on marine organisms and its impact on the trophic chain. Indeed, Company et al. (*2008*) has shown how the lateral input of particulate organic matter and energy by DSWC enhanced the larval recruitment of *Aristeus antennatus* through increased food availability. And we have shown that in the deep canyon environments, sediment-bound contaminants displayed moderate anthropogenic contribution. Hence, one can wonder what would be the consequence of this important uptake by juvenile. Danovaro et al. (*2009*) have found high level of As, Cd, Cu, Hg, Pb and Zn in deep-sea sharks sampled in this same environment, implying biomagnification in the food chain.

- In order to sort out the geographical sources of particulate material by their REE signatures, identification of potential candidates needs to be refined, by sampling the Rhone tributaries in particular. First results show that REE concentrations and signatures of southern tributaries are very different (*Gairoard et al., 2012*). Other potential contributors such as

coastal rivers, canyon walls as well as Saharan dust should not be neglected. For the latter, results from the SOERE MOOSE survey should answer some questions. The acid-leaching procedure could also be performed in the same samples to strengthen any conclusion, as well as the use of Nd isotopes for example.

References

Company, J.B., Puig, P., Sarda, F., Palanques, A., Latasa, M., Scharek, R. (2008). Climate influence on deep sea populations. *PLoS ONE*, 3(1), doi: 10.1371/journal.pone.0001431.

Danovaro, R., Mea, M., Dell'Anno, A., Pusceddu, A. (2009). Deep-sea sharks: sentinels for evaluating anthropogenic impacts on continental margins? *HERMIONE Newsletter*, 2, 6.

Durrieu de Madron, X., Houpert, L., Puig, P., Sanchez-Vidal, A., Testor, P., Bosse, A., Estournel, C., Somot, S., Bourrin, F., Bouin, M.N., Beauverger, M., Beguery, L., Calafat, A., Canals, M., Cassou, C., Coppola, L., Dausse, D., D'Ortenzio, F., Font, J., Heussner, S., Kunesch, S., Lefevre, D., Le Goff, H., Martin, J., Mortier, L., Palanques, A., Raimbault, P. (2013). Interaction of dense shelf water cascading and open-sea convection in the northwestern Mediterranean during winter 2012. *Geophysical Research Letters*, 40, 1-7.

Ferrand, E., Eyrolle, F., Radakovitch, O., Provansal, M., Dufour, S., Vella, C., Raccasi, G., Gurriaran, R. (2012). Historical levels of heavy metals and artificial radionucleides reconstructed from overbank sediment records in lower Rhône River (South-East France). *Geochimica et Cosmochimica Acta*, 82, 163–182.

Gairoard, S., Radakovitch, O., Angeletti, B., Raimbault, P., Fornier, M. (2012). Caractérisations chimiques des particules en suspension transitant dans le Rhône et de ses affluents méridionaux. Détermination des flux. *Observatoire des Sédiments du Rhône*, http://www.graie.org/osr/spip.php?article127.

Heimbürger, L.E., Migon, C., Losno, R., Miquel, J.C., Thibodeau, B., Stabholz, M., Dufour, A., Leblond, N. (2014). Vertical export flux of metals in the Mediterranean Sea. *Deep Sea Research Part I: Oceanographic Research Papers*, 87, 14-23.

Houpert, L., Testor, P., Durrieu de Madron, X. (2012). Variability of open-sea deep convection and deep water masses in the North- western Mediterranean basin over the recent period (2007–2011) from in-situ measurements. *Ocean Science Meeting*, 20-24th February 2012, Salt Lake City, USA.

Roussiez, V., Ludwig, W., Monaco, A., Probst, J.-L., Bouloubassi, I., Buscail, R., Saragoni, G. (2006)a. Sources and sinks of sediment-bound contaminants in the Gulf of Lions (NW Mediterranean Sea): a multi-tracer approach. *Continental Shelf Research*, 26, 1843-1857.

Roussiez, V. (2006)b. Les éléments métalliques. Traceurs de la pression anthropique et du fonctionnement hydro-sédimentarie du golfe du Lion. *Ph.D. thesis*, University of Perpignan Via Domitia, p.247.

Stabholz, M. (2013)a. Impact of dense water formation on particulate organic matter dynamics : application to the Gulf of Lions margin. *Ph.D. thesis*, University of Perpignan Via Domitia, p.168.

Stabholz, M., Durrieu de Madron, X., Canals, M., Khripounoff, A., Taupier-Letage, I., Testor, P., Heussner, S., Kerhervé, P., Delsaut, N., Houpert, L., Lastras, G., Dennielou, B. (2013)b. Impact of open-ocean convection on particle fluxes and sediment dynamics in the deep margin of the Gulf of Lions. *Biogeosciences*, 10, 1097-1116.

Wedepohl, K.H. (1995). The composition of the continental crust. *Geochimica et Cosmochimica Acta*, 59(7), 1217-1232.

Chapitre VI

Conclusion

Au travers d'études spatiales et temporelles des flux de métaux lourds exportés et de la sédimentation dans le Golfe du Lion (GdL), les principaux objectifs de ce travail étaient les suivants:

- Dans un premier temps, nous souhaitions quantifier les apports en métaux traces (Cr, Co, Ni, Cu, Zn, Cd et Pb en particulier) transférés par les rivières au GdL. Le Rhône, ainsi que les rivières côtières grâce à l'exemple de la Têt furent étudiées. Une attention particulière fut portée à la contribution des événements de crues aux flux géochimiques.
- La signature des métaux traces déposés sur le plateau continental ayant déjà été largement étudiée, nous nous sommes intéressés aux flux de métaux exportés du plateau vers le bassin profond, ainsi qu'aux dépôts le long de ce continuum fluviomarin. Cet export, en Méditerranée Nord-Occidentale, se fait surtout lors d'événements hydrodynamiques intenses comme les tempêtes d'E-SE et les événements de cascading d'eaux denses côtières sur lesquels nous nous sommes particulièrement penchés.
- Un autre objectif de ce travail était de caractériser l'origine des ces métaux traces particulaires (MTP) dans les différentes zones et types de matériels étudiés, c'est-à-dire d'identifier la source géographique des particules initialement distribuées par les rivières. Nous voulions également évaluer la contribution anthropique aux flux de métaux traces exportés. Pour cela, nous avons utilisé divers outils géochimiques tels que les facteurs d'enrichissement (FE), les terres rares ou encore la méthode des fractions naturelle/résiduelle .

Ce travail s'appuie sur d'importants jeux de données : le suivi à long terme (2006-2011) de deux fleuves côtiers méditerranéens que j'ai analysé en partie; des échantillons de sédiment, de pièges à particules et de matières en suspension, récoltés lors de la campagne océanographique CASCADE à laquelle j'ai participé activement; et le suivi sur 6 mois (2005-2006, premier déploiement du programme européen HERMES) de 9 pièges à particules que j'ai entièrement analysé en ce qui concerne leurs concentrations en métaux traces.

Transfert des métaux traces particulaires par les fleuves côtiers au Golfe du Lion

Un suivi sur 6 ans a pas de temps mensuel a fourni le jeu de données le plus important à ce jour concernant les concentrations et les flux particulaires de métaux traces du Rhône et de la Têt. Ce suivi a également permis la détermination de paramètres (débit, matière particulaire

en suspension et carbone organique particulaire) qui sont essentiels pour la compréhension des processus de transport et de comportement des métaux traces. Cela nous a permis de déterminer l'influence du débit liquide et solide sur la composition des flux particulaires. De bonnes relations de corrélation ont pu être calculées grâce à cet important jeu de données, ainsi que le calcul précis des flux annuels de matière particulaire et de métaux traces. Par la juste estimation des apports en métaux traces au GdL, ce modèle pourra aider à la mise en place de mesures de gestion.

De précédentes études dans le GdL avaient déjà montré que les fleuves côtiers ont un régime à caractère torrentiel mais sont soumis aux événements de crues éclair alors que les fleuves plus importants, tels que le Rhône ont un débit plus constant et plus diffus. Cette étude a en outre permis de montrer que pendant les crues éclair sur les rivières côtières, la composition des particules varie de manière importante au cours de l'événement. Les métaux traces dont une part significative est d'origine anthropique, et plus labile, sont préférentiellement exportés très tôt dès l'initiation de la crue. Il est donc essentiel d'adapter la stratégie d'échantillonnage afin de mieux définir les flux de métaux traces exportés. Sur cette étude, l'utilisation d'une station d'échantillonnage automatisée fut utile au bon suivi d'événements hydrométéorologiques intenses mais imprévisibles. L'analyse du set de données de 2006-2011 et sa comparaison avec des études précédentes sur des années ou des événements antérieurs a mis en lumière la grande variabilité temporelle des apports en matières particulaires en suspension et métaux traces associés.

Sur cette période, deux événements de crues différents furent étudiés sur chaque système. Sur un même système, ces deux événements montraient cependant la même dynamique, que ce soit en période d'étiage printanière ou automnale. Sur un même système, ils représentaient aux alentours de 80% de l'apport annuel en MTP. Cependant, des concentrations différentes de certains éléments traces (les métaux dits « lithogènes » étaient en moyenne plus concentrés sur le Rhône, alors que Cu et Zn avaient des concentrations moyennes plus élevées sur la Têt) furent observées, de par les différences de lithologie des deux bassins versants mais aussi la diversité de leurs affluents. Le Rhône représente tout de même la source majeure des apports en matières particulaires en suspension, ainsi qu'en métaux traces associés, vers le plateau continental du GdL (70 à 90%).

Transfert des métaux traces particulaires vers le domaine profond du Golfe du Lion par les canyons sous-marins

Une fois délivrées au plateau continental, les matières en suspension et les métaux traces associés sont soumis aux transports le long et en travers du plateau puis aux phénomènes d'advection vers les canyons sous-marins.

- Dans la deuxième partie de ce manuscrit, nous avons, dans un premier temps, discuté de l'importance du transport induit par les événements de tempêtes. La tempête E-SE de Mars 2011, d'importance modérée et de récurrence annuelle, s'est avérée être un processus d'export efficace d'un mélange de particules (provenant à la fois du Rhône et des fleuves côtiers) puisque nous avons estimé que l'équivalent de 30 à 50% de l'apport annuel du Rhône en MTP fut exporté par le canyon du Cap de Creus. La grande diversité des échantillons collectés et de leurs pas de temps d'échantillonnage nous a également permis d'étudier la variabilité temporelle des flux de MTP et de la composition du matériel exporté hors du plateau. Nous en avons conclu que la variabilité de la composition du flux particulaire observée grâce aux prélèvements CTD était bien retranscrite par les pièges à particules, bien qu'ils fonctionnent sur des pas de temps d'échantillonnage plus grands. Les particules exportées dans le canyon étaient plus fines pendant les 3 jours de tempête que pendant le reste de la période d'étude et montraient des concentrations variables de carbone organique particulaire (COP) et de MTP (apports occasionnels en particules riches en métaux d'origine anthropique, ex. Cu, Zn, Pb). A l'issue de ces 3 jours de tempête, un dépôt centimétrique de sédiments fins a été observé uniquement à 442m de profondeur sur le flanc du canyon. Ces dépôts temporaires sont eux-mêmes susceptibles d'être remobilisés et exportés vers des environnements plus profonds lors d'événements hydrodynamiques intenses tels que les cascading d'eaux denses côtières qui dévalent périodiquement le long des canyons.

- Nous avons également étudié les échantillons du premier déploiement de la campagne HERMES, qui ont enregistré l'événement de cascading d'eaux denses côtières (DSWC) de l'hiver 2005-2006, afin d'étudier la variabilité spatiale et temporelle des concentrations de MTP et d'en quantifier les flux exportés. Des études antérieures sur ces mêmes échantillons avaient déjà décrit le contexte hydrodynamique. Si l'on compare les capacités d'export en matière particulaire en suspension (MPS) et MTP d'une tempête E-SE et du transport hors plateau induit par le DSWC, ce dernier est 20 à 30 fois plus efficace principalement en raison de sa durée. Les deux événements ayant exportés le même matériel (i.e. du sédiment de

plateau resuspendu ayant globalement les mêmes caractéristiques géochimiques), les flux journaliers moyens de MTP dans le canyon du Cap de Creus étaient comparables. Contrairement aux tempêtes, les événements de cascading ne se produisent pas tous les ans dans le GdL et n'ont pas la même intensité. Cependant l'étude de l'événement (2005-2006) a démontré leur forte capacité d'épuration côtière. En effet, nous avons estimé que l'équivalent de 300% des apports moyens annuels en MPS et MTP dus au Rhône a été exporté cet hiver là.

Caractéristiques géochimiques des sédiments profonds récents du Golfe du Lion

Des études récentes ont donc détecté la présence de masses d'eaux formées pendant l'hiver 2005-2006 sur toute la surface du bassin NO méditerranéen. Après avoir dévalé le long des canyons sous-marins, la couche néphéloide dense s'étend et se stabilise.

Les conclusions du chapitre 4.2 démontraient que la matière organique, ainsi que les métaux d'origine anthropique, étaient distribués préférentiellement dans les pièges profonds des canyons sous-marins. Il n'est donc pas trivial de se demander quelle est l'empreinte anthropique dans les sédiments profonds, et les métaux traces sont un bon élément de réponse à cette question.

Les carottes profondes analysées dans cette étude ont en effet enregistré des événements d'apport différents ou du moins des changements de sources de sédiment. Ces changements ont été identifiés grâce aux inclusions d'organismes côtiers, aux niveaux de granulométrie différentes, à la composition et à la qualité du matériel organique et/ou grâce aux augmentations concomitantes de différents paramètres géochimiques.

Traçage de l'origine des particules exportées

- Les méthodes de traçage (terres rares et fraction résiduelle) nous ont permis de décrire l'origine géographique fluviatile mixte (mélange de particules provenant du Rhône et des rivières côtières) des particules collectées dans le canyon (pièges et sédiment) du Cap de Creus et les carottes profondes. Mais dans les environnements les plus profonds, autour de la carotte située le plus au sud en particulier, nous suspectons des apports particulaires provenant soit de dépôts temporaires au sein des canyons (comme ceux décrits lors de la tempête), de l'érosion des flancs de canyon, de la remise en suspension des sédiments du plancher océanique sous l'action de la convection profonde intense, des glissements gravitaires ou encore de dépôts atmosphériques de poussières sahariennes et de la production pélagique.

- Grâce au calcul des facteurs d'enrichissement, nous avons précisé l'origine

naturelle ou anthropique des particules et la contribution de la part anthropique aux flux totaux de MTP. Les FEs ont montré que, pendant les événements de crues, les premières particules exportées vers le GdL étaient les plus riches en matière organique et donc celles qui renfermaient le plus de métaux traces d'origine anthropique et labiles.

Les extractions par lessivages acides confirment également que les particules mobilisées lors de la tempête de Mars 2011contenaient une large proportion de MTP labiles. Les FEs calculés dans les sédiments de surface échantillonnés à 442 m dans le canyon du Cap de Creus après cette tempête nous ont permis de caractériser le matériel déposé dans le canyon par les courants de tempête. Ces caractéristiques nous ont amené à la conclusion qu'il s'agissait du même matériel que celui échantillonné dans les pièges et que celui-ci provenait de la remise en suspension des sédiments du plateau continental.

Les FEs ont également montré que les processus hydrodynamiques ont un impact sur la composition de la MPS (teneur en COP et argiles notamment) ce qui influence la qualité et la quantité des flux de métaux traces associés. En effet, ce travail a démontré que le gradient géochimique de COP dû au cascading dans le canyon du Cap de Creus était également responsable de la distribution spatiale des MTP d'origine anthropique dans ce même canyon. Les facteurs d'enrichissement ont également démontrés le rôle des courants induits par le cascading dans le mélange occasionnel des sédiments du plateau remis en suspension avec les dépôts de crues.

- Ainsi, la contribution anthropique est détectable jusqu'à des dizaines de kilomètres du Littoral et dans le milieu profond. Mais quelle est son ampleur ? Les FEs moyens dans l'ensemble des échantillons analysés démontrent une pollution faible à modérée des sédiments du GdL (i.e. 1,5 < FE < 3, *Roussiez et al., 2006a*). Afin de mieux représenter ces résultats, nous avons rassemblé notre set de données de concentrations en MTP avec ceux d'autres travaux (thèse de *Roussiez et al., 2006b;* thèse de *Stabholz et al., 2013a*) afin d'établir une cartographie des concentrations normalisées de MTP et leurs FEs correspondants. Ces résultats sont présentés ci-dessous et démontrent le rôle de source en nombreux MTP des fleuves côtiers méditerranéens.

Afin de rester cohérent avec les méthodes utilisées tout au long de ce travail, nous avons représenté les concentrations en MTP normalisées à Al, afin d'éviter tout biais granulométrique, surtout en prenant en compte des environnements divers aux caractéristiques granulométriques différentes. Dans le dernier chapitre nous avons montré que les normalisations par Al se révélaient peu satisfaisantes dans les premiers centimètres de la

carotte SC2400, très influencée par des apports liés aux événements hydrodynamiques intenses dans les environnements profonds. Ces cartes mettent en évidence le dépôt préférentiel de la plupart des MTP dans les prodeltas des fleuves côtiers. Le plateau continental se trouve peu enrichi ou plus probablement régulièrement remanié par les courants induits par les processus hydrodynamiques très fréquents. Dans les environnements plus profonds, le dépôt en Zn et Pb semble plus important sur la pente continentale sud du canyon du Cap de Creus, à l'endroit ou les masses d'eau débordent du chenal du canyon. Les concentrations normalisées par Al du Zn et du Pb sont aussi élevées dans le point le plus au sud (M01) à cause des faibles concentrations en Al en ce point. En ce qui concerne Cu, cet élément semble assez concentré dans tous les sédiments de la plaine abyssale.

Les mêmes cartographies des FEs du sédiment superficiel ont été réalisées. Pour ce calcul, c'est la référence locale du bas de la carotte prélevée sur les berges du Rhône (*Ferrand et al., 2012*) qui a été choisie, puisqu'elle a été utilisée dans la majorité de ce travail. Les mêmes calculs ont été réalisés avec la référence de la croûte continentale (*Wedepohl, 1995*) et les profils étaient la aussi très similaires aux précédents. Pour tous les éléments, les valeurs de FE calculés par rapport à la composition de la croûte continentale étaient plus élevées par rapport à celles calculées avec une référence locale, sauf pour le Pb. Ceci s'explique par le fait que la composition de la croute continentale ne reflète pas forcément la lithologie locale qui est parfois enrichie en certains éléments, ici en Cu et en Zn par exemple.
Ces cartes soulignent le fait que les dépôts-centres identifiés par les cartographies des concentrations normalisées sont également enrichies en MTP d'origine anthropique.

Perspectives

- Après l'étude de l'impact des crues, tempêtes, et du cascading sur les flux de MTP, reste en suspens l'impact de la convection profonde qui a également été identifié comme un processus majeur de remise en suspension du sédiment profond (*Stabholz et al., 2013b*). En effet, nous avons mentionné dans le chapitre 4.2 que la convection profonde interagissait avec les flux de masses induis par le cascading et nous savons désormais que la convection est un phénomène récurrent dans le GdL (*Houpert et al., 2012; Durrieu de Madron et al., 2013).* Ce serait donc une perspective d'investigation intéressante puisque la convection remobilise un stock de particules différent de tous les autres processus hydrodynamiques étudiés ici (i.e. les sédiments du plateau continental remis en suspension). Plus à l'est, Heimburger et al. (*2014*)

ont montré l'impact de la convection sur les flux verticaux de MTP à DYFAMED mais qu'en est-il de son impact sur la redistribution des MTP dans le GdL?
Pour répondre à cette question, une large étude des caractéristiques géochimiques des sédiments du bassin profond NO devra être menée. En effet, afin d'étudier un éventuel mélange avec des particules provenant d'autres sources comme la production biologique, la signature de ces sédiments devra être mieux connue.

- Ce travail a souligné l'importance des quantités de matière exportées du plateau continental vers les canyons et les environnements profonds. Les cartes ci-dessus ont résumé l'importance de la contribution en MTP d'origine anthropique dans ces flux. Et on sait que les métaux d'origine anthropique sont les plus labiles et potentiellement biodisponibles. Ainsi, il serait intéressant d'étudier l'impact de cette distribution en MTP sur les organismes marins et la chaine trophique. Company et al. (*2008*) ont mis en évidence que l'apport latéral de matière organique particulaire et d'énergie par le cascading accroissait par la suite le recrutement larvaire par une meilleure disponibilité de nourriture. Dans ce travail de thèse, nous avons montré que dans les environnements profonds du canyon, les contaminants associés au sédiment affichent une contribution anthropique modérée. Aussi le lien semble possible entre accroissement de biomasse et contamination potentielle de celle-ci. Ainsi, il serait normal de se demander quelle serait la conséquence de consommation par des juvéniles. Danovaro et al. (*2009*) ont relevé des concentrations élevées de As, Cd, Cu, Hg, Pb et Zn chez une espèce de requins vivant en milieu profond, prélevés dans ces mêmes environnements, suggérant ainsi l'existence de la bioamplification des ces composés le long de la chaine trophique.

- Aussi, afin de différencier les sources géographiques de matériel particulaire au travers de leurs signatures par les terres rares, l'identification des candidats devra être affinée par l'échantillonnage des affluents du Rhône en particulier. Des premiers résultats montrent que les concentrations ainsi que les signatures en REE des affluents méridionaux sont très différentes (*Gairoard et al., 2012*). Il ne faut pas négliger d'autres contributeurs potentiels tels que les fleuves côtiers, les flancs de canyons, ainsi que les poussières sahariennes. Pour ces dernières les résultats issus des collectes du SOERE MOOSE devraient lever les doutes. La méthode des lessivages acides, ainsi que l'étude des isotopes du Nd par exemple, pourront aussi être réalisées sur ces mêmes échantillons afin de renforcer toute conclusion.

APPENDICES

A. Particulate trace metal concentrations in suspended particulate matter

		Q	SPM	OC	^{27}Al	^{47}Ti	^{51}V	^{52}Cr	^{56}Fe	^{59}Co	^{60}Ni	^{65}Cu	^{66}Zn	^{75}As	^{107}Ag	^{114}Cd	^{133}Cs	^{139}La	^{146}Nd	^{147}Sm	^{208}Pb
		(m^3/s)	(mg/L)	(%)	(µg/g)	(µg/g)	(µg/g)	(µg/g)	(µg/g)	(µg/g)	(µg/g)	(µg/g)	(µg/g)	(µg/g)	(µg/g)	(µg/g)	(µg/g)	(µg/g)	(µg/g)	(µg/g)	(µg/g)
TET (low flow)	09/01/06 18:10	7,89	17,14	7,0		3066	90,89	64,27	39839	14,40	32,61	109,2	247,1	31,43		0,46	7,90	37,46	33,11	6,59	64,87
	08/02/06 17:40	11,30	9,14	6,7		2934	75,27	61,61	34821	12,74	33,14	90,4	205,5	29,12		0,55	6,93	39,69	33,48	6,56	46,91
	09/03/06 17:50	3,69	9,06	6,9		3604	94,79	75,66	37079	12,59	52,34	96,2	343,4	36,45		0,92	8,00	50,70	34,81	6,90	50,16
	06/04/06 18:25	9,72	11,48	4,7		2655	49,09	48,08	26654	11,09	25,91	59,5	176,4	10,11		0,51	5,88	30,30	27,23	5,29	40,87
	05/07/06 19:02	0,21	6,78	14,2	40439	2159	52,33	37,98	39221	11,79	20,54	67,4	238,4	50,68	2,40	2,47	4,34	23,91	21,85	4,49	60,51
	06/09/06 19:00	0,84	20,28	12,0	55303	1902	60,58	48,17	36773	12,34	28,75	118,0	334,0	44,04	3,10	0,95	5,07	24,52	23,23	4,38	77,20
	04/10/06 16:45	1,99	21,75	10,1	65976	2194	69,29	56,79	37336	12,56	28,35	111,1	309,8	31,22	2,46	0,71	6,09	27,40	25,57	4,91	73,31
	07/11/06 16:42	1,38	5,46	12,8	51522	2009	60,03	46,59	44893	18,42	32,80	104,5	313,7	61,39	2,76	1,15	4,69	23,08	21,08	4,10	72,40
	12/12/06 16:35	2,58	5,96	15,7	35198	1141	39,83	38,68	33277	11,75	16,90	92,1	226,1	43,96	3,44	0,77	3,36	15,96	14,67	2,94	52,16
	17/01/07 16:15	3,65	15,24	17,5	45557	2039	51,91	42,99	28662	14,22	19,59	112,7	265,5	33,82	5,02	0,84	4,43	21,67	19,07	3,71	63,51
	05/02/07 16:30	1,72	8,26	18,6	44648	1678	47,35	44,45	40572	10,35	22,45	129,7	336,1	66,19	2,92	1,04	4,14	18,64	17,31	3,41	56,55
	07/03/07 17:30	0,40	6,98	9,4	59378	2588	69,58	63,31	42953	14,42	26,99	192,6	625,1	69,43	4,33	1,64	5,52	28,21	24,55	4,96	89,39
	04/04/07 16:25	0,83	26,32	15,6	55829	2572	67,60	56,03	29276	12,08	26,54	197,7	432,4	39,76	5,58	1,18	5,25	28,06	23,77	4,51	78,11
	02/05/07 16:30	8,58	115,86	4,5	88905	3955	91,25	63,92	29875	13,41	29,58	79,7	253,4	24,16	1,08	0,50	7,84	35,39	30,86	6,33	59,91
	12/06/07 15:15	2,15	13,11	7,9	71115	2909	80,57	62,82	36724	16,88	29,16	143,4	426,0	42,82	2,98	0,84	6,56	33,42	29,23	5,81	90,03
	04/07/07 18:15	0,64	16,98	13,3	51549	2136	65,50	50,55	46133	15,03	28,86	122,6	312,8	58,73	2,40	0,80	5,58	24,85	22,32	4,60	68,46
	05/09/07 17:20	0,58	14,70	12,7	59856	2463	73,98	51,54	37628	13,74	27,20	119,4	414,3	82,72	2,37	0,85	5,67	27,58	23,77	4,74	80,87
	08/11/07 16:05	0,47	7,69	14,8	36509	1957	43,66	37,86	39325	14,43	17,99	84,0	257,9	53,98	2,61	0,81	3,51	20,01	17,50	3,54	54,79
	05/12/07 17:09	0,79	6,23	16,2	44300	1401	49,22	42,53	42384	12,12	20,68	109,7	275,7	47,39	2,43	0,75	4,04	20,12	17,63	3,59	66,18
	08/01/08 16:40	2,07	10,44	12,1	54137	2629	66,73	48,52	37425	11,61	24,90	92,6	279,0	29,47	2,42	0,65	5,28	25,95	22,71	4,60	58,58
	06/02/08 17:38	0,81	11,66	12,6	55400	2695	58,60	47,30	38679	16,01	27,98	142,4	310,1	35,46	2,79	0,73	5,02	24,82	21,51	4,31	78,52
	06/03/08 17:20	1,01	9,35	11,4	39044	1970	49,94	36,06	19337	5,79	18,96	27,2	159,8	11,27	0,92	0,25	3,32	14,44	12,77	2,47	18,48
	06/04/08 15:50	0,66	5,80	13,0	61588	2577	81,92	66,41	28739	11,35	30,18	104,0	332,7	28,37	1,97	0,55	6,68	25,85	21,99	4,39	56,38
	06/05/08 16:52	0,51	4,18	11,0	49501	2081	55,65	50,55	28394	8,87	23,76	120,8	470,4	21,03	2,39	0,53	5,07	21,65	18,72	3,73	71,53
	06/06/08 18:15	9,97	159,99	4,8	81149	2756	74,73	53,31	36267	10,38	26,69	38,6	148,0	21,38	0,54	0,14	7,73	30,36	26,20	5,19	30,10
	06/07/08 16:30	0,89	17,30	8,9	66701	2924	67,29	50,73	26721	10,87	23,60	69,5	320,7	21,58	1,08	0,34	6,21	29,07	25,67	5,25	55,55
	06/08/08 17:50	0,59	24,91	9,5	65490	2700	70,20	55,78	27853	10,86	26,07	74,7	368,3	19,50	1,42	0,36	6,78	30,58	26,69	5,33	70,05
	06/09/08 17:00	0,96	39,28	9,3	17242	772	17,57	13,07	8785	2,33	6,19	18,6	51,2	4,47	0,33	0,07	1,59	7,95	6,97	1,38	15,21
	06/10/08 17:55	1,01	15,20	10,9	55562	1705	53,34	45,45	29346	9,12	25,73	78,6	366,6	17,65	1,32	0,53	4,75	21,56	19,26	3,87	72,74
	05/11/08 16:20	7,13	30,05	5,1	72153	3666	94,02	65,70	33733	14,70	31,97	73,7	260,7	32,93	0,86	0,52	5,75	31,23	28,26	5,71	71,15
	06/12/08 16:20	3,21	3,76	10,2	65858	2458	70,88	56,61	27079	11,98	27,30	86,7	321,0	23,80	1,32	0,42	6,39	28,69	24,81	5,04	59,94
	15/01/09 16:35	3,22	4,51	4,5	71622	2394	84,38	80,93	43609	15,27	40,11	120,5	368,6	28,83	1,73	0,65	7,71	43,64	39,57	7,80	65,12
	11/02/09 16:30	4,97	4,46	8,5	68016	2547	64,87	46,90	30797	10,64	24,71	72,2	211,5	21,09	0,84	0,39	6,30	31,90	28,42	5,72	41,77
	12/03/09 16:30	0,82	9,62	8,8	53684	2457	56,71	53,44	20456	8,81	25,91	64,6	1343,8	18,09	0,67	0,27	4,88	23,61	20,50	4,13	39,64
	08/04/09 16:43	24,60	140,30	3,7	82962	3759	85,40	59,21	28808	12,81	30,09	66,6	207,3	26,97	0,34	0,38	7,48	38,50	33,75	6,60	37,13
	10/06/09 16:40	4,00	9,82	4,2	77517	3400	81,48	60,78	30716	14,30	29,04	73,1	299,8	31,28	0,66	0,80	7,84	35,60	31,84	6,35	55,81
	10/07/09 17:33	2,74	16,66	6,6	85686	3675	92,91	66,04	32361	15,10	32,53	94,8	338,2	28,37	0,85	0,54	8,48	39,27	34,73	7,06	60,13
	10/08/09 17:15	1,78	7,96	8,1	71954	3227	78,63	58,71	28539	12,34	26,61	85,6	318,0	23,47	1,05	0,33	7,31	32,74	28,97	5,81	66,59
	10/09/09 17:00	2,75	26,06	9,3	69339	3471	77,21	57,65	26034	11,64	26,00	105,5	399,2	19,50	1,88	0,68	6,82	32,81	28,38	5,59	73,35
	10/10/09 16:15	1,65	10,25	9,7	58120	2593	60,48	47,66	24070	10,87	22,42	60,7	345,9	18,29	0,89	0,32	5,71	26,35	23,35	4,70	72,46
	10/11/09 16:56	1,53	2,80	15,8	39308	1884	45,03	43,13	20753	9,16	18,58	88,3	316,7	19,24	1,33	0,48	3,97	20,86	17,45	3,56	66,88
	10/12/09 16:56	1,28	7,48	12,2	50120	2398	56,30	45,99	22227	9,88	22,06	85,1	318,2	17,34	1,05	0,50	5,10	23,55	20,38	4,03	56,46
	06/01/10 11:17	2,52	7,58	14,7	104250	4155	118,99	84,12	52411	16,17	40,14	47,6	141,2	35,47	0,25	0,24	9,59	47,81	42,31	8,58	51,34

	03/02/10 11:15	2,57	5,04	13,1	53409	2598	62,91	56,07	31080	11,63	26,44	98,8	300,9	14,07	1,61	0,96	5,65	25,87	23,19	4,65	54,87
	03/03/10 11:33	3,37	78,15	10,5	46461	2265	57,33	47,47	29364	10,95	23,00	76,1	314,5	14,60	1,08	0,48	5,29	22,11	19,54	4,04	61,04
	07/04/10 11:26	2,61	13,73	8,7	62124	3490	88,92	69,66	37164	13,05	32,73	168,6	552,5	20,78	1,64	0,82	6,54	28,51	24,56	4,95	90,46
	05/05/10 11:15	24,90	48,89	3,6	49903	2491	62,61	47,50	29293	10,71	25,30	73,8	293,6	14,95	1,22	0,54	5,49	26,35	23,57	4,65	48,66
	09/06/10 11:15	6,39	16,24		90824	4394	94,87	65,76	43638	14,37	31,55	60,7	214,4	29,34	0,47	0,37	8,77	41,42	36,95	7,57	45,80
	21/07/10 11:30	1,53	8,64		45932	3210	69,98	50,88	32337	12,21	25,14	64,3	218,5	19,84	0,46	0,44	5,34	25,10	22,78	4,70	46,99
	08/09/10 11:45	1,82	19,91		63737	3288	71,70	56,13	36577	12,45	28,16	67,0	263,8	17,12	2,09	0,26	7,05	37,64	33,10	6,55	79,93
	13/10/10 12:00	150,00	159,69		54342	2827	66,90	53,38	33198	11,25	25,91	76,3	287,7	15,87	0,83	0,42	6,11	30,04	26,81	5,33	64,37
	04/11/10 12:10	6,42	12,06		59151	3922	96,83	65,19	41817	13,98	32,43	39,5	146,0	34,81	0,21	0,27	6,22	32,70	29,25	5,75	37,43
	08/12/10 12:00	8,75	10,97		68461	4044	92,41	71,60	42609	15,32	32,12	74,0	212,1	24,87	0,48	0,41	7,87	36,32	32,77	6,49	65,48
	12/01/11 12:00	6,44	6,20		51690	2346	56,56	42,31	24034	9,30	20,40	61,3	229,9	17,92	0,72	0,39	5,44	25,33	21,83	4,32	37,98
	04/02/11 12:00	4,84	8,33		64930	3237	83,25	61,99	32600	14,04	28,52	85,8	299,7	24,32	0,94	0,56	7,00	33,06	28,70	5,61	53,58
	04/03/11 18:00	4,49	9,96		54523	2684	63,29	49,95	26487	12,07	24,57	99,6	320,4	17,04	1,26	0,70	5,69	26,74	22,67	4,53	51,45
	06/04/11 18:00	366,00	19,07		79707	3349	83,45	59,74	34833	12,92	31,25	65,1	253,1	28,22	0,46	0,41	7,72	43,13	38,24	7,61	51,41
	11/05/11 18:00	12,70	9,73		65498	3290	78,74	57,30	31579	12,65	27,28	62,6	210,8	22,33	0,49	0,38	7,00	33,69	29,63	5,87	50,67
(turbid)	13/11/05 19:00	7,26	74,73	7,4	51437	2675	62,70	54,47	28501	9,96	14,30	123,8	1180,0	17,14	2,84	0,88	5,85	24,02	20,79	4,21	75,98
	14/11/05 05:00	10,76	223,99	5,0	77595	2461	75,79	54,07	36157	11,89	25,92	93,2	259,2	24,00	1,51	0,58	7,20	29,92	26,67	5,26	61,00
	14/11/05 06:00	11,34	236,76	5,1	73841	3414	91,85	75,77	40817	14,69	24,15	132,2	333,9	29,83	2,17	0,76	8,23	32,59	29,06	5,86	97,16
	14/11/05 07:00	12,50	197,37	5,8	78846	2877	81,61	80,14	37034	13,51	39,96	125,9	347,1	27,71	2,39	0,73	7,15	34,66	29,94	5,67	91,41
	14/11/05 09:00	12,50	92,50	6,2	70046	2972	87,79	72,17	40162	14,28	23,42	123,5	325,0	30,71	1,93	0,78	8,03	30,83	27,99	5,79	89,38
	14/11/05 16:00	89,59	735,30	2,4	80987	3103	98,24	72,07	41060	13,95	25,13	98,1	205,9	28,23	0,75	0,50	8,85	33,39	30,03	6,14	57,40
	14/11/05 19:00	135,91	647,54	3,8	82743	3171	107,59	74,97	48150	15,76	38,06	109,3	204,9	32,40	0,63	0,45	9,29	34,66	33,31	6,99	53,27
	14/11/05 22:00	326,13	935,45	2,0	89694	4322	104,78	77,27	43926	14,96	27,35	89,5	153,2	28,70	0,40	0,27	7,87	41,48	37,12	7,43	44,75
	15/11/05 01:00	503,16	1529,60	1,5	83807	3870	117,90	80,14	47493	16,25	39,30	91,7	148,9	29,12	0,32	0,27	3,49	39,30	35,38	7,17	39,01
	15/11/05 04:00	343,13	1014,80	1,4	97217	3754	139,84	90,01	52954	18,53	45,69	90,6	157,9	32,32	0,32	0,31	10,21	37,48	36,85	7,36	40,87
	15/11/05 07:00	275,11	389,17	1,6	109364	3734	119,28	78,90	45707	16,92	39,67	71,7	134,7	31,49	0,20	0,29	9,24	40,97	36,20	7,37	38,38
	15/11/05 10:00	229,03	327,14	1,5	102522	3461	102,53	69,08	42912	15,23	35,02	58,0	132,1	30,55	0,17	0,29	8,39	40,36	34,13	6,74	37,35
	15/11/05 13:00	196,11	259,01	1,7	84179	3482	94,15	69,75	40268	13,79	23,92	47,6	132,6	28,94	0,34	0,33	8,68	38,00	34,47	6,92	38,51
	15/11/05 16:00	163,20	219,82	1,9	103133	3019	101,48	66,18	44784	15,07	32,39	54,8	90,2	34,24	0,28	0,27	9,13	39,78	35,92	7,23	39,36
	15/11/05 19:00	134,12	220,56	1,7	91299	3765	103,29	70,92	45950	15,46	26,42	56,9	149,1	36,19	0,40	0,37	9,34	43,70	40,64	8,34	44,45
	16/11/05 07:00	63,85	130,64	1,7	90521	3721	94,95	67,57	43362	14,31	24,97	52,2	157,3	36,68	0,38	0,36	8,70	42,38	37,98	7,61	40,32
	16/11/05 13:00	63,85	100,44	1,5	90556	3833	95,94	67,25	43188	14,17	24,79	58,1	161,0	34,99	0,45	0,32	8,82	43,74	39,71	7,90	42,56
	16/11/05 22:00	48,30	92,87	1,7	82754	3379	85,18	65,58	39925	13,35	20,82	52,7	157,4	30,71	0,58	0,35	8,13	42,79	38,24	7,44	41,89
	17/11/05 10:00	41,62	76,72	2,0	82997	3655	87,77	63,88	40572	12,78	21,44	58,8	190,1	28,94	0,55	0,37	8,23	39,46	35,36	7,09	42,14
	11/04/07 06:00	0,46	6,79		35210	1136	31,67	32,90	32697	11,83	15,15	82,8	281,0	50,97	4,44	0,77	2,13	10,02	9,19	1,80	43,67
	12/04/07 18:00	2,94	201,00	12,9	56668	2829	63,03	54,67	32494	9,09	26,28	172,3	422,2	28,09	4,29	1,03	5,12	21,84	19,74	4,02	73,34
	13/04/07 16:00	3,10	37,20	10,1	64862	2836	71,10	62,80	34504	11,50	30,86	197,1	560,5	24,09	5,05	1,32	5,80	29,53	25,64	5,02	81,46
	14/04/07 07:00	25,46	383,64	4,8	65716	3931	95,83	66,42	41406	14,38	33,55	74,6	221,6	33,08	0,51	0,51	4,91	31,87	29,62	6,17	53,70
	14/04/07 15:00	86,16	714,68	3,9	58198	4260	94,95	64,83	40514	13,84	31,92	62,0	190,4	26,35	0,43	0,38	4,43	23,88	23,13	4,82	44,15
	15/04/07 07:00	52,12	159,66	3,1	66113	4278	106,17	73,56	45464	16,25	36,76	106,5	221,8	40,85	0,62	0,34	6,31	25,12	20,69	3,86	48,46
	15/04/07 16:00	41,85	129,46	2,6	93149	4291	105,62	72,72	47957	16,75	36,44	56,7	205,4	41,71	0,38	0,47	5,46	38,99	36,06	7,29	52,03
	16/04/07 00:00	32,78	111,05	2,2	94714	4114	98,54	67,21	44848	15,62	33,35	51,3	210,4	38,84	0,33	0,42	6,12	38,38	35,55	7,26	50,21
	16/04/07 10:00	37,52	78,87	2,4	65147	4447	111,33	74,66	49078	17,66	38,74	60,1	222,7	45,95	0,40	0,48	5,17	25,09	21,30	4,29	58,17
	18/04/07 08:00	24,40	33,22		86722	3934	90,86	92,22	42625	15,79	32,88	50,3	216,9	35,55	0,37	0,43	8,14	40,43	36,63	7,79	51,18
	19/04/07 08:00	16,59	45,80		84302	4065	87,53	60,91	40397	14,50	30,11	55,4	229,3	32,34	0,70	0,47	7,27	28,03	26,37	5,63	48,14
	20/04/07 08:00	17,16	48,56		77181	4188	85,42	58,55	38901	13,77	29,41	57,1	217,0	29,04	0,60	0,43	5,55	30,89	27,91	5,92	45,72

	21/04/07 08:00	12,60	36,92		84883	3766	78,73	55,62	36460	12,99	26,88	53,1	224,9	27,43	0,50	0,44	7,22	32,32	30,30	6,31	46,81
	22/04/07 08:00		34,95		85987	3629	74,52	54,79	35638	13,06	26,99	62,9	256,1	26,86	0,49	0,53	7,22	28,76	26,40	5,50	48,43
	23/04/07 08:00		24,14		100584	3982	87,23	71,07	42232	14,96	36,58	69,9	299,8	30,74	0,73	0,64	8,13	38,04	33,90	6,81	58,12
	15/03/11 09:50	366,00	460,46		95931	4183	121,33	80,36	41845	17,02	39,71	76,3	196,6	37,05	0,25	0,34	9,25	42,91	37,52	7,41	44,14
RHONE (low flow)	09/01/06 11:15	652	11,94			3115	112,7	98,3	32078	15,36	52,85	59,57	271,2	20,82		0,46	15,02	35,08	27,10	5,30	53,40
	08/02/06 11:15	624	5,86			2491	92,0	83,5	26104	16,55	54,63	58,16	244,1	22,54		0,55	14,85	27,95	21,57	4,07	48,21
	09/03/06 11:20	2184	126,67			2641	73,4	73,5	21971	12,31	40,88	44,01	182,3	13,28		0,69	9,62	26,87	22,05	4,42	37,66
	06/04/06 11:20	2923	128,56			2781	76,8	76,8	24204	13,63	42,22	36,79	159,3	3,73		0,45	9,43	23,43	20,14	4,08	35,41
	05/07/06 11:40	871	10,02	4,2	68446	3002	97,3	84,6	27769	15,96	45,61	57,48	220,0	17,95	0,75	0,45	10,89	24,58	21,77	3,96	45,36
	08/08/06 10:48	625	10,49	2,2	59583	2902	97,1	88,4	28540	15,40	53,62	56,38	197,1	16,80	0,99	0,57	13,23	20,46	18,33	3,77	47,96
	06/09/06 11:37	622	7,79	2,9	71596	2304	100,4	89,8	29924	16,90	48,72	67,56	241,4	16,34	0,92	0,58	12,69	19,87	19,05	3,94	52,64
	04/10/06 10:41	2075	58,75	1,8	76594	3060	108,3	123,7	32348	16,98	57,33	58,69	216,3	19,10	0,90	0,47	13,10	26,58	24,74	4,87	60,74
	07/11/06 11:10	948	10,92	3,6	78982	3282	118,4	99,7	30812	17,10	51,77	54,87	210,2	19,94	0,70	0,44	14,36	31,08	27,09	4,75	56,17
	12/12/06 11:00	2774	96,38	2,5	77002	3080	118,1	98,3	35313	15,88	53,77	48,89	201,7	19,03	0,63	0,57	13,90	32,68	29,22	5,47	47,75
	17/01/07 11:00	1514	24,68	4,1	72384	3510	112,8	102,1	27475	16,08	55,23	54,71	269,5	20,98	1,06	0,63	16,49	35,35	30,36	5,80	50,71
	05/02/07 11:00	992	11,06	5,4	71438	2954	105,9	93,8	35005	16,59	52,05	64,45	254,2	22,06	0,85	0,52	16,19	33,85	30,78	5,93	51,36
	07/03/07 11:40	3541	259,38	1,9	70111	3476	107,9	97,1	24884	14,58	51,90	45,58	179,0	18,39	0,51	0,48	11,33	32,21	27,44	5,40	39,15
	04/04/07 10:45	1318	23,27	3,1	56116	3661	84,0	83,7	21337	13,56	39,83	44,78	189,6	16,46	0,84	0,29	9,88	40,02	37,81	7,41	41,84
	02/05/07 11:30	807	18,64	2,8	65616	3559	100,5	102,4	24592	21,93	52,73	75,34	247,5	21,33	1,10	0,58	14,63	46,46	40,38	7,35	52,83
	12/06/07 17:50	1822	40,53	2,0	83998	3592	131,5	104,4	26712	17,07	54,55	162,35	227,5	19,63	0,44	0,30	13,16	30,80	25,65	4,82	41,47
	04/07/07 11:45	1563	32,99	2,8	62953	3436	103,5	97,8	32303	16,97	60,15	80,23	235,7	21,86	0,87	0,52	13,06	25,18	22,56	4,71	50,63
	05/09/07 11:10	581	36,33	3,0	69922	3619	108,3	97,4	25089	17,67	54,54	47,77	371,4	21,02	0,74	0,48	13,36	38,74	32,44	6,18	47,43
	08/10/07 11:00	679	12,69	5,0	65073	3408	83,4	79,5	29477	14,29	38,42	63,87	443,3	17,54	0,97	0,43	13,47	29,48	25,36	4,99	101,02
	08/11/07 11:20	270	4,78	6,3	74497	3988	101,0	81,0	35232	14,34	42,93	56,53	229,0	40,61	0,51	0,46	13,20	32,78	29,26	5,72	80,19
	08/01/08 11:10	1535	29,46	4,3	65169	2988	89,0	75,4	27646	13,40	39,31	41,99	306,3	23,15	0,81	0,50	12,06	28,03	23,55	4,50	53,99
	06/02/08 12:00	1506	9,97	4,6	84487	3702	112,4	95,9	32480	16,60	52,40	57,44	235,7	26,55	0,93	0,42	18,21	34,07	28,19	5,24	59,03
	06/04/08 11:00	1509	5,34	4,8	50893	2300	80,6	75,7	19226	12,41	37,13	49,03	207,9	14,90	0,76	0,35	12,20	22,40	18,96	3,60	51,31
	06/05/08 11:15	1532	7,89	4,8	71553	3275	114,6	101,4	26104	17,45	50,35	56,38	266,7	22,43	0,79	0,49	15,61	31,13	25,79	4,88	48,54
	06/07/08 11:00	1366	16,53	2,1	67084	2944	105,5	87,5	22069	15,69	47,41	50,00	188,8	18,89	0,42	0,30	10,71	23,57	20,31	3,93	52,43
	06/08/08 12:30	704	11,02	3,4	64651	2862	102,5	85,6	22210	16,72	46,10	54,00	173,6	18,49	0,51	0,31	11,24	23,83	20,39	4,05	38,22
	06/09/08 11:35	2133	173,60	1,6	71250	3326	95,0	82,7	30320	16,78	47,18	37,73	149,2	18,97	0,34	0,44	9,34	25,71	22,30	4,44	47,63
	06/10/08 00:00	659	7,75	3,5	68570	3455	95,2	84,7	29321	15,35	47,37	66,06	173,7	16,11	0,67	0,37	9,98	26,51	22,93	4,66	191,61
	05/11/08 11:20	3639	307,68	2,7	81902	4342	122,9	100,4	31109	18,04	49,68	70,55	267,2	50,20	0,40	0,60	15,50	37,79	33,78	6,66	89,23
	06/12/08 11:35	1851	16,76	3,6	71561	3182	113,4	96,5	26661	16,65	50,01	57,05	223,4	22,35	0,75	0,51	13,53	27,48	23,71	4,74	49,22
	15/01/09 11:15	1119	8,25	3,6	70591	2388	103,1	98,1	34429	15,09	53,01	58,87	311,0	21,82	0,74	0,55	11,87	24,75	22,90	4,54	62,93
	11/02/09 11:10	3132	345,39	1,3	61642	3231	83,2	70,4	27070	12,15	38,83	28,65	119,3	15,57	0,25	0,68	7,99	25,00	21,96	4,41	37,80
	12/03/09 11:50	2118	40,99	1,2	71032	3443	110,5	99,2	27504	15,44	53,87	54,74	439,1	24,39	0,52	0,46	13,56	30,35	25,47	4,87	68,22
	08/04/09 11:49	1784	12,53	2,4	57041	2900	89,4	79,1	20662	13,40	39,55	38,21	193,6	17,40	0,50	0,27	10,27	27,27	23,07	4,38	37,83
	07/05/09 11:20	1131	7,05	3,6	57144	2843	89,8	74,2	20161	13,76	39,19	36,42	169,1	15,37	0,38	0,42	10,75	23,96	20,90	4,05	39,81
	10/06/09 11:34	1521	18,92	2,8	63544	3043	98,9	84,1	21802	14,37	44,45	48,46	200,4	17,13	0,48	0,43	11,69	25,53	22,57	4,49	39,52
	10/07/09 11:26	855	3,18	5,6	57554	2637	89,4	78,3	21120	17,28	41,31	69,88	233,3	20,19	0,56	0,58	11,80	22,60	19,18	3,67	81,64
	10/08/09 12:00	760	4,80	6,7	59447	2690	90,9	78,2	21606	15,97	42,31	65,46	218,3	19,48	0,68	0,50	11,49	22,43	19,43	3,81	48,60
	10/09/09 11:20	811	11,17	3,1	64496	3035	98,8	87,0	23427	16,45	51,97	53,99	253,3	20,51	0,69	0,50	12,85	24,72	21,30	4,06	66,32
	10/10/09 11:02	774	3,69	5,9	55575	2578	85,8	77,6	21244	14,29	41,57	82,10	213,2	17,84	1,17	0,53	10,53	20,85	18,12	3,60	126,09
	10/11/09 11:30	751	11,22	3,0	68135	3393	107,2	91,3	23711	16,21	46,59	53,54	193,6	16,49	0,75	0,43	13,28	27,45	22,68	4,40	46,63

	10/12/09 11:30	1780	33,92	4,6	71806	3601	114,2	95,5	26691	15,48	48,37	51,85	203,9	18,74	0,64	0,42	14,68	31,09	26,25	4,97	43,98
	06/01/10 16:35	2929	128,03	10,5	59245	2505	103,0	83,6	26069	8,28	33,77	23,29	109,7	12,54	0,26	0,13	10,05	24,29	20,49	3,68	30,73
	03/02/10 00:00	1364	11,85	7,8	50397	2883	112,2	87,5	25122	10,12	74,34	24,68	146,2	15,92	0,34	0,58	9,58	26,66	22,93	4,34	42,22
	03/03/10 00:00	2879	76,28	4,7	60088	2722	114,0	92,2	28600	9,40	38,40	24,67	181,2	13,79	0,33	0,17	10,77	25,78	21,93	3,99	36,30
	07/04/10 16:54	2984	64,46	1,9	52933	2436	94,0	87,3	25839	8,21	33,84	17,90	105,6	14,24	0,28	0,21	8,38	23,04	20,19	3,75	39,59
	05/05/10 00:00	1627	20,75	2,4	70617	3028	113,8	92,0	34407	11,23	43,88	35,79	177,0	18,02	0,31	0,32	11,06	29,69	26,11	4,99	58,03
	09/06/10 00:00	1868	24,35		58224	2896	100,5	83,6	28819	9,58	33,55	25,10	118,4	17,73	0,26	0,21	8,09	24,88	22,34	4,33	38,10
	21/07/10 16:30	744	12,20		75382	3232	118,4	84,1	34694	11,18	37,84	34,71	127,4	23,20	0,23	0,20	10,71	31,50	27,24	5,25	42,48
	08/09/10 17:20	2190			75900	3933	124,2	90,2	38690	12,60	38,92	57,13	137,9	43,69	0,24	0,39	9,65	30,20	27,47	5,32	45,60
	13/10/10 00:00	691	270,27		113662	5198	172,4	125,8	54986	17,49	51,68	77,97	170,0	54,67	0,35	0,54	14,24	45,30	40,47	7,91	64,95
	04/11/10 18:00	1461	6,00		70260	3600	115,6	85,3	35821	11,59	36,59	51,73	132,3	39,17	0,25	0,37	8,90	27,78	24,93	4,77	41,84
	08/12/10 00:00	1259	117,80		22653	1069	42,7	43,6	10802	4,27	16,04	14,18	136,1	7,06	0,24	0,24	3,65	10,14	8,74	1,65	20,50
	12/01/11 00:00	2959	39,95		55175	3029	96,7	81,4	26197	13,41	42,87	43,49	224,6	18,28	0,51	0,49	12,95	25,31	21,74	4,31	44,83
	04/02/11 00:00	1064	8,53		56356	2903	94,5	85,5	26046	16,64	40,90	53,36	153,0	14,71	0,62	0,25	12,82	25,67	20,20	3,93	43,72
	04/03/11 13:15	1246	12,43		55381	2920	90,2	78,1	25367	16,60	40,32	46,79	211,8	17,17	0,61	0,35	13,40	25,62	21,94	4,28	44,47
	06/04/11 10:43	1134	4,42		52735	2502	83,0	77,2	23952	15,08	38,80	49,28	220,0	18,25	0,82	0,54	12,88	22,26	19,15	3,79	52,58
	11/05/11 11:30	580	6,32		47268	2399	78,9	80,6	23009	14,43	37,62	40,35	199,4	18,81	0,49	0,45	10,92	21,50	18,21	3,47	43,88
(turbid)	14/04/08 12:15				59596	2853	94,4	90,4	29699	12,8	54,5	37,7	165,6	15,2	0,5	0,5	9,6	24,9	23,1	4,4	37,2
	14/04/08 12:45				51562	3073	83,0	77,4	26462	12,85	46,54	41,57	190,7	17,04	0,59	0,50	9,47	26,31	23,06	4,55	39,97
	14/04/08 15:00				50003	2731	83,8	77,6	27022	11,82	45,64	39,08	167,9	16,41	0,60	0,50	9,47	25,19	22,26	4,50	40,01
	21/04/08 15:20				60349	2976	97,4	81,2	29817	13,37	44,64	38,69	195,1	21,74	0,75	0,55	11,76	29,04	25,12	4,92	48,22
	21/04/08 17:00				61473	2932	95,9	80,4	29762	13,39	44,49	39,51	199,4	23,07	0,67	0,58	11,79	27,88	23,76	4,96	49,38
	21/04/08 19:30				56549	3124	88,2	77,9	27834	12,28	41,96	39,91	196,8	20,81	0,65	0,51	10,82	28,22	23,96	4,64	45,31
	21/04/08 23:30				56929	2431	88,3	74,3	26877	11,89	40,07	37,33	202,5	19,90	0,60	0,58	11,39	24,90	21,64	4,24	46,69
	22/04/08 02:00				46942	2749	71,9	61,4	22286	10,33	32,78	28,01	162,6	15,58	0,42	0,49	9,42	24,31	20,74	3,98	41,13
	22/04/08 06:30				43236	2462	59,5	53,3	18528	8,58	27,62	23,40	127,3	13,45	0,42	0,39	8,50	20,93	17,84	3,48	41,33
	30/05/08 12:30	3870	290	0,8	23816	1293	39,5	29,5	10309	5,19	18,11	13,54	57,0	5,31	0,14	0,10	3,65	9,65	8,10	1,62	11,65
	31/05/08 16:45	4247	2590	0,8	50497	3001	84,2	63,4	23111	11,45	41,15	24,63	97,5	9,95	0,27	0,19	6,82	23,44	19,35	3,67	20,48
	03/06/08 12:40	3732	839	0,7	54228	2239	85,9	64,4	24873	11,92	42,80	26,11	95,4	11,79	0,24	0,20	7,08	21,09	19,13	3,84	23,95
	10/06/08 17:10	2866	610		53163	3004	85,9	141,5	25130	12,49	75,93	26,74	104,2	16,92	0,31	0,24	7,45	21,78	18,75	3,76	28,61
	09/09/08 10:00	2459	246,9		48834	2551	74,0	60,8	22854	10,84	38,26	26,79	104,7	12,03	0,25	0,23	6,35	17,55	15,25	3,54	27,03
	22/10/08 17:00	3295	216,7		50196	2866	81,3	66,3	25806	12,83	37,51	39,85	146,8	23,24	0,43	0,50	8,94	23,58	20,98	4,08	53,31
	23/10/08 10:25	2853	308,1		67274	2737	90,8	70,1	29886	13,18	37,25	37,27	183,1	25,93	0,42	0,56	15,57	30,43	26,74	5,85	80,29
	23/10/08 12:25	2612	268,7		72003	3181	99,3	77,3	32056	14,74	41,22	42,55	196,7	28,35	0,48	0,63	16,48	33,69	29,13	5,70	86,82
	23/10/08 14:25	2472	233,9		71441	3066	96,6	75,3	31509	14,53	40,30	39,04	190,7	26,66	0,48	0,56	16,23	33,48	28,60	5,62	81,79
	02/11/08 15:30	4786	122,8	1,4	55280	3080	81,8	67,6	26923	12,66	37,00	35,65	157,6	23,24	0,62	0,49	10,17	25,31	23,71	4,72	60,10
	02/11/08 17:00	4976,5	331,45	1,7	64771	2952	89,7	73,8	30076	14,49	41,68	39,09	183,9	31,77	0,50	0,60	11,88	30,76	27,01	5,25	82,66
	03/11/08 12:00	4770	318,35	1,6	51340	2816	65,3	56,9	24473	11,25	31,60	28,08	133,9	23,35	0,41	0,43	9,10	28,99	25,64	5,23	60,22
	03/11/08 14:00	4801	240,9	1,5	68836	3009	88,9	75,3	32282	14,74	41,70	38,58	176,3	32,20	0,53	0,52	11,69	31,57	27,33	5,54	72,67
	04/11/08 13:00	3999	206,2	2,1	32832	3395	87,6	86,5	32353	14,04	43,05	48,07	203,0	34,70	0,44	0,44	8,01	19,03	17,81	3,27	64,82

B. Particulate trace metal concentrations in sediment traps

		Ref. date	Lat. (deg.)	Long. (deg.)	Depth (m)	^{27}Al (µg/g)	^{47}Ti (µg/g)	^{51}V (µg/g)	^{52}Cr (µg/g)	^{56}Fe (µg/g)	^{59}Co (µg/g)	^{60}Ni (µg/g)	^{65}Cu (µg/g)	^{66}Zn (µg/g)	^{75}As (µg/g)	^{107}Ag (µg/g)	^{114}Cd (µg/g)	^{133}Cs (µg/g)	^{139}La (µg/g)	^{146}Nd (µg/g)	^{147}Sm (µg/g)	^{208}Pb (µg/g)
CASCADE	*T1*	04/03/11	42.0268	3.0070	290	58608	3132	108.11	78.60	25123	10.82	36.55	60.63	190.65	17.75	0.10	0.12	8.91	27.42	24.03	4.57	40.47
		05/03/11				57427	3023	104.64	75.24	24944	10.50	35.24	41.91	163.25	17.32	0.06	0.12	8.60	26.95	23.88	4.77	38.96
		07/03/11				59417	3116	110.33	79.06	25134	10.93	38.21	54.84	184.22	18.72	0.09	0.41	9.22	27.48	23.94	4.61	39.94
		08/03/11				58224	3031	103.70	75.52	24652	10.60	35.36	37.12	164.30	18.44	0.07	0.11	8.77	25.42	22.31	4.30	38.76
		10/03/11				57737	3118	107.97	81.38	24962	10.99	39.65	64.49	188.13	16.95	0.07	0.11	8.91	26.63	23.20	4.42	40.18
		11/03/11				59020	3097	109.73	82.06	25135	11.39	40.70	55.91	184.30	16.40	0.07	0.21	9.01	27.46	23.88	4.42	40.64
		13/03/11				57111	3307	103.74	73.19	25156	10.13	33.03	38.07	161.60	18.68	0.08	0.15	8.16	27.22	23.88	4.52	39.66
		14/03/11				57229	3221	108.09	76.32	25210	9.70	34.39	40.23	161.38	19.43	0.09	0.14	8.60	27.00	23.33	4.57	41.14
		16/03/11				60744	3451	117.22	82,31	26936	10,72	37,17	40,91	153,46	19,28	0,09	0,14	9,21	29,74	25,68	4,94	44,51
		17/03/11				56186	3126	103,25	80,55	24255	11,11	39,29	58,75	171,37	16,77	0,07	0,11	8,72	33,49	28,31	5,19	39,37
		19/03/11				55052	2977	102,70	81,44	23623	10,91	41,98	68,54	181,60	15,30	0,06	0,11	8,40	27,15	23,51	4,50	39,40
	T2	04/03/11	42,0052	3,0538	365	59900	3124	111,73	80,72	25367	11,24	37,75	48,71	140,37	17,79	0,06	0,70	9,28	28,26	24,32	4,54	40,51
		05/03/11				61533	3177	111,22	82,89	26197	11,67	39,98	44,62	152,36	18,62	0,07	0,14	9,68	28,78	24,35	4,69	40,31
		07/03/11				59484	3100	110,82	78,81	25382	11,20	38,32	32,87	144,46	17,70	0,07	0,13	9,32	28,14	24,22	4,75	39,22
		08/03/11				59198	3151	107,44	78,09	25513	10,94	36,60	40,36	146,08	17,36	0,08	0,13	8,95	27,63	23,98	4,65	40,86
		10/03/11				58909	3044	107,77	79,72	24907	11,07	38,78	45,88	159,45	17,52	0,07	0,11	9,16	26,15	22,75	4,43	39,93
		11/03/11				57760	3012	105,94	79,08	24558	11,09	39,38	49,21	164,78	17,20	0,06	0,15	8,95	26,52	23,57	4,40	38,40
		13/03/11				59476	3176	107,26	76,04	25918	10,60	35,55	37,77	184,55	18,74	0,09	0,23	8,83	26,43	23,44	4,60	41,28
		14/03/11				59227	3290	107,00	78,45	25778	10,20	35,36	41,09	172,35	19,46	0,07	0,13	9,03	28,11	24,30	4,67	41,94
		16/03/11				60791	3290	108,71	80,25	26017	10,65	36,86	41,22	172,85	18,92	0,08	0,06	9,39	28,52	24,96	4,78	41,81
		17/03/11				59826	3066	107,26	82,77	25214	11,41	41,13	47,42	181,12	17,87	0,06	0,19	9,21	30,05	25,78	4,83	39,44
		19/03/11				59150	3140	103,45	82,55	25381	11,25	40,46	54,44	181,45	17,78	0,07	0,12	8,88	27,45	23,43	4,57	39,77
HERMES	*CCC300*	27/10/05	42,0585	3,1533	310	58609	2958	102,95	86,77	29185	12,03	42,51	49,42	207,59	17,21	0,57	0,15	8,01			4,83	41,57
	CCC1000	27/10/05	42,1450	3,0650	1000	56439	2650	100,81	84,06	27469	11,77	44,05	42,40	153,57	16,24	0,51	0,13	8,38			4,27	41,11
		07/11/05				66301	3025	115,24	97,70	31365	14,49	54,44	58,27	247,78	19,05	0,42	0,24	9,94			5,10	52,59
		23/11/05				63682	2894	111,91	99,20	30837	13,69	52,19	59,67	229,77	17,89	0,28	0,47	9,33			4,99	49,94
		07/12/05				47750	2283	92,14	86,82	25294	11,92	46,56	54,60	173,18	14,45	0,28	0,16	6,85			3,79	40,30
		23/12/05				64455	3071	116,53	100,48	32313	14,73	52,46	73,95	190,45	20,30	0,22	0,14	8,94			5,00	48,45
		06/01/06				56198	2931	97,37	73,84	29423	11,36	36,30	37,32	139,92	16,54	0,19	0,22	7,79			4,80	39,03
		22/01/06				57473	3055	97,39	73,95	29260	11,28	37,18	36,65	146,20	16,98	0,21	0,16	8,38			5,06	40,21
		05/02/06				61467	3094	105,25	87,25	30599	12,81	47,17	44,47	134,42	16,73	0,17	0,22	9,56			5,19	43,14
		21/02/06				74814	3958	135,60	118,54	37878	17,31	65,86	52,44	213,47	24,89	0,23	0,49	10,38			6,25	56,33
		08/03/06				60602	3071	109,12	92,25	30769	12,71	48,11	46,13	179,84	18,51	0,20	0,19	8,19			4,91	41,33
		23/03/06				67644	3623	113,25	93,10	34214	12,38	44,21	37,41	154,28	17,68	0,18	0,15	8,71			5,51	42,65
		06/04/06				61936	3108	110,98	105,87	31661	13,48	63,45	63,27	246,30	17,12	0,25	0,33	9,43			5,32	46,09
	CCC1500	07/11/05	42,0573	3,1598	1490	51464	2627	93,72	97,00	27554	18,61	54,04	104,07	238,77	13,67	0,33	0,28	6,81			4,67	56,33
		23/12/05				79402	4071	147,47	149,14	41911	27,81	82,85	125,60	409,36	23,07	0,49	0,55	10,74			6,96	85,94
		06/01/06				58253	3205	109,25	94,34	30661	14,14	48,78	57,80	166,13	16,98	0,19	0,14	8,86			5,30	46,68
		22/01/06				60579	3502	118,52	113,12	33332	17,68	59,90	67,79	184,20	18,45	0,48	0,18	8,81			5,82	55,99
		05/02/06				59919	4077	124,03	128,19	34901	18,54	63,38	63,21	131,77	19,58	0,29	0,25	8,43			5,82	58,31
		21/02/06				57917	3417	114,79	115,54	32717	16,08	60,08	69,14	185,51	19,69	0,30	0,26	7,89			5,44	52,90
		08/03/06				54300	3538	125,87	128,29	34677	17,83	64,82	65,11	168,80	20,62	0,28	0,32	7,42			5,91	58,08
		23/03/06				64107	3666	121,12	123,03	34640	15,40	59,70	60,24	187,81	19,10	0,34	5,92	8,98			5,86	54,09
		06/04/06				53723	3724	122,84	132,31	33722	16,86	63,47	67,89	218,81	19,01	0,36	0,31	7,37			5,60	59,48
	LDC300	27/10/05	42,0960	3,0633	300	72629	3269	122,85	94,94	33262	13,18	53,78	48,05	170,35	19,63	0,19	0,26	10,59			5,44	47,08
		07/11/05				55751	2459	93,90	75,62	26073	10,12	41,94	59,45	157,56	14,26	0,14		8,01			4,35	38,97
		23/11/05				62048	2894	109,01	88,08	30112	11,77	41,92	44,45	239,45	16,79	0,25	0,13	8,89			4,76	41,27
		07/12/05				77954	3574	134,43	103,65	36757	14,32	49,90	51,21	246,95	19,56	0,28	0,17	11,14			5,72	47,69
		23/12/05				64752	3034	114,21	97,92	31183	12,52	45,32	62,81	210,17	16,84	0,21	0,21	9,14			4,96	43,74
		06/01/06				61921	3025	110,37	84,29	29980	12,61	43,60	39,36	152,87	16,66	0,25	0,15	10,06			5,23	43,96
		22/01/06				49071	2599	94,54	72,52	25793	11,26	37,83	25,96	119,38	14,83	0,25	0,12	7,64			4,75	40,04
		05/02/06				58391	2982	106,94	83,56	29036	12,31	43,94	37,60	147,16	15,58	0,16	0,18	9,49			5,09	42,78
		21/02/06				66429	3196	119,51	110,18	32805	13,47	52,29	58,49	180,76	17,95	0,22	0,31	9,35			5,21	46,41
		08/03/06				94248	4571	163,76	141,03	45407	19,02	68,80	63,49	243,89	25,30	0,31	0,25	13,11			7,18	63,00
		23/03/06				57471	2603	101,97	87,13	28573	11,78	43,30	41,51	170,10	14,42	0,15	0,52	7,92			4,36	38,93
		06/04/06				60930	2910	102,11	84,62	29097	11,78	41,82	32,73	182,33	14,01	0,15	0,21	8,48			4,58	38,26
	LDC1000	27/10/05	42,0937	3,0440	1050	59032	2907	107,82	91,09	29502	17,02	51,50	45,44	152,03	17,76	0,19	0,18	9,26			4,99	44,25
	(30mab)	07/11/05				52468	2498	97,28	80,77	26369	14,78	44,35	59,06	1443,01	15,63	0,24	0,73	8,59			4,47	43,19
		23/11/05				53099	2525	100,11	86,63	27327	15,74	46,18	61,05	1035,18	15,76	0,41	0,58	8,02			4,71	46,57
		07/12/05				56052	2729	104,47	88,33	28134	17,08	46,82	54,98	175,36	16,75	0,19	0,19	8,67			4,82	44,47

	23/12/05				61115	2986	109,37	91,15	30369	17,04	49,32	61,63	156,08	18,05	0,20	0,19	9,37	5,25	46,98
	22/01/06				54545	2778	101,80	83,35	28394	12,05	42,43	51,91	172,30	16,14	0,17	0,16	8,40	5,14	40,72
	05/02/06				60896	3018	106,52	111,37	30453	12,69	58,76	42,05	153,15	16,23	0,23	0,29	9,34	5,18	43,87
LDC1000	27/10/05	42,0937	3,0440	1050	61367	2889	112,17	93,29	30068	16,71	49,98	47,93	165,12	17,75	0,24	0,14	9,83	5,09	47,34
(550mab)	07/11/05				56950	2855	103,08	120,47	28312	15,14	65,54	59,21	216,68	16,37	0,31	0,37	8,68	4,76	45,73
	23/11/05				60780	2743	111,14	96,09	29813	18,38	49,74	64,25	217,01	17,53	0,26	0,27	9,80	5,09	50,38
	07/12/05				50848	2378	95,37	80,13	25262	17,47	42,52	47,36	159,62	14,93	0,18	0,13	8,04	4,15	42,47
	23/12/05				54559	2556	99,40	87,15	26848	18,87	44,90	70,01	191,98	15,37	0,21	1,26	8,44	4,63	45,53
	22/01/06				57093	2788	102,60	88,54	28513	13,00	44,10	53,76	203,35	16,35	0,18	0,17	8,70	4,75	43,70
	05/02/06				52266	2765	101,16	89,32	28361	13,74	46,97	44,26	145,94	14,83	0,18	0,14	7,61	4,62	41,21
	21/02/06				45337	2505	91,90	94,68	25048	12,78	47,48	31,00	125,37	15,26	0,19	0,23	6,70	4,39	36,31
	08/03/06				58525	2944	110,17	93,82	30102	15,65	49,64	50,41	170,36	17,31	0,23	0,18	9,08	4,93	44,11
	23/03/06				60376	2889	109,18	101,17	30230	15,27	52,93	84,46	215,52	17,34	0,21	0,79	9,43	5,01	47,62
	06/04/06				61913	3015	113,56	107,35	31581	17,74	56,51	62,14	279,75	17,33	0,23	0,24	9,54	5,13	49,88
LDC1500	23/12/05	42,0333	3,0023	1510	64581	3378	119,41	134,02	34201	34,78	71,05	109,87	335,12	17,93	0,44	1,79	9,18	5,64	69,82
	21/02/06				63101	3713	121,58	124,79	34697	18,73	64,84	83,88	178,98	20,76	0,33	1,82	8,59	6,17	56,20
	08/03/06				60248	3580	113,13	114,01	32799	16,53	56,78	51,43	162,46	17,72	0,24	0,23	8,54	5,72	50,90
	23/03/06				60703	3199	112,32	105,76	31504	14,24	53,45	51,80	185,93	17,51	0,25	0,25	8,90	5,19	47,40
	06/04/06				65359	3419	120,05	123,39	33743	15,84	61,09	68,14	259,88	17,43	0,33	0,30	9,50	5,86	53,89
CCC1900	07/11/05	42,0527	4,0947	1920	52616	2683	90,86	95,10	27060	19,49	49,36	131,14	251,45	13,80	0,21	0,20	5,67	4,19	52,19
	23/12/05				52693	2824	86,18	107,31	28193	18,65	60,32	128,80	392,64	12,87	0,25	0,24	5,77	4,28	54,24
	06/01/06				54666	3551	105,58	112,28	30804	17,49	54,72	92,36	262,35	15,35	0,23	0,24	7,21	5,52	54,40
	22/01/06				52630	3324	100,96	103,06	29288	15,14	56,24	80,07	167,78	15,95	0,23	0,19	7,09	5,15	46,91
	05/02/06				47849	3174	105,81	99,99	29632	17,65	55,28	61,88	121,51	15,85	0,22	0,17	6,54	5,28	51,41
	21/02/06				56349	3534	108,78	110,49	31470	16,18	53,76	60,93	169,40	17,36	0,19	0,20	6,59	4,89	47,77
	08/03/06				50584	3148	94,73	97,10	27788	14,03	46,37	56,72	141,23	15,34	0,21	0,36	5,77	4,72	40,79
	23/03/06				55274	3742	109,43	114,68	32153	16,36	56,20	76,48	152,24	16,58	0,43	0,27	7,19	5,86	55,95
	06/04/06				52332	3306	104,82	114,82	29744	15,75	55,25	76,93	186,30	16,07	0,40	0,36	6,95	5,20	54,40
SOS1000	27/10/05	42,1282	3,1092	970	68699	3549	128,65	135,11	36561	24,38	73,41	135,36	306,02	21,60	0,42	0,37	9,88	6,22	73,10
	07/11/05				69777	3408	126,84	119,10	36103	21,80	64,50	99,63	275,26	19,33	0,38	0,22	9,94	5,93	61,45
	23/11/05				68825	3332	128,43	114,55	35531	21,11	61,93	78,68	237,76	20,40	0,30	2,07	10,16	5,82	59,23
	07/12/05				62676	3963	128,84	129,78	36805	22,36	66,57	77,61	201,38	21,25	0,30	0,52	7,76	6,30	62,66
	23/12/05				56751	2855	105,09	96,96	29528	20,74	53,35	74,99	212,26	17,59	0,26	0,36	8,44	5,09	52,08
	06/01/06				46701	3165	82,90	64,26	24329	9,33	30,53	23,88	98,48	13,25	0,24	0,14	6,11	5,41	28,50
	22/01/06				62135	3472	124,83	112,85	34619	18,04	61,69	66,72	167,33	19,80	0,26	0,24	9,55	5,63	55,23
	05/02/06				65441	3434	122,35	95,39	33737	13,31	47,89	36,95	134,68	20,36	0,31	0,16	10,48	5,70	45,24
	21/02/06				50952	2752	92,55	83,44	26770	12,18	43,56	34,84	127,80	16,02	0,17	0,18	7,29	4,56	38,70
	08/03/06				58365	3325	115,18	104,98	32074	15,17	53,37	57,36	172,39	18,73	0,26	0,52	8,10	5,06	47,72
	23/03/06				55187	3055	100,10	86,48	29458	11,87	41,97	40,89	152,59	17,11	0,23	0,28	7,54	4,98	39,49
	06/04/06				94542	4841	176,27	191,04	49998	23,21	89,30	125,42	356,18	27,85	0,45	0,53	13,25	8,28	79,60
SOS2000	23/11/05	42,1100	4,0488	1900	276748	14026	517,34	472,71	144022	96,78	256,28	325,48	997,03	78,99	1,48	0,89	39,49	23,90	259,09
	21/02/06				47163	3172	107,00	110,10	29833	18,26	54,95	75,28	174,56	17,52	0,28	0,24	5,51	4,93	50,81
	08/03/06				11324	579	21,06	221,02	6116	7,85	13,79	33,25	77,65	3,05	0,07	0,17	1,33	0,97	12,93
	23/03/06				57176	3532	111,87	114,45	32177	18,40	57,38	68,72	159,49	18,06	0,30	1,01	7,37	5,60	53,99

C. Particulate mercury concentrations in sediment trap and core samples (DMA extraction)

		Ref. date	Lat.	Long.	Depth	Particulate Hg concentration		
						Total	*After HCl extraction*	*After H2O2 extraction*
			(deg.)	(deg.)	(m)	(µg/kg)	(µg/kg)	(µg/kg)
CASCADE	*T1*	04/03/11	42.0268	3.0070	290	577,2	196,8	54,2
(sediment trap)		05/03/11				773,6	326,4	93,6
		07/03/11				189,1	89,8	54,6
		08/03/11				136,2	71,3	59,8
		10/03/11				310,7	108,8	
		11/03/11				730,1	186,4	47,9
		13/03/11				201,9	123,3	31,6
		14/03/11				130,3	65,2	29,2
		16/03/11				137,5	68,3	
		17/03/11				159,3	73,3	41,2
	T2	04/03/11	42.0268	3.0070	290	1843,1	419,2	137,0
		05/03/11				127,4	61,9	37,7
		07/03/11				114,1	59,1	33,2
		08/03/11				129,5	62,6	38,3
		10/03/11				150,2	88,4	50,7
		11/03/11				146,0	82,1	
		13/03/11				126,1	69,5	47,7
		14/03/11				138,2	93,8	33,8
		16/03/11				120,5	85,7	38,0
		17/03/11				130,2	89,3	
		19/03/11				1463,6	842,6	
HERMES	*LDC300*	06/01/06	42,0960	3,0633	300	79,2		
(sediment trap)		22/01/06	42,0960	3,0633		87,6		
		05/02/06	42,0960	3,0633		100,7		
	CCC1000	06/01/06	42,1450	3,0650	1000	89,6		
		22/01/06	42,1450	3,0650		111,5		

		05/02/06	42,1450	3,0650		104,0		
	CCC1500	06/01/06	42,0573	3,1598	1490	116,2		
		22/01/06	42,0573	3,1598		113,6		
		05/02/06	42,0573	3,1598		108,3		
	CCC1900	06/01/06	42,0527	4,0947	1920	115,7		
		22/01/06	42,0527	4,0947		107,7		
		05/02/06	42,0527	4,0947		104,5		
	SOS1000	06/01/06	42,1282	3,1092	970	93,5		
		22/01/06	42,1282	3,1092		117,4		
		05/02/06	42,1282	3,1092		100,3		
CASCADE	*M08 (0-0,5)*				1957	75,8	58,6	21,4
(deep cores)	*(0,5-1)*					72,5	43,7	23,3
	M01 (0-0,5)				2657	80,3	51,7	21,7
	(0,5-1)					144,2	47,8	25,6
DEEP3	*SC2400 (0-0,5)*				2400	78,9	49,6	29,9
(deep cores)	*(0,5-1)*					65,6	47,5	26,0

SUMMARY

Coastal areas represent the connexion between continent, ocean and atmosphere domains. They are the scene for production, transformation, transfer, export and storage of both natural and anthropogenic particulate inputs, the latter arising from constant increase in population density and industrialization. Sedimentological cycle in the coastal environment has been well studied but gaps need to be filled to better understand the fate, and hence, the impact of contaminated particles in the whole land-to-sea continuum. Through the long-term survey of coastal Mediterranean rivers, we better estimated inter-annual variability of riverine particulate trace metal fluxes delivered to the sea. We confirmed by tracing methods, that it is the main source towards the marine environment. We were able to quantify export budgets due to E-SE storms and Dense Shelf Water Cascading. Export fluxes are temporarily stored in canyons then periodically flushed by those high energetic, depurating processes. This depuration induces moderate enrichment of the deep basin, relatively far from sources.

Key words: trace metals, Gulf of Lion, flood, storm, dense shelf water cascading, submarine canyons, metal budget, contamination, sediment.

RESUME

Les zones côtières représentent l'interface entre les domaines continentaux, océaniques et atmosphériques. Elles sont le lieu de production, de transformation, de transferts, d'export et de stockage des apports particulaires à la fois naturels et anthropiques, ces derniers étant dus à une constante augmentation de la densité de population et de l'industrialisation. Le cycle des sédiments dans l'environnement côtier à été largement étudié mais certains manques restent à combler afin de bien comprendre le devenir, et par là, l'impact des particules contaminées dans tout le continuum terre-mer. Le suivi à long terme des rivières côtières méditerranéennes, a permis une meilleure estimation de la variabilité interannuelle des apports fluviatiles en métaux traces. Les méthodes de traçage utilisées dans cette étude prouvent qu'ils constituent la source principale vers le domaine marin. Ces apports sont temporairement stockés dans les canyons et périodiquement balayés par ces processus énergétiques qui épurent alors la zone. Cette épuration se traduit par un enrichissement modéré du bassin profond, relativement loin des zones sources.

Mots-clefs : métaux traces, Golfe du Lion, crue, tempête, cascading d'eaux denses côtières, canyons sous-marins, bilan de métaux, contamination, sédiment.